

GCA Technical Report No. 66-20-N

GEOPOTENTIAL VERSUS GEOMETRIC ALTITUDE
FROM 0 TO 10,000 KILOMETERS FOR VARIOUS LATITUDES

R. A. Minzner
S. Mello

Contract No. NASW-1463

This work was partially supported by the United States Air Force under
Contract No. AF19(628)-6085.

GCA CORPORATION
GCA TECHNOLOGY DIVISION
Bedford, Massachusetts

April 1967

Prepared for

NATIONAL AERONAUTICS AND SPACE ADMINISTRATION
HEADQUARTERS
WASHINGTON, D.C.

N67-30623

FACILITY FORM 602

(ACCESSION NUMBER)	(THRU)
91	
(PAGES)	
UR-85566	
(NASA CR OR TMX OR AD NUMBER)	(CODE)
	/3
	(CATEGORY)

ABSTRACT

Simple analytical relationships between geopotential H_ϕ and geometric altitude Z_ϕ for various latitudes ϕ are presented with the required constants for relating H_ϕ to Z , and Z_ϕ to H at each of eight latitudes 0° , 15° , 30° , 45° , 60° , 75° , 90° , and at the reference latitude R equal to $45^\circ 32'33''$ which latitude corresponds to the standard sea-level gravity, $9.80665 \text{ m sec}^{-2}$. Values of $H_R(Z)$ were computed for geometric altitudes between 0 and 10,000 km; values of $Z_R(H)$ were computed for the equivalent range of geopotentials, between 0 and 3900 standard geopotential kilometers (km'). Computed values of Z_ϕ and H_ϕ for the other latitudes are presented as differences $(Z_\phi - Z_R)$ and $(H_\phi - H_R)$ as functions of both argument pairs $H_R(Z)$ and $Z_R(H)$, thereby leading to four sets of tables. Values of $H_R(Z)$ and $Z_R(H)$ are compared with the corresponding values from the U. S. Standard Atmosphere $H_S(Z)$ and $Z_S(H)$. These comparisons show the difference $(H_S - H_R)$ to be -33 meters at $Z_R = 700 \text{ km}$, while the difference $(Z_S - Z_R)$ is shown to be 55 meters at the corresponding value of $H_R = 630 \text{ km}'$.

TABLE OF CONTENTS

<u>Section</u>	<u>Title</u>	<u>Page</u>
I	INTRODUCTION	1
II	DEFINITIONS AND METHOD OF CALCULATION	3
III	GENERAL DESCRIPTION OF THE TABLES	9
IV	SPECIFIC DESCRIPTION OF THE TABLES 1A AND 1B	11
V	SPECIFIC DESCRIPTION OF TABLES 2A AND 2B	27
VI	SPECIFIC DESCRIPTION OF TABLES 3A AND 3B	45
VII	SPECIFIC DESCRIPTION OF TABLES 4A AND 4B	63
VIII	UNCERTAINTY CONSIDERATIONS	79
	REFERENCES	81
APPENDIX A:	VALUES OF r_ϕ AND g_ϕ EMPLOYED IN THE CALCULATION OF GEOPOTENTIAL AT VARIOUS LATITUDES	83
APPENDIX B:	PROGRAM FOR TABLE 2	85
APPENDIX C:	PROGRAM FOR TABLE 4	87

SECTION I

INTRODUCTION

Atmospheric properties are tabulated not only as a function of geometric height but frequently as a function of a height parameter called geopotential H (Ref. 1 through 5). Geopotential H is used as an independent variable because many atmospheric relationships are materially simplified by its introduction. The single variable, geopotential H , can replace two variables, the acceleration of gravity g and the geometric altitude Z . Accordingly, differential equations initially containing both variables g and Z may be restated in terms of the single variable geopotential so that integration of these transformed expressions is much simpler.

Most atmospheric models published since 1952, which include tabulations in terms of geopotential (those cited above) use the standard geopotential meter as the unit of geopotential, and some of these models provide tables for relating geopotential to geometric altitude, and vice versa, to heights of 700 km. These transformation tables have usually been calculated for that single latitude associated with the so-called standard sea-level value of gravity equal to $9.80665 \text{ m sec}^{-2}$. No similar transformation tables are associated with the above cited models for other latitudes. One recent set of models (Ref. 6) does distinguish between atmospheric properties at 15° , 30° , 45° , 60° , and 75° , and accordingly includes values of geometric altitude as a function of geopotential argument for each of these latitudes. These tabulations are limited to geopotentials between 0 and 90,000 m' (except for the model depicting 75° latitude, in which case the tabulation extends only to 31,000 m'). No tabulations are given for geopotential as a function of geometric altitude for these five latitudes, and no tabulations of any kind are given in these models for 0° and 90° latitude.

Harrison (Ref. 7) in a paper adapted for the Smithsonian Meteorological tables (Ref. 8) describes a simple but accurate method of calculating geopotential and provides two tables: (1) a tabulation of geopotential at various latitudes from 0° to 90° as a function of integral multiples of one geometric kilometer between sea level and 630 km; and (2) a tabulation (for the same latitudes) of geometric altitude as a function of integral multiples of one geopotential kilometer from sea level to 630 geopotential kilometers. The geopotential meter defined by Harrison, however, is slightly smaller than the currently used standard geopotential meter, which was first defined in the ICAO Standard Atmosphere (Ref. 1). The relative size of these two units of geopotential is expressed by the ratio $9.8/9.80665$, whereby the difference is about 0.678 percent of the former. Primarily because of this difference in

basic units, the Harrison tabulations are not consistent with the related tabulations of the United States Standard Atmosphere, 1962 (Ref. 5) and of other currently used model atmospheres.

Recent atmospheric measurements, particularly those involving high perigee satellites, have yielded values of atmospheric properties for altitudes considerably above 630 kilometers, and various atmospheric models (Ref. 9 and 10) have consequently been extended to altitudes of 1000 km. The desirability of applying these models to latitudes other than 45°, plus the limitations of the existing geopotential tables in previous publications, has prompted the calculation of the geopotential-geometric altitude tables which comprise the major contribution of this report.

SECTION II

DEFINITIONS AND METHOD OF CALCULATION

Geopotential H_ϕ of a unit mass, at a given latitude ϕ , relative to the reference geopotential at the earth's surface Z_0 at the same latitude, varies with geometric altitude Z and with the altitude-dependent acceleration of gravity $g_\phi(Z)$ for that latitude in accordance with the following integral equation:

$$H_\phi = \int_{Z_0}^Z g_\phi(Z) dZ \quad (1)$$

Approaches of considerable though varying sophistication have been employed in recent years in the determination of a function of Z which would permit the perfect integration of Equation (1) and would thus lead to numerical values of H_ϕ (Ref. 2, 3, 4, 5, and 7), for specified values of Z . The extreme differences in the values of H_ϕ for a given value of Z as determined by any of these methods are very small compared with the uncertainties of the atmospheric properties with which these geopotentials are commonly associated. Thus, it is reasonable that the simpler of these sophisticated methods (Ref. 2 and 7) be employed in the calculation of geopotential for use with atmospheric properties as is the intent in these tables. The most complicated and most sophisticated of these referenced methods, that is, the method used in the United States Standard Atmosphere 1962 (Ref. 5), yields a value of H_ϕ at 700 km which differs by less than 0.007 percent from that computed for these tables for the same latitude.

Analytical relationships for H_ϕ as a function of Z , and for Z_ϕ as a function of H , both stemming from Equation (1), are arrived at by replacing $g_\phi(Z)$ with a specialized form of the inverse-square law prior to the integration of Equation (1). The resulting relationships are:

$$H_\phi(Z) = H_\phi = \frac{r_\phi Z}{r_\phi + Z} \cdot \frac{g_\phi}{G} \quad (2)$$

and

$$Z_\phi(H) = Z_\phi = \frac{\frac{r_\phi H}{r_\phi g_\phi}}{\frac{G}{r_\phi g_\phi} - H} \quad (3)$$

where

$H_\phi(Z) = H_\phi =$ geopotential in geopotential meters (m') at latitude ϕ as a function of geometric altitude, Z ,

$Z_\phi(H) = Z_\phi =$ geometric altitude in geometric meters (m) at latitude ϕ as a function of geopotential H ,

$G = 9.80665 m^2 sec^{-2} (m')^{-1}$, which value implicitly defines one standard geopotential meter

$g_\phi =$ the sea-level value of the acceleration of gravity at latitude ϕ , ($m sec^{-2}$)

$r_\phi =$ the effective earth's radius for latitude ϕ , (m)

For any latitude ϕ , the value of r_ϕ is generally not equal to the earth's radius for that latitude, but rather is a quantity calculated to meet certain boundary conditions (Ref. 2, Appendix M, and Ref. 7), such that the relationships of Equations (2) and (3) retain a high degree of validity over an extended range of altitudes at all latitudes.

The values of g_ϕ and r_ϕ applicable to latitudes 0° , 15° , 30° , 45° , 60° , 75° , and 90° as used in this report were taken from Table 167 and Table 49, respectively, of the Smithsonian Meteorological Tables (Ref. 8). No value of g_ϕ or r_ϕ is given in the Smithsonian Tables, however, for the reference latitude, $R = 45^\circ 32' 33''$ (45.5424°).

The reference latitude R is not an arbitrary value for which the appropriate value of g_ϕ must be found, but rather is the latitude associated with the so-called standard acceleration of gravity equal to $9.80665 m sec^{-2}$ as designated in all United States Standard Atmospheres published after 1922. If the latitude variation of the sea-level value of the acceleration gravity is assumed to follow the Lambert equation (Ref. 8, page 491), that is,

$$g_\phi = 9.806160 (1 - 0.0026373 \cos 2\phi + 0.0000059 \cos^2 2\phi) \quad (4)$$

the value of ϕ which satisfies this equation for $g_\phi = 9.80665 \text{ m sec}^{-2}$ is found to be $\phi = 45^\circ 32' 33'' = R$. The value of r_ϕ for this latitude was computed in the manner described for the computation of values in Smithsonian Table 49 (Ref. 8) or as previously discussed by Minzner and Ripley (Ref. 2).

The values of g_ϕ and r_ϕ associated with the various latitudes employed in these calculations are listed in Appendix A. The use of the particular value of g_ϕ and r_ϕ for latitude R in Equation (2) yields values of H_R as a function of integral values of Z . These corresponding values of Z and H for latitude R are hereafter referred to as Z_R and H_R and serve as the first argument pair Z_R and H_R , that is, the pair in which Z_R is given in integral multiples of one geometric meter while H_R is expressed in non-integral multiples of the geopotential unit. The use of this same pair of values for g_ϕ and r_ϕ (for latitude R) in Equation (3) yields values of Z_R as a function of integral values of H . These corresponding values of H and Z which hereafter also bear the subscript R , are designated as the second argument pair H_R and Z_R , that is, the pair in which H_R is expressed in integral multiples of one standard geopotential meter and Z_R is expressed in non-integral multiples of a geometric meter.

The use in Equation (3) of the appropriate values of g_ϕ and r_ϕ successively for each of the other seven latitudes permits the calculation of two corresponding sets of values of Z_ϕ as a function of H_R , for each latitude, one set for the non-integral values of H_R from the first argument pair, and another set for the integral values of H_R from the second argument pair. A considerable reduction in the number of columns of tabular print resulted, however, by listing values of the departure of the above values of Z_ϕ from Z_R in the form $Z_\phi - Z_R$ for each of seven latitudes as a function of the values of H_R in each of the argument-pair sets.

Similarly, Equation (2) and the appropriate values of g_ϕ and r_ϕ led to seven sets of difference values, $H_\phi - H_R$, one set for each latitude as a function of the integral values of Z_R of the first argument pair, while seven additional sets of $H_\phi - H_R$ were computed as a function of the non-integral values of Z_R of the second argument pair. Thus, two sets of differences, $(Z_\phi - Z_R)$ and $(H_\phi - H_R)$, as well as two sets of argument pairs $(Z_R$ and $H_R)$ and $(H_R$ and $Z_R)$ led to the four tables of this report.

A comparison of the values of geopotential as a function of Z in the 1962 United States Standard Atmosphere with values of H_R as computed by Equation (2) for the same values of Z at the reference latitude R shows that these two sets of values of H depart slowly from each other in accordance with some function of increasing values of Z . The analytical expression for computing the Standard-Atmosphere values of geopotential

has not been published, but Minzner (Ref. 11) has shown that the unrounded Standard-Atmosphere values of geopotential as a function of Z are very closely approximated by an empirical function H_S which is defined by the following pair of equations:

$$H_S = \frac{r_R Z}{r_R + Z} \cdot \frac{g_R}{G} - f(Z) \quad (5)$$

and

$$f(Z) = A + BZ + CZ^2 + DZ^3 + EZ^4 \quad (6)$$

where

$$\begin{aligned} r_R &= \text{the value of } r_\phi \text{ for } \phi = R \\ g_R &= \text{the value of } g_\phi \text{ for } \phi = R \\ A &= 0.4858124 \times 10^{-2} \text{ m'} \\ B &= 0.1338918 \times 10^{-10} \text{ m''/m} \\ C &= 0.1903029 \times 10^{-10} \text{ m''/m}^2 \\ D &= 0.8288881 \times 10^{-16} \text{ m''/m}^3 \\ E &= 0.1822113 \times 10^{-22} \text{ m''/m}^4 \end{aligned}$$

Similarly Minzner (Ref. 10) has shown that the unrounded values of Standard Atmosphere Z as a function of H are very closely approximated by an empirical function Z_S which is defined by the following pair of equations:

$$Z_S = \frac{r_R [H + f(H)]}{\frac{r_R g_R}{G} - [H + f(H)]} \quad (7)$$

and

$$f(H) = A' + B'H + C'H^2 + D'H^3 + E'H^4 \quad (8)$$

where

$$\begin{aligned} A' &= 0.2579651 \times 10^{-2} \text{ m'} \\ B' &= 0.2161710 \times 10^{-7} \text{ m''/m'} \\ C' &= 0.1807561 \times 10^{-10} \text{ m''/(m')}^2 \\ D' &= 0.9153012 \times 10^{-16} \text{ m''/(m')}^3 \\ E' &= 0.2006785 \times 10^{-22} \text{ m''/(m')}^4 \end{aligned}$$

Since the 1962 Standard Atmosphere, like the earlier Standards, uses $9.80665 \text{ m sec}^{-2}$ as the sea-level value of the acceleration of gravity, the 1962 Standard Atmosphere may be associated with the reference latitude $45^{\circ} 32' 33''$, at least at sea level. Consequently, a comparison of $Z_S(H)$ with $Z_R(H)$ in the form of $Z_S - Z_R$ and a comparison of $H_S(Z)$ with $H_R(Z)$ in the form of $H_S - H_R$ gives an overall indication of the uncertainties introduced into the H to Z relationship by using the simplified expressions of Equations (2) and (3) rather than the complicated unpublished method used in the 1962 Standard.

PRECEDING PAGE BLANK NOT FILMED.

SECTION III

GENERAL DESCRIPTION OF THE TABLES

As already indicated, the two sets of differences, $(Z_\phi - Z_R)$ and $(H_\phi - H_R)$, applied to the two sets of argument pairs, $(Z_R$ and $H_R)$ and $(H_R$ and $Z_R)$, lead to four tables each having separate columns of differences for each of seven latitudes. Each of these four tables is divided into an "A" section and a "B" section. The "A" sections cover the argument range from 0 to 1000 km (or km') with differences in units of meters (or standard geopotential meters). The particular increments in the "A" sections of the tables are chosen to agree with the U. S. Standard Atmosphere Supplements, 1966, (Ref. 12).

The "B" section of each table includes the data for values of the argument pairs between 1000 and 10,000 km or between 1000 and 3,900 km'. All entries in the "B" sections are in kilometers (or Standard geopotential kilometers) and the number of significant figures presented decreases with increasing height to indicate, at least to a first approximation, the degree of uncertainty.

SECTION IV

SPECIFIC DESCRIPTION OF THE TABLES 1A AND 1B

Tables 1A and 1B present geometric altitude differences $Z_\phi - Z_R$ for various latitudes ϕ as a function of the second argument pair, that is, as a function of integral values of H_R . The first two columns give the values of the argument pair H_R and Z_R respectively, and 3 through 9 give the corresponding sets of values of $Z_\phi - Z_R$, one column for each latitude as indicated in the heading. The addition of the appropriate values of reference height Z_R to these differences leads to values of Z_ϕ as a function of H_R , that is, the same kind of information as that presented with different geopotential units in Table 51 of the Smithsonian Meteorological Tables (Ref. 8).

Column 10 of Table 1A lists the differences $Z_S - Z_R$ where Z_S approximates the set of standard-atmosphere geometric altitudes corresponding to the independent set of values of H_R . The values of Z_S corresponding to H_R were not taken directly from the tabulations of the United States Standard Atmosphere but from Equations (7) and (8) since (1) not all of the values of geopotential listed as H_R appear in that document and (2) the Standard Atmosphere values $Z(H)$ have been rounded to the nearest meter such that they are not smooth in the scale of 0.01 meter as required for smooth values of $Z_S - Z_R$. This function Z_S which accurately fits the Z to H relationship employed in the Standard Atmosphere, 1962, permits the recovery of at least two significant figures lost in the Standard-Atmosphere procedure of rounding to the nearest meter. Thus, differences $Z_S - Z_R$ may certainly be tabulated to the nearest tenth of a meter as given. No values of $Z_S - Z_R$ are given for Z_R greater than 700 km because the United States Standard Atmosphere terminates at that altitude. Consequently no values of $Z_S - Z_R$ appear in Table 1B.

Tables 1A and 1B should be useful as a means of determining geometric altitude as a function of geopotential for each of seven latitudes. With latitude used as the independent variable, this table also shows the altitude variation with latitude for each of a large number of equal geopotential surfaces having values expressed in integral multiples of one m'.

Graphical presentations of the data of Tables 1A and 1B are given in Figures 1.1A, 1.1B, 1.2A, and 1.2B. The figures with "A" designations are limited to the data for the region between sea level and 1,000 km (or km') while those with the "B" designation display the data for the region between sea level and 10,000 km (or 3,900 km'). The digit to the left of the decimal point associates the figure with the table. The digit "1" to the right of the decimal point indicates the independent

variable of the graph to be either geometric altitude or geopotential, while the digit "2" to the right of the decimal point indicates the independent variable of the graph to be latitude. Values of $Z_S - Z_R$ are not included in any of the figures.

TABLE 1A

GEOMETRIC ALTITUDE DIFFERENCES BETWEEN A SERIES OF GEOPOTENTIAL SURFACES AT A REFERENCE LATITUDE, AND THE SAME GEOPOTENTIAL SURFACES AT OTHER LATITUDES, INCLUDING THOSE OF THE US STANDARD ATMOSPHERE, ALL AS A FUNCTION OF GEOPOTENTIAL, 0 to 1,000 km²

GEOPOTENTIAL	GEOMETRIC ALTITUDE	LATITUDE φ (DEG)							
		0	15	30	45	60	75	90	
H _R (m ²)	Z _R (m)	Z _φ - Z _R	Z _S - Z _R						
0.	0.0	0.0	0.0	0.0	0.0	0.0	0.0	0.0	0.0
250.	250.0	0.7	0.6	0.3	0.0	-0.3	-0.6	-0.6	0.0
500.	500.0	1.3	1.2	0.7	0.0	-0.6	-1.1	-1.3	0.0
750.	750.0	2.0	1.8	1.0	0.0	-1.0	-1.7	-1.9	0.0
1000.	1000.1	2.7	2.3	1.4	0.1	-1.3	-2.2	-2.6	0.0
1250.	1250.2	3.4	2.9	1.7	0.1	-1.6	-2.8	-3.2	0.0
1500.	1500.3	4.0	3.5	2.1	0.1	-1.9	-3.4	-3.9	0.0
1750.	1750.4	4.7	4.1	2.4	0.1	-2.2	-3.9	-4.5	0.0
2000.	2000.6	5.4	4.7	2.7	0.1	-2.5	-4.5	-5.2	0.0
2250.	2250.7	6.1	5.3	3.1	0.1	-2.9	-5.0	-5.8	0.0
2500.	2500.9	6.7	5.8	3.4	0.1	-3.2	-5.6	-6.5	0.0
2750.	2751.1	7.4	6.4	3.8	0.1	-3.5	-6.2	-7.1	0.0
3000.	3001.4	8.1	7.0	4.1	0.2	-3.8	-6.7	-7.8	0.0
3250.	3251.6	8.8	7.6	4.5	0.2	-4.1	-7.3	-8.4	0.0
3500.	3501.9	9.4	8.2	4.8	0.2	-4.4	-7.8	-9.1	0.0
3750.	3752.2	10.1	8.8	5.1	0.2	-4.8	-8.4	-9.7	0.0
4000.	4002.5	10.8	9.4	5.5	0.2	-5.1	-9.0	-10.4	0.0
4250.	4252.8	11.4	9.9	5.8	0.2	-5.4	-9.5	-11.0	0.0
4500.	4503.1	12.1	10.5	6.2	0.2	-5.7	-10.1	-11.7	0.0
4750.	4753.5	12.8	11.1	6.5	0.2	-6.0	-10.6	-12.3	0.0
5000.	5003.9	13.5	11.7	6.9	0.3	-6.4	-11.2	-13.0	0.0
5250.	5254.3	14.2	12.3	7.2	0.3	-6.7	-11.8	-13.6	0.0
5500.	5504.7	14.8	12.9	7.6	0.3	-7.0	-12.3	-14.3	0.0
5750.	5755.2	15.5	13.5	7.9	0.3	-7.3	-12.9	-14.9	0.0
6000.	6005.6	16.2	14.1	8.2	0.3	-7.6	-13.4	-15.6	0.0
6250.	6256.1	16.9	14.6	8.6	0.3	-8.0	-14.0	-16.2	0.0
6500.	6506.6	17.5	15.2	8.9	0.3	-8.3	-14.6	-16.9	0.0
6750.	6757.1	18.2	15.8	9.3	0.3	-8.6	-15.1	-17.5	0.0
7000.	7007.7	18.9	16.4	9.6	0.4	-8.9	-15.7	-18.2	0.0
7250.	7258.2	19.6	17.0	10.0	0.4	-9.2	-16.3	-18.8	0.0
7500.	7508.8	20.2	17.6	10.3	0.4	-9.6	-16.8	-19.5	0.0
7750.	7759.4	20.9	18.2	10.7	0.4	-9.9	-17.4	-20.1	0.0
8000.	8010.0	21.6	18.8	11.0	0.4	-10.2	-17.9	-20.8	0.0
8250.	8260.7	22.3	19.3	11.3	0.4	-10.5	-18.5	-21.4	0.0
8500.	8511.3	22.9	19.9	11.7	0.4	-10.8	-19.1	-22.1	0.0
8750.	8762.0	23.6	20.5	12.0	0.4	-11.2	-19.6	-22.7	0.0
9000.	9012.7	24.3	21.1	12.4	0.5	-11.5	-20.2	-23.4	0.0
9250.	9263.4	25.0	21.7	12.7	0.5	-11.8	-20.8	-24.0	0.0
9500.	9514.2	25.7	22.3	13.1	0.5	-12.1	-21.3	-24.7	0.0
9750.	9764.9	26.3	22.9	13.4	0.5	-12.4	-21.9	-25.3	0.0

TABLE 1A CONTINUED

GEOPOTENTIAL	GEOMETRIC ALTITUDE	0	LATITUDE ϕ (DEG)						$Z_S - Z_R$
			15	30	45	60	75	90	
H_R (m')	Z_R (m)	$Z_\phi - Z_R$	$Z_\phi - Z_R$	$Z_\phi - Z_R$	$Z_\phi - Z_R$	$Z_\phi - Z_R$	$Z_\phi - Z_R$	$Z_\phi - Z_R$	$Z_S - Z_R$
10000.	10015.7	27.0	23.5	13.8	0.5	-12.8	-22.4	-26.0	0.0
10250.	10266.5	27.7	24.1	14.1	0.5	-13.1	-23.0	-26.7	0.0
10500.	10517.3	28.4	24.6	14.5	0.5	-13.4	-23.6	-27.3	0.0
10750.	10768.2	29.1	25.2	14.8	0.5	-13.7	-24.1	-28.0	0.0
11000.	11019.0	29.7	25.8	15.1	0.6	-14.0	-24.7	-28.6	0.0
11500.	11520.8	31.1	27.0	15.8	0.6	-14.7	-25.8	-29.9	0.0
12000.	12022.6	32.5	28.2	16.5	0.6	-15.3	-27.0	-31.2	0.0
12500.	12524.6	33.8	29.4	17.2	0.6	-16.0	-28.1	-32.5	0.0
13000.	13026.6	35.2	30.6	17.9	0.7	-16.6	-29.2	-33.9	0.0
13500.	13528.7	36.5	31.7	18.6	0.7	-17.3	-30.4	-35.2	0.0
14000.	14030.9	37.9	32.9	19.3	0.7	-17.9	-31.5	-36.5	0.0
14500.	14533.1	39.3	34.1	20.0	0.7	-18.5	-32.6	-37.8	0.0
15000.	15035.4	40.6	35.3	20.7	0.8	-19.2	-33.8	-39.1	0.0
15500.	15537.8	42.0	36.5	21.4	0.8	-19.8	-34.9	-40.4	0.0
16000.	16040.3	43.4	37.7	22.1	0.8	-20.5	-36.0	-41.7	0.0
16500.	16542.9	44.7	38.9	22.8	0.8	-21.1	-37.2	-43.0	0.0
17000.	17045.5	46.1	40.0	23.5	0.9	-21.8	-38.3	-44.4	0.0
17500.	17548.3	47.5	41.2	24.2	0.9	-22.4	-39.4	-45.7	0.0
18000.	18051.1	48.8	42.4	24.9	0.9	-23.1	-40.6	-47.0	0.0
18500.	18553.9	50.2	43.6	25.6	0.9	-23.7	-41.7	-48.3	0.0
19000.	19056.9	51.6	44.8	26.3	1.0	-24.3	-42.8	-49.6	0.0
19500.	19560.0	52.9	46.0	27.0	1.0	-25.0	-44.0	-50.9	0.0
20000.	20063.1	54.3	47.2	27.7	1.0	-25.6	-45.1	-52.3	0.0
20500.	20566.3	55.7	48.4	28.4	1.0	-26.3	-46.3	-53.6	0.0
21000.	21069.6	57.1	49.6	29.1	1.1	-26.9	-47.4	-54.9	0.0
21500.	21572.9	58.4	50.8	29.8	1.1	-27.6	-48.5	-56.2	0.0
22000.	22076.4	59.8	51.9	30.5	1.1	-28.2	-49.7	-57.5	0.0
22500.	22579.9	61.2	53.1	31.2	1.1	-28.9	-50.8	-58.9	0.0
23000.	23083.5	62.6	54.3	31.9	1.2	-29.5	-52.0	-60.2	0.0
23500.	23587.1	63.9	55.5	32.6	1.2	-30.2	-53.1	-61.5	0.0
24000.	24090.9	65.3	56.7	33.3	1.2	-30.8	-54.3	-62.8	0.0
24500.	24594.7	66.7	57.9	34.0	1.2	-31.5	-55.4	-64.2	0.0
25000.	25098.7	68.1	59.1	34.7	1.3	-32.1	-56.6	-65.5	0.0
25500.	25602.7	69.5	60.3	35.4	1.3	-32.8	-57.7	-66.8	0.0
26000.	26106.7	70.8	61.5	36.1	1.3	-33.4	-58.8	-68.2	0.0
26500.	26610.9	72.2	62.7	36.8	1.3	-34.1	-60.0	-69.5	0.0
27000.	27115.1	73.6	63.9	37.5	1.4	-34.7	-61.1	-70.8	0.0
27500.	27619.4	75.0	65.1	38.2	1.4	-35.4	-62.3	-72.1	0.0
28000.	28123.8	76.4	66.3	38.9	1.4	-36.0	-63.4	-73.5	0.0
28500.	28628.3	77.7	67.5	39.6	1.4	-36.7	-64.6	-74.8	0.0
29000.	29132.9	79.1	68.7	40.3	1.5	-37.4	-65.7	-76.1	0.0
29500.	29637.5	80.5	69.9	41.0	1.5	-38.0	-66.9	-77.5	0.0

TABLE 1A CONTINUED

GEOPOTENTIAL ALTITUDE	GEOMETRIC ALTITUDE	LATITUDE ϕ (DEG)							
		0	15	30	45	60	75	90	
H (m')	Z_R (m)	Z_phi - Z_R	Z_phi - Z_R	Z_phi - Z_R	Z_phi - Z_R	Z_phi - Z_R	Z_phi - Z_R	Z_phi - Z_R	Z_phi - Z_R
30000.	30142.2	81.9	71.1	41.7	1.5	-38.7	-68.0	-78.8	0.0
30500.	30647.0	83.3	72.3	42.4	1.6	-39.3	-69.2	-80.1	0.0
31000.	31151.9	84.7	73.5	43.1	1.6	-40.0	-70.3	-81.5	0.0
31500.	31656.8	86.1	74.7	43.8	1.6	-40.6	-71.5	-82.8	0.0
32000.	32161.9	87.5	76.0	44.5	1.6	-41.3	-72.7	-84.1	0.0
33000.	33172.2	90.2	78.4	46.0	1.7	-42.6	-75.0	-86.8	0.0
34000.	34182.8	93.0	80.8	47.4	1.7	-43.9	-77.3	-89.5	0.0
35000.	35193.7	95.8	83.2	48.8	1.8	-45.2	-79.6	-92.2	0.0
36000.	36205.0	98.6	85.6	50.2	1.8	-46.5	-81.9	-94.8	0.0
37000.	37216.6	101.4	88.0	51.6	1.9	-47.9	-84.2	-97.5	0.0
38000.	38228.5	104.2	90.5	53.1	1.9	-49.2	-86.5	-100.2	0.0
39000.	39240.7	107.0	92.9	54.5	2.0	-50.5	-88.9	-102.9	0.0
40000.	40253.2	109.8	95.3	55.9	2.0	-51.8	-91.2	-105.6	0.0
41000.	41266.1	112.6	97.8	57.3	2.1	-53.1	-93.5	-108.3	0.0
42000.	42279.3	115.4	100.2	58.8	2.1	-54.5	-95.8	-111.0	0.0
43000.	43292.8	118.2	102.6	60.2	2.2	-55.8	-98.2	-113.7	0.0
44000.	44306.6	121.0	105.1	61.6	2.3	-57.1	-100.5	-116.4	0.0
45000.	45320.8	123.8	107.5	63.1	2.3	-58.4	-102.9	-119.1	0.0
46000.	46335.3	126.6	110.0	64.5	2.4	-59.8	-105.2	-121.8	0.1
47000.	47350.0	129.4	112.4	65.9	2.4	-61.1	-107.5	-124.5	0.1
48000.	48365.2	132.3	114.9	67.4	2.5	-62.4	-109.9	-127.3	0.1
49000.	49380.6	135.1	117.3	68.8	2.5	-63.8	-112.2	-130.0	0.1
50000.	50396.3	137.9	119.8	70.3	2.6	-65.1	-114.6	-132.7	0.1
51000.	51412.4	140.8	122.2	71.7	2.6	-66.4	-116.9	-135.4	0.1
52000.	52428.8	143.6	124.7	73.1	2.7	-67.8	-119.3	-138.1	0.1
53000.	53445.6	146.4	127.2	74.6	2.7	-69.1	-121.6	-140.9	0.1
54000.	54462.6	149.3	129.6	76.0	2.8	-70.5	-124.0	-143.6	0.1
55000.	55480.0	152.1	132.1	77.5	2.8	-71.8	-126.4	-146.3	0.1
56000.	56497.7	155.0	134.6	78.9	2.9	-73.1	-128.7	-149.1	0.1
57000.	57515.7	157.8	137.1	80.4	2.9	-74.5	-131.1	-151.8	0.1
58000.	58534.0	160.7	139.5	81.8	3.0	-75.8	-133.5	-154.6	0.1
59000.	59552.7	163.5	142.0	83.3	3.0	-77.2	-135.8	-157.3	0.1
60000.	60571.7	166.4	144.5	84.7	3.1	-78.5	-138.2	-160.1	0.1
61000.	61591.0	169.2	147.0	86.2	3.1	-79.9	-140.6	-162.8	0.1
62000.	62610.6	172.1	149.5	87.7	3.2	-81.2	-143.0	-165.6	0.1
63000.	63630.6	175.0	151.9	89.1	3.3	-82.6	-145.3	-168.3	0.1
64000.	64650.9	177.8	154.4	90.6	3.3	-83.9	-147.7	-171.1	0.1
65000.	65671.5	180.7	156.9	92.0	3.4	-85.3	-150.1	-173.8	0.1
66000.	66692.4	183.6	159.4	93.5	3.4	-86.6	-152.5	-176.6	0.1
67000.	67713.6	186.5	161.9	95.0	3.5	-88.0	-154.9	-179.4	0.1
68000.	68735.2	189.3	164.4	96.4	3.5	-89.4	-157.3	-182.1	0.1
69000.	69757.1	192.2	166.9	97.9	3.6	-90.7	-159.7	-184.9	0.1

TABLE 1A CONTINUED

GEOPOTENTIAL	GEOMETRIC ALTITUDE	LATITUDE ϕ (DEG)							
		0	15	30	45	60	75	90	
H_R (m')	Z_R (m)	$Z_\phi - Z_R$	$Z_\phi - Z_R$	$Z_\phi - Z_R$	$Z_\phi - Z_R$	$Z_\phi - Z_R$	$Z_\phi - Z_R$	$Z_\phi - Z_R$	$Z_S - Z_R$
70000.	70779.4	195.1	169.4	99.4	3.6	-92.1	-162.1	-187.7	0.1
71000.	71801.9	198.0	172.0	100.9	3.7	-93.5	-164.5	-190.5	0.1
72000.	72824.8	200.9	174.5	102.3	3.7	-94.8	-166.9	-193.3	0.1
73000.	73848.0	203.8	177.0	103.8	3.8	-96.2	-169.3	-196.0	0.1
74000.	74871.5	206.7	179.5	105.3	3.8	-97.5	-171.7	-198.8	0.1
75000.	75895.4	209.6	182.0	106.8	3.9	-98.9	-174.1	-201.6	0.1
76000.	76919.6	212.5	184.5	108.2	3.9	-100.3	-176.5	-204.4	0.2
77000.	77944.1	215.4	187.1	109.7	4.0	-101.7	-178.9	-207.2	0.2
78000.	78968.9	218.3	189.6	111.2	4.1	-103.0	-181.3	-210.0	0.2
79000.	79994.1	221.2	192.1	112.7	4.1	-104.4	-183.7	-212.8	0.2
80000.	81019.6	224.1	194.7	114.2	4.2	-105.8	-186.2	-215.6	0.2
81000.	82045.4	227.1	197.2	115.7	4.2	-107.2	-188.6	-218.4	0.2
82000.	83071.5	230.0	199.7	117.2	4.3	-108.5	-191.0	-221.2	0.2
83000.	84098.0	232.9	202.3	118.6	4.3	-109.9	-193.4	-224.0	0.2
84000.	85124.8	235.8	204.8	120.1	4.4	-111.3	-195.9	-226.9	0.2
85000.	86151.9	238.8	207.4	121.6	4.4	-112.7	-198.3	-229.7	0.2
86000.	87179.4	241.7	209.9	123.1	4.5	-114.1	-200.8	-232.5	0.2
87000.	88207.2	244.6	212.5	124.6	4.5	-115.5	-203.2	-235.3	0.2
88000.	89235.3	247.6	215.0	126.1	4.6	-116.8	-205.6	-238.1	0.2
89000.	90263.7	250.5	217.6	127.6	4.7	-118.2	-208.1	-241.0	0.2
90000.	91292.5	253.5	220.1	129.1	4.7	-119.6	-210.5	-243.8	0.2
92000.	93351.0	259.4	225.2	132.1	4.8	-122.4	-215.4	-249.5	0.2
94000.	95410.8	265.3	230.4	135.1	4.9	-125.2	-220.3	-255.2	0.3
96000.	97472.0	271.2	235.5	138.1	5.0	-128.0	-225.3	-260.9	0.3
98000.	99534.4	277.1	240.7	141.2	5.2	-130.8	-230.2	-266.6	0.3
100000.	101598.2	283.1	245.9	144.2	5.3	-133.6	-235.1	-272.3	0.3
102000.	103663.3	289.1	251.0	147.2	5.4	-136.4	-240.1	-278.0	0.3
104000.	105729.7	295.0	256.2	150.3	5.5	-139.2	-245.0	-283.8	0.3
106000.	107797.5	301.0	261.4	153.3	5.6	-142.1	-250.0	-289.5	0.3
108000.	109866.6	307.0	266.6	156.4	5.7	-144.9	-255.0	-295.3	0.4
110000.	111937.0	313.0	271.8	159.4	5.8	-147.7	-260.0	-301.1	0.4
112000.	114008.7	319.0	277.1	162.5	5.9	-150.6	-265.0	-306.9	0.4
114000.	116081.7	325.1	282.3	165.6	6.1	-153.4	-270.0	-312.7	0.4
116000.	118156.1	331.1	287.6	168.7	6.2	-156.3	-275.0	-318.5	0.4
118000.	120231.8	337.2	292.8	171.7	6.3	-159.1	-280.0	-324.3	0.4
120000.	122308.8	343.2	298.1	174.8	6.4	-162.0	-285.1	-330.2	0.5
125000.	127507.3	358.5	311.3	182.6	6.7	-169.2	-297.7	-344.8	0.5
130000.	132714.0	373.8	324.6	190.4	7.0	-176.4	-310.4	-359.5	0.6
135000.	137929.2	389.2	338.0	198.2	7.2	-183.7	-323.2	-374.3	0.6
140000.	143152.7	404.6	351.4	206.1	7.5	-191.0	-336.1	-389.2	0.7
145000.	148384.7	420.2	364.9	214.0	7.8	-198.3	-348.9	-404.1	0.7
150000.	153625.0	435.8	378.5	222.0	8.1	-205.7	-361.9	-419.1	0.8
155000.	158873.9	451.5	392.1	230.0	8.4	-213.1	-374.9	-434.2	0.9
160000.	164131.1	467.3	405.8	238.0	8.7	-220.5	-388.0	-449.4	1.0
165000.	169396.9	483.1	419.6	246.1	9.0	-228.0	-401.2	-464.6	1.0

TABLE 1A CONTINUED

GEOPO- TENTIAL	GEOMET. ALTITUDE	LATITUDE ϕ (DEG)							
		0	15	30	45	60	75	90	
H _R (km')	Z _R (m)	Z _φ -Z _R	Z _S -Z _R						
170.	174671.2	499.1	433.4	254.2	9.3	-235.5	-414.4	-479.9	1.1
175.	179954.0	515.1	447.3	262.4	9.6	-243.0	-427.7	-495.3	1.2
180.	185245.4	531.2	461.3	270.5	9.9	-250.7	-441.1	-510.8	1.3
185.	190545.4	547.4	475.3	278.8	10.2	-258.3	-454.5	-526.3	1.4
190.	195853.9	563.6	489.4	287.1	10.5	-265.9	-468.0	-542.0	1.5
195.	201171.1	579.9	503.6	295.4	10.8	-273.6	-481.5	-557.7	1.6
200.	206496.9	596.4	517.9	303.8	11.1	-281.4	-495.2	-573.4	1.7
205.	211831.3	612.9	532.2	312.2	11.4	-289.2	-508.9	-589.3	1.8
210.	217174.5	629.4	546.6	320.6	11.7	-297.0	-522.6	-605.3	2.0
215.	222526.3	646.1	561.1	329.1	12.0	-304.9	-536.4	-621.3	2.1
220.	227886.8	662.8	575.6	337.6	12.3	-312.7	-550.4	-637.4	2.2
225.	233256.1	679.7	590.3	346.2	12.7	-320.7	-564.3	-653.5	2.4
230.	238634.2	696.6	604.9	354.8	13.0	-328.7	-578.3	-669.8	2.5
235.	244021.0	713.6	619.7	363.5	13.3	-336.7	-592.5	-686.1	2.7
240.	249416.7	730.7	634.5	372.1	13.6	-344.7	-606.6	-702.5	2.8
245.	254821.2	747.8	649.4	380.9	13.9	-352.8	-620.9	-719.0	3.0
250.	260234.5	765.1	664.4	389.7	14.2	-361.0	-635.2	-735.6	3.2
255.	265656.7	782.4	679.5	398.5	14.6	-369.1	-649.5	-752.2	3.4
260.	271087.8	799.8	694.6	407.4	14.9	-377.3	-664.0	-769.0	3.5
265.	276527.8	817.3	709.8	416.3	15.2	-385.6	-678.6	-785.8	3.7
270.	281976.7	835.0	725.1	425.3	15.5	-393.9	-693.1	-802.7	3.9
275.	287434.7	852.6	740.4	434.2	15.8	-402.2	-707.8	-819.7	4.2
280.	292901.5	870.4	755.9	443.3	16.2	-410.6	-722.5	-836.7	4.4
285.	298377.4	888.2	771.4	452.4	16.5	-419.0	-737.4	-853.9	4.6
290.	303862.4	906.2	786.9	461.5	16.8	-427.5	-752.2	-871.2	4.8
295.	309356.3	924.2	802.6	470.7	17.2	-436.0	-767.2	-888.5	5.1
300.	314859.4	942.3	818.3	479.9	17.5	-444.5	-782.2	-905.9	5.3
310.	325892.7	978.8	850.1	498.5	18.2	-461.7	-812.5	-940.9	5.9
320.	336962.7	1015.7	882.0	517.3	18.9	-479.1	-843.1	-976.4	6.4
330.	348069.4	1052.9	914.4	536.2	19.6	-496.7	-873.9	-1012.1	7.1
340.	359212.9	1090.5	947.0	555.4	20.3	-514.4	-905.1	-1048.2	7.7
350.	370393.6	1128.5	980.0	574.7	21.0	-532.3	-936.6	-1084.6	8.4
360.	381611.6	1166.8	1013.2	594.2	21.7	-550.4	-968.4	-1121.5	9.1
370.	392867.1	1205.5	1046.9	613.9	22.4	-568.6	-1000.5	-1158.6	9.9
380.	404160.2	1244.6	1080.8	633.8	23.1	-587.0	-1032.8	-1196.1	10.8
390.	415491.1	1284.0	1115.1	653.9	23.9	-605.6	-1065.5	-1234.0	11.7
400.	426860.2	1323.8	1149.6	674.2	24.6	-624.4	-1098.6	-1272.2	12.6
410.	438267.4	1364.1	1184.6	694.6	25.3	-643.3	-1131.9	-1310.8	13.6
420.	449713.1	1404.7	1219.8	715.3	26.1	-662.4	-1165.6	-1349.8	14.7
430.	461197.4	1445.7	1255.4	736.2	26.9	-681.8	-1199.5	-1389.1	15.8
440.	472720.5	1487.1	1291.4	757.3	27.6	-701.3	-1233.9	-1428.9	17.0
450.	484282.7	1528.9	1327.7	778.6	28.4	-721.0	-1268.5	-1469.0	18.2
460.	495884.0	1571.1	1364.3	800.1	29.2	-740.8	-1303.5	-1509.5	19.5
470.	507524.8	1613.6	1401.3	821.7	30.0	-761.0	-1338.9	-1550.4	20.9
480.	519205.2	1656.7	1438.6	843.6	30.8	-781.2	-1374.5	-1591.7	22.4
490.	530925.4	1700.1	1476.4	865.7	31.6	-801.6	-1410.4	-1633.4	23.9

TABLE 1A CONCLUDED

GEOPO- TENTIAL	GEOMET. ALTITUDE	LATITUDE ϕ (DEG)							
		0	15	30	45	60	75	90	
H_R (km)	Z_R (m)	$Z_\phi - Z_R$	$Z_\phi - Z_R$	$Z_\phi - Z_R$	$Z_\phi - Z_R$	$Z_\phi - Z_R$	$Z_\phi - Z_R$	$Z_\phi - Z_R$	$Z_S - Z_R$
500.	542685.6	1744.0	1514.4	888.1	32.4	-822.3	-1446.8	-1675.4	25.5
510.	554486.1	1788.2	1552.8	910.5	33.2	-843.2	-1483.5	-1717.9	27.2
520.	566327.0	1832.9	1591.7	933.3	34.1	-864.2	-1520.5	-1760.8	29.0
530.	578208.5	1878.0	1630.8	956.3	34.9	-885.4	-1557.8	-1804.0	30.9
540.	590130.9	1923.6	1670.4	979.5	35.8	-906.9	-1595.6	-1847.7	32.9
550.	602094.4	1969.5	1710.3	1002.9	36.6	-928.6	-1633.7	-1891.9	34.9
560.	614099.1	2015.9	1750.6	1026.5	37.5	-950.4	-1672.1	-1936.4	37.1
570.	626145.3	2062.8	1791.3	1050.4	38.3	-972.5	-1710.9	-1981.3	39.4
580.	638233.3	2110.0	1832.3	1074.4	39.2	-994.8	-1750.1	-2026.7	41.7
590.	650363.1	2157.8	1873.8	1098.7	40.1	-1017.3	-1789.7	-2072.5	44.2
600.	662535.1	2206.0	1915.7	1123.2	41.0	-1040.0	-1829.6	-2118.7	46.8
610.	674749.4	2254.7	1957.9	1148.0	41.9	-1062.8	-1869.9	-2165.3	49.5
620.	687006.4	2303.8	2000.5	1173.0	42.8	-1086.0	-1910.6	-2212.5	52.4
630.	699306.1	2353.4	2043.6	1198.2	43.7	-1109.3	-1951.6	-2260.0	55.4
640.	711648.8	2403.4	2087.1	1223.7	44.7	-1132.9	-1993.0	-2308.0	
650.	724034.8	2454.0	2131.0	1249.5	45.6	-1156.6	-2034.9	-2356.4	
660.	736464.4	2504.9	2175.2	1275.4	46.5	-1180.7	-2077.1	-2405.3	
670.	748937.6	2556.4	2219.9	1301.6	47.5	-1204.9	-2119.8	-2454.7	
680.	761454.8	2608.4	2265.0	1328.0	48.5	-1229.4	-2162.7	-2504.5	
690.	774016.2	2660.8	2310.5	1354.7	49.4	-1254.1	-2206.2	-2554.8	
700.	786621.9	2713.8	2356.5	1381.7	50.4	-1279.0	-2250.0	-2605.5	
710.	799272.3	2767.2	2403.0	1408.9	51.4	-1304.2	-2294.3	-2656.7	
720.	811967.5	2821.2	2449.8	1436.4	52.4	-1329.5	-2338.9	-2708.4	
730.	824708.0	2875.6	2497.0	1464.0	53.4	-1355.2	-2384.0	-2760.7	
740.	837493.8	2930.6	2544.8	1492.0	54.4	-1381.1	-2429.5	-2813.3	
750.	850325.1	2986.1	2593.0	1520.3	55.5	-1407.2	-2475.4	-2866.4	
760.	863202.4	3042.1	2641.6	1548.8	56.5	-1433.5	-2521.7	-2920.1	
770.	876125.8	3098.6	2690.6	1577.5	57.5	-1460.2	-2568.6	-2974.3	
780.	889095.4	3155.6	2740.2	1606.5	58.6	-1487.0	-2615.7	-3028.9	
790.	902111.7	3213.2	2790.2	1635.8	59.7	-1514.1	-2663.3	-3084.1	
800.	915174.8	3271.4	2840.7	1665.4	60.8	-1541.4	-2711.4	-3139.7	
820.	941442.7	3389.2	2943.0	1725.4	62.9	-1596.9	-2809.0	-3252.7	
840.	967901.0	3509.2	3047.2	1786.4	65.1	-1653.4	-2908.4	-3367.8	
860.	994551.8	3631.6	3153.5	1848.7	67.4	-1710.9	-3009.5	-3484.9	
880.	1021397.3	3756.2	3261.6	1912.1	69.7	-1769.6	-3112.6	-3604.3	
900.	1048439.5	3883.2	3371.9	1976.7	72.1	-1829.3	-3217.6	-3725.8	
920.	1075680.8	4012.4	3484.0	2042.4	74.4	-1890.2	-3324.6	-3849.7	
940.	1103123.1	4144.2	3598.5	2109.5	76.9	-1952.0	-3433.4	-3975.7	
960.	1130768.9	4278.4	3715.0	2177.8	79.4	-2015.2	-3544.4	-4104.2	
980.	1158620.3	4415.1	3833.6	2247.3	82.0	-2079.4	-3657.4	-4234.9	
1000.	1186679.8	4554.2	3954.4	2318.1	84.5	-2144.9	-3772.5	-4368.3	

TABLE 1B

GEOMETRIC ALTITUDE DIFFERENCES BETWEEN A SERIES OF GEOPOTENTIAL SURFACES AT A REFERENCE LATITUDE, AND THE SAME GEOPOTENTIAL SURFACES AT OTHER LATITUDES, ALL AS A FUNCTION OF GEOPOTENTIAL, 1,000 to 3,900 km²

GEOPOTENTIAL TEN.	GEOMETRIC ALT.	LATITUDE φ (DEG)						
		0	15	30	45	60	75	90
H_R (km ²)	Z_R (km)	$Z_\phi - Z_R$	$Z_\phi - Z_R$	$Z_\phi - Z_R$	$Z_\phi - Z_R$	$Z_\phi - Z_R$	$Z_\phi - Z_R$	$Z_\phi - Z_R$
1000.	1186.68	4.55	3.95	2.32	.08	-2.14	-3.77	-4.37
1020.	1214.95	4.70	4.08	2.39	.09	-2.21	-3.89	-4.50
1040.	1243.43	4.84	4.20	2.46	.09	-2.28	-4.01	-4.64
1060.	1272.13	4.99	4.33	2.54	.09	-2.35	-4.13	-4.78
1080.	1301.04	5.14	4.46	2.61	.10	-2.42	-4.25	-4.93
1100.	1330.18	5.29	4.59	2.69	.10	-2.49	-4.38	-5.07
1120.	1359.54	5.45	4.73	2.77	.10	-2.56	-4.51	-5.22
1140.	1389.12	5.60	4.87	2.85	.10	-2.64	-4.64	-5.37
1160.	1418.93	5.77	5.01	2.93	.11	-2.71	-4.77	-5.53
1180.	1448.97	5.93	5.15	3.02	.11	-2.79	-4.91	-5.68
1200.	1479.24	6.10	5.29	3.10	.11	-2.87	-5.05	-5.84
1220.	1509.75	6.27	5.44	3.19	.12	-2.95	-5.19	-6.01
1240.	1540.50	6.44	5.59	3.28	.12	-3.03	-5.33	-6.17
1260.	1571.49	6.62	5.75	3.37	.12	-3.11	-5.48	-6.34
1280.	1602.73	6.80	5.90	3.46	.13	-3.20	-5.63	-6.51
1300.	1634.21	6.98	6.06	3.55	.13	-3.29	-5.78	-6.69
1320.	1665.94	7.17	6.22	3.65	.13	-3.37	-5.93	-6.87
1340.	1697.92	7.36	6.39	3.74	.14	-3.46	-6.09	-7.05
1360.	1730.16	7.55	6.56	3.84	.14	-3.55	-6.25	-7.23
1380.	1762.66	7.75	6.73	3.94	.14	-3.65	-6.41	-7.42
1400.	1795.42	7.95	6.90	4.05	.15	-3.74	-6.58	-7.62
1420.	1828.45	8.16	7.08	4.15	.15	-3.84	-6.75	-7.81
1440.	1861.74	8.36	7.26	4.26	.16	-3.94	-6.92	-8.01
1460.	1895.31	8.58	7.45	4.36	.16	-4.03	-7.09	-8.21
1480.	1929.15	8.79	7.64	4.47	.16	-4.14	-7.27	-8.42
1500.	1963.27	9.01	7.83	4.59	.17	-4.24	-7.45	-8.63
1520.	1997.67	9.24	8.02	4.70	.17	-4.35	-7.64	-8.85
1540.	2032.36	9.47	8.22	4.82	.18	-4.45	-7.83	-9.06
1560.	2067.34	9.70	8.42	4.94	.18	-4.56	-8.02	-9.29
1580.	2102.61	9.94	8.63	5.06	.18	-4.67	-8.22	-9.51
1600.	2138.18	10.18	8.84	5.18	.19	-4.79	-8.42	-9.74
1620.	2174.05	10.43	9.05	5.30	.19	-4.90	-8.62	-9.98
1640.	2210.22	10.68	9.27	5.43	.20	-5.02	-8.83	-10.22
1660.	2246.70	10.93	9.49	5.56	.20	-5.14	-9.04	-10.46
1680.	2283.49	11.20	9.72	5.70	.21	-5.26	-9.25	-10.71
1700.	2320.60	11.46	9.95	5.83	.21	-5.39	-9.47	-10.96
1720.	2358.03	11.73	10.19	5.97	.22	-5.51	-9.69	-11.22
1740.	2395.78	12.01	10.42	6.11	.22	-5.64	-9.92	-11.49
1760.	2433.86	12.29	10.67	6.25	.23	-5.78	-10.15	-11.75
1780.	2472.28	12.58	10.92	6.40	.23	-5.91	-10.39	-12.03

TABLE 1B CONTINUED

GEOPO- TEN.	GEOMET. ALT.	0	15	30	45	LATITUDE	ϕ (DEG)	75	90
						60			
1800.	2511.03	12.87	11.17	6.54	.24	-6.05	-10.63	-12.30	
1820.	2550.12	13.16	11.43	6.70	.24	-6.19	-10.87	-12.59	
1840.	2589.56	13.47	11.69	6.85	.25	-6.33	-11.12	-12.88	
1860.	2629.35	13.78	11.96	7.01	.26	-6.47	-11.38	-13.17	
1880.	2669.50	14.09	12.23	7.17	.26	-6.62	-11.63	-13.47	
1900.	2710.00	14.41	12.51	7.33	.27	-6.77	-11.90	-13.77	
1920.	2750.88	14.74	12.79	7.49	.27	-6.92	-12.17	-14.09	
1940.	2792.12	15.07	13.08	7.66	.28	-7.08	-12.44	-14.40	
1960.	2833.73	15.41	13.38	7.84	.29	-7.24	-12.72	-14.73	
1980.	2875.73	15.76	13.68	8.01	.29	-7.40	-13.00	-15.05	
2000.	2918.11	16.11	13.98	8.19	.30	-7.56	-13.29	-15.39	
2020.	2960.89	16.47	14.30	8.37	.31	-7.73	-13.59	-15.73	
2040.	3004.06	16.83	14.61	8.56	.31	-7.90	-13.89	-16.08	
2060.	3047.63	17.21	14.94	8.75	.32	-8.08	-14.20	-16.44	
2080.	3091.61	17.59	15.27	8.94	.33	-8.26	-14.51	-16.80	
2100.	3136.00	17.98	15.60	9.14	.33	-8.44	-14.83	-17.17	
2120.	3180.81	18.37	15.95	9.34	.34	-8.62	-15.15	-17.54	
2140.	3226.05	18.78	16.30	9.55	.35	-8.81	-15.49	-17.93	
2160.	3271.71	19.19	16.66	9.75	.36	-9.01	-15.82	-18.32	
2180.	3317.82	19.61	17.02	9.97	.36	-9.20	-16.17	-18.72	
2200.	3364.37	20.03	17.39	10.18	.37	-9.40	-16.52	-19.12	
2220.	3411.37	20.47	17.77	10.41	.38	-9.61	-16.88	-19.54	
2240.	3458.82	20.91	18.15	10.63	.39	-9.81	-17.24	-19.96	
2260.	3506.74	21.4	18.5	10.9	.40	-10.0	-17.6	-20.4	
2280.	3555.13	22.8	18.9	11.1	.40	-10.2	-18.0	-20.8	
2300.	3603.99	22.3	19.4	11.3	.41	-10.5	-18.3	-21.3	
2320.	3653.34	22.8	19.8	11.6	.42	-10.7	-18.7	-21.7	
2340.	3703.19	23.3	20.2	11.8	.43	-10.9	-19.1	-22.2	
2360.	3753.53	23.8	20.6	12.1	.44	-11.2	-19.5	-23.7	
2380.	3804.37	24.3	21.1	12.3	.45	-11.4	-19.9	-23.2	
2400.	3855.73	24.8	21.5	12.6	.46	-11.6	-20.2	-23.6	
2420.	3907.62	25.3	22.0	12.8	.47	-11.9	-20.7	-24.2	
2440.	3960.03	25.9	22.5	13.2	.48	-12.1	-21.1	-24.7	
2460.	4012.98	26.4	23.9	13.4	.49	-12.4	-21.5	-25.2	
2480.	4066.48	27.0	23.4	13.7	.50	-12.7	-22.0	-25.7	
2500.	4120.53	27.6	23.9	14.0	.51	-12.9	-22.5	-26.3	
2520.	4175.14	28.2	24.4	14.3	.52	-13.2	-23.0	-26.8	
2540.	4230.33	28.7	25.0	14.6	.53	-13.5	-23.6	-27.4	
2560.	4286.10	29.4	25.5	14.9	.54	-13.8	-24.1	-28.0	
2580.	4342.46	30.0	26.0	15.2	.55	-14.1	-24.6	-28.6	

TABLE 1B CONTINUED

GEOPOTENTIAL TEN.	GEOMETRIC ALT.	0	15	30	45	60	LATITUDE ϕ (DEG)	
							Z _φ - Z _R	Z _φ - Z _R
H _R (km')	Z _R (km)	Z _φ - Z _R						
2600.	4399.4	31.	27.	16.	.6	-14.	-25.	-29.
2620.	4457.0	31.	27.	16.	.6	-15.	-26.	-30.
2640.	4515.2	32.	28.	16.	.6	-15.	-26.	-30.
2660.	4574.0	33.	28.	17.	.6	-15.	-27.	-31.
2680.	4633.5	33.	29.	17.	.6	-16.	-27.	-32.
2700.	4693.6	34.	30.	17.	.6	-16.	-28.	-32.
2720.	4754.3	35.	30.	18.	.6	-16.	-29.	-33.
2740.	4815.8	35.	31.	18.	.7	-17.	-29.	-34.
2760.	4877.9	36.	31.	18.	.7	-17.	-30.	-34.
2780.	4940.7	37.	32.	19.	.7	-17.	-30.	-35.
2800.	5004.2	38.	33.	19.	.7	-18.	-31.	-36.
2820.	5068.5	39.	34.	20.	.7	-18.	-32.	-37.
2840.	5133.5	39.	34.	20.	.7	-18.	-32.	-37.
2860.	5199.2	40.	35.	20.	.7	-19.	-33.	-38.
2880.	5265.7	41.	36.	21.	.8	-19.	-34.	-39.
2900.	5332.9	42.	36.	21.	.8	-20.	-35.	-40.
2920.	5400.9	43.	37.	22.	.8	-20.	-35.	-41.
2940.	5469.8	44.	38.	22.	.8	-20.	-36.	-42.
2960.	5539.4	45.	39.	23.	.8	-21.	-37.	-43.
2980.	5609.9	46.	40.	23.	.8	-21.	-38.	-43.
3000.	5681.2	47.	41.	24.	.9	-22.	-38.	-44.
3020.	5753.3	48.	41.	24.	.9	-22.	-39.	-45.
3040.	5826.3	49.	42.	25.	.9	-23.	-40.	-46.
3060.	5900.2	50.	43.	25.	.9	-23.	-41.	-47.
3080.	5975.0	51.	44.	26.	.9	-24.	-42.	-48.
3100.	6050.8	52.	45.	26.	1.0	-24.	-43.	-49.
3120.	6127.4	53.	46.	27.	1.0	-25.	-43.	-50.
3140.	6205.1	54.	47.	27.	1.0	-25.	-44.	-51.
3160.	6283.7	55.	48.	28.	1.0	-26.	-45.	-53.
3180.	6363.2	57.	49.	29.	1.0	-26.	-46.	-54.
3200.	6443.8	58.	50.	29.	1.1	-27.	-47.	-55.
3220.	6525.4	59.	51.	30.	1.1	-28.	-48.	-56.
3240.	6608.1	60.	52.	31.	1.1	-28.	-49.	-57.
3260.	6691.8	62.	53.	31.	1.1	-29.	-50.	-58.
3280.	6776.7	63.	55.	32.	1.2	-29.	-52.	-60.
3300.	6862.6	64.	56.	33.	1.2	-30.	-53.	-61.
3320.	6949.7	66.	57.	33.	1.2	-31.	-54.	-62.
3340.	7037.9	67.	58.	34.	1.2	-31.	-55.	-64.
3360.	7127.3	69.	60.	35.	1.3	-32.	-56.	-65.
3380.	7217.9	70.	61.	36.	1.3	-33.	-57.	-66.

TABLE 1B CONCLUDED

GEOPOTENTIAL TEN.	GEOMETRIC ALT.	0	LATITUDE ϕ (DEG)					
			15	30	45	60	75	90
H_R (km')	Z_R (km)	$Z_\phi - Z_R$	$Z_\phi - Z_R$	$Z_\phi - Z_R$	$Z_\phi - Z_R$	$Z_\phi - Z_R$	$Z_\phi - Z_R$	$Z_\phi - Z_R$
3400.	7309.7	72.	62.	36.	1.3	-33.	-59.	-68.
3420.	7402.7	73.	64.	37.	1.4	-34.	-60.	-69.
3440.	7497.1	75.	65.	38.	1.4	-35.	-61.	-71.
3460.	7592.7	77.	66.	39.	1.4	-36.	-63.	-73.
3480.	7689.7	78.	68.	40.	1.4	-37.	-64.	-74.
3500.	7788.1	80.	69.	41.	1.5	-37.	-65.	-76.
3520.	7887.8	82.	71.	42.	1.5	-38.	-67.	-77.
3540.	7988.9	84.	73.	42.	1.5	-39.	-68.	-79.
3560.	8091.5	86.	74.	43.	1.6	-40.	-70.	-81.
3580.	8195.6	88.	76.	44.	1.6	-41.	-72.	-83.
3600.	8301.2	90.	78.	45.	1.6	-42.	-73.	-85.
3620.	8408.3	92.	79.	46.	1.7	-43.	-75.	-87.
3640.	8517.0	94.	81.	47.	1.7	-44.	-76.	-88.
3660.	8627.3	96.	83.	49.	1.8	-45.	-78.	-91.
3680.	8739.2	98.	85.	50.	1.8	-46.	-80.	-93.
3700.	8852.9	100.	87.	51.	1.8	-47.	-82.	-95.
3720.	8968.2	103.	89.	52.	1.9	-48.	-84.	-97.
3740.	9085.4	105.	91.	53.	1.9	-49.	-86.	-99.
3760.	9204.3	107.	93.	54.	2.0	-50.	-88.	-101.
3780.	9325.1	110.	95.	56.	2.0	-51.	-90.	-104.
3800.	9447.8	113.	98.	57.	2.1	-52.	-92.	-106.
3820.	9572.4	115.	100.	58.	2.1	-54.	-94.	-109.
3840.	9698.9	118.	102.	60.	2.2	-55.	-96.	-111.
3860.	9827.6	121.	105.	61.	2.2	-56.	-98.	-114.
3880.	9958.2	124.	107.	63.	2.3	-57.	-101.	-116.
3900.	10091.1	127.	110.	64.	2.3	-59.	-103.	-119.

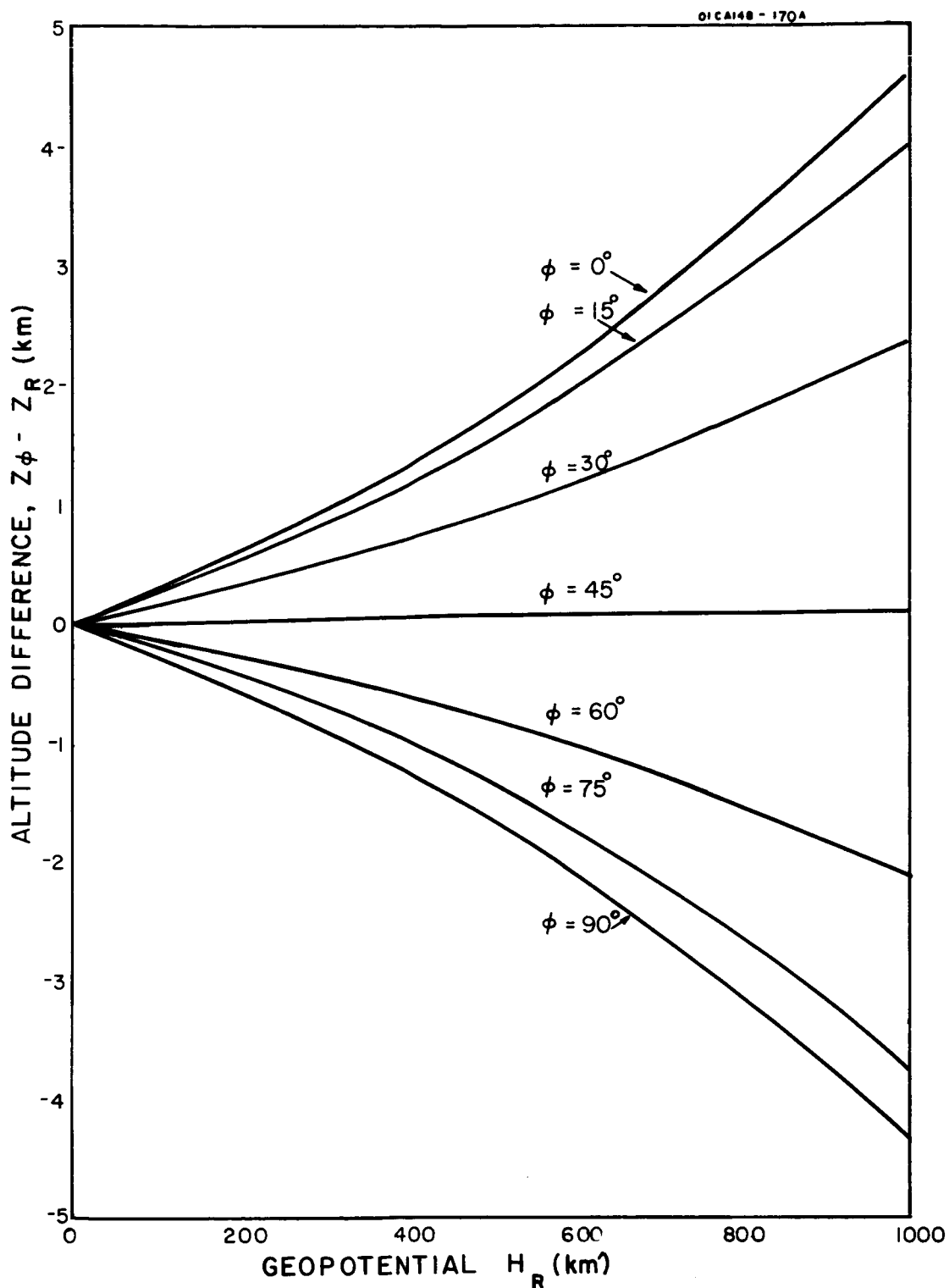


Figure 1.1A. Geometric altitude differences between geopotential surfaces at a reference latitude, and the same geopotential surfaces at each of seven other latitudes, all as a function of geopotential from 0 to 1,000 km'.

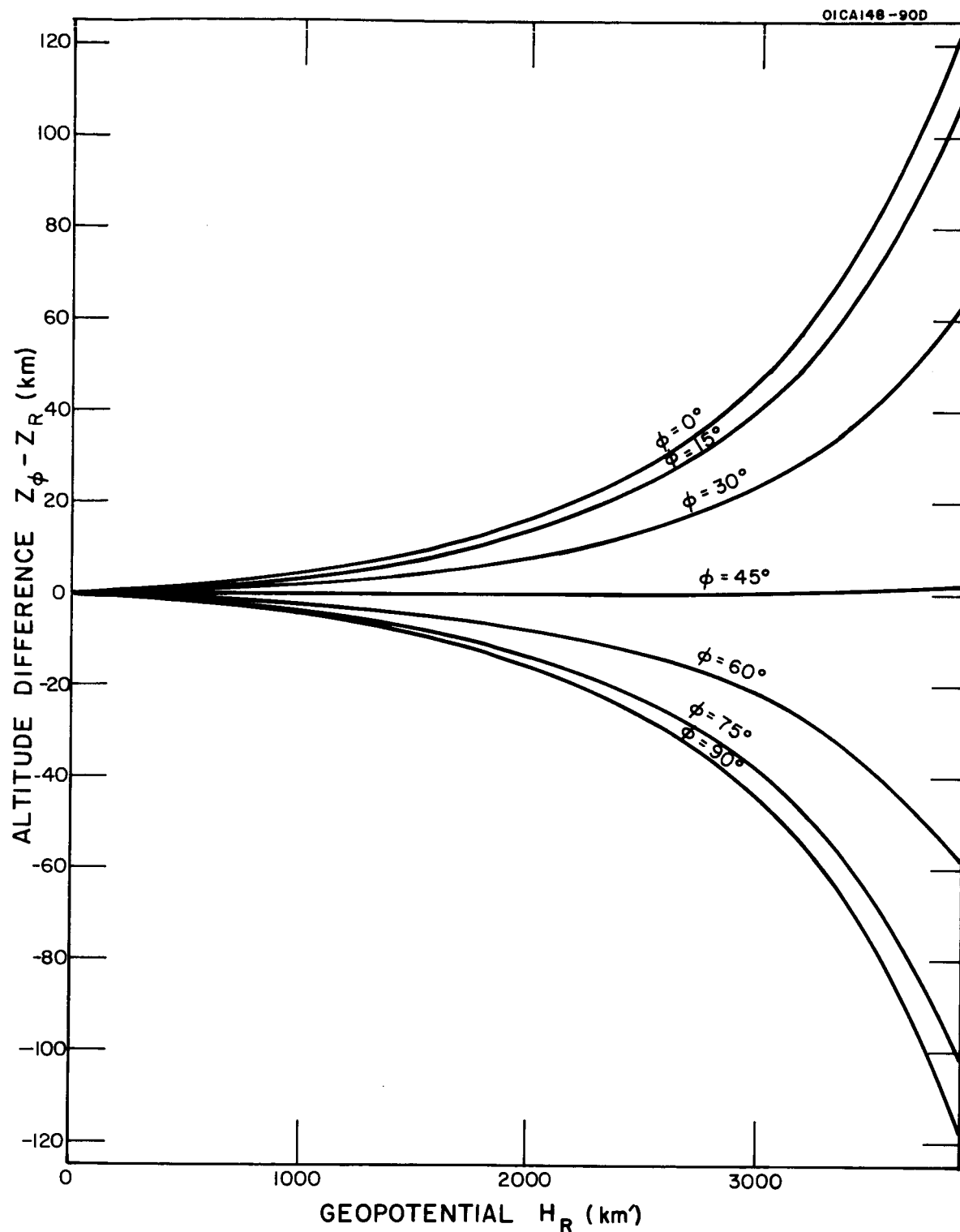


Figure 1.1B. Geometric altitude differences between geopotential surfaces at a reference latitude, and the same geopotential surfaces at each of seven other latitudes, all as a function of geopotential from 0 to 3,900 km'.

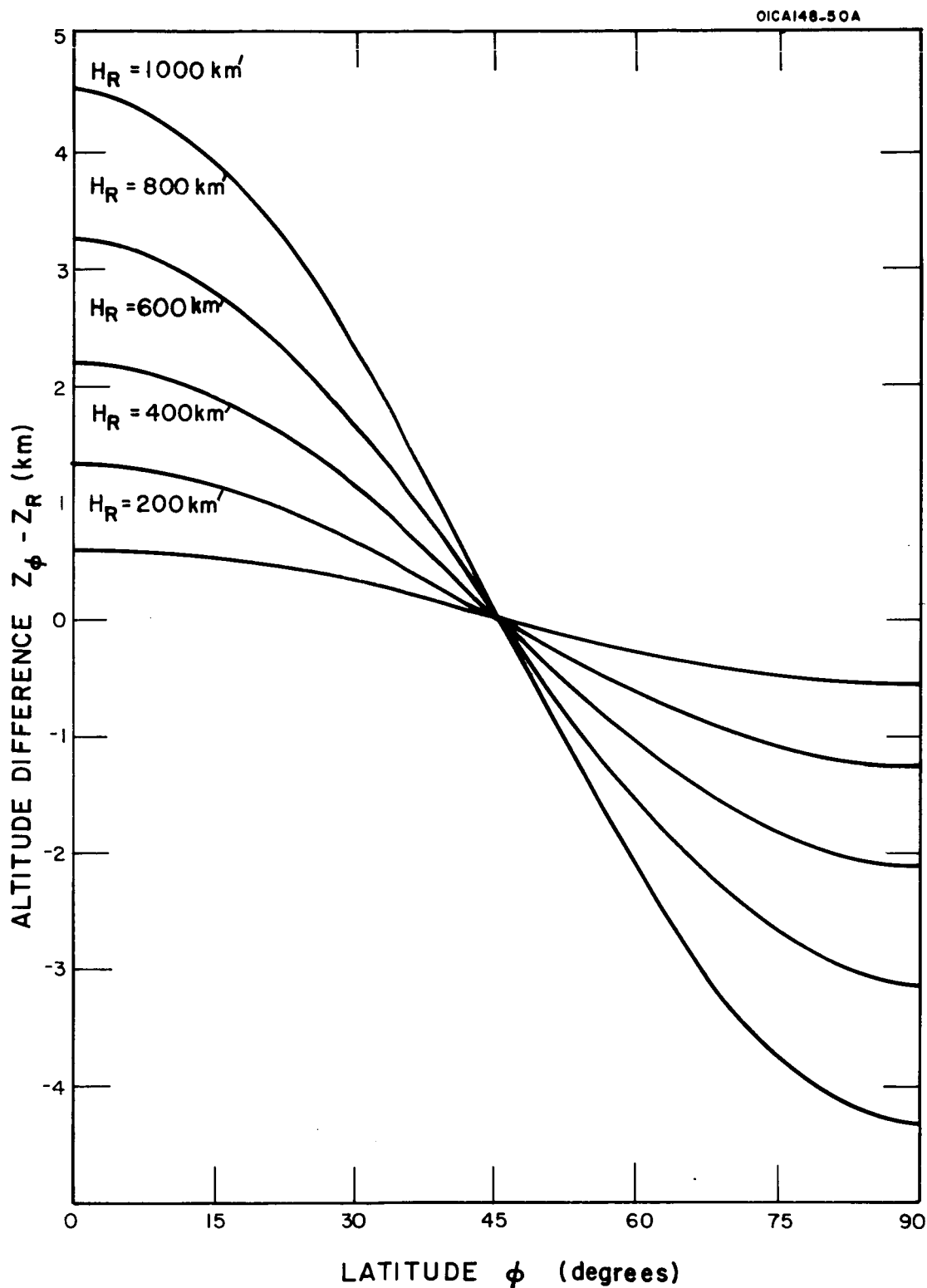


Figure 1.2A. Geometric altitude differences between each of five geopotential surfaces (from 200 to 1,000 km') at a reference latitude and the same five geopotential surfaces at other latitudes, all as a function of latitude from 0 to 90 degrees.

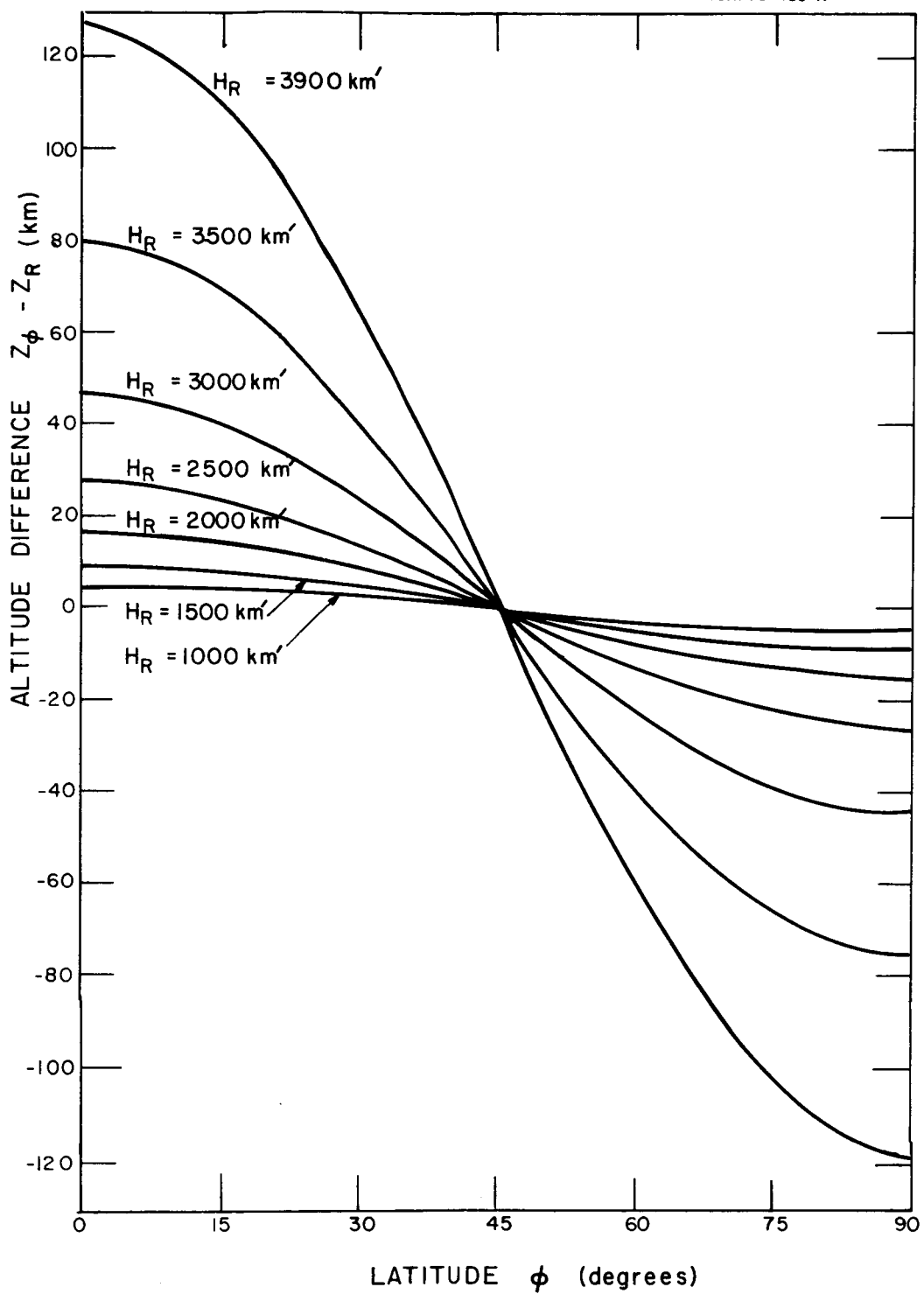


Figure 1.2B. Geometric altitude differences between each of seven geopotential surfaces (from 200 to 1,000 km') at a reference latitude and the same seven geopotential surfaces at other latitudes, all as a function of latitude from 0 to 90 degrees.

SECTION V

SPECIFIC DESCRIPTION OF TABLES 2A AND 2B

Tables 2A and 2B are formally arranged to present geometric altitude differences $Z_\phi - Z_R$ (for various latitudes) as a function of the first argument pair such that the differences $Z_\phi - Z_R$ are related to the integral values of Z_R through the non-integral values of H_R . The concept of the variation of the values of $Z_\phi - Z_R$ as a function of Z_R , implicit in the format of this table, is not very meaningful without some consideration of the intervening relationships. It appears to be more meaningful, therefore, to consider these tables as the altitude variation of $Z_\phi - Z_R$ of a certain set of equal-geopotential surfaces H_R as a function of latitude.

The values of $Z_\phi - Z_R$ for each latitude are given successively in columns 3 through 9 while column 10 of Table 2A contains values of $Z_S - Z_R$ corresponding to the set of non-integral values of H_R in column 2 of this table. These values of $Z_S - Z_R$ were obtained in the same way as those of column 10 of Table 1A. Tables 2A and 2B are intended primarily to provide the altitude adjustment required when atmospheric models expressed as a function of geometric altitude at 45° latitude are applied to other latitudes.

Graphical presentations of the data of Tables 2A and 2B are given in Figures 2.1A, 2.1B, 2.2A, and 2.2B where the significance of the digits and letters of this series of figure designations are as explained above. No graphical presentations of $Z_S - Z_R$ are given. Table 2A as well as Figures 2.1A and 2.2A are to be published as a part of the U. S. Standard Atmosphere Supplements, 1966, (Ref. 12).

TABLE 2A
GEOMETRIC ALTITUDE DIFFERENCES BETWEEN A SERIES OF GEOPOTENTIAL SURFACES AT
A REFERENCE LATITUDE, AND THE SAME GEOPOTENTIAL SURFACES AT OTHER LATITUDES,
INCLUDING THOSE OF THE US STANDARD ATMOSPHERE, ALL AS A FUNCTION OF THE GEO-
METRIC-ALTITUDE EQUIVALENT OF THE EQUAL-GEOPOTENTIAL SURFACES, 0 to 1,000 km

GEOMFT. ALTITUDE	GEOPO- TENTIAL	0	15	LATITUDE ϕ (DEG)					$Z_s - Z_R$
				30	45	60	75	90	
0.	0.0	0.0	0.0	0.0	0.0	0.0	0.0	0.0	0.0
250.	249.9	0.7	0.6	0.3	0.0	-0.3	-0.6	-0.6	0.0
500.	499.9	1.3	1.2	0.7	0.0	-0.6	-1.1	-1.3	0.0
750.	749.9	2.0	1.8	1.0	0.0	-1.0	-1.7	-1.9	0.0
1000.	999.8	2.7	2.3	1.4	0.0	-1.3	-2.2	-2.6	0.0
1250.	1249.7	3.4	2.9	1.7	0.1	-1.6	-2.8	-3.2	0.0
1500.	1499.6	4.0	3.5	2.1	0.1	-1.9	-3.4	-3.9	0.0
1750.	1749.5	4.7	4.1	2.4	0.1	-2.2	-3.9	-4.5	0.0
2000.	1999.3	5.4	4.7	2.7	0.1	-2.5	-4.5	-5.2	0.0
2250.	2249.2	6.1	5.3	3.1	0.1	-2.9	-5.0	-5.8	0.0
2500.	2499.0	6.7	5.8	3.4	0.1	-3.2	-5.6	-6.5	0.0
2750.	2748.8	7.4	6.4	3.8	0.1	-3.5	-6.1	-7.1	0.0
3000.	2998.5	8.1	7.0	4.1	0.2	-3.8	-6.7	-7.8	0.0
3250.	3248.3	8.7	7.6	4.5	0.2	-4.1	-7.3	-8.4	0.0
3500.	3498.0	9.4	8.2	4.8	0.2	-4.4	-7.8	-9.1	0.0
3750.	3747.7	10.1	8.8	5.1	0.2	-4.8	-8.4	-9.7	0.0
4000.	3997.4	10.8	9.4	5.5	0.2	-5.1	-8.9	-10.4	0.0
4250.	4247.1	11.4	9.9	5.8	0.2	-5.4	-9.5	-11.0	0.0
4500.	4496.8	12.1	10.5	6.2	0.2	-5.7	-10.1	-11.7	0.0
4750.	4746.4	12.8	11.1	6.5	0.2	-6.0	-10.6	-12.3	0.0
5000.	4996.0	13.5	11.7	6.9	0.3	-6.4	-11.2	-13.0	0.0
5250.	5245.6	14.1	12.3	7.2	0.3	-6.7	-11.7	-13.6	0.0
5500.	5495.2	14.8	12.9	7.5	0.3	-7.0	-12.3	-14.3	0.0
5750.	5744.8	15.5	13.5	7.9	0.3	-7.3	-12.9	-14.9	0.0
6000.	5994.3	16.2	14.0	8.2	0.3	-7.6	-13.4	-15.6	0.0
6250.	6243.8	16.8	14.6	8.6	0.3	-7.9	-14.0	-16.2	0.0
6500.	6493.3	17.5	15.2	8.9	0.3	-8.3	-14.5	-16.9	0.0
6750.	6742.8	18.2	15.8	9.3	0.3	-8.6	-15.1	-17.5	0.0
7000.	6992.3	18.9	16.4	9.6	0.4	-8.9	-15.7	-18.2	0.0
7250.	7241.7	19.5	17.0	10.0	0.4	-9.2	-16.2	-18.8	0.0
7500.	7491.1	20.2	17.6	10.3	0.4	-9.5	-16.8	-19.4	0.0
7750.	7740.5	20.9	18.1	10.6	0.4	-9.9	-17.4	-20.1	0.0
8000.	7989.9	21.6	18.7	11.0	0.4	-10.2	-17.9	-20.8	0.0
8250.	8239.3	22.2	19.3	11.3	0.4	-10.5	-18.5	-21.4	0.0
8500.	8488.6	22.9	19.9	11.7	0.4	-10.8	-19.0	-22.1	0.0
8750.	8737.9	23.6	20.5	12.0	0.4	-11.1	-19.6	-22.7	0.0
9000.	8987.2	24.3	21.1	12.4	0.5	-11.5	-20.2	-23.4	0.0
9250.	9236.5	24.9	21.7	12.7	0.5	-11.8	-20.7	-24.0	0.0
9500.	9485.8	25.6	22.3	13.1	0.5	-12.1	-21.3	-24.7	0.0
9750.	9735.0	26.3	22.8	13.4	0.5	-12.4	-21.8	-25.3	0.0

TABLE 2A CONTINUED

GEOMET. ALTITUDE	GEOPOTENTIAL	LATITUDE ϕ (DEG)							
		0	15	30	45	60	75	90	
Z_R (m)	H_R (m')	$Z_\phi - Z_R$	$Z_\phi - Z_R$	$Z_\phi - Z_R$	$Z_\phi - Z_R$	$Z_\phi - Z_R$	$Z_\phi - Z_R$	$Z_S - Z_R$	
10000.	9984.2	27.0	23.4	13.7	0.5	-12.7	-22.4	-26.0	0.0
10250.	10233.4	27.7	24.0	14.1	0.5	-13.1	-23.0	-26.6	0.0
10500.	10482.6	28.3	24.6	14.4	0.5	-13.4	-23.5	-27.3	0.0
10750.	10731.8	29.0	25.2	14.8	0.5	-13.7	-24.1	-27.9	0.0
11000.	10980.9	29.7	25.8	15.1	0.6	-14.0	-24.7	-28.6	0.0
11500.	11479.2	31.0	27.0	15.8	0.6	-14.7	-25.8	-29.9	0.0
12000.	11977.3	32.4	28.1	16.5	0.6	-15.3	-26.9	-31.2	0.0
12500.	12475.4	33.8	29.3	17.2	0.6	-15.9	-28.0	-32.5	0.0
13000.	12973.4	35.1	30.5	17.9	0.7	-16.6	-29.2	-33.8	0.0
13500.	13471.3	36.5	31.7	18.6	0.7	-17.2	-30.3	-35.1	0.0
14000.	13969.2	37.8	32.8	19.3	0.7	-17.9	-31.4	-36.4	0.0
14500.	14467.0	39.2	34.0	20.0	0.7	-18.5	-32.5	-37.7	0.0
15000.	14964.6	40.5	35.2	20.7	0.8	-19.1	-33.7	-39.0	0.0
15500.	15462.2	41.9	36.4	21.3	0.8	-19.8	-34.8	-40.3	0.0
16000.	15959.8	43.3	37.6	22.0	0.8	-20.4	-35.9	-41.6	0.0
16500.	16457.2	44.6	38.7	22.7	0.8	-21.1	-37.1	-42.9	0.0
17000.	16954.6	46.0	39.9	23.4	0.9	-21.7	-38.2	-44.2	0.0
17500.	17451.9	47.3	41.1	24.1	0.9	-22.3	-39.3	-45.5	0.0
18000.	17949.1	48.7	42.3	24.8	0.9	-23.0	-40.5	-46.9	0.0
18500.	18446.3	50.1	43.5	25.5	0.9	-23.6	-41.6	-48.2	0.0
19000.	18943.3	51.4	44.7	26.2	1.0	-24.3	-42.7	-49.5	0.0
19500.	19440.3	52.8	45.8	26.9	1.0	-24.9	-43.9	-50.8	0.0
20000.	19937.2	54.1	47.0	27.6	1.0	-25.6	-45.0	-52.1	0.0
20500.	20434.1	55.5	48.2	28.3	1.0	-26.2	-46.1	-53.4	0.0
21000.	20930.8	56.9	49.4	29.0	1.1	-26.8	-47.3	-54.7	0.0
21500.	21427.5	58.2	50.6	29.7	1.1	-27.5	-48.4	-56.0	0.0
22000.	21924.1	59.6	51.8	30.4	1.1	-28.1	-49.5	-57.3	0.0
22500.	22420.6	61.0	53.0	31.1	1.1	-28.8	-50.7	-58.7	0.0
23000.	22917.0	62.3	54.1	31.8	1.2	-29.4	-51.8	-60.0	0.0
23500.	23413.4	63.7	55.3	32.5	1.2	-30.1	-52.9	-61.3	0.0
24000.	23909.7	65.1	56.5	33.1	1.2	-30.7	-54.1	-62.6	0.0
24500.	24405.9	66.4	57.7	33.8	1.2	-31.4	-55.2	-63.9	0.0
25000.	24902.0	67.8	58.9	34.5	1.3	-32.0	-56.3	-65.2	0.0
25500.	25398.1	69.2	60.1	35.2	1.3	-32.7	-57.5	-66.6	0.0
26000.	25894.0	70.5	61.3	35.9	1.3	-33.3	-58.6	-67.9	0.0
26500.	26389.9	71.9	62.5	36.6	1.3	-33.9	-59.7	-69.2	0.0
27000.	26885.8	73.3	63.6	37.3	1.4	-34.6	-60.9	-70.5	0.0
27500.	27381.5	74.7	64.8	38.0	1.4	-35.2	-62.0	-71.8	0.0
28000.	27877.2	76.0	66.0	38.7	1.4	-35.9	-63.2	-73.1	0.0
28500.	28372.7	77.4	67.2	39.4	1.4	-36.5	-64.3	-74.5	0.0
29000.	28868.3	78.8	68.4	40.1	1.5	-37.2	-65.4	-75.8	0.0
29500.	29363.7	80.1	69.6	40.8	1.5	-37.8	-66.6	-77.1	0.0

TABLE 2A CONTINUED

GEOMETRIC ALTITUDE	GEOPOTENTIAL	0	LATITUDE ϕ (DEG)					
			15	30	45	60	75	90
Z_R (m)	H_R (m')	$Z_\phi - Z_R$	$Z_\phi - Z_R$	$Z_\phi - Z_R$	$Z_\phi - Z_R$	$Z_\phi - Z_R$	$Z_\phi - Z_R$	$Z_S - Z_R$
30000.	29859.0	81.5	70.8	41.5	1.5	-38.5	-67.7	-78.4 0.0
30500.	30354.3	82.9	72.0	42.2	1.5	-39.1	-68.9	-79.7 0.0
31000.	30849.5	84.3	73.2	42.9	1.6	-39.8	-70.0	-81.1 0.0
31500.	31344.6	85.6	74.4	43.6	1.6	-40.4	-71.1	-82.4 0.0
32000.	31839.7	87.0	75.6	44.3	1.6	-41.1	-72.3	-83.7 0.0
33000.	32829.5	89.8	78.0	45.7	1.7	-42.4	-74.6	-86.4 0.0
34000.	33819.1	92.5	80.3	47.1	1.7	-43.7	-76.9	-89.0 0.0
35000.	34808.3	95.3	82.7	48.5	1.8	-45.0	-79.1	-91.7 0.0
36000.	35797.2	98.0	85.1	49.9	1.8	-46.3	-81.4	-94.3 0.0
37000.	36785.8	100.8	87.5	51.3	1.9	-47.6	-83.7	-97.0 0.0
38000.	37774.1	103.5	89.9	52.7	1.9	-48.9	-86.0	-99.6 0.0
39000.	38762.1	106.3	92.3	54.2	2.0	-50.2	-88.3	-102.3 0.0
40000.	39749.8	109.1	94.7	55.6	2.0	-51.5	-90.6	-104.9 0.0
41000.	40737.2	111.8	97.1	57.0	2.1	-52.8	-92.9	-107.6 0.0
42000.	41724.3	114.6	99.5	58.4	2.1	-54.1	-95.2	-110.3 0.0
43000.	42711.0	117.4	101.9	59.8	2.2	-55.4	-97.5	-112.9 0.0
44000.	43697.5	120.1	104.3	61.2	2.2	-56.7	-99.8	-115.6 0.0
45000.	44683.6	122.9	106.8	62.6	2.3	-58.0	-102.1	-118.3 0.0
46000.	45669.5	125.7	109.2	64.0	2.3	-59.3	-104.4	-120.9 0.0
47000.	46655.0	128.5	111.6	65.4	2.4	-60.6	-106.7	-123.6 0.0
48000.	47640.2	131.3	114.0	66.9	2.4	-62.0	-109.0	-126.3 0.1
49000.	48625.1	134.0	116.4	68.3	2.5	-63.3	-111.3	-129.0 0.1
50000.	49609.7	136.8	118.8	69.7	2.5	-64.6	-113.7	-131.6 0.1
51000.	50594.0	139.6	121.2	71.1	2.6	-65.9	-116.0	-134.3 0.1
52000.	51578.0	142.4	123.7	72.5	2.6	-67.2	-118.3	-137.0 0.1
53000.	52561.7	145.2	126.1	74.0	2.7	-68.5	-120.6	-139.7 0.1
54000.	53545.1	148.0	128.5	75.4	2.7	-69.8	-122.9	-142.4 0.1
55000.	54528.2	150.8	130.9	76.8	2.8	-71.2	-125.2	-145.0 0.1
56000.	55510.9	153.6	133.4	78.2	2.9	-72.5	-127.6	-147.7 0.1
57000.	56493.4	156.4	135.8	79.7	2.9	-73.8	-129.9	-150.4 0.1
58000.	57475.5	159.2	138.2	81.1	3.0	-75.1	-132.2	-153.1 0.1
59000.	58457.4	162.0	140.7	82.5	3.0	-76.4	-134.5	-155.8 0.1
60000.	59438.9	164.8	143.1	83.9	3.1	-77.8	-136.9	-158.5 0.1
61000.	60420.2	167.6	145.5	85.4	3.1	-79.1	-139.2	-161.2 0.1
62000.	61401.1	170.4	148.0	86.8	3.2	-80.4	-141.5	-163.9 0.1
63000.	62381.7	173.2	150.4	88.2	3.2	-81.7	-143.9	-166.6 0.1
64000.	63362.0	176.0	152.8	89.7	3.3	-83.1	-146.2	-169.3 0.1
65000.	64342.0	178.8	155.3	91.1	3.3	-84.4	-148.5	-172.0 0.1
66000.	65321.7	181.6	157.7	92.5	3.4	-85.7	-150.9	-174.7 0.1
67000.	66301.1	184.4	160.2	93.9	3.4	-87.1	-153.2	-177.4 0.1
68000.	67280.2	187.3	162.6	95.4	3.5	-88.4	-155.5	-180.1 0.1
69000.	68259.0	190.1	165.1	96.8	3.5	-89.7	-157.9	-182.9 0.1

TABLE 2A CONTINUED

GEOMET. ALTITUDE	GEOPOTENTIAL	LATITUDE φ (DEG)							
		0	15	30	45	60	75	90	
70000.	69237.5	192.9	167.5	98.3	3.6	-91.0	-160.2	-185.6	0.1
71000.	70215.7	195.7	170.0	99.7	3.6	-92.4	-162.6	-188.3	0.1
72000.	71193.6	198.6	172.4	101.1	3.7	-93.7	-164.9	-191.0	0.1
73000.	72171.2	201.4	174.9	102.6	3.7	-95.0	-167.3	-193.7	0.1
74000.	73148.4	204.2	177.4	104.0	3.8	-96.4	-169.6	-196.4	0.1
75000.	74125.4	207.0	179.8	105.5	3.8	-97.7	-172.0	-199.2	0.1
76000.	75102.0	209.9	182.3	106.9	3.9	-99.1	-174.3	-201.9	0.1
77000.	76078.4	212.7	184.7	108.4	4.0	-100.4	-176.7	-204.6	0.1
78000.	77054.5	215.6	187.2	109.8	4.0	-101.7	-179.0	-207.4	0.2
79000.	78030.2	218.4	189.7	111.2	4.1	-103.1	-181.4	-210.1	0.2
80000.	79005.7	221.2	192.1	112.7	4.1	-104.4	-183.8	-212.8	0.2
81000.	79980.8	224.1	194.6	114.1	4.2	-105.8	-186.1	-215.6	0.2
82000.	80955.7	226.9	197.1	115.6	4.2	-107.1	-188.5	-218.3	0.2
83000.	81930.2	229.8	199.5	117.0	4.3	-108.5	-190.9	-221.0	0.2
84000.	82904.4	232.6	202.0	118.5	4.3	-109.8	-193.2	-223.8	0.2
85000.	83878.4	235.5	204.5	119.9	4.4	-111.1	-195.6	-226.5	0.2
86000.	84852.0	238.3	207.0	121.4	4.4	-112.5	-198.0	-229.3	0.2
87000.	85825.3	241.2	209.5	122.9	4.5	-113.8	-200.3	-232.0	0.2
88000.	86798.4	244.0	211.9	124.3	4.5	-115.2	-202.7	-234.8	0.2
89000.	87771.1	246.9	214.4	125.8	4.6	-116.5	-205.1	-237.5	0.2
90000.	88743.5	249.8	216.9	127.2	4.6	-117.9	-207.4	-240.3	0.2
92000.	90687.4	255.5	221.9	130.1	4.7	-120.6	-212.2	-245.8	0.2
94000.	92630.2	261.2	226.9	133.1	4.9	-123.3	-217.0	-251.3	0.2
96000.	94571.7	267.0	231.9	136.0	5.0	-126.0	-221.7	-256.8	0.2
98000.	96512.1	272.7	236.9	138.9	5.1	-128.7	-226.5	-262.3	0.3
100000.	98451.2	278.5	241.8	141.8	5.2	-131.4	-231.3	-267.9	0.3
102000.	100389.1	284.3	246.9	144.8	5.3	-134.2	-236.1	-273.4	0.3
104000.	102325.9	290.0	251.9	147.7	5.4	-136.9	-240.9	-279.0	0.3
106000.	104261.4	295.8	256.9	150.7	5.5	-139.6	-245.7	-284.5	0.3
108000.	106195.7	301.6	261.9	153.6	5.6	-142.3	-250.5	-290.1	0.3
110000.	108128.8	307.4	267.0	156.6	5.7	-145.1	-255.3	-295.7	0.3
112000.	110060.8	313.2	272.0	159.5	5.8	-147.8	-260.1	-301.3	0.4
114000.	111991.5	319.0	277.1	162.5	5.9	-150.6	-265.0	-306.8	0.4
116000.	113921.1	324.8	282.1	165.5	6.0	-153.3	-269.8	-312.5	0.4
118000.	115849.5	330.7	287.2	168.4	6.1	-156.1	-274.6	-318.1	0.4
120000.	117776.6	336.5	292.2	171.4	6.3	-158.8	-279.5	-323.7	0.4
125000.	122589.3	351.1	304.9	178.9	6.5	-165.7	-291.6	-337.7	0.5
130000.	127394.6	365.8	317.7	186.3	6.8	-172.6	-303.8	-351.9	0.5
135000.	132192.6	380.5	330.5	193.8	7.1	-179.6	-316.0	-366.0	0.6
140000.	136983.1	395.3	343.3	201.3	7.3	-186.6	-328.3	-380.2	0.6
145000.	141766.2	410.1	356.2	208.9	7.6	-193.5	-340.6	-394.4	0.7
150000.	146542.0	425.0	369.1	216.5	7.9	-200.6	-352.9	-408.7	0.7
155000.	151310.5	439.9	382.0	224.1	8.2	-207.6	-365.3	-423.1	0.8
160000.	156071.6	454.9	395.0	231.7	8.5	-214.6	-377.7	-437.5	0.8
165000.	160825.5	469.9	408.1	239.3	8.7	-221.7	-390.2	-451.9	0.9

TABLE 2A CONTINUED

GEOMET. ALTITUDE	GEOPO- TENTIAL	LATITUDE ϕ (DEG)							
		0	15	30	45	60	75	90	
Z_R (km)	H_R (m')	$Z_\phi - Z_R$	$Z_\phi - Z_R$	$Z_\phi - Z_R$	$Z_\phi - Z_R$	$Z_\phi - Z_R$	$Z_\phi - Z_R$	$Z_S - Z_R$	
170.	165572.0	484.9	421.1	247.0	9.0	-228.9	-402.7	-466.4	1.0
175.	170311.3	500.1	434.3	254.7	9.3	-236.0	-415.2	-480.9	1.0
180.	175043.4	515.2	447.4	262.4	9.6	-243.1	-427.8	-495.5	1.1
185.	179768.2	530.4	460.6	270.2	9.9	-250.3	-440.4	-510.1	1.2
190.	184485.8	545.7	473.9	277.9	10.2	-257.5	-453.1	-524.7	1.3
195.	189196.2	561.0	487.2	285.7	10.4	-264.7	-465.8	-539.5	1.4
200.	193899.4	576.3	500.5	293.6	10.7	-271.9	-478.5	-554.2	1.5
205.	198595.4	591.7	513.9	301.4	11.0	-279.2	-491.3	-569.0	1.6
210.	203284.3	607.2	527.3	309.3	11.3	-286.5	-504.2	-583.9	1.7
215.	207966.1	622.7	540.8	317.2	11.6	-293.8	-517.0	-598.7	1.8
220.	212640.7	638.2	554.3	325.1	11.9	-301.1	-529.9	-613.7	1.9
225.	217308.2	653.8	567.8	333.0	12.1	-308.5	-542.9	-628.7	2.0
230.	221968.7	669.5	581.4	341.0	12.5	-315.9	-555.8	-643.7	2.1
235.	226622.1	685.1	595.0	349.0	12.7	-323.3	-568.9	-658.8	2.2
240.	231268.4	700.9	608.7	357.0	13.0	-330.7	-581.9	-673.9	2.3
245.	235907.7	716.7	622.4	365.0	13.3	-338.1	-595.0	-689.1	2.4
250.	240539.9	732.5	636.1	373.1	13.6	-345.6	-608.2	-704.3	2.6
255.	245165.2	748.4	650.0	381.2	13.9	-353.1	-621.3	-719.5	2.7
260.	249783.5	764.3	663.8	389.3	14.2	-360.6	-634.6	-734.9	2.8
265.	254394.8	780.3	677.6	397.4	14.5	-368.2	-647.8	-750.2	3.0
270.	258999.1	796.3	691.6	405.6	14.8	-375.7	-661.1	-765.6	3.1
275.	263596.5	812.4	705.5	413.8	15.1	-383.3	-674.5	-781.1	3.3
280.	268187.0	828.5	719.5	422.0	15.4	-390.9	-687.9	-796.6	3.5
285.	272770.5	844.7	733.6	430.2	15.7	-398.5	-701.2	-812.1	3.6
290.	277347.2	860.9	747.7	438.5	16.0	-406.2	-714.7	-827.7	3.8
295.	281917.0	877.2	761.8	446.8	16.3	-413.8	-728.2	-843.3	4.0
300.	286479.9	893.5	776.0	455.1	16.6	-421.5	-741.7	-859.0	4.1
310.	295585.2	926.3	804.4	471.8	17.2	-437.0	-768.9	-890.5	4.5
320.	304663.2	959.3	833.1	488.6	17.8	-452.6	-796.3	-922.2	4.9
330.	313714.0	992.5	861.9	505.5	18.4	-468.2	-823.8	-954.1	5.3
340.	322737.9	1025.9	890.9	522.5	19.1	-483.9	-851.5	-986.1	5.7
350.	331734.8	1059.4	920.0	539.6	19.7	-499.7	-879.3	-1018.3	6.2
360.	340704.9	1093.2	949.3	556.7	20.3	-515.7	-907.3	-1050.8	6.7
370.	349648.4	1127.1	978.8	574.0	20.9	-531.6	-935.5	-1083.4	7.2
380.	358565.3	1161.3	1008.5	591.4	21.6	-547.7	-963.8	-1116.1	7.7
390.	367455.8	1195.6	1038.2	608.9	22.2	-564.0	-992.3	-1149.1	8.3
400.	376320.0	1230.1	1068.2	626.4	22.8	-580.2	-1020.9	-1182.3	8.9
410.	385158.0	1264.9	1098.4	644.1	23.5	-596.6	-1049.7	-1215.6	9.5
420.	393969.9	1299.8	1128.7	661.9	24.2	-613.0	-1078.6	-1249.1	10.1
430.	402755.7	1334.9	1159.2	679.8	24.8	-629.6	-1107.8	-1282.9	10.8
440.	411515.8	1370.2	1189.9	697.8	25.5	-646.2	-1137.0	-1316.7	11.4
450.	420250.1	1405.7	1220.7	715.8	26.1	-663.0	-1166.4	-1350.8	12.2
460.	428958.9	1441.4	1251.7	734.0	26.8	-679.7	-1196.0	-1385.0	12.9
470.	437642.0	1477.2	1282.8	752.3	27.4	-696.7	-1225.8	-1419.5	13.7
480.	446299.8	1513.3	1314.2	770.6	28.1	-713.7	-1255.7	-1454.1	14.5
490.	454932.3	1549.6	1345.7	789.1	28.8	-730.8	-1285.7	-1488.9	15.3

TABLE 2A CONCLUDED

GEOMET. ALTITUDE	GEOPOTENTIAL	LATITUDE ϕ (DEG)							
		0	15	30	45	60	75	90	
Z_R (km)	H_R (m')	$Z_\phi - Z_R$	$Z_\phi - Z_R$	$Z_\phi - Z_R$	$Z_\phi - Z_R$	$Z_\phi - Z_R$	$Z_\phi - Z_R$	$Z_S - Z_R$	
500.	463539.6	1586.1	1377.4	807.7	29.5	-747.9	-1316.0	-1523.9	16.2
510.	472121.8	1622.7	1409.2	826.3	30.1	-765.2	-1346.4	-1559.2	17.1
520.	480679.1	1659.6	1441.2	845.1	30.8	-782.6	-1376.9	-1594.5	18.0
530.	489211.6	1696.7	1473.4	864.0	31.5	-800.0	-1407.6	-1630.1	19.0
540.	497719.2	1733.9	1505.7	882.9	32.2	-817.6	-1438.5	-1665.8	20.0
550.	506202.3	1771.3	1538.2	902.0	32.9	-835.2	-1469.5	-1701.7	21.0
560.	514660.8	1809.0	1570.9	921.1	33.6	-853.0	-1500.7	-1737.8	22.1
570.	523095.0	1846.8	1603.7	940.4	34.3	-870.8	-1532.0	-1774.1	23.2
580.	531504.7	1884.8	1636.7	959.7	35.0	-888.7	-1563.5	-1810.6	24.3
590.	539890.3	1923.0	1669.9	979.2	35.7	-906.7	-1595.2	-1847.3	25.5
600.	548251.8	1961.4	1703.3	998.7	36.4	-924.8	-1627.0	-1884.1	26.7
610.	556589.3	2000.1	1736.8	1018.4	37.2	-942.9	-1658.9	-1921.1	28.0
620.	564902.8	2038.8	1770.5	1038.1	37.8	-961.3	-1691.1	-1958.4	29.3
630.	573192.6	2077.8	1804.3	1058.0	38.6	-979.6	-1723.4	-1995.7	30.6
640.	581458.6	2117.0	1838.4	1077.9	39.3	-998.0	-1755.8	-2033.3	32.0
650.	589701.1	2156.3	1872.5	1097.9	40.0	-1016.6	-1788.5	-2071.1	33.4
660.	597920.1	2195.9	1906.9	1118.1	40.8	-1035.2	-1821.3	-2109.1	34.8
670.	606115.7	2235.7	1941.4	1138.3	41.5	-1054.0	-1854.2	-2147.2	36.3
680.	614288.0	2275.7	1976.1	1158.7	42.3	-1072.8	-1887.3	-2185.5	37.8
690.	622437.0	2315.8	2011.0	1179.1	43.0	-1091.7	-1920.6	-2224.0	39.4
700.	630563.0	2356.2	2046.0	1199.7	43.7	-1110.7	-1954.0	-2262.7	41.0
710.	638666.1	2396.7	2081.2	1220.3	44.5	-1129.8	-1987.5	-2301.6	
720.	646746.2	2437.5	2116.6	1241.1	45.3	-1148.9	-2021.2	-2340.6	
730.	654803.4	2478.4	2152.1	1261.8	46.0	-1168.2	-2055.2	-2379.9	
740.	662838.0	2519.5	2187.8	1282.8	46.8	-1187.6	-2089.2	-2419.3	
750.	670850.0	2560.8	2223.7	1303.8	47.6	-1207.0	-2123.4	-2458.9	
760.	678839.5	2602.4	2259.8	1325.0	48.4	-1226.5	-2157.7	-2498.6	
770.	686806.5	2644.0	2296.0	1346.2	49.1	-1246.2	-2192.3	-2538.7	
780.	694751.3	2685.9	2332.3	1367.5	49.9	-1265.9	-2227.0	-2578.8	
790.	702673.8	2728.0	2368.9	1388.9	50.7	-1285.7	-2261.8	-2619.2	
800.	710574.1	2770.3	2405.6	1410.4	51.4	-1305.7	-2296.9	-2659.7	
820.	726308.7	2855.5	2479.6	1453.8	53.0	-1345.7	-2367.3	-2741.3	
840.	741955.9	2941.3	2554.1	1497.5	54.6	-1386.2	-2438.5	-2823.7	
860.	757516.4	3028.1	2629.4	1541.6	56.2	-1427.0	-2510.2	-2906.7	
880.	772990.8	3115.6	2705.4	1586.1	57.8	-1468.2	-2582.6	-2990.6	
900.	788380.0	3203.9	2782.0	1631.1	59.5	-1509.7	-2655.6	-3075.1	
920.	803684.5	3292.9	2859.3	1676.3	61.1	-1551.6	-2729.3	-3160.5	
940.	818905.2	3382.7	2937.3	1722.1	62.8	-1593.8	-2803.6	-3246.4	
960.	834042.7	3473.3	3015.9	1768.1	64.5	-1636.5	-2878.6	-3333.3	
980.	849097.6	3564.7	3095.3	1814.7	66.2	-1679.4	-2954.1	-3420.7	
1000.	864070.7	3656.7	3175.2	1861.5	67.8	-1722.8	-3030.4	-3509.0	

TABLE 2B

GEOMETRIC ALTITUDE DIFFERENCES BETWEEN A SERIES OF GEOPOTENTIAL SURFACES AT
A REFERENCE LATITUDE, AND THE SAME GEOPOTENTIAL SURFACES AT OTHER LATITUDES,
ALL AS A FUNCTION OF THE GEOMETRIC-ALTITUDE EQUIV-
ALENT OF THE EQUAL GEOPOTENTIAL SURFACES, 1,000 to 10,000 km

GEOMET. ALT.	GEOPO- TENTIAL	0	15	30	45	LATITUDE ϕ (DEG)		
						60	75	90
Z_R (km)	H_R (km ^{1/2})	$Z_\phi - Z_R$	$Z_\phi - Z_R$	$Z_\phi - Z_R$				
1000.	864.07	3.66	3.18	1.86	.07	-1.72	-3.03	-3.51
1020.	878.96	3.75	3.26	1.91	.07	-1.77	-3.11	-3.60
1040.	893.77	3.84	3.34	1.96	.07	-1.81	-3.18	-3.69
1060.	908.51	3.94	3.42	2.00	.07	-1.86	-3.26	-3.78
1080.	923.16	4.03	3.50	2.05	.07	-1.90	-3.34	-3.87
1100.	937.73	4.13	3.59	2.10	.08	-1.95	-3.42	-3.96
1120.	952.23	4.23	3.67	2.15	.08	-1.99	-3.50	-4.05
1140.	966.65	4.32	3.75	2.20	.08	-2.04	-3.58	-4.15
1160.	980.99	4.42	3.84	2.25	.08	-2.08	-3.66	-4.24
1180.	995.25	4.52	3.93	2.30	.08	-2.13	-3.75	-4.34
1200.	1009.44	4.62	4.01	2.35	.09	-2.18	-3.83	-4.43
1220.	1023.56	4.72	4.10	2.40	.09	-2.22	-3.91	-4.53
1240.	1037.60	4.82	4.19	2.45	.09	-2.27	-3.99	-4.63
1260.	1051.57	4.93	4.28	2.51	.09	-2.32	-4.08	-4.72
1280.	1065.46	5.03	4.37	2.56	.09	-2.37	-4.16	-4.82
1300.	1079.28	5.13	4.46	2.61	.10	-2.42	-4.25	-4.92
1320.	1093.03	5.24	4.55	2.67	.10	-2.47	-4.34	-5.02
1340.	1106.71	5.34	4.64	2.72	.10	-2.52	-4.42	-5.12
1360.	1120.31	5.45	4.73	2.77	.10	-2.57	-4.51	-5.22
1380.	1133.85	5.56	4.82	2.83	.10	-2.62	-4.60	-5.33
1400.	1147.32	5.66	4.92	2.88	.10	-2.67	-4.69	-5.43
1420.	1160.71	5.77	5.01	2.94	.11	-2.72	-4.78	-5.53
1440.	1174.04	5.88	5.11	2.99	.11	-2.77	-4.87	-5.64
1460.	1187.30	5.99	5.20	3.05	.11	-2.82	-4.96	-5.74
1480.	1200.50	6.10	5.30	3.10	.11	-2.87	-5.05	-5.85
1500.	1213.62	6.21	5.39	3.16	.12	-2.92	-5.14	-5.95
1520.	1226.68	6.33	5.49	3.22	.12	-2.98	-5.24	-6.06
1540.	1239.67	6.44	5.59	3.28	.12	-3.03	-5.33	-6.17
1560.	1252.60	6.55	5.69	3.33	.12	-3.08	-5.42	-6.28
1580.	1265.46	6.67	5.79	3.39	.12	-3.14	-5.52	-6.39
1600.	1278.26	6.78	5.89	3.45	.13	-3.19	-5.61	-6.50
1620.	1290.99	6.90	5.99	3.51	.13	-3.25	-5.71	-6.61
1640.	1303.66	7.02	6.09	3.57	.13	-3.30	-5.81	-6.72
1660.	1316.27	7.13	6.19	3.63	.13	-3.36	-5.90	-6.83
1680.	1328.81	7.25	6.30	3.69	.13	-3.41	-6.00	-6.95
1700.	1341.30	7.37	6.40	3.75	.14	-3.47	-6.10	-7.06
1720.	1353.71	7.49	6.50	3.81	.14	-3.52	-6.20	-7.18
1740.	1366.07	7.61	6.61	3.87	.14	-3.58	-6.30	-7.29
1760.	1378.37	7.73	6.71	3.94	.14	-3.64	-6.40	-7.41
1780.	1390.61	7.86	6.82	4.00	.15	-3.70	-6.50	-7.52

TABLE 2B CONTINUED

GEOMET. ALT.	GEOPO- TENTIAL	0	LATITUDE ϕ (DEG)					
			15	30	45	60	75	90
		Z_R (km)	H_R (km')	$Z_\phi - Z_R$				
1800.	1402.78	7.98	6.93	4.06	.15	-3.75	-6.60	-7.64
1820.	1414.90	8.10	7.04	4.12	.15	-3.81	-6.70	-7.76
1840.	1426.96	8.23	7.14	4.19	.15	-3.87	-6.81	-7.88
1860.	1438.96	8.35	7.25	4.25	.15	-3.93	-6.91	-8.00
1880.	1450.90	8.48	7.36	4.31	.16	-3.99	-7.01	-8.12
1900.	1462.78	8.61	7.47	4.38	.16	-4.05	-7.12	-8.24
1920.	1474.61	8.74	7.58	4.44	.16	-4.11	-7.22	-8.36
1940.	1486.38	8.86	7.70	4.51	.16	-4.17	-7.33	-8.49
1960.	1498.09	8.99	7.81	4.58	.17	-4.23	-7.44	-8.61
1980.	1509.75	9.12	7.92	4.64	.17	-4.29	-7.54	-8.73
2000.	1521.35	9.25	8.03	4.71	.17	-4.35	-7.65	-8.86
2020.	1532.89	9.39	8.15	4.78	.17	-4.41	-7.76	-8.99
2040.	1544.38	9.52	8.26	4.84	.18	-4.48	-7.87	-9.11
2060.	1555.82	9.65	8.38	4.91	.18	-4.54	-7.98	-9.24
2080.	1567.20	9.79	8.50	4.98	.18	-4.60	-8.09	-9.37
2100.	1578.52	9.92	8.61	5.05	.18	-4.67	-8.20	-9.50
2120.	1589.80	10.06	8.73	5.12	.19	-4.73	-8.31	-9.63
2140.	1601.02	10.19	8.85	5.19	.19	-4.79	-8.43	-9.76
2160.	1612.19	10.33	8.97	5.26	.19	-4.86	-8.54	-9.89
2180.	1623.30	10.47	9.09	5.33	.19	-4.92	-8.65	-10.02
2200.	1634.37	10.61	9.21	5.40	.20	-4.99	-8.77	-10.15
2220.	1645.38	10.75	9.33	5.47	.20	-5.05	-8.88	-10.28
2240.	1656.34	10.89	9.45	5.54	.20	-5.12	-9.00	-10.42
2260.	1667.25	11.03	9.58	5.61	.20	-5.18	-9.11	-10.55
2280.	1678.11	11.17	9.70	5.68	.21	-5.25	-9.23	-10.69
2300.	1688.92	11.31	9.82	5.75	.21	-5.32	-9.35	-10.82
2320.	1699.68	11.46	9.95	5.83	.21	-5.39	-9.47	-10.96
2340.	1710.39	11.60	10.07	5.90	.21	-5.45	-9.59	-11.10
2360.	1721.05	11.75	10.20	5.97	.22	-5.52	-9.71	-11.24
2380.	1731.66	11.89	10.32	6.05	.22	-5.59	-9.83	-11.38
2400.	1742.22	12.04	10.45	6.12	.22	-5.66	-9.95	-11.51
2420.	1752.74	12.19	10.58	6.20	.23	-5.73	-10.07	-11.66
2440.	1763.21	12.33	10.71	6.27	.23	-5.80	-10.19	-11.80
2460.	1773.63	12.48	10.84	6.35	.23	-5.87	-10.31	-11.94
2480.	1784.00	12.63	10.97	6.43	.23	-5.94	-10.44	-12.08
2500.	1794.32	12.78	11.10	6.50	.24	-6.01	-10.56	-12.22
2520.	1804.60	12.93	11.23	6.58	.24	-6.08	-10.68	-12.37
2540.	1814.84	13.09	11.36	6.66	.24	-6.15	-10.81	-12.51
2560.	1825.03	13.24	11.49	6.73	.25	-6.22	-10.93	-12.66
2580.	1835.17	13.39	11.63	6.81	.25	-6.29	-11.06	-12.81
2600.	1845.26	13.55	11.76	6.89	.25	-6.37	-11.19	-12.95
2620.	1855.31	13.70	11.90	6.97	.25	-6.44	-11.32	-13.10
2640.	1865.32	13.86	12.03	7.05	.26	-6.51	-11.44	-13.25
2660.	1875.28	14.02	12.17	7.13	.26	-6.58	-11.57	-13.40
2680.	1885.20	14.17	12.30	7.21	.26	-6.66	-11.70	-13.55

TABLE 2B CONTINUED

GEOMET. ALT.	GEOPOTENTIAL	0	LATITUDE ϕ (DEG)					
			15	30	45	60	75	90
Z_R (km)	H_R (km')	$Z_\phi - Z_R$	$Z_\phi - Z_R$	$Z_\phi - Z_R$	$Z_\phi - Z_R$	$Z_\phi - Z_R$	$Z_\phi - Z_R$	$Z_\phi - Z_R$
2700.	1895.08	14.33	12.44	7.29	.27	-6.73	-11.83	-13.70
2720.	1904.91	14.49	12.58	7.37	.27	-6.81	-11.96	-13.85
2740.	1914.70	14.65	12.72	7.45	.27	-6.88	-12.10	-14.00
2760.	1924.44	14.81	12.86	7.53	.27	-6.96	-12.23	-14.16
2780.	1934.14	14.97	13.00	7.61	.28	-7.03	-12.36	-14.31
2800.	1943.80	15.13	13.14	7.70	.28	-7.11	-12.49	-14.46
2820.	1953.42	15.30	13.28	7.78	.28	-7.18	-12.63	-14.62
2840.	1963.00	15.46	13.42	7.86	.29	-7.26	-12.76	-14.77
2860.	1972.53	15.63	13.56	7.95	.29	-7.34	-12.90	-14.93
2880.	1982.02	15.79	13.71	8.03	.29	-7.42	-13.03	-15.09
2900.	1991.48	15.96	13.85	8.11	.30	-7.49	-13.17	-15.25
2920.	2000.89	16.12	14.00	8.20	.30	-7.57	-13.31	-15.40
2940.	2010.26	16.29	14.14	8.28	.30	-7.65	-13.45	-15.56
2960.	2019.59	16.46	14.29	8.37	.30	-7.73	-13.58	-15.72
2980.	2028.88	16.63	14.44	8.46	.31	-7.81	-13.72	-15.89
3000.	2038.13	16.80	14.58	8.54	.31	-7.89	-13.86	-16.05
3020.	2047.34	16.97	14.73	8.63	.31	-7.97	-14.00	-16.21
3040.	2056.51	17.14	14.88	8.72	.32	-8.05	-14.14	-16.37
3060.	2065.65	17.31	15.03	8.80	.32	-8.13	-14.29	-16.54
3080.	2074.74	17.49	15.18	8.89	.32	-8.21	-14.43	-16.70
3100.	2083.80	17.66	15.33	8.98	.33	-8.29	-14.57	-16.87
3120.	2092.81	17.84	15.48	9.07	.33	-8.37	-14.71	-17.03
3140.	2101.79	18.01	15.64	9.16	.33	-8.46	-14.86	-17.20
3160.	2110.74	18.19	15.79	9.25	.34	-8.54	-15.00	-17.37
3180.	2119.64	18.36	15.94	9.34	.34	-8.62	-15.15	-17.54
3200.	2128.51	18.54	16.10	9.43	.34	-8.70	-15.29	-17.70
3220.	2137.34	18.72	16.25	9.52	.35	-8.79	-15.44	-17.87
3240.	2146.13	18.90	16.41	9.61	.35	-8.87	-15.59	-18.05
3260.	2154.89	19.08	16.56	9.70	.35	-8.96	-15.74	-18.22
3280.	2163.61	19.26	16.72	9.79	.36	-9.04	-15.89	-18.39
3300.	2172.29	19.44	16.88	9.88	.36	-9.13	-16.03	-18.56
3320.	2180.94	19.63	17.04	9.98	.36	-9.21	-16.18	-18.73
3340.	2189.55	19.81	17.20	10.07	.37	-9.30	-16.34	-18.91
3360.	2198.13	19.99	17.36	10.16	.37	-9.38	-16.49	-19.08
3380.	2206.67	20.18	17.52	10.26	.37	-9.47	-16.64	-19.26
3400.	2215.18	20.36	17.68	10.35	.38	-9.56	-16.79	-19.44
3420.	2223.65	20.55	17.84	10.45	.38	-9.64	-16.94	-19.61
3440.	2232.09	20.74	18.00	10.54	.38	-9.73	-17.10	-19.79
3460.	2240.49	20.93	18.16	10.64	.39	-9.82	-17.25	-19.97
3480.	2248.86	21.11	18.33	10.73	.39	-9.91	-17.41	-20.15
3500.	2257.20	21.30	18.49	10.83	.39	-9.99	-17.56	-20.33
3520.	2265.50	21.49	18.66	10.93	.40	-10.08	-17.72	-21.51
3540.	2273.77	21.69	18.82	11.02	.40	-10.17	-17.87	-20.69
3560.	2282.00	21.88	18.99	11.12	.40	-10.26	-18.03	-20.87
3580.	2290.20	22.07	19.15	11.22	.41	-10.35	-18.19	-21.06

TABLE 2B CONTINUED

GEOMET. ALT.	GEOPO- TENTIAL	0	15	LATITUDE ϕ (DEG)				
				30	45	60	75	90
Z_R (km)	H_R (km')	$Z_\phi - Z_R$	$Z_\phi - Z_R$	$Z_\phi - Z_R$	$Z_\phi - Z_R$	$Z_\phi - Z_R$	$Z_\phi - Z_R$	$Z_\phi - Z_R$
3600.	2298.4	22.	19.	11.	.4	-10.	-18.	-21.
3620.	2306.5	22.	19.	11.	.4	-11.	-19.	-21.
3640.	2314.6	23.	20.	12.	.4	-11.	-19.	-22.
3660.	2322.7	23.	20.	12.	.4	-11.	-19.	-22.
3680.	2330.7	23.	20.	12.	.4	-11.	-19.	-22.
3700.	2338.7	23.	20.	12.	.4	-11.	-19.	-22.
3720.	2346.7	23.	20.	12.	.4	-11.	-19.	-22.
3740.	2354.6	24.	21.	12.	.4	-11.	-19.	-23.
3760.	2362.6	24.	21.	12.	.4	-11.	-20.	-23.
3780.	2370.4	24.	21.	12.	.4	-11.	-20.	-23.
3800.	2378.3	24.	21.	12.	.4	-11.	-20.	-23.
3820.	2386.1	24.	21.	12.	.5	-11.	-20.	-23.
3840.	2393.9	25.	21.	13.	.5	-12.	-20.	-24.
3860.	2401.7	25.	22.	13.	.5	-12.	-20.	-24.
3880.	2409.4	25.	22.	13.	.5	-12.	-21.	-24.
3900.	2417.1	25.	22.	13.	.5	-12.	-21.	-24.
3920.	2424.7	25.	22.	13.	.5	-12.	-21.	-24.
3940.	2432.4	26.	22.	13.	.5	-12.	-21.	-24.
3960.	2440.0	26.	22.	13.	.5	-12.	-21.	-25.
3980.	2447.6	26.	23.	13.	.5	-12.	-21.	-25.
4000.	2455.1	26.	23.	13.	.5	-12.	-22.	-25.
4020.	2462.6	27.	23.	13.	.5	-12.	-22.	-25.
4040.	2470.1	27.	23.	14.	.5	-13.	-22.	-25.
4060.	2477.6	27.	23.	14.	.5	-13.	-22.	-26.
4080.	2485.0	27.	24.	14.	.5	-13.	-22.	-26.
4100.	2492.4	27.	24.	14.	.5	-13.	-23.	-26.
4120.	2499.8	28.	24.	14.	.5	-13.	-23.	-26.
4140.	2507.2	28.	24.	14.	.5	-13.	-23.	-26.
4160.	2514.5	28.	24.	14.	.5	-13.	-23.	-27.
4180.	2521.8	28.	24.	14.	.5	-13.	-23.	-27.
4200.	2529.0	28.	25.	14.	.5	-13.	-23.	-27.
4220.	2536.3	29.	25.	15.	.5	-13.	-24.	-27.
4240.	2543.5	29.	25.	15.	.5	-14.	-24.	-28.
4260.	2550.7	29.	25.	15.	.5	-14.	-24.	-28.
4280.	2557.8	29.	25.	15.	.5	-14.	-24.	-28.
4300.	2565.0	30.	26.	15.	.5	-14.	-24.	-28.
4320.	2572.1	30.	26.	15.	.5	-14.	-24.	-28.
4340.	2579.1	30.	26.	15.	.6	-14.	-25.	-29.
4360.	2586.2	30.	26.	15.	.6	-14.	-25.	-29.
4380.	2593.2	30.	26.	15.	.6	-14.	-25.	-29.
4400.	2600.2	31.	27.	16.	.6	-14.	-25.	-29.
4420.	2607.2	31.	27.	16.	.6	-14.	-25.	-29.
4440.	2614.1	31.	27.	16.	.6	-15.	-26.	-30.
4460.	2621.0	31.	27.	16.	.6	-15.	-26.	-30.
4480.	2627.9	32.	27.	16.	.6	-15.	-26.	-30.

TABLE 2B CONTINUED

GEOMET. ALT.	GEOPOTENTIAL	LATITUDE ϕ (DEG)						
		0	15	30	45	60	75	90
Z_R (km)	H_R (km')	$Z_\phi - Z_R$	$Z_\phi - Z_R$	$Z_\phi - Z_R$	$Z_\phi - Z_R$	$Z_\phi - Z_R$	$Z_\phi - Z_R$	$Z_\phi - Z_R$
4500.	2634.8	32.	28.	16.	.6	-15.	-26.	-30.
4520.	2641.6	32.	28.	16.	.6	-15.	-26.	-30.
4540.	2648.5	32.	28.	16.	.6	-15.	-27.	-31.
4560.	2655.3	32.	28.	16.	.6	-15.	-27.	-31.
4580.	2662.0	33.	28.	17.	.6	-15.	-27.	-31.
4600.	2668.8	33.	29.	17.	.6	-15.	-27.	-31.
4620.	2675.5	33.	29.	17.	.6	-16.	-27.	-32.
4640.	2682.2	33.	29.	17.	.6	-16.	-27.	-32.
4660.	2688.9	34.	29.	17.	.6	-16.	-28.	-32.
4680.	2695.5	34.	29.	17.	.6	-16.	-28.	-32.
4700.	2702.1	34.	30.	17.	.6	-16.	-28.	-32.
4720.	2708.7	34.	30.	17.	.6	-16.	-28.	-33.
4740.	2715.3	35.	30.	18.	.6	-16.	-28.	-33.
4760.	2721.9	35.	30.	18.	.6	-16.	-29.	-33.
4780.	2728.4	35.	30.	18.	.6	-16.	-29.	-33.
4800.	2734.9	35.	31.	18.	.7	-17.	-29.	-34.
4820.	2741.4	36.	31.	18.	.7	-17.	-29.	-34.
4840.	2747.8	36.	31.	18.	.7	-17.	-29.	-34.
4860.	2754.3	36.	31.	18.	.7	-17.	-30.	-34.
4880.	2760.7	36.	31.	18.	.7	-17.	-30.	-35.
4900.	2767.1	37.	32.	19.	.7	-17.	-30.	-35.
4920.	2773.4	37.	32.	19.	.7	-17.	-30.	-35.
4940.	2779.8	37.	32.	19.	.7	-17.	-30.	-35.
4960.	2786.1	37.	32.	19.	.7	-17.	-31.	-35.
4980.	2792.4	38.	33.	19.	.7	-18.	-31.	-36.
5000.	2798.7	38.	33.	19.	.7	-18.	-31.	-36.
5050.	2814.3	38.	33.	19.	.7	-18.	-32.	-37.
5100.	2829.7	39.	34.	20.	.7	-18.	-32.	-37.
5150.	2845.1	40.	34.	20.	.7	-19.	-33.	-38.
5200.	2860.2	40.	35.	20.	.7	-19.	-33.	-38.
5250.	2875.3	41.	36.	21.	.8	-19.	-34.	-39.
5300.	2890.2	42.	36.	21.	.8	-19.	-34.	-40.
5350.	2905.0	42.	37.	21.	.8	-20.	-35.	-40.
5400.	2919.7	43.	37.	22.	.8	-20.	-35.	-41.
5450.	2934.3	44.	38.	22.	.8	-20.	-36.	-41.
5500.	2948.7	44.	38.	22.	.8	-21.	-36.	-42.
5550.	2963.0	45.	39.	23.	.8	-21.	-37.	-43.
5600.	2977.2	46.	40.	23.	.8	-21.	-37.	-43.
5650.	2991.3	46.	40.	23.	.9	-22.	-38.	-44.
5700.	3005.2	47.	41.	24.	.9	-22.	-39.	-45.
5750.	3019.1	48.	41.	24.	.9	-22.	-39.	-45.
5800.	3032.8	48.	42.	25.	.9	-23.	-40.	-46.
5850.	3046.4	49.	43.	25.	.9	-23.	-40.	-47.
5900.	3059.9	50.	43.	25.	.9	-23.	-41.	-47.
5950.	3073.3	50.	44.	26.	.9	-24.	-41.	-48.

TABLE 2B CONTINUED

GEOMFT. ALT.	GEOFPO- TENTIAL	LATITUDE ϕ (DEG)						
		0	15	30	45	60	75	90
Z_R (km)	H_R (km')	$Z_\phi - Z_R$	$Z_\phi - Z_R$	$Z_\phi - Z_R$	$Z_\phi - Z_R$	$Z_\phi - Z_R$	$Z_\phi - Z_R$	$Z_\phi - Z_R$
6000.	3086.6	51.	44.	26.	.9	-24.	-42.	-49.
6050.	3099.8	52.	45.	26.	.0	-24.	-43.	-49.
6100.	3112.9	53.	46.	27.	.0	-25.	-43.	-50.
6150.	3125.8	53.	46.	27.	.0	-25.	-44.	-51.
6200.	3138.7	54.	47.	27.	.0	-25.	-44.	-51.
6250.	3151.5	55.	48.	28.	.0	-26.	-45.	-52.
6300.	3164.1	56.	48.	28.	.0	-26.	-46.	-53.
6350.	3176.7	56.	49.	29.	.0	-26.	-46.	-53.
6400.	3189.2	57.	50.	29.	.1	-27.	-47.	-54.
6450.	3201.5	58.	50.	29.	.1	-27.	-47.	-55.
6500.	3213.8	59.	51.	30.	.1	-27.	-48.	-56.
6550.	3226.0	59.	52.	30.	.1	-28.	-49.	-56.
6600.	3238.1	60.	52.	31.	.1	-28.	-49.	-57.
6650.	3250.0	61.	53.	31.	.1	-28.	-50.	-58.
6700.	3261.9	62.	54.	31.	.1	-29.	-51.	-59.
6750.	3273.7	63.	54.	32.	.2	-29.	-51.	-59.
6800.	3285.5	63.	55.	32.	.2	-30.	-52.	-60.
6850.	3297.1	64.	56.	33.	.2	-30.	-53.	-61.
6900.	3308.6	65.	56.	33.	.2	-30.	-53.	-62.
6950.	3320.1	66.	57.	33.	.2	-31.	-54.	-62.
7000.	3331.4	67.	58.	34.	.2	-31.	-55.	-63.
7050.	3342.7	67.	58.	34.	.2	-31.	-55.	-64.
7100.	3353.9	68.	59.	35.	.3	-32.	-56.	-65.
7150.	3365.0	69.	60.	35.	.3	-32.	-57.	-65.
7200.	3376.1	70.	61.	35.	.3	-33.	-57.	-66.
7250.	3387.0	71.	61.	36.	.3	-33.	-58.	-67.
7300.	3397.9	72.	62.	36.	.3	-33.	-59.	-68.
7350.	3408.7	72.	63.	37.	.3	-34.	-59.	-69.
7400.	3419.4	73.	64.	37.	.4	-34.	-60.	-69.
7450.	3430.1	74.	64.	38.	.4	-35.	-61.	-70.
7500.	3440.6	75.	65.	38.	.4	-35.	-61.	-71.
7550.	3451.1	76.	66.	38.	.4	-35.	-62.	-72.
7600.	3461.5	77.	67.	39.	.4	-36.	-63.	-73.
7650.	3471.8	78.	67.	39.	.4	-36.	-63.	-73.
7700.	3482.1	79.	68.	40.	.4	-37.	-64.	-74.
7750.	3492.3	79.	69.	40.	.5	-37.	-65.	-75.
7800.	3502.4	80.	70.	41.	.5	-37.	-66.	-76.
7850.	3512.5	81.	70.	41.	.5	-38.	-66.	-77.
7900.	3522.4	82.	71.	42.	.5	-38.	-67.	-78.
7950.	3532.3	83.	72.	42.	.5	-39.	-68.	-79.
8000.	3542.2	84.	73.	43.	.5	-39.	-69.	-79.
8050.	3551.9	85.	74.	43.	.6	-40.	-69.	-80.
8100.	3561.6	86.	74.	43.	.6	-40.	-70.	-81.
8150.	3571.3	87.	75.	44.	.6	-40.	-71.	-82.
8200.	3580.8	88.	76.	44.	.6	-41.	-72.	-83.

TABLE 2B CONCLUDED

GEOMETRIC ALT.	GEOPOTENTIAL	0	LATITUDE ϕ (DEG)					
			15	30	45	60	75	90
Z_R (km)	H_R (km')	$Z_\phi - Z_R$	$Z_\phi - Z_R$	$Z_\phi - Z_R$	$Z_\phi - Z_R$	$Z_\phi - Z_R$	$Z_\phi - Z_R$	$Z_\phi - Z_R$
8250.	3590.3	89.	77.	45.	.6	-41.	-72.	-84.
8300.	3599.8	90.	78.	45.	.6	-42.	-73.	-85.
8350.	3609.2	90.	78.	46.	.7	-42.	-74.	-85.
8400.	3618.5	91.	79.	46.	.7	-43.	-75.	-86.
8450.	3627.7	92.	80.	47.	.7	-43.	-75.	-87.
8500.	3636.9	93.	81.	47.	.7	-43.	-76.	-88.
8550.	3646.0	94.	82.	48.	.7	-44.	-77.	-89.
8600.	3655.1	95.	83.	48.	.8	-44.	-78.	-90.
8650.	3664.1	96.	84.	49.	.8	-45.	-79.	-91.
8700.	3673.0	97.	84.	49.	.8	-45.	-79.	-92.
8750.	3681.9	98.	85.	50.	.8	-46.	-80.	-93.
8800.	3690.7	99.	86.	50.	.8	-46.	-81.	-94.
8850.	3699.5	100.	87.	51.	.8	-47.	-82.	-95.
8900.	3708.2	101.	88.	51.	.9	-47.	-83.	-96.
8950.	3716.9	102.	89.	52.	.9	-48.	-83.	-97.
9000.	3725.5	103.	90.	52.	.9	-48.	-84.	-97.
9050.	3734.0	104.	90.	53.	.9	-49.	-85.	-98.
9100.	3742.5	105.	91.	53.	.9	-49.	-86.	-99.
9150.	3750.9	106.	92.	54.	.0	-49.	-87.	-100.
9200.	3759.3	107.	93.	54.	.0	-50.	-88.	-101.
9250.	3767.6	108.	94.	55.	.0	-50.	-88.	-102.
9300.	3775.9	109.	95.	55.	.0	-51.	-89.	-103.
9350.	3784.1	111.	96.	56.	.0	-51.	-90.	-104.
9400.	3792.3	112.	97.	57.	.1	-52.	-91.	-105.
9450.	3800.4	113.	98.	57.	.1	-52.	-92.	-106.
9500.	3808.4	114.	99.	58.	.1	-53.	-93.	-107.
9550.	3816.4	115.	100.	58.	.1	-53.	-94.	-108.
9600.	3824.4	116.	100.	59.	.1	-54.	-94.	-109.
9650.	3832.3	117.	101.	59.	.2	-54.	-95.	-110.
9700.	3840.2	118.	102.	60.	.2	-55.	-96.	-111.
9750.	3848.0	119.	103.	60.	.2	-55.	-97.	-112.
9800.	3855.7	120.	104.	61.	.2	-56.	-98.	-113.
9850.	3863.5	121.	105.	61.	.2	-56.	-99.	-114.
9900.	3871.1	122.	106.	62.	.3	-57.	-100.	-115.
9950.	3878.7	123.	107.	63.	.3	-57.	-101.	-116.
10000.	3886.3	125.	108.	63.	.3	-58.	-101.	-117.

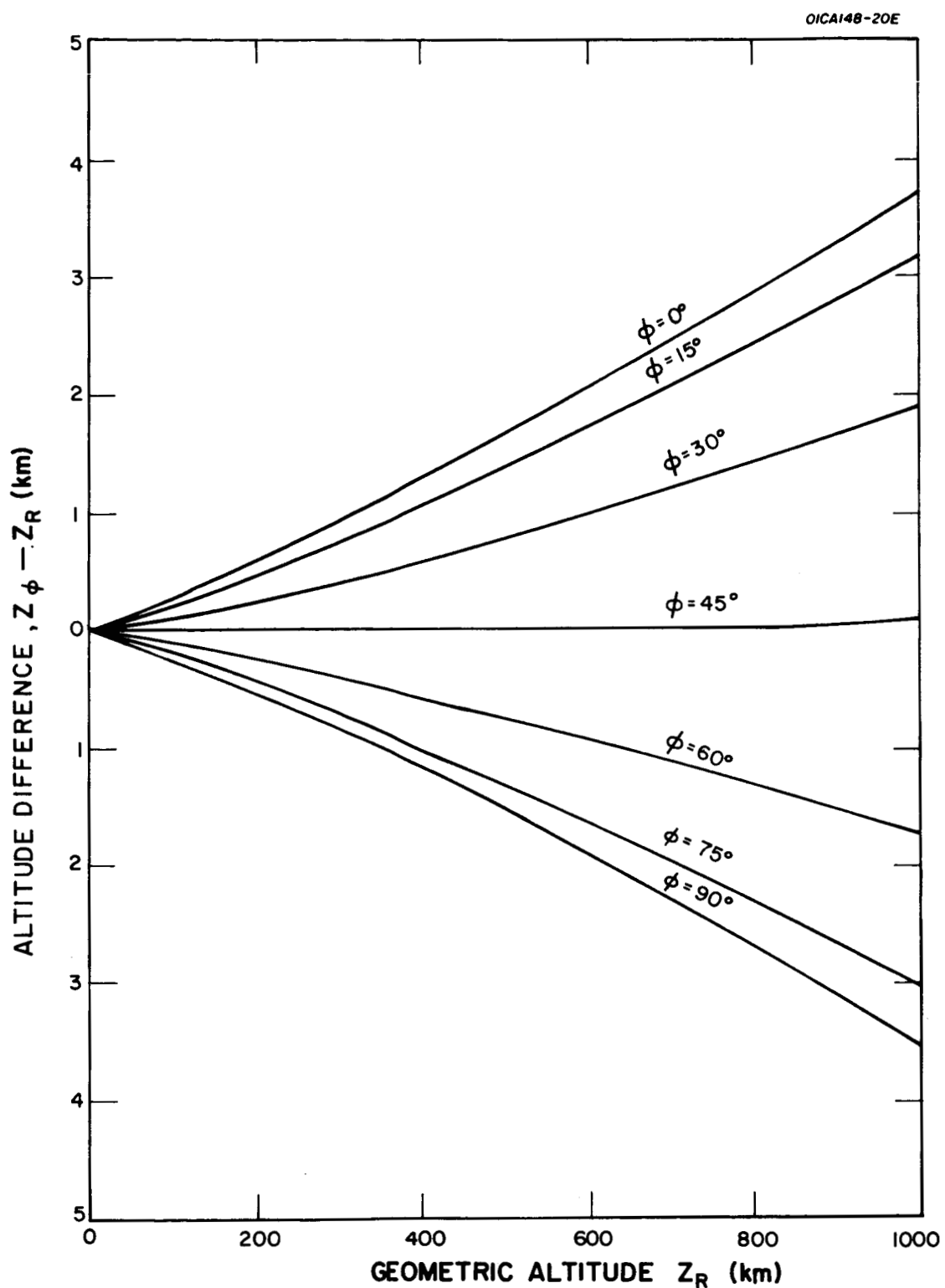


Figure 2.1A. Geometric altitude differences between geopotential surfaces at a reference latitude, and the same geopotential surfaces at each of seven other latitudes all as a function of the geometric-altitude equivalents of the equal-geopotential surfaces, 0 to 1,000 km.

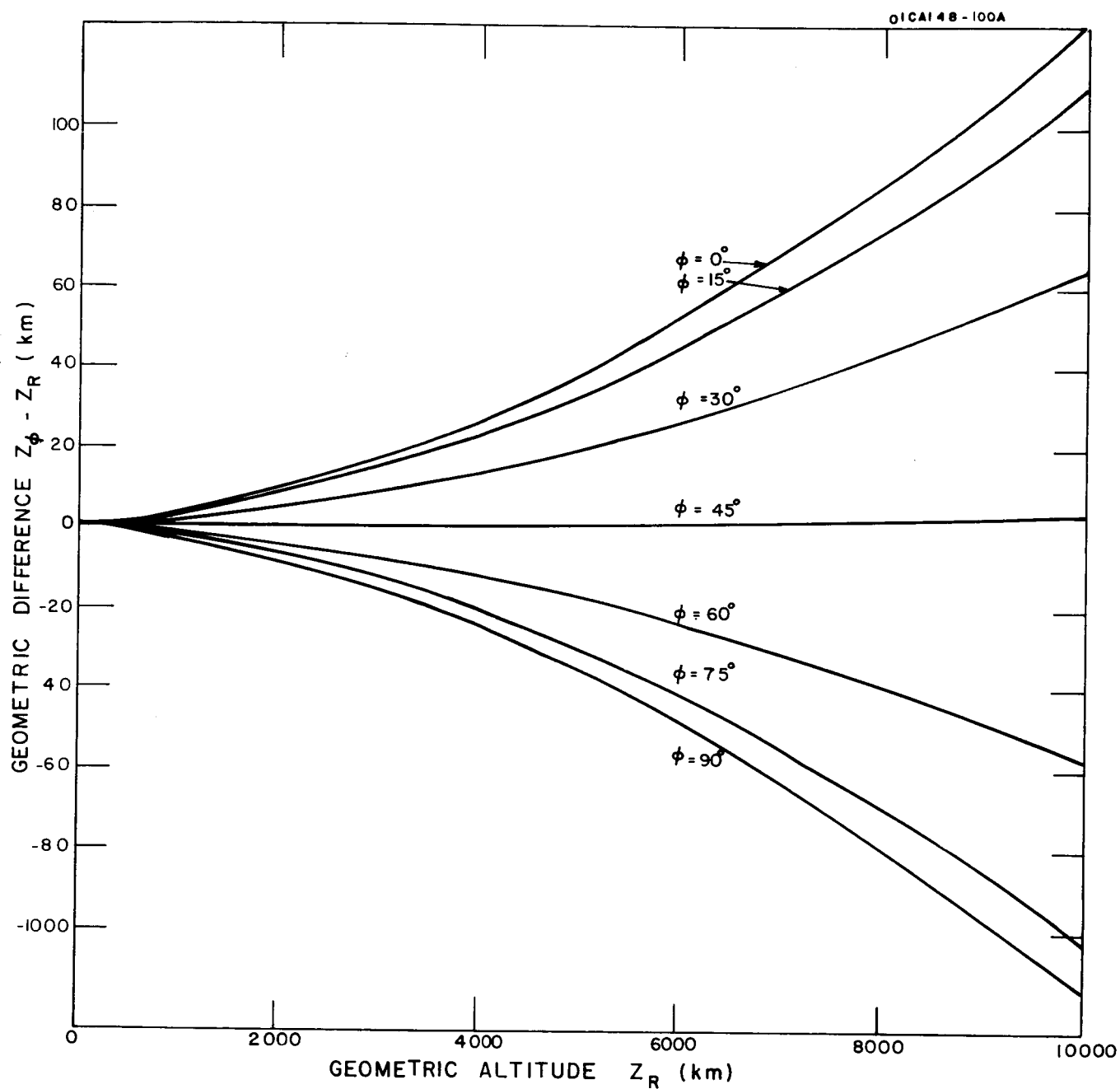


Figure 2.1B. Geometric altitude differences between geopotential surfaces at a reference latitude, and the same geopotential surface at each of seven other latitudes, all as a function of the geometric-altitude equivalents of the equal-geopotential surfaces, 0 to 10,000 km.

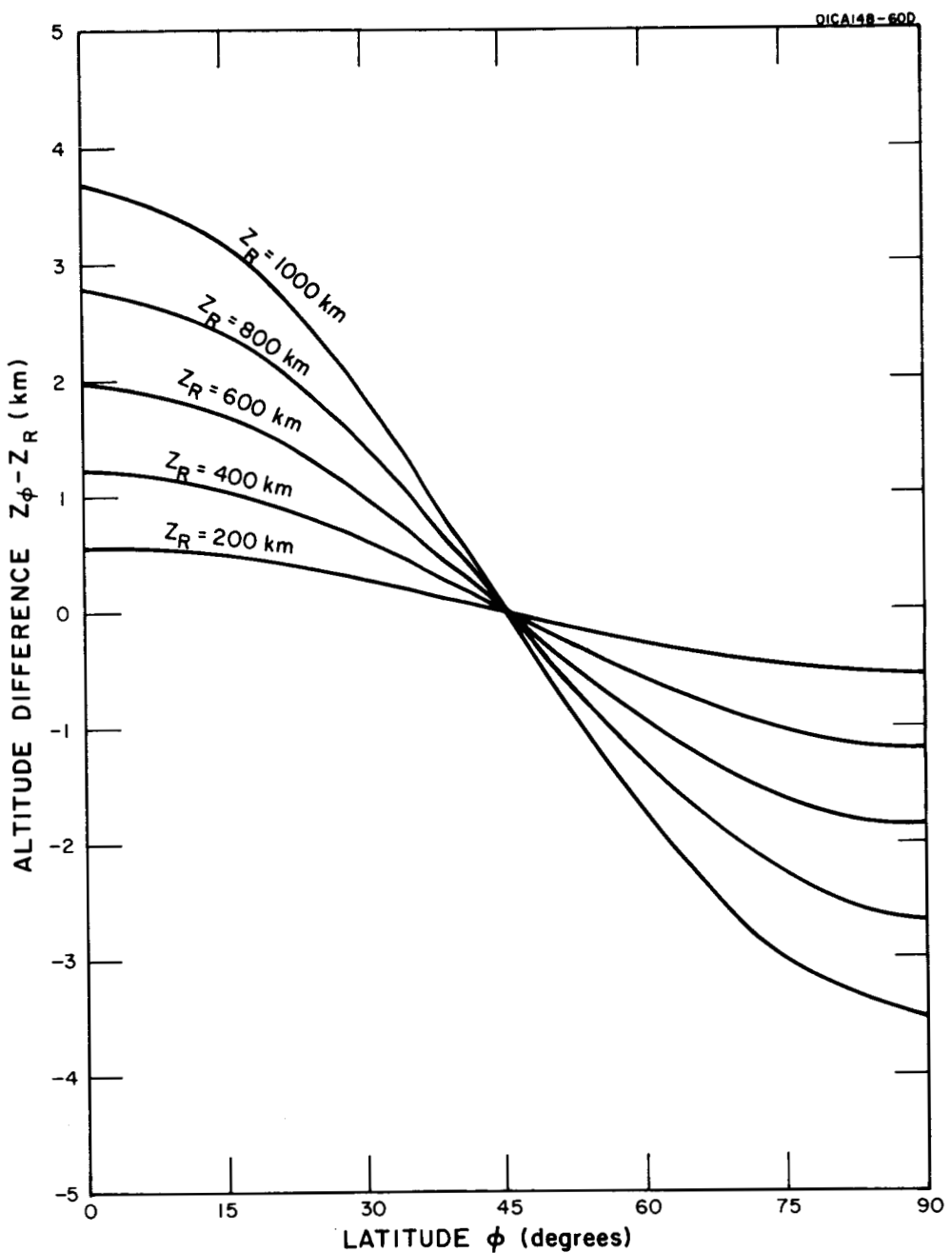


Figure 2.2A. Geometric altitude differences between each of five geopotential surfaces, expressed in equivalent geometric altitudes (200 to 1,000 km) at a reference latitude, and the same five surfaces at other latitudes, all as a function of latitude from 0 to 90 degrees.

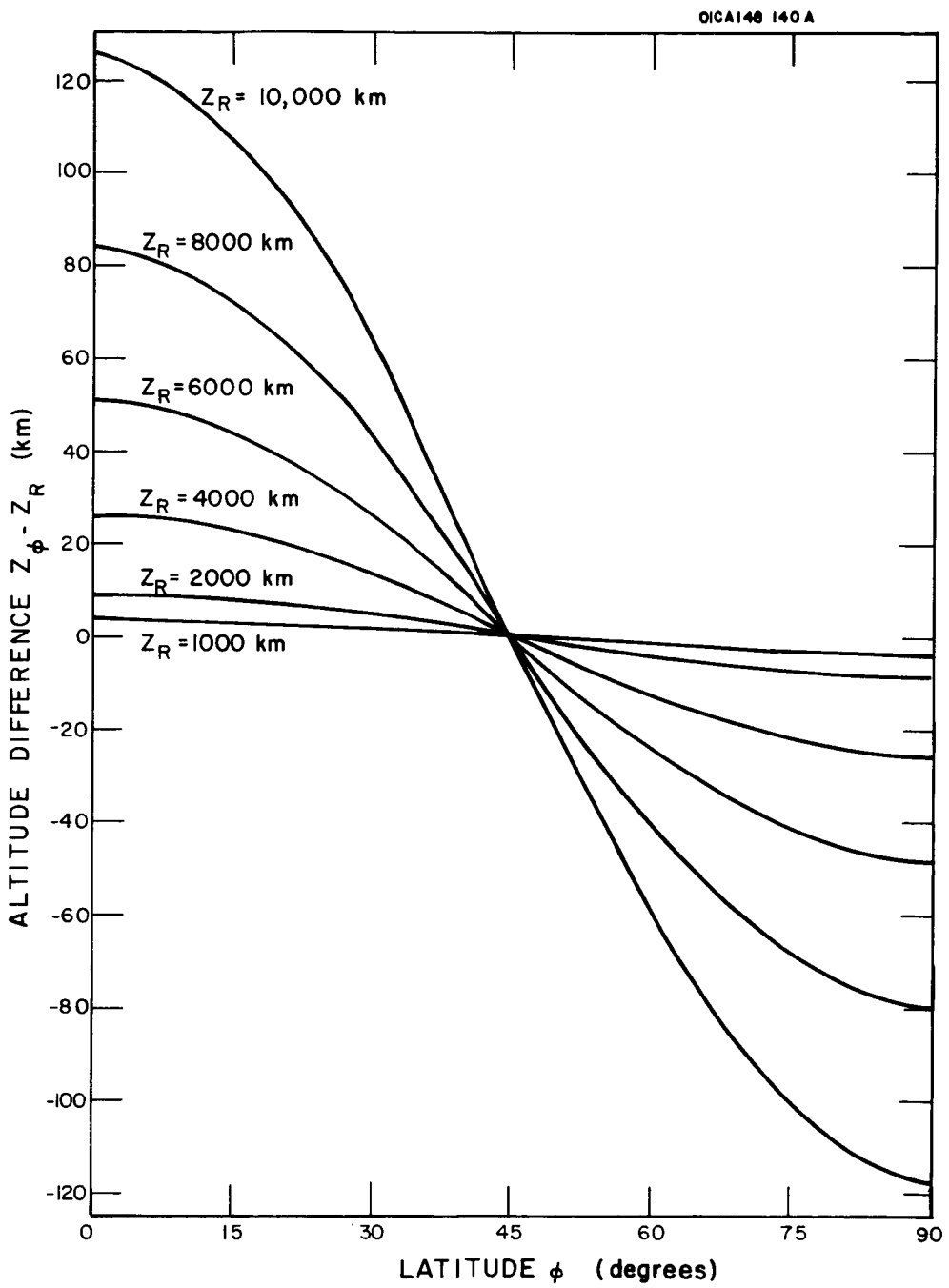


Figure 2.2B. Geometric altitude differences between each of six geopotential surfaces, expressed in equivalent geometric altitudes (1000 to 10,000 km) at a reference latitude, and the same six surfaces at other latitudes, all as a function of latitude from 0 to 90 degrees.

SECTION VI

SPECIFIC DESCRIPTION OF TABLES 3A AND 3B

Tables 3A and 3B present geopotential differences $H_\phi - H_R$ as a function of the first argument pair (columns 1 and 2) for each of seven latitudes (columns 3 through 9). The addition of these differences to the appropriate reference values H_R which appear as the second column of the argument pair leads to the same kind of information as that presented in slightly different geopotential units in Table 50 of the Smithsonian Meteorological Tables (Ref. 8). These data may also be considered as the variation of geopotential of equal geometric altitude surfaces as a function of latitude.

Values of $H_S - H_R$ are given in column 10 of Table 3A with no similar listing in Table 3B. Values of H_S determined from Equations (5) and (6) closely approximate the corresponding values of Standard Atmosphere geopotentials as a function Z prior to the latter set being rounded for tabulation purposes. No values of geopotential are given in the Standard Atmosphere for altitudes above 700 km and consequently no values of $H_S - H_R$ are given in Table 3B for these altitudes.

Figures 3.1A, 3.1B, 3.2A, and 3.2B provide graphical representations of the data of Tables 3A and 3B. Again, the figure notation follows the pattern explained above for Figures 1.1A, etc. and no values of $H_S - H_R$ are given in any of the figures.

TABLE 3A

GEOPOTENTIAL DIFFERENCES BETWEEN A SERIES OF GEOMETRIC ALTITUDE SURFACES AT A
REFERENCE LATITUDE AND THE SAME GEOMETRIC-ALTITUDE SURFACES AT OTHER LATITUDES,
INCLUDING THOSE IN THE US STANDARD ATMOSPHERE,
ALL AS A FUNCTION OF GEOMETRIC ALTITUDE 0 to 1,000 km

GEOMET. ALTITUDE	GEOPO- TENTIAL	LATITUDE ϕ (DEG)							
		0	15	30	45	60	75	90	
z_R (m)	H_R (m')	$H_\phi - H_R$	$H_\phi - H_R$	$H_\phi - H_R$	$H_\phi - H_R$	$H_\phi - H_R$	$H_\phi - H_R$	$H_S - H_R$	
0.	0.0	-0.0	-0.0	-0.0	-0.0	0.0	0.0	0.0	-0
250.	249.9	-0.7	-0.6	-0.3	-0.0	0.3	0.6	0.6	-0
500.	499.9	-1.3	-1.2	-0.7	-0.0	0.6	1.1	1.3	-0
750.	749.9	-2.0	-1.7	-1.0	-0.0	1.0	1.7	1.9	-0
1000.	999.8	-2.7	-2.3	-1.4	-0.0	1.3	2.2	2.6	-0
1250.	1249.7	-3.4	-2.9	-1.7	-0.1	1.6	2.8	3.2	-0
1500.	1499.6	-4.0	-3.5	-2.1	-0.1	1.9	3.4	3.9	-0
1750.	1749.5	-4.7	-4.1	-2.4	-0.1	2.2	3.9	4.5	-0
2000.	1999.3	-5.4	-4.7	-2.7	-0.1	2.5	4.5	5.2	-0
2250.	2249.2	-6.0	-5.2	-3.1	-0.1	2.9	5.0	5.8	-0
2500.	2499.0	-6.7	-5.8	-3.4	-0.1	3.2	5.6	6.5	-0
2750.	2748.8	-7.4	-6.4	-3.8	-0.1	3.5	6.2	7.1	-0
3000.	2998.5	-8.0	-7.0	-4.1	-0.2	3.8	6.7	7.8	-0
3250.	3248.3	-8.7	-7.6	-4.4	-0.2	4.1	7.3	8.4	-0
3500.	3498.0	-9.4	-8.2	-4.8	-0.2	4.4	7.8	9.1	-0
3750.	3747.7	-10.1	-8.7	-5.1	-0.2	4.8	8.4	9.7	-0
4000.	3997.4	-10.7	-9.3	-5.5	-0.2	5.1	9.0	10.4	-0
4250.	4247.1	-11.4	-9.9	-5.8	-0.2	5.4	9.5	11.0	-0
4500.	4496.8	-12.1	-10.5	-6.2	-0.2	5.7	10.1	11.7	-0
4750.	4746.4	-12.7	-11.1	-6.5	-0.2	6.0	10.6	12.3	-0
5000.	4996.0	-13.4	-11.6	-6.8	-0.2	6.4	11.2	13.0	-0
5250.	5245.6	-14.1	-12.2	-7.2	-0.3	6.7	11.8	13.6	-0
5500.	5495.2	-14.7	-12.8	-7.5	-0.3	7.0	12.3	14.3	-0
5750.	5744.8	-15.4	-13.4	-7.9	-0.3	7.3	12.9	14.9	-0
6000.	5994.3	-16.1	-14.0	-8.2	-0.3	7.6	13.4	15.6	-0
6250.	6243.8	-16.8	-14.6	-8.5	-0.3	7.9	14.0	16.2	-0
6500.	6493.3	-17.4	-15.1	-8.9	-0.3	8.3	14.6	16.9	-0
6750.	6742.8	-18.1	-15.7	-9.2	-0.3	8.6	15.1	17.5	-0
7000.	6992.3	-18.8	-16.3	-9.6	-0.3	8.9	15.7	18.2	-0
7250.	7241.7	-19.4	-16.9	-9.9	-0.4	9.2	16.2	18.8	-0
7500.	7491.1	-20.1	-17.5	-10.3	-0.4	9.5	16.8	19.5	-0
7750.	7740.5	-20.8	-18.1	-10.6	-0.4	9.8	17.4	20.1	-0
8000.	7989.9	-21.5	-18.6	-10.9	-0.4	10.2	17.9	20.8	-0
8250.	8239.3	-22.1	-19.2	-11.3	-0.4	10.5	18.5	21.4	-0
8500.	8488.6	-22.8	-19.8	-11.6	-0.4	10.8	19.0	22.0	-0
8750.	8737.9	-23.5	-20.4	-12.0	-0.4	11.1	19.6	22.7	-0
9000.	8987.2	-24.1	-21.0	-12.3	-0.4	11.4	20.2	23.3	-0
9250.	9236.5	-24.8	-21.6	-12.7	-0.5	11.8	20.7	24.0	-0
9500.	9485.8	-25.5	-22.1	-13.0	-0.5	12.1	21.3	24.6	-0
9750.	9735.0	-26.1	-22.7	-13.3	-0.5	12.4	21.8	25.3	-0

TABLE 3A CONTINUED

GEOMET. ALTITUDE	GEOPO- TENTIAL	LATITUDE ϕ (DEG)							
		0	15	30	45	60	75	90	
Z_R (m)	H_R (m')	$H - H_R$	$H_\phi - H_R$	$H_\phi - H_R$	$H_\phi - H_R$	$H_\phi - H_R$	$H_\phi - H_R$	$H_S - H_R$	
10000.	9984.2	-26.8	-23.3	-13.7	-0.5	12.7	22.4	25.9	-0.0
10250.	10233.4	-27.5	-23.9	-14.0	-0.5	13.0	23.0	26.6	-0.0
10500.	10482.6	-28.2	-24.5	-14.4	-0.5	13.3	23.5	27.2	-0.0
10750.	10731.8	-28.8	-25.0	-14.7	-0.5	13.7	24.1	27.9	-0.0
11000.	10980.9	-29.5	-25.6	-15.0	-0.6	14.0	24.6	28.5	-0.0
11500.	11479.2	-30.8	-26.8	-15.7	-0.6	14.6	25.8	29.8	-0.0
12000.	11977.3	-32.2	-28.0	-16.4	-0.6	15.3	26.9	31.1	-0.0
12500.	12475.4	-33.5	-29.1	-17.1	-0.6	15.9	28.0	32.4	-0.0
13000.	12973.4	-34.9	-30.3	-17.8	-0.7	16.5	29.1	33.7	-0.0
13500.	13471.3	-36.2	-31.5	-18.5	-0.7	17.2	30.2	35.0	-0.0
14000.	13969.2	-37.6	-32.6	-19.2	-0.7	17.8	31.4	36.3	-0.0
14500.	14467.0	-38.9	-33.8	-19.8	-0.7	18.4	32.5	37.6	-0.0
15000.	14964.6	-40.2	-35.0	-20.5	-0.8	19.1	33.6	38.9	-0.0
15500.	15462.2	-41.6	-36.1	-21.2	-0.8	19.7	34.7	40.2	-0.0
16000.	15959.8	-42.9	-37.3	-21.9	-0.8	20.3	35.8	41.5	-0.0
16500.	16457.2	-44.3	-38.5	-22.6	-0.8	21.0	37.0	42.8	-0.0
17000.	16954.6	-45.6	-39.6	-23.3	-0.9	21.6	38.1	44.1	-0.0
17500.	17451.9	-46.9	-40.8	-23.9	-0.9	22.3	39.2	45.4	-0.0
18000.	17949.1	-48.3	-42.0	-24.6	-0.9	22.9	40.3	46.7	-0.0
18500.	18446.3	-49.6	-43.1	-25.3	-0.9	23.5	41.4	48.0	-0.0
19000.	18943.3	-51.0	-44.3	-26.0	-1.0	24.2	42.6	49.3	-0.0
19500.	19440.3	-52.3	-45.5	-26.7	-1.0	24.8	43.7	50.6	-0.0
20000.	19937.2	-53.7	-46.6	-27.4	-1.0	25.4	44.8	51.9	-0.0
20500.	20434.1	-55.0	-47.8	-28.1	-1.0	26.1	45.9	53.2	-0.0
21000.	20930.8	-56.3	-49.0	-28.7	-1.1	26.7	47.0	54.5	-0.0
21500.	21427.5	-57.7	-50.1	-29.4	-1.1	27.3	48.2	55.8	-0.0
22000.	21924.1	-59.0	-51.3	-30.1	-1.1	28.0	49.3	57.1	-0.0
22500.	22420.6	-60.4	-52.5	-30.8	-1.1	28.6	50.4	58.4	-0.0
23000.	22917.0	-61.7	-53.6	-31.5	-1.1	29.3	51.5	59.7	-0.0
23500.	23413.4	-63.1	-54.8	-32.2	-1.2	29.9	52.7	61.0	-0.0
24000.	23909.7	-64.4	-56.0	-32.9	-1.2	30.5	53.8	62.3	-0.0
24500.	24405.9	-65.7	-57.1	-33.5	-1.2	31.2	54.9	63.6	-0.0
25000.	24902.0	-67.1	-58.3	-34.2	-1.3	31.8	56.0	64.9	-0.0
25500.	25398.1	-68.4	-59.5	-34.9	-1.3	32.4	57.1	66.2	-0.0
26000.	25894.0	-69.8	-60.6	-35.6	-1.3	33.1	58.3	67.5	-0.0
26500.	26389.9	-71.1	-61.8	-36.3	-1.3	33.7	59.4	68.8	-0.0
27000.	26885.8	-72.5	-63.0	-37.0	-1.4	34.3	60.5	70.1	-0.0
27500.	27381.5	-73.8	-64.1	-37.6	-1.4	35.0	61.6	71.4	-0.0
28000.	27877.2	-75.2	-65.3	-38.3	-1.4	35.6	62.7	72.7	-0.0
28500.	28372.7	-76.5	-66.5	-39.0	-1.4	36.3	63.9	74.0	-0.0
29000.	28868.3	-77.8	-67.6	-39.7	-1.5	36.9	65.0	75.3	-0.0
29500.	29363.7	-79.2	-68.8	-40.4	-1.5	37.5	66.1	76.6	-0.0

TABLE 3A CONTINUED

GEOMET. ALTITUDE	GEOPOTENTIAL	0	LATITUDE ϕ (DEG)						
			15	30	45	60	75	90	
20000.	29859.0	-80.5	-70.0	-41.1	-1.5	38.2	67.2	77.9	-0.0
30500.	30354.3	-81.9	-71.1	-41.8	-1.5	38.8	68.4	79.2	-0.0
31000.	30849.5	-83.2	-72.3	-42.4	-1.6	39.4	69.5	80.5	-0.0
31500.	31344.6	-84.6	-73.5	-43.1	-1.6	40.1	70.6	81.8	-0.0
32000.	31839.7	-85.9	-74.6	-43.8	-1.6	40.7	71.7	83.1	-0.0
33000.	32829.5	-88.6	-77.0	-45.2	-1.7	42.0	74.0	85.7	-0.0
34000.	33819.1	-91.3	-79.3	-46.6	-1.7	43.3	76.2	88.3	-0.0
35000.	34808.3	-94.0	-81.6	-47.9	-1.8	44.5	78.5	90.9	-0.0
36000.	35797.2	-96.7	-84.0	-49.3	-1.8	45.8	80.7	93.5	-0.0
37000.	36785.8	-99.3	-86.3	-50.7	-1.9	47.1	82.9	96.1	-0.0
38000.	37774.1	-102.0	-88.6	-52.0	-1.9	48.4	85.2	98.7	-0.0
39000.	38762.1	-104.7	-91.0	-53.4	-2.0	49.6	87.4	101.3	-0.0
40000.	39749.8	-107.4	-93.3	-54.8	-2.0	50.9	89.7	103.9	-0.0
41000.	40737.2	-110.1	-95.7	-56.2	-2.1	52.2	91.9	106.5	-0.0
42000.	41724.3	-112.8	-98.0	-57.5	-2.1	53.5	94.2	109.1	-0.0
43000.	42711.0	-115.5	-100.3	-58.9	-2.2	54.7	96.4	111.7	-0.0
44000.	43697.5	-118.2	-102.7	-60.3	-2.2	56.0	98.7	114.3	-0.0
45000.	44683.6	-120.9	-105.0	-61.7	-2.3	57.3	100.9	116.9	-0.0
46000.	45669.5	-123.6	-107.3	-63.0	-2.3	58.6	103.2	119.5	-0.0
47000.	46655.0	-126.2	-109.7	-64.4	-2.4	59.8	105.4	122.1	-0.0
48000.	47640.2	-128.9	-112.0	-65.8	-2.4	61.1	107.7	124.7	-0.1
49000.	48625.1	-131.6	-114.4	-67.1	-2.5	62.4	109.9	127.3	-0.1
50000.	49609.7	-134.3	-116.7	-68.5	-2.5	63.7	112.1	129.9	-0.1
51000.	50594.0	-137.0	-119.0	-69.9	-2.6	64.9	114.4	132.5	-0.1
52000.	51578.0	-139.7	-121.4	-71.3	-2.6	66.2	116.6	135.1	-0.1
53000.	52561.7	-142.4	-123.7	-72.6	-2.7	67.5	118.9	137.7	-0.1
54000.	53545.1	-145.1	-126.1	-74.0	-2.7	68.8	121.1	140.3	-0.1
55000.	54528.2	-147.8	-128.4	-75.4	-2.8	70.0	123.4	142.9	-0.1
56000.	55510.9	-150.5	-130.7	-76.8	-2.8	71.3	125.6	145.6	-0.1
57000.	56493.4	-153.2	-133.1	-78.1	-2.9	72.6	127.9	148.2	-0.1
58000.	57475.5	-155.9	-135.4	-79.5	-2.9	73.9	130.1	150.8	-0.1
59000.	58457.4	-158.6	-137.8	-80.9	-3.0	75.1	132.4	153.4	-0.1
60000.	59438.9	-161.2	-140.1	-82.2	-3.0	76.4	134.6	156.0	-0.1
61000.	60420.2	-163.9	-142.4	-83.6	-3.1	77.7	136.9	158.6	-0.1
62000.	61401.1	-166.6	-144.8	-85.0	-3.1	79.0	139.1	161.2	-0.1
63000.	62381.7	-169.3	-147.1	-86.4	-3.2	80.3	141.4	163.8	-0.1
64000.	63362.0	-172.0	-149.5	-87.7	-3.2	81.5	143.6	166.4	-0.1
65000.	64342.0	-174.7	-151.8	-89.1	-3.3	82.8	145.9	169.0	-0.1
66000.	65321.7	-177.4	-154.1	-90.5	-3.3	84.1	148.1	171.6	-0.1
67000.	66301.1	-180.1	-156.5	-91.9	-3.4	85.4	150.4	174.2	-0.1
68000.	67280.2	-182.8	-158.8	-93.2	-3.4	86.6	152.6	176.8	-0.1
69000.	68259.0	-185.5	-161.2	-94.6	-3.5	87.9	154.9	179.4	-0.1

TABLE 3A CONTINUED

GEOMETRIC ALTITUDE	GEOPOTENTIAL	0	15	LATITUDE ϕ (DEG)					
				30	45	60	75	90	
Z _R (m)	H _R (m')	H _φ -H _R	H _S -H _R						
70000.	69237.5	-188.2	-163.5	-96.0	-3.5	89.2	157.1	182.0	-0.1
71000.	70215.7	-190.9	-165.8	-97.4	-3.6	90.5	159.4	184.6	-0.1
72000.	71193.6	-193.6	-168.2	-98.7	-3.6	91.7	161.6	187.3	-0.1
73000.	72171.2	-196.3	-170.5	-100.1	-3.7	93.0	163.9	189.9	-0.1
74000.	73148.4	-199.0	-172.9	-101.5	-3.7	94.3	166.1	192.5	-0.1
75000.	74125.4	-201.7	-175.2	-102.9	-3.8	95.6	168.4	195.1	-0.1
76000.	75102.0	-204.4	-177.6	-104.2	-3.8	96.9	170.6	197.7	-0.1
77000.	76078.4	-207.1	-179.9	-105.6	-3.9	98.1	172.9	200.3	-0.1
78000.	77054.5	-209.8	-182.2	-107.0	-3.9	99.4	175.1	202.9	-0.1
79000.	78030.2	-212.5	-184.6	-108.4	-4.0	100.7	177.4	205.5	-0.2
80000.	79005.7	-215.2	-186.9	-109.8	-4.0	102.0	179.6	208.1	-0.2
81000.	79980.8	-217.9	-189.3	-111.1	-4.1	103.2	181.9	210.7	-0.2
82000.	80955.7	-220.6	-191.6	-112.5	-4.1	104.5	184.1	213.3	-0.2
83000.	81930.2	-223.3	-194.0	-113.9	-4.2	105.8	186.4	216.0	-0.2
84000.	82904.4	-226.0	-196.3	-115.3	-4.2	107.1	188.7	218.6	-0.2
85000.	83878.4	-228.7	-198.7	-116.6	-4.3	108.4	190.9	221.2	-0.2
86000.	84852.0	-231.4	-201.0	-118.0	-4.3	109.6	193.2	223.8	-0.2
87000.	85825.3	-234.1	-203.3	-119.4	-4.4	110.9	195.4	226.4	-0.2
88000.	86798.4	-236.8	-205.7	-120.8	-4.4	112.2	197.7	229.0	-0.2
89000.	87771.1	-239.5	-208.0	-122.1	-4.5	113.5	199.9	231.6	-0.2
90000.	88743.5	-242.2	-210.4	-123.5	-4.5	114.8	202.2	234.2	-0.2
92000.	90687.4	-247.6	-215.1	-126.3	-4.6	117.3	206.7	239.5	-0.2
94000.	92630.2	-253.0	-219.8	-129.0	-4.7	119.9	211.2	244.7	-0.2
96000.	94571.7	-258.4	-224.5	-131.8	-4.8	122.4	215.7	249.9	-0.2
98000.	96512.1	-263.8	-229.1	-134.5	-4.9	125.0	220.2	255.1	-0.3
100000.	98451.2	-269.2	-233.8	-137.3	-5.0	127.6	224.7	260.4	-0.3
102000.	100389.1	-274.6	-238.5	-140.1	-5.1	130.1	229.2	265.6	-0.3
104000.	102325.9	-280.0	-243.2	-142.8	-5.2	132.7	233.7	270.8	-0.3
106000.	104261.4	-285.4	-247.9	-145.6	-5.3	135.2	238.2	276.0	-0.3
108000.	106195.7	-290.8	-252.6	-148.3	-5.4	137.8	242.8	281.3	-0.3
110000.	108128.8	-296.2	-257.3	-151.1	-5.5	140.4	247.3	286.5	-0.3
112000.	110060.8	-301.6	-262.0	-153.8	-5.6	142.9	251.8	291.7	-0.3
114000.	111991.5	-307.0	-266.7	-156.6	-5.7	145.5	256.3	296.9	-0.4
116000.	113921.1	-312.4	-271.4	-159.4	-5.8	148.1	260.8	302.2	-0.4
118000.	115849.5	-317.8	-276.1	-162.1	-5.9	150.6	265.3	307.4	-0.4
120000.	117776.6	-323.2	-280.8	-164.9	-6.0	153.2	269.9	312.6	-0.4
125000.	122589.3	-336.8	-292.6	-171.8	-6.3	159.6	281.1	325.7	-0.4
130000.	127394.6	-350.3	-304.3	-178.7	-6.5	166.0	292.5	338.8	-0.5
135000.	132192.6	-363.8	-316.1	-185.6	-6.8	172.4	303.7	351.9	-0.5
140000.	136983.1	-377.4	-327.8	-192.5	-7.0	178.8	315.1	365.0	-0.6
145000.	141766.2	-390.9	-339.6	-199.4	-7.3	185.2	326.3	378.1	-0.6
150000.	146542.0	-404.4	-351.4	-206.3	-7.5	191.7	337.7	391.2	-0.7
155000.	151310.5	-418.0	-363.1	-213.2	-7.8	198.1	349.0	404.3	-0.7
160000.	156071.6	-431.5	-374.9	-220.1	-8.1	204.5	360.3	417.4	-0.8
165000.	160825.5	-445.1	-386.7	-227.0	-8.3	210.9	371.6	430.5	-0.9

TABLE 3A CONTINUED

GEOMFT. ALTITUDE	GEOPO- TENTIAL	0	15	30	45	60	LATITUDE ϕ (DEG)		90
							H _{φ-H} _R	H _{φ-H} _R	
170.	165572.0	-458.6	-398.5	-233.9	-8.5	217.4	382.9	443.7	-0.9
175.	170311.3	-472.2	-410.3	-240.9	-8.8	223.8	394.3	456.8	-1.0
180.	175043.4	-485.8	-422.0	-247.8	-9.1	230.2	405.6	469.9	-1.1
185.	179768.2	-499.4	-433.9	-254.7	-9.3	236.7	416.9	483.0	-1.1
190.	184485.8	-512.9	-445.6	-261.6	-9.6	243.1	428.2	496.2	-1.2
195.	189196.2	-526.5	-457.4	-268.6	-9.8	249.5	439.6	509.3	-1.3
200.	193899.4	-540.1	-469.2	-275.5	-10.1	256.0	450.9	522.4	-1.4
205.	198595.4	-553.7	-481.0	-282.4	-10.3	262.4	462.3	535.6	-1.5
210.	203284.3	-567.3	-492.8	-289.3	-10.6	268.9	473.6	548.7	-1.5
215.	207966.1	-580.9	-504.6	-296.3	-10.8	275.3	484.9	561.8	-1.6
220.	212640.7	-594.5	-516.4	-303.2	-11.1	281.7	496.3	575.0	-1.7
225.	217308.2	-608.0	-528.3	-310.2	-11.3	288.2	507.7	588.2	-1.8
230.	221968.7	-621.7	-540.1	-317.1	-11.6	294.6	519.0	601.3	-1.9
235.	226622.1	-635.2	-551.9	-324.0	-11.8	301.1	530.4	614.5	-2.0
240.	231268.4	-648.9	-563.7	-331.0	-12.1	307.5	541.7	627.6	-2.2
245.	235907.7	-662.5	-575.5	-337.9	-12.4	313.9	553.1	640.8	-2.3
250.	240539.9	-676.0	-587.3	-344.8	-12.6	320.4	564.4	653.9	-2.4
255.	245165.2	-689.7	-599.2	-351.8	-12.9	326.9	575.8	667.1	-2.5
260.	249783.5	-703.3	-611.0	-358.7	-13.1	333.3	587.2	680.3	-2.6
265.	254394.8	-716.9	-622.8	-365.7	-13.4	339.8	598.5	693.5	-2.8
270.	258999.1	-730.5	-634.7	-372.6	-13.6	346.2	609.9	706.6	-2.9
275.	263596.5	-744.1	-646.5	-379.6	-13.9	352.7	621.3	719.8	-3.0
280.	268187.0	-757.7	-658.3	-386.5	-14.1	359.2	632.7	733.0	-3.2
285.	272770.5	-771.4	-670.2	-393.5	-14.4	365.6	644.0	746.1	-3.3
290.	277347.2	-785.0	-682.0	-400.4	-14.6	372.1	655.4	759.3	-3.5
295.	281917.0	-798.7	-693.9	-407.4	-14.9	378.5	666.8	772.5	-3.6
300.	286479.9	-812.3	-705.7	-414.3	-15.1	385.0	678.2	785.7	-3.8
310.	295585.2	-839.5	-729.4	-428.2	-15.7	397.9	700.9	812.1	-4.1
320.	304663.2	-866.8	-753.1	-442.1	-16.1	410.8	723.7	838.5	-4.4
330.	313714.0	-894.1	-776.8	-456.1	-16.7	423.8	746.5	864.9	-4.8
340.	322737.9	-921.4	-800.5	-470.0	-17.2	436.7	769.3	891.2	-5.2
350.	331734.8	-948.7	-824.2	-483.9	-17.7	449.6	792.0	917.6	-5.6
360.	340704.9	-976.0	-847.9	-497.8	-18.2	462.6	814.9	944.1	-6.0
370.	349648.4	-1003.3	-871.6	-511.8	-18.7	475.5	837.7	970.5	-6.4
380.	358565.3	-1030.6	-895.4	-525.7	-19.2	488.4	860.4	996.9	-6.9
390.	367455.8	-1057.9	-919.1	-539.6	-19.7	501.4	883.3	1023.3	-7.3
400.	376320.0	-1085.2	-942.8	-553.5	-20.2	514.4	906.1	1049.8	-7.8
410.	385158.0	-1112.6	-966.6	-567.5	-20.7	527.3	928.9	1076.2	-8.3
420.	393969.9	-1139.9	-990.3	-581.4	-21.3	540.2	951.7	1102.6	-8.9
430.	402755.7	-1167.2	-1014.0	-595.3	-21.7	553.2	974.5	1129.1	-9.4
440.	411515.8	-1194.5	-1037.8	-609.3	-22.3	566.2	997.3	1155.5	-10.0
450.	420250.1	-1221.9	-1061.5	-623.3	-22.8	579.1	1020.1	1181.9	-10.6
460.	428958.9	-1249.2	-1085.3	-637.2	-23.3	592.0	1043.0	1208.3	-11.2
470.	437642.0	-1276.5	-1109.0	-651.1	-23.8	605.0	1065.3	1234.8	-11.9
480.	446299.8	-1303.9	-1132.8	-665.1	-24.3	618.0	1088.6	1261.2	-12.5
490.	454932.3	-1331.2	-1156.6	-679.0	-24.8	630.9	1111.4	1287.7	-13.2

TABLE 3A CONCLUDED

GEOMETRIC ALTITUDE	GEOPOTENTIAL	LATITUDE ϕ (DEG)							
		0	15	30	45	60	75	90	
γ_R (km)	H_R (m')	$H_\phi - H_R$	$H_\phi - H_R$	$H_\phi - H_R$	$H_\phi - H_R$	$H_\phi - H_R$	$H_\phi - H_R$	$H_\phi - H_R$	$H_S - H_R$
500.	463539.6	-1358.6	-1180.3	-693.0	-25.3	643.9	1134.3	1314.1	-13.9
510.	472121.8	-1385.9	-1204.0	-706.9	-25.8	656.9	1157.1	1340.6	-14.6
520.	480679.1	-1413.2	-1227.8	-720.9	-26.4	669.8	1179.9	1367.0	-15.4
530.	489211.6	-1440.6	-1251.6	-734.8	-26.9	682.8	1202.7	1393.5	-16.2
540.	497719.2	-1467.9	-1275.3	-748.7	-27.3	695.7	1225.6	1419.9	-17.0
550.	506202.3	-1495.2	-1299.0	-762.7	-27.9	708.7	1248.4	1446.4	-17.8
560.	514660.8	-1522.6	-1322.8	-776.6	-28.4	721.6	1271.2	1472.8	-18.7
570.	523095.0	-1549.9	-1346.5	-790.6	-28.9	734.6	1294.0	1499.2	-19.5
580.	531504.7	-1577.2	-1370.2	-804.5	-29.4	747.6	1316.9	1525.7	-20.4
590.	539890.3	-1604.5	-1394.0	-818.4	-29.9	760.5	1339.7	1552.1	-21.4
600.	548251.8	-1631.9	-1417.8	-832.4	-30.4	773.4	1362.5	1578.5	-22.3
610.	556589.3	-1659.2	-1441.5	-846.3	-30.9	786.4	1385.3	1604.9	-23.3
620.	564902.8	-1686.5	-1465.2	-860.2	-31.4	799.4	1408.1	1631.4	-24.3
630.	573192.6	-1713.8	-1488.9	-874.2	-31.9	812.3	1430.9	1657.8	-25.3
640.	581458.6	-1741.1	-1512.7	-888.1	-32.5	825.2	1453.7	1684.2	-26.4
650.	589701.1	-1768.4	-1536.4	-902.0	-32.9	838.2	1476.5	1710.7	-27.5
660.	597920.1	-1795.7	-1560.1	-915.9	-33.5	851.1	1499.3	1737.1	-28.6
670.	606115.7	-1823.0	-1583.8	-929.9	-34.0	864.0	1522.1	1763.4	-29.7
680.	614288.0	-1850.3	-1607.5	-943.8	-34.5	876.9	1544.8	1789.8	-30.9
690.	622437.0	-1877.6	-1631.2	-957.7	-35.0	889.9	1567.7	1816.3	-32.1
700.	630563.0	-1904.8	-1654.9	-971.6	-35.5	902.8	1590.4	1842.6	-33.3
710.	638666.1	-1932.1	-1678.6	-985.6	-36.0	915.8	1613.2	1869.0	
720.	646746.2	-1959.4	-1702.3	-999.5	-36.5	928.7	1635.9	1895.3	
730.	654803.4	-1986.6	-1726.0	-1013.3	-37.0	941.6	1658.7	1921.8	
740.	662838.0	-2013.9	-1749.6	-1027.2	-37.5	954.5	1681.5	1948.1	
750.	670850.0	-2041.1	-1773.3	-1041.2	-38.1	967.4	1704.2	1974.4	
760.	678839.5	-2068.4	-1797.0	-1055.1	-38.6	980.3	1726.9	2000.8	
770.	686806.5	-2095.6	-1820.6	-1068.9	-39.1	993.2	1749.7	2027.1	
780.	694751.3	-2122.8	-1844.3	-1082.8	-39.6	1006.1	1772.4	2053.5	
790.	702673.8	-2150.0	-1867.9	-1096.7	-40.1	1019.0	1795.1	2079.8	
800.	710574.1	-2177.2	-1891.5	-1110.5	-40.6	1032.0	1817.9	2106.1	
820.	726308.7	-2231.6	-1938.8	-1138.3	-41.6	1057.7	1863.2	2158.7	
840.	741955.9	-2285.9	-1985.9	-1166.0	-42.6	1083.5	1908.6	2211.3	
860.	757516.4	-2340.2	-2033.2	-1193.7	-43.6	1109.2	1953.9	2263.8	
880.	772990.8	-2394.4	-2080.3	-1221.4	-44.6	1134.9	1999.3	2316.3	
900.	788380.0	-2448.7	-2127.4	-1249.1	-45.7	1160.6	2044.5	2368.7	
920.	803684.5	-2502.8	-2174.4	-1276.6	-46.6	1186.3	2089.8	2421.2	
940.	818905.2	-2557.0	-2221.5	-1304.3	-47.7	1211.9	2134.9	2473.5	
960.	834042.7	-2611.0	-2268.4	-1331.8	-48.7	1237.6	2180.1	2525.8	
980.	849097.6	-2665.1	-2315.4	-1359.4	-49.7	1263.2	2225.2	2578.1	
1000.	864070.7	-2719.0	-2362.3	-1386.9	-50.7	1288.8	2270.3	2630.3	

TABLE 3B

GEOPOTENTIAL DIFFERENCES BETWEEN A SERIES OF GEOMETRIC-ALTITUDE SURFACES AT A
REFERENCE LATITUDE AND THE SAME GEOMETRIC-ALTITUDE SURFACES AT OTHER LATITUDES,
ALL AS A FUNCTION OF GEOMETRIC ALTITUDE, 1,000 to 10,000 km

GEOMET. ALT.	GEOPO- TEN.	LATITUDE (DEG)						
		0	15	30	45	60	75	90
Z_R (km)	H_R (km')	$H_\phi - H_R$	$H_\phi - H_R$	$H_\phi - H_R$	$H_\phi - H_\phi$	$H_\phi - H_R$	$H_\phi - H_R$	$H_\phi - H_R$
1000.	864.07	-2.72	-2.36	-1.39	-0.05	1.29	2.27	2.63
1020.	878.96	-2.77	-2.41	-1.41	-0.05	1.31	2.32	2.68
1040.	893.77	-2.83	-2.46	-1.44	-0.05	1.34	2.36	2.73
1060.	908.51	-2.88	-2.50	-1.47	-0.05	1.37	2.41	2.79
1080.	923.16	-2.93	-2.55	-1.50	-0.05	1.39	2.45	2.84
1100.	937.73	-2.99	-2.60	-1.52	-0.06	1.42	2.49	2.89
1120.	952.23	-3.04	-2.64	-1.55	-0.06	1.44	2.54	2.94
1140.	966.65	-3.10	-2.69	-1.58	-0.06	1.47	2.58	2.99
1160.	980.99	-3.15	-2.74	-1.61	-0.06	1.49	2.63	3.05
1180.	995.25	-3.20	-2.78	-1.63	-0.06	1.52	2.67	3.10
1200.	1009.44	-3.26	-2.83	-1.66	-0.06	1.54	2.72	3.15
1220.	1023.56	-3.31	-2.87	-1.69	-0.06	1.57	2.76	3.20
1240.	1037.60	-3.36	-2.92	-1.72	-0.06	1.59	2.81	3.25
1260.	1051.57	-3.42	-2.97	-1.74	-0.06	1.62	2.85	3.30
1280.	1065.46	-3.47	-3.01	-1.77	-0.06	1.64	2.90	3.36
1300.	1079.28	-3.52	-3.06	-1.80	-0.07	1.67	2.94	3.41
1320.	1093.03	-3.57	-3.11	-1.82	-0.07	1.69	2.98	3.46
1340.	1106.71	-3.63	-3.15	-1.85	-0.07	1.72	3.03	3.51
1360.	1120.31	-3.68	-3.20	-1.88	-0.07	1.74	3.07	3.56
1380.	1133.85	-3.73	-3.24	-1.90	-0.07	1.77	3.12	3.61
1400.	1147.32	-3.79	-3.29	-1.93	-0.07	1.79	3.16	3.66
1420.	1160.71	-3.84	-3.33	-1.96	-0.07	1.82	3.20	3.71
1440.	1174.04	-3.89	-3.38	-1.98	-0.07	1.84	3.25	3.76
1460.	1187.30	-3.94	-3.43	-2.01	-0.07	1.87	3.29	3.81
1480.	1200.50	-4.00	-3.47	-2.04	-0.07	1.89	3.34	3.87
1500.	1213.62	-4.05	-3.52	-2.06	-0.08	1.92	3.38	3.92
1520.	1226.68	-4.10	-3.56	-2.09	-0.08	1.94	3.42	3.97
1540.	1239.67	-4.15	-3.61	-2.12	-0.08	1.97	3.47	4.02
1560.	1252.60	-4.20	-3.65	-2.14	-0.08	1.99	3.51	4.07
1580.	1265.46	-4.26	-3.70	-2.17	-0.08	2.02	3.55	4.12
1600.	1278.26	-4.31	-3.74	-2.20	-0.08	2.04	3.60	4.17
1620.	1290.99	-4.36	-3.79	-2.22	-0.08	2.07	3.64	4.22
1640.	1303.66	-4.41	-3.83	-2.25	-0.08	2.09	3.68	4.27
1660.	1316.27	-4.46	-3.88	-2.28	-0.08	2.12	3.73	4.32
1680.	1328.81	-4.51	-3.92	-2.30	-0.08	2.14	3.77	4.37
1700.	1341.30	-4.57	-3.97	-2.33	-0.09	2.16	3.81	4.42
1720.	1353.71	-4.62	-4.01	-2.36	-0.09	2.19	3.86	4.47
1740.	1366.07	-4.67	-4.06	-2.38	-0.09	2.21	3.90	4.52
1760.	1378.37	-4.72	-4.10	-2.41	-0.09	2.24	3.94	4.57
1780.	1390.61	-4.77	-4.14	-2.43	-0.09	2.26	3.98	4.62

TABLE 3B CONTINUED

GEOMET. ALT.	GEOPO- TEN.	0	LATITUDE ϕ (DEG)					
			15	30	45	60	75	90
Z _R (km)	H _R (km')	H _φ -H _R						
1800.	1402.78	-4.82	-4.19	-2.46	-.09	2.29	4.03	4.67
1820.	1414.90	-4.87	-4.23	-2.49	-.09	2.31	4.07	4.71
1840.	1426.96	-4.92	-4.28	-2.51	-.09	2.33	4.11	4.76
1860.	1438.96	-4.97	-4.32	-2.54	-.09	2.36	4.15	4.81
1880.	1450.90	-5.02	-4.37	-2.56	-.09	2.38	4.20	4.86
1900.	1462.78	-5.07	-4.41	-2.59	-.09	2.41	4.24	4.91
1920.	1474.61	-5.13	-4.45	-2.61	-.10	2.43	4.28	4.96
1940.	1486.38	-5.18	-4.50	-2.64	-.10	2.45	4.32	5.01
1960.	1498.09	-5.23	-4.54	-2.67	-.10	2.48	4.36	5.06
1980.	1509.75	-5.28	-4.58	-2.69	-.10	2.50	4.41	5.11
2000.	1521.35	-5.33	-4.63	-2.72	-.10	2.53	4.45	5.15
2020.	1532.89	-5.38	-4.67	-2.74	-.10	2.55	4.49	5.20
2040.	1544.38	-5.43	-4.71	-2.77	-.10	2.57	4.53	5.25
2060.	1555.82	-5.48	-4.76	-2.79	-.10	2.60	4.57	5.30
2080.	1567.20	-5.53	-4.80	-2.82	-.10	2.62	4.61	5.35
2100.	1578.52	-5.57	-4.84	-2.84	-.10	2.64	4.66	5.39
2120.	1589.80	-5.62	-4.89	-2.87	-.10	2.67	4.70	5.44
2140.	1601.02	-5.67	-4.93	-2.89	-.11	2.69	4.74	5.49
2160.	1612.19	-5.72	-4.97	-2.92	-.11	2.71	4.78	5.54
2180.	1623.30	-5.77	-5.01	-2.94	-.11	2.74	4.82	5.59
2200.	1634.37	-5.82	-5.06	-2.97	-.11	2.76	4.86	5.63
2220.	1645.38	-5.87	-5.10	-2.99	-.11	2.78	4.90	5.68
2240.	1656.34	-5.92	-5.14	-3.02	-.11	2.81	4.94	5.73
2260.	1667.25	-5.97	-5.19	-3.04	-.11	2.83	4.98	5.77
2280.	1678.11	-6.02	-5.23	-3.07	-.11	2.85	5.02	5.82
2300.	1688.92	-6.07	-5.27	-3.09	-.11	2.88	5.07	5.87
2320.	1699.68	-6.11	-5.31	-3.12	-.11	2.90	5.11	5.92
2340.	1710.39	-6.16	-5.35	-3.14	-.11	2.92	5.15	5.96
2360.	1721.05	-6.21	-5.40	-3.17	-.12	2.94	5.19	6.01
2380.	1731.66	-6.26	-5.44	-3.19	-.12	2.97	5.23	6.06
2400.	1742.22	-6.31	-5.48	-3.22	-.12	2.99	5.27	6.10
2420.	1752.74	-6.35	-5.52	-3.24	-.12	3.01	5.31	6.15
2440.	1763.21	-6.40	-5.56	-3.27	-.12	3.04	5.35	6.20
2460.	1773.63	-6.45	-5.60	-3.29	-.12	3.06	5.39	6.24
2480.	1784.00	-6.50	-5.65	-3.31	-.12	3.08	5.43	6.29
2500.	1794.32	-6.55	-5.69	-3.34	-.12	3.10	5.47	6.33
2520.	1804.60	-6.59	-5.73	-3.36	-.12	3.13	5.51	6.38
2540.	1814.84	-6.64	-5.77	-3.39	-.12	3.15	5.55	6.43
2560.	1825.03	-6.69	-5.81	-3.41	-.12	3.17	5.59	6.47
2580.	1835.17	-6.73	-5.85	-3.44	-.13	3.19	5.63	6.52
2600.	1845.26	-6.78	-5.89	-3.46	-.13	3.22	5.66	6.56
2620.	1855.31	-6.83	-5.93	-3.48	-.13	3.24	5.70	6.61
2640.	1865.32	-6.88	-5.97	-3.51	-.13	3.26	5.74	6.65
2660.	1875.28	-6.92	-6.01	-3.53	-.13	3.28	5.78	6.70
2680.	1885.20	-6.97	-6.06	-3.56	-.13	3.30	5.82	6.74

TABLE 3B CONTINUED

GEOMET. ALT.	GEOPO- TEN.	0	LATITUDE ϕ (DEG)					
			15	30	45	60	75	90
Z _R (km)	H _R (km')	H _φ -H _R						
2700.	1895.08	-7.02	-6.10	-3.58	-1.13	3.33	5.86	6.79
2720.	1904.91	-7.06	-6.14	-3.60	-1.13	3.35	5.90	6.83
2740.	1914.70	-7.11	-6.18	-3.63	-1.13	3.37	5.94	6.88
2760.	1924.44	-7.15	-6.22	-3.65	-1.13	3.39	5.98	6.92
2780.	1934.14	-7.20	-6.26	-3.67	-1.13	3.41	6.01	6.97
2800.	1943.80	-7.25	-6.30	-3.70	-1.13	3.44	6.05	7.01
2820.	1953.42	-7.29	-6.34	-3.72	-1.14	3.46	6.09	7.06
2840.	1963.00	-7.34	-6.38	-3.74	-1.14	3.48	6.13	7.10
2860.	1972.53	-7.38	-6.42	-3.77	-1.14	3.50	6.17	7.15
2880.	1982.02	-7.43	-6.46	-3.79	-1.14	3.52	6.21	7.19
2900.	1991.48	-7.48	-6.50	-3.81	-1.14	3.54	6.24	7.24
2920.	2000.89	-7.52	-6.53	-3.84	-1.14	3.57	6.28	7.28
2940.	2010.26	-7.57	-6.57	-3.86	-1.14	3.59	6.32	7.32
2960.	2019.59	-7.61	-6.61	-3.88	-1.14	3.61	6.36	7.37
2980.	2028.88	-7.66	-6.65	-3.91	-1.14	3.63	6.40	7.41
3000.	2038.13	-7.70	-6.69	-3.93	-1.14	3.65	6.43	7.45
3020.	2047.34	-7.75	-6.73	-3.95	-1.14	3.67	6.47	7.50
3040.	2056.51	-7.79	-6.77	-3.98	-1.15	3.69	6.51	7.54
3060.	2065.65	-7.84	-6.81	-4.00	-1.15	3.72	6.55	7.58
3080.	2074.74	-7.88	-6.85	-4.02	-1.15	3.74	6.58	7.63
3100.	2083.80	-7.93	-6.89	-4.04	-1.15	3.76	6.62	7.67
3120.	2092.81	-7.97	-6.93	-4.07	-1.15	3.78	6.66	7.71
3140.	2101.79	-8.01	-6.96	-4.09	-1.15	3.80	6.70	7.76
3160.	2110.74	-8.06	-7.00	-4.11	-1.15	3.82	6.73	7.80
3180.	2119.64	-8.10	-7.04	-4.13	-1.15	3.84	6.77	7.84
3200.	2128.51	-8.15	-7.08	-4.16	-1.15	3.86	6.81	7.89
3220.	2137.34	-8.19	-7.12	-4.18	-1.15	3.88	6.84	7.93
3240.	2146.13	-8.24	-7.16	-4.20	-1.15	3.91	6.88	7.97
3260.	2154.89	-8.28	-7.19	-4.22	-1.15	3.93	6.92	8.01
3280.	2163.61	-8.32	-7.23	-4.25	-1.16	3.95	6.95	8.06
3300.	2172.29	-8.37	-7.27	-4.27	-1.16	3.97	6.99	8.10
3320.	2180.94	-8.41	-7.31	-4.29	-1.16	3.99	7.03	8.14
3340.	2189.55	-8.45	-7.34	-4.31	-1.16	4.01	7.06	8.18
3360.	2198.13	-8.50	-7.38	-4.33	-1.16	4.03	7.10	8.22
3380.	2206.67	-8.54	-7.42	-4.36	-1.16	4.05	7.13	8.27
3400.	2215.18	-8.58	-7.46	-4.38	-1.16	4.07	7.17	8.31
3420.	2223.65	-8.63	-7.49	-4.40	-1.16	4.09	7.21	8.35
3440.	2232.09	-8.67	-7.53	-4.42	-1.16	4.11	7.24	8.39
3460.	2240.49	-8.71	-7.57	-4.44	-1.16	4.13	7.28	8.43
3480.	2248.86	-8.75	-7.61	-4.47	-1.16	4.15	7.31	8.47
3500.	2257.20	-8.80	-7.64	-4.49	-1.16	4.17	7.35	8.51
3520.	2265.50	-8.84	-7.68	-4.51	-1.16	4.19	7.38	8.56
3540.	2273.77	-8.88	-7.72	-4.53	-1.17	4.21	7.42	8.60
3560.	2282.00	-8.92	-7.75	-4.55	-1.17	4.23	7.45	8.64
3580.	2290.20	-8.97	-7.79	-4.57	-1.17	4.25	7.49	8.68

TABLE 3B CONTINUED

GEOMET. ALT.	GEOPO- TEN.	0	LATITUDE ϕ (DEG)					
			15	30	45	60	75	90
3600.	2298.37	-9.01	-7.83	-4.60	-0.17	4.27	7.53	8.72
3620.	2306.51	-9.05	-7.86	-4.62	-0.17	4.29	7.56	8.76
3640.	2314.61	-9.09	-7.90	-4.64	-0.17	4.31	7.60	8.80
3660.	2322.68	-9.13	-7.94	-4.66	-0.17	4.33	7.63	8.84
3680.	2330.72	-9.18	-7.97	-4.68	-0.17	4.35	7.67	8.88
3700.	2338.73	-9.22	-8.01	-4.70	-0.17	4.37	7.70	8.92
3720.	2346.70	-9.26	-8.04	-4.72	-0.17	4.39	7.73	8.96
3740.	2354.65	-9.30	-8.08	-4.74	-0.17	4.41	7.77	9.00
3760.	2362.56	-9.34	-8.12	-4.77	-0.17	4.43	7.80	9.04
3780.	2370.44	-9.38	-8.15	-4.79	-0.18	4.45	7.84	9.08
3800.	2378.29	-9.42	-8.19	-4.81	-0.18	4.47	7.87	9.12
3820.	2386.11	-9.46	-8.22	-4.83	-0.18	4.49	7.91	9.16
3840.	2393.89	-9.51	-8.26	-4.85	-0.18	4.51	7.94	9.20
3860.	2401.65	-9.55	-8.29	-4.87	-0.18	4.53	7.98	9.24
3880.	2409.38	-9.59	-8.33	-4.89	-0.18	4.55	8.01	9.28
3900.	2417.08	-9.63	-8.36	-4.91	-0.18	4.57	8.04	9.32
3920.	2424.74	-9.67	-8.40	-4.93	-0.18	4.59	8.08	9.36
3940.	2432.38	-9.71	-8.44	-4.95	-0.18	4.60	8.11	9.40
3960.	2439.99	-9.75	-8.47	-4.97	-0.18	4.62	8.14	9.44
3980.	2447.57	-9.79	-8.51	-4.99	-0.18	4.64	8.18	9.48
4000.	2455.12	-9.83	-8.54	-5.01	-0.18	4.66	8.21	9.51
4020.	2462.64	-9.87	-8.57	-5.04	-0.18	4.68	8.25	9.55
4040.	2470.13	-9.91	-8.61	-5.06	-0.18	4.70	8.28	9.59
4060.	2477.59	-9.95	-8.64	-5.08	-0.19	4.72	8.31	9.63
4080.	2485.02	-9.99	-8.68	-5.10	-0.19	4.74	8.35	9.67
4100.	2492.43	-10.03	-8.71	-5.12	-0.19	4.76	8.38	9.71
4120.	2499.81	-10.07	-8.75	-5.14	-0.19	4.78	8.41	9.75
4140.	2507.15	-10.11	-8.78	-5.16	-0.19	4.79	8.45	9.78
4160.	2514.48	-10.15	-8.82	-5.18	-0.19	4.81	8.48	9.82
4180.	2521.77	-10.19	-8.85	-5.20	-0.19	4.83	8.51	9.86
4200.	2529.03	-10.23	-8.88	-5.22	-0.19	4.85	8.54	9.90
4220.	2536.27	-10.26	-8.92	-5.24	-0.19	4.87	8.58	9.94
4240.	2543.48	-10.30	-8.95	-5.26	-0.19	4.89	8.61	9.97
4260.	2550.67	-10.34	-8.99	-5.28	-0.19	4.91	8.64	10.01
4280.	2557.82	-10.38	-9.02	-5.30	-0.19	4.92	8.67	10.05
4300.	2564.95	-10.42	-9.05	-5.32	-0.19	4.94	8.71	10.09
4320.	2572.05	-10.46	-9.09	-5.34	-0.20	4.96	8.74	10.13
4340.	2579.13	-10.50	-9.12	-5.36	-0.20	4.98	8.77	10.16
4360.	2586.18	-10.54	-9.15	-5.38	-0.20	5.00	8.80	10.20
4380.	2593.21	-10.57	-9.19	-5.39	-0.20	5.02	8.84	10.24
4400.	2600.20	-10.61	-9.22	-5.41	-0.20	5.03	8.87	10.27
4420.	2607.17	-10.65	-9.25	-5.43	-0.20	5.05	8.90	10.31
4440.	2614.12	-10.69	-9.29	-5.45	-0.20	5.07	8.93	10.35
4460.	2621.04	-10.73	-9.32	-5.47	-0.20	5.09	8.96	10.39
4480.	2627.93	-10.77	-9.35	-5.49	-0.20	5.11	9.00	10.42

TABLE 3B CONTINUED

GEOMET. ALT.	GFOPO- TEN.	0	LATITUDE ϕ (DEG)					
			15	30	45	60	75	90
Z _R (km)	H _R (km')	H _φ -H _R						
4500.	2634.80	-10.80	-9.39	-5.51	-20	5.12	9.03	10.46
4520.	2641.65	-10.84	-9.42	-5.53	-20	5.14	9.06	10.50
4540.	2648.47	-10.88	-9.45	-5.55	-20	5.16	9.09	10.53
4560.	2655.26	-10.92	-9.48	-5.57	-20	5.18	9.12	10.57
4580.	2662.03	-10.95	-9.52	-5.59	-20	5.20	9.15	10.61
4600.	2668.77	-10.99	-9.55	-5.61	-20	5.21	9.18	10.64
4620.	2675.49	-11.03	-9.58	-5.63	-21	5.23	9.22	10.68
4640.	2682.19	-11.07	-9.61	-5.65	-21	5.25	9.25	10.71
4660.	2688.86	-11.10	-9.65	-5.66	-21	5.27	9.28	10.75
4680.	2695.51	-11.14	-9.68	-5.68	-21	5.28	9.31	10.79
4700.	2702.13	-11.18	-9.71	-5.70	-21	5.30	9.34	10.82
4720.	2708.73	-11.21	-9.74	-5.72	-21	5.32	9.37	10.86
4740.	2715.30	-11.25	-9.78	-5.74	-21	5.34	9.40	10.89
4760.	2721.85	-11.29	-9.81	-5.76	-21	5.35	9.43	10.93
4780.	2728.38	-11.32	-9.84	-5.78	-21	5.37	9.46	10.96
4800.	2734.89	-11.36	-9.87	-5.80	-21	5.39	9.49	11.00
4820.	2741.37	-11.40	-9.90	-5.81	-21	5.41	9.52	11.03
4840.	2747.82	-11.43	-9.93	-5.83	-21	5.42	9.55	11.07
4860.	2754.26	-11.47	-9.97	-5.85	-21	5.44	9.58	11.11
4880.	2760.67	-11.51	-10.00	-5.87	-21	5.46	9.61	11.14
4900.	2767.06	-11.54	-10.03	-5.89	-22	5.47	9.65	11.18
4920.	2773.43	-11.58	-10.06	-5.91	-22	5.49	9.68	11.21
4940.	2779.77	-11.61	-10.09	-5.93	-22	5.51	9.71	11.25
4960.	2786.09	-11.65	-10.12	-5.94	-22	5.53	9.74	11.28
4980.	2792.39	-11.69	-10.15	-5.96	-22	5.54	9.77	11.31
5000.	2798.67	-11.72	-10.18	-5.98	-22	5.56	9.80	11.35
5050.	2814.27	-11.81	-10.26	-6.03	-22	5.60	9.87	11.44
5100.	2829.73	-11.90	-10.34	-6.07	-22	5.64	9.94	11.52
5150.	2845.05	-11.99	-10.42	-6.12	-22	5.69	10.02	11.61
5200.	2860.25	-12.07	-10.49	-6.16	-23	5.73	10.09	11.69
5250.	2875.31	-12.16	-10.56	-6.20	-23	5.77	10.16	11.78
5300.	2890.24	-12.25	-10.64	-6.25	-23	5.81	10.23	11.86
5350.	2905.05	-12.33	-10.71	-6.29	-23	5.86	10.30	11.94
5400.	2919.73	-12.42	-10.97	-6.34	-23	5.89	10.37	12.03
5450.	2934.28	-12.50	-10.86	-6.38	-23	5.93	10.43	12.11
5500.	2948.71	-12.59	-10.94	-6.42	-23	5.97	10.50	12.19
5550.	2963.03	-12.67	-11.01	-6.47	-24	6.01	10.57	12.27
5600.	2977.22	-12.76	-11.08	-6.51	-24	6.05	10.64	12.35
5650.	2991.29	-12.83	-11.15	-6.55	-24	6.09	10.70	12.43
5700.	3005.25	-12.92	-11.23	-6.59	-24	6.13	10.77	12.51
5750.	3019.09	-13.00	-11.30	-6.63	-24	6.17	10.84	12.59
5800.	3032.82	-13.08	-11.37	-6.68	-24	6.21	10.91	12.67
5850.	3046.43	-13.16	-11.44	-6.72	-25	6.25	10.97	12.75
5900.	3059.94	-13.25	-12.51	-6.76	-25	6.28	11.04	12.83
5950.	3073.33	-13.32	-12.58	-6.80	-25	6.32	11.10	12.90

TABLE 3B CONTINUED

GEOMET. ALT.	GEOPO- TEN.	0	15	LATITUDE ϕ (DEG)				
				30	45	60	75	90
Z _R (km)	H _R (km')	H _φ -H _R						
6000.	3086.6	-13.	-12.	-6.8	-3	6.4	11.	13.
6050.	3099.8	-13.	-12.	-6.9	-3	6.4	11.	13.
6100.	3112.9	-14.	-12.	-6.9	-3	6.4	11.	13.
6150.	3125.8	-14.	-12.	-7.0	-3	6.5	11.	13.
6200.	3138.7	-14.	-12.	-7.0	-3	6.5	11.	13.
6250.	3151.5	-14.	-12.	-7.0	-3	6.5	12.	13.
6300.	3164.1	-14.	-12.	-7.1	-3	6.6	12.	13.
6350.	3176.7	-14.	-12.	-7.1	-3	6.6	12.	14.
6400.	3189.2	-14.	-12.	-7.2	-3	6.7	12.	14.
6450.	3201.5	-14.	-12.	-7.2	-3	6.7	12.	14.
6500.	3213.8	-14.	-12.	-7.2	-3	6.7	12.	14.
6550.	3226.0	-14.	-12.	-7.3	-3	6.8	12.	14.
6600.	3238.1	-14.	-12.	-7.3	-3	6.8	12.	14.
6650.	3250.0	-14.	-13.	-7.3	-3	6.8	12.	14.
6700.	3261.9	-14.	-13.	-7.4	-3	6.9	12.	14.
6750.	3273.7	-15.	-13.	-7.4	-3	6.9	12.	14.
6800.	3285.5	-15.	-13.	-7.5	-3	6.9	12.	14.
6850.	3297.1	-15.	-13.	-7.5	-3	7.0	12.	14.
6900.	3308.6	-15.	-13.	-7.5	-3	7.0	12.	14.
6950.	3320.1	-15.	-13.	-7.6	-3	7.0	12.	14.
7000.	3331.4	-15.	-13.	-7.6	-3	7.1	12.	14.
7050.	3342.7	-15.	-13.	-7.6	-3	7.1	13.	15.
7100.	3353.9	-15.	-13.	-7.7	-3	7.1	13.	15.
7150.	3365.0	-15.	-13.	-7.7	-3	7.2	13.	15.
7200.	3376.1	-15.	-13.	-7.7	-3	7.2	13.	15.
7250.	3387.0	-15.	-13.	-7.8	-3	7.2	13.	15.
7300.	3397.9	-15.	-13.	-7.8	-3	7.3	13.	15.
7350.	3408.7	-15.	-13.	-7.9	-3	7.3	13.	15.
7400.	3419.4	-15.	-13.	-7.9	-3	7.3	13.	15.
7450.	3430.1	-16.	-13.	-7.9	-3	7.4	13.	15.
7500.	3440.6	-16.	-14.	-8.0	-3	7.4	13.	15.
7550.	3451.1	-16.	-14.	-8.0	-3	7.4	13.	15.
7600.	3461.5	-16.	-14.	-8.0	-3	7.5	13.	15.
7650.	3471.8	-16.	-14.	-8.1	-3	7.5	13.	15.
7700.	3482.1	-16.	-14.	-8.1	-3	7.5	13.	15.
7750.	3492.3	-16.	-14.	-8.1	-3	7.6	13.	15.
7800.	3502.4	-16.	-14.	-8.2	-3	7.6	13.	15.
7850.	3512.5	-16.	-14.	-8.2	-3	7.6	13.	16.
7900.	3522.4	-16.	-14.	-8.2	-3	7.7	13.	16.
7950.	3532.3	-16.	-14.	-8.3	-3	7.7	14.	16.
8000.	3542.2	-16.	-14.	-8.3	-3	7.7	14.	16.
8050.	3551.9	-16.	-14.	-8.3	-3	7.7	14.	16.
8100.	3561.6	-16.	-14.	-8.4	-3	7.8	14.	16.
8150.	3571.3	-16.	-14.	-8.4	-3	7.8	14.	16.
8200.	3580.8	-17.	-14.	-8.4	-3	7.8	14.	16.

TABLE 3B CONCLUDED

GEOMET. ALT.	GEOPO- TEN.	0	LATITUDE ϕ (DEG)					
			15	30	45	60	75	90
Z _R (km)	H _R (km)	H _φ -H _R						
8250.	3590.3	-17.	-14.	-8.5	-3	7.9	14.	16.
8300.	3599.8	-17.	-14.	-8.5	-3	7.9	14.	16.
8350.	3609.2	-17.	-15.	-8.5	-3	7.9	14.	16.
8400.	3618.5	-17.	-15.	-8.5	-3	7.9	14.	16.
8450.	3627.7	-17.	-15.	-8.6	-3	8.0	14.	16.
8500.	3636.9	-17.	-15.	-8.6	-3	8.0	14.	16.
8550.	3646.0	-17.	-15.	-8.6	-3	8.0	14.	16.
8600.	3655.1	-17.	-15.	-8.7	-3	8.1	14.	16.
8650.	3664.1	-17.	-15.	-8.7	-3	8.1	14.	17.
8700.	3673.0	-17.	-15.	-8.7	-3	8.1	14.	17.
8750.	3681.9	-17.	-15.	-8.8	-3	8.1	14.	17.
8800.	3690.7	-17.	-15.	-8.8	-3	8.2	14.	17.
8850.	3699.5	-17.	-15.	-8.8	-3	8.2	14.	17.
8900.	3708.2	-17.	-15.	-8.9	-3	8.2	15.	17.
8950.	3716.9	-17.	-15.	-8.9	-3	8.3	15.	17.
9000.	3725.5	-17.	-15.	-8.9	-3	8.3	15.	17.
9050.	3734.0	-18.	-15.	-8.9	-3	8.3	15.	17.
9100.	3742.5	-18.	-15.	-9.0	-3	8.3	15.	17.
9150.	3750.9	-18.	-15.	-9.0	-3	8.4	15.	17.
9200.	3759.3	-18.	-15.	-9.0	-3	8.4	15.	17.
9250.	3767.6	-18.	-15.	-9.1	-3	8.4	15.	17.
9300.	3775.9	-18.	-15.	-9.1	-3	8.4	15.	17.
9350.	3784.1	-18.	-16.	-9.1	-3	8.5	15.	17.
9400.	3792.3	-18.	-16.	-9.1	-3	8.5	15.	17.
9450.	3800.4	-18.	-16.	-9.2	-3	8.5	15.	17.
9500.	3808.4	-18.	-16.	-9.2	-3	8.6	15.	17.
9550.	3816.4	-18.	-16.	-9.2	-3	8.6	15.	18.
9600.	3824.4	-18.	-16.	-9.2	-3	8.6	15.	18.
9650.	3832.3	-18.	-16.	-9.3	-3	8.6	15.	18.
9700.	3840.2	-18.	-16.	-9.3	-3	8.7	15.	18.
9750.	3848.0	-18.	-16.	-9.3	-3	8.7	15.	18.
9800.	3855.7	-18.	-16.	-9.4	-3	8.7	15.	18.
9850.	3863.5	-18.	-16.	-9.4	-3	8.7	15.	18.
9900.	3871.1	-18.	-16.	-9.4	-3	8.8	15.	18.
9950.	3878.7	-18.	-16.	-9.4	-3	8.8	15.	18.
10000.	3886.3	-19.	-16.	-9.5	-3	8.8	16.	18.

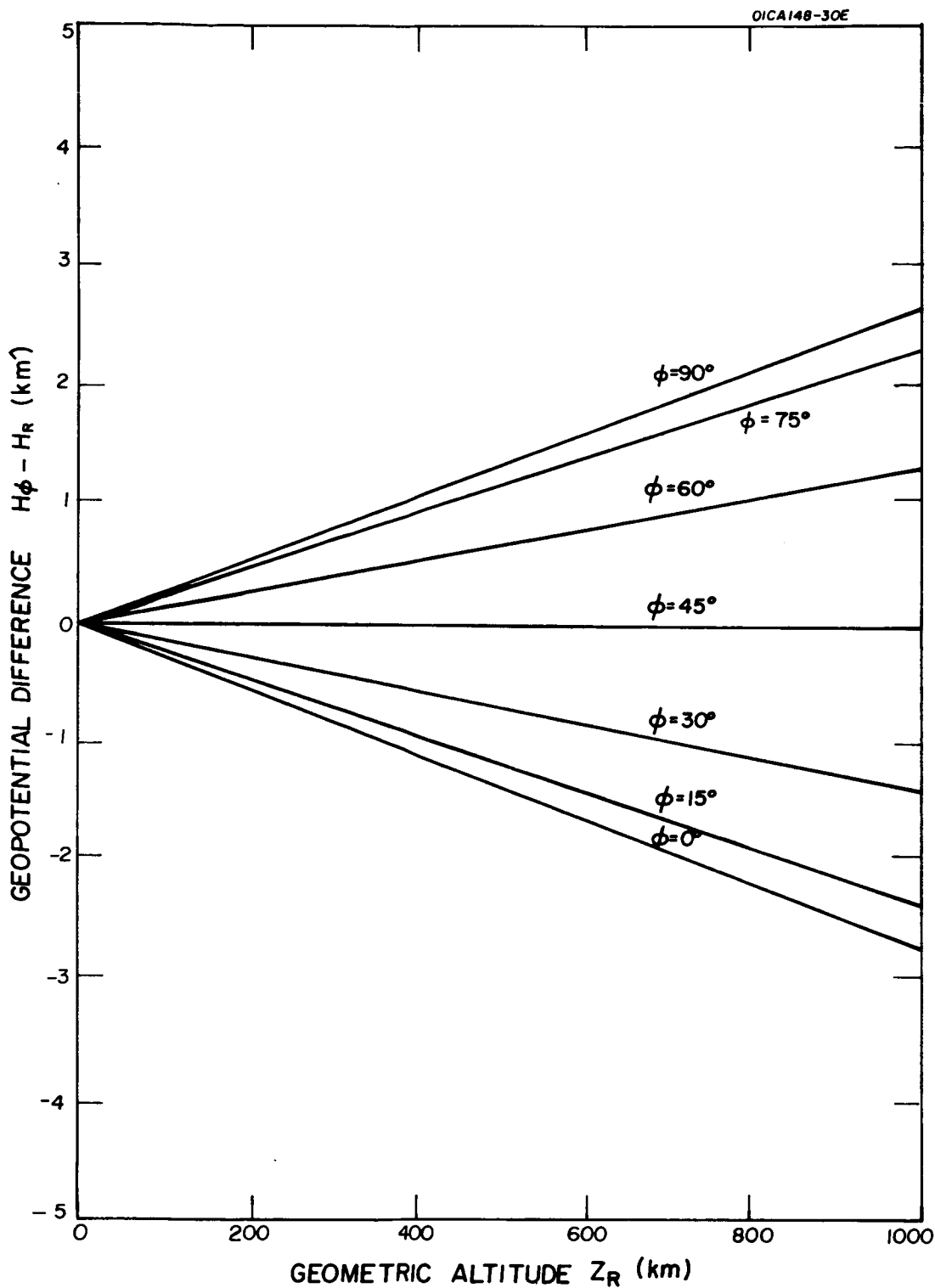


Figure 3.1A. Geopotential differences between geometric-altitude surfaces at a reference latitude, and the same geometric-altitude surfaces at each of seven other latitudes, all as a function of geometric altitude, 0 to 1,000 km.

FOREWORD

This final report is based upon research carried out during the past year under NASA contract NASw-1227, Planetary Meteorology. It contains complete discussions of two aspects of our research: 1) Seasonal and Latitudinal Variations of the Average Surface Temperature and Vertical Temperature Profile on Mars, and 2) The General Circulation of the Martian Atmosphere. A third task in our research, a review of available information on the meteorology of Mars and Venus, is discussed in a previously published technical report entitled Comprehensive Summary of Available Knowledge of the Meteorology of Mars and Venus by Edward M. Brooks (GCA Technical Report No. 66-21-N).

Abstracts for the two papers presented in this report may be found on the following pages; all references are listed together, starting on p. 61.

SEASONAL AND LATITUDINAL VARIATIONS OF THE AVERAGE SURFACE
TEMPERATURE AND VERTICAL TEMPERATURE PROFILE ON MARS

George Ohring and Joseph Mariano

ABSTRACT

The seasonal and latitudinal variations of the average surface temperature and vertical profile of atmospheric temperature on Mars are computed using a thermal equilibrium model. In thermal equilibrium, the computed temperature profiles satisfy the following equilibrium conditions: 1) a balance at the top of the atmosphere between net incoming solar radiation and outgoing infrared radiation; 2) a balance at the surface between the net gain of heat by radiation and the loss of heat by convective transport into the atmosphere, the amount of convective loss being determined from the net integrated radiative cooling of the convective layer — the troposphere; and 3) the stratosphere is in radiative equilibrium. It is assumed that carbon dioxide is the sole radiating gas in a model atmosphere that is composed of 60 percent carbon dioxide and has a surface pressure of 10 mb. The results are presented in the form of pole-to-pole temperature cross-sections from the surface to about 40 km for each Martian season. Because the model does not allow for latitudinal transport of heat energy by the atmospheric circulation, the computed temperatures are too low at polar latitudes during the winter half of the year and probably too high at equatorial latitudes during the solstices and at polar latitudes during summer; they should be most representative of actual conditions at middle latitudes during the equinoxes and at low latitudes during the solstices. The computed temperature cross-sections indicate: 1) extremely small latitudinal temperature gradients in the summer hemisphere, with the maximum temperature occurring at the pole; 2) a decrease of tropopause altitude with latitude from a maximum at the equator during the equinoctial seasons and at the summer pole during the solstices; and 3) relatively isothermal vertical structure at high latitudes during the equinoxes and winter. Comparisons, where possible, of the present results with other theoretical studies and with the microwave and Mariner IV observational indications of Martian temperatures yield generally good agreement.

THE GENERAL CIRCULATION OF THE MARTIAN ATMOSPHERE

Wen Tang

ABSTRACT

Dynamic models simulating the Martian atmospheric circulation are constructed. Model I, based on a terrestrial atmospheric circulation model due to Adem (1962), is a vertically integrated model and is used to compute meridional profiles of mean mid-atmospheric zonal wind and temperature for both northern and southern hemispheres of Mars during the two equinoxes and the two solstices. In these experiments, the value of the eddy exchange coefficient is assumed to be $10^{10} \text{ cm}^2 \text{ sec}^{-1}$, similar to that in the Earth's atmosphere. The numerical results indicate that the maximum mid-atmospheric wind is about 45 m sec^{-1} and occurs at about 40° latitude in the winter hemisphere. The direction of the mean zonal wind for all seasons except summer is generally from the west. The mean mid-atmospheric temperatures during the solstices range from a maximum of 200°K at the summer pole to 110°K at the winter pole. During the equinoxes, the mean mid-atmospheric temperatures range from 175°K to 195°K at the equator to 140°K to 142°K at the poles.

Model II is a more sophisticated two-level, quasi-geostrophic numerical model. This model can be used to compute the latitudinal variation of surface temperature, zonal and meridional winds, and mid-atmospheric vertical velocities as a function of time during the course of a Martian year. The model is described in the text; application to Mars is planned during the coming year.

TABLE OF CONTENTS

<u>Section</u>	<u>Title</u>	<u>Page</u>
1	SEASONAL AND LATITUDINAL VARIATIONS OF THE AVERAGE SURFACE TEMPERATURE AND VERTICAL TEMPERATURE PROFILE ON MARS	1
	1.1 Introduction	1
	1.2 Basic Model	1
	1.3 Infrared Cooling	3
	1.4 Solar Heating	7
	1.5 Numerical Methods	10
	1.6 Atmospheric Composition, Surface Pressure and Other Input Parameters	15
	1.7 Results and Discussion	16
	1.8 Concluding Remarks	35
2.	THE GENERAL CIRCULATION OF THE MARTIAN ATMOSPHERE	39
	2.1 Seasonal Variation of the Mean Zonal Wind Velocity and Temperature of the Martian Atmosphere	39
	2.2 A Numerical Model of the Martian Atmospheric General Circulation	47
	REFERENCES	61
	APPENDIX	65

LIST OF ILLUSTRATIONS

<u>Figure</u>	<u>Caption</u>	<u>Page</u>
1	Schematic diagram of computational model at time step, τ .	11
2	Comparison of Martian temperature profiles computed for 10 mb, 60% CO ₂ atmosphere (dashed line) and 5 mb, 100% CO ₂ atmosphere (solid line) for Southern Hemisphere summer solstice, latitude 80°S. Tropopause indicated by short horizontal line.	17
3	Comparison of Martian temperature profiles computed with 4-layer model (x) and 10-layer model (0) for Southern Hemisphere summer solstice, latitude 80°S.	18
4	Computed latitudinal temperature cross-section for Northern Hemisphere spring equinox on Mars. Temperatures in °K; tropopause indicated by dashed line.	19
5	Computed latitudinal temperature cross-section for Northern Hemisphere summer solstice on Mars. Temperatures in °K; tropopause indicated by dashed line.	20
6	Computed latitudinal temperature cross-section for Northern Hemisphere fall equinox on Mars. Temperatures in °K; tropopause indicated by dashed line.	21
7	Computed latitudinal temperature cross-section for Northern Hemisphere winter solstice on Mars. Temperatures in °K; tropopause indicated by dashed line.	22
8	Comparison of computed latitudinal variation of Martian surface temperature for Northern Hemisphere fall equinox with that of Leovy (1966). Solid line - present model; dashed line - Leovy (1966).	26
9	Comparison of computed latitudinal variation of Martian surface temperature for Northern Hemisphere winter solstice with that of Leovy (1966). Solid line - present model; dashed line - Leovy (1966).	27
10	Comparison of computed latitudinal variation of mean annual Martian surface temperature with that of Leighton and Murray (1966). Solid line - present model; dashed line - Leighton and Murray (1966).	28

LIST OF ILLUSTRATIONS (Cont.)

<u>Figure</u>	<u>Caption</u>	<u>Page</u>
11	Comparison of computed latitudinal variation of Martian temperature at atmospheric level $p/p_0 = 0.31$ for Northern Hemisphere fall equinox with that of Leovy (1966). Solid line - present model; dashed line - Leovy (1966).	30
12	Comparison of computed latitudinal variation of Martian temperature at atmospheric level $p/p_0 = 0.31$ for Northern Hemisphere winter solstice with that of Leovy (1966). Solid line - present model; dashed line - Leovy (1966).	31
13	Computed temperature profile of the Martian atmosphere for the date of the Mariner IV immersion occultation experiment (50°S , solar declination $+15^{\circ}$, late Southern Hemisphere winter).	32
14	Computed temperature profile of the Martian atmosphere for the date of the Mariner IV emmersion occultation experiment (60°N , solar declination $+15^{\circ}$, late Northern Hemisphere summer).	34
15	Martian surface temperature as a function of time at equator. Solid line: time dependent case starting with initial thermal equilibrium condition at Northern Hemisphere spring equinox. X: computed on basis of thermal equilibrium.	36
16	Martian surface temperature as a function of time at 80°N . Solid line: time dependent case starting with initial thermal equilibrium condition at 45 days prior to spring equinox. X: computed on the basis of thermal equilibrium.	37
17	Latitudinal profile of mean atmospheric temperature for the four Martian seasons.	43
18	Latitudinal profile of mean zonal wind for the four Martian seasons.	44

1. SEASONAL AND LATITUDINAL VARIATIONS OF THE AVERAGE SURFACE TEMPERATURE AND VERTICAL TEMPERATURE PROFILE ON MARS

George Ohring and Joseph Mariano

1.1 Introduction

Previous theoretical estimates of the average vertical temperature profile in the lower Martian atmosphere have been based upon convective-radiative equilibrium models (see, for example, Goody, 1957; Prabhakara and Hogan, 1965; and Ohring and Mariano, 1966). In such models, a surface temperature is assumed and the vertical temperature profile is computed on the basis of a convective troposphere and radiative equilibrium stratosphere. In the present study, we actually compute the average surface temperature as well as the average vertical temperature profile as a function of latitude and season. The computations are based upon the thermal equilibrium concept of Manabe and Strickler (1964), which is a slight modification of the convective-radiative equilibrium model. Although the effect on Martian temperatures of latitudinal transport of heat by the atmospheric circulation is not included in the model, the computed temperatures should be useful for many purposes. Where possible, we compare the computed temperatures with observational and previous theoretical indications of Martian temperatures.

1.2 Basic Model

Under the concept of thermal equilibrium, the computed temperature profile must satisfy the following equilibrium conditions: 1) a balance at the top of the atmosphere between net incoming solar radiation and net outgoing infrared radiation; 2) a balance at the surface between the net gain of heat by radiation and the loss of heat by convective transport into the atmosphere; the loss of heat by convective transfer into the atmosphere is determined from the net integrated radiative cooling of the convective layer — the troposphere; and 3) the stratosphere is in radiative equilibrium.

The thermal equilibrium temperature profile is computed with the use of an iterative procedure based upon the initial value method of computing radiative equilibrium temperatures. Starting with an initial temperature profile, one computes the vertical distribution of the rate of radiational temperature change. These rates are applied to the initial profile for a unit time step to obtain a new temperature profile. This process is continued until the three equilibrium conditions are satisfied. At each stage of the calculations any layers with lapse rates greater than a specified convective lapse rate are corrected to the convective lapse rate. Numerically, this is accomplished as follows.

(1) In a non-convective layer, the net rate of temperature change at time step τ is equal to the computed rate of radiational temperature change:

$$\left(\frac{\partial \theta}{\partial t} \right)_{\text{net}}^{\tau} = \left(\frac{\partial \theta}{\partial t} \right)_{\text{rad}}^{\tau} . \quad (1)$$

(2) In a convective layer (that is, a layer that would have a super-convective lapse rate if no correction were made) that does not extend to the surface, the net rate of temperature change must satisfy the following requirements:

$$\int_{p_t}^{p_b} \left(\frac{\partial \theta}{\partial t} \right)_{\text{net}}^{\tau} dp = \int_{p_t}^{p_b} \left(\frac{\partial \theta}{\partial t} \right)_{\text{rad}}^{\tau} dp \quad (2)$$

where p_t and p_b are the pressures at the top and base of the layer, respectively, and

$$\left(\frac{\partial \theta}{\partial p} \right)^{\tau+1} = \text{convective lapse rate} \quad (3)$$

where

$$\theta^{\tau+1} = \theta^{\tau} + \left(\frac{\partial \theta}{\partial t} \right)_{\text{net}}^{\tau} \Delta t \quad (4)$$

(3) In a convective layer that extends to the surface, the net rate of temperature change must satisfy (3) and (4) and

$$\begin{aligned} \frac{c_p}{g} \int_{p_t}^{p_0} \left(\frac{\partial \theta}{\partial t} \right)_{\text{net}}^{\tau} dp &= \frac{c_p}{g} \int_{p_t}^{p_0} \left(\frac{\partial \theta}{\partial t} \right)_{\text{rad}}^{\tau} dp + s_g \\ &\quad + (F_{\downarrow g})^{\tau} - (\sigma \theta g^4)^{\tau+1} \end{aligned} \quad (5)$$

where c_p is the specific heat of the atmosphere at constant pressure, g is the gravitational acceleration, p_0 is the surface pressure, s_g is the net downward flux of solar radiation at the surface, $(F_{\downarrow g})^{\tau}$ is the downward flux of infrared radiation at the surface at time step τ , and $(\sigma \theta g^4)^{\tau+1}$ is the upward flux of radiation at the surface at time step $\tau+1$. This equation is a result of the second equilibrium condition; it enables us to compute the surface temperature at each succeeding time step. At each time step, Equations (1) through (5) must be satisfied before computations for the next time step begin.

1.3 Infrared Cooling

The radiative rates of temperature change depend upon two factors — infrared cooling and solar heating. Thus,

$$\left(\frac{\partial \theta}{\partial t} \right)_{\text{rad}} = \left(\frac{\partial \theta}{\partial t} \right)_s + \left(\frac{\partial \theta}{\partial t} \right)_{\text{IR}} . \quad (6)$$

In this section, we discuss the model used to compute infrared fluxes and cooling rates $(\partial \theta / \partial t)_{\text{IR}}$ in the Martian atmosphere. In the next section, we discuss the model to compute the solar heating rates, $(\partial \theta / \partial t)_s$.

We shall make use of the computational model discussed by Rodgers and Walshaw (1966). They take as vertical coordinate the unit z , where

$$z = -\ell \ln \varphi \quad (7)$$

and $\varphi = p/p_0$, where p_0 is the surface pressure. Then $(\partial \theta / \partial t)_{\text{IR}}$ can be written as

$$\left(\frac{\partial \theta}{\partial t} \right)_{\text{IR}} = - \frac{g}{c_p} \frac{C}{p} \quad (8)$$

where g is the gravitational acceleration, c_p is specific heat at constant pressure, and C is the derivative with respect to z of the net flux of infrared radiation. At any level z , C for an absorption band can be written as

$$C(z) = B(Z) \frac{dT}{dz}(z, Z) - \int_0^Z \frac{dT}{dz}(z, z') \frac{dB}{dz}(z') dz' \quad (9)$$

where B is the blackbody flux for the absorption band, Z is the highest level considered, and T is the transmission function for the absorption band. For the Martian atmosphere, we can assume that only the $15\mu \text{ CO}_2$ band contributes to the infrared cooling. Local thermodynamic equilibrium is also assumed. Curtis and Goody (1956) have found this to be a good assumption for the $15\mu \text{ CO}_2$ band in the Earth's atmosphere down to pressures as low as 3.4×10^{-2} mb.

For a band transmission model we assume the Goody random model, for which the transmission of Lorentz lines (the applicability of the Lorentz line shape for the Martian atmosphere is discussed in the Appendix) along a path at constant pressure can be written as

$$T = \exp \left[- \frac{1.66 \text{ km}}{\delta} \left(1 + \frac{1.66 \text{ km}}{\pi \alpha} \right)^{-\frac{1}{2}} \right] \quad (10)$$

where k is the mean line intensity, α is the half-width of the absorption lines, m is the amount of carbon dioxide in g cm^{-2} , δ is the mean line spacing, and the factor 1.66 is introduced as a multiple of m to approximate flux transmission. For an atmosphere with constant mass mixing ratio, w , of CO_2 , m between any two levels z and z' is given by

$$m = \frac{wp_o}{g} [\phi(z) - \phi(z')] . \quad (11)$$

Equation (10) is for a homogeneous path, i.e., constant pressure and temperature. In the actual atmosphere, both pressure and temperature vary along the path. Pressure affects the half-widths of the absorption lines while temperature affects both their half-widths and intensities. However, the effect of temperature is a second order effect compared to the effect of pressure and CO_2 amount on the transmission. The Lorentz half-width of an absorption line at pressure p and temperature θ can be written as

$$\alpha = \alpha_s \left(\frac{p}{p_s} \right) \left(\frac{\theta_s}{\theta} \right)^{\frac{1}{2}} = \alpha_s \frac{p_o \Phi}{p_s} \left(\frac{\theta_s}{\theta} \right)^{\frac{1}{2}} \quad (12)$$

where α_s is the half-width at standard pressure, p_s , and standard temperature, θ_s . Since the temperature variation with altitude is much smaller than the pressure variation, and since the temperature correction is proportional to the square root of temperature, we may approximate the temperature effect by assuming an appropriate isothermal atmosphere for Mars with a temperature equal to θ . For an isothermal atmosphere, the Curtis-Godson approximation for the mean half-width of an absorption line for an atmospheric path with varying pressure yields

$$\bar{\alpha} = \frac{\int \alpha dm}{\int dm} \quad (13)$$

or, upon substitution of (12),

$$\bar{\alpha} = \frac{\alpha_s \left(\frac{\theta_s}{\theta} \right)^{\frac{1}{2}} \left(\frac{p_o}{p_s} \right) \int \phi dm}{\int dm} \quad (14)$$

After integration, (14) can be reduced to

$$\bar{\alpha} = \frac{\alpha_s}{2} \left(\frac{\theta_s}{\theta} \right)^{\frac{1}{2}} \left(\frac{p_o}{p_s} \right) \left[\frac{\varphi(z)^2 - \varphi(z')^2}{\varphi(z) - \varphi(z')} \right] . \quad (15)$$

The effect of temperature on the line intensities can be incorporated following Rodgers and Walshaw (1966). The mean absorber amount between any two levels is corrected by the formula

$$\bar{m} = \int \Phi(\theta) dm \quad (16)$$

where

$$\Phi(\theta) = \frac{\sum k_i(\theta)}{\sum k_i(\theta_s)}$$

in which k is the line intensity and the summation is over all lines contributing to the absorption interval. Rodgers and Walshaw present the following empirical equation for $\Phi(\theta)$.

$$\log_e \Phi(\theta) = a(\theta - 260) + b(\theta - 260)^2 \quad (17)$$

where $a = 3.49 \times 10^{-3}$ and $b = -1.28 \times 10^{-6}$ for the 15μ CO₂ band. If we again assume that we can use a constant temperature correction, $\Phi(\theta)$ can come out of the integral and (16) becomes

$$\bar{m} = \Phi(\theta) \int dm = \frac{\Phi(\theta) w p_o}{g} [\varphi(z) - \varphi(z')] . \quad (18)$$

$\bar{\alpha}$ and \bar{m} can now be substituted into the expression for the transmittance, Equation (10). For the CO₂ content and pressures prevailing on Mars,

$$\frac{1.66 k \bar{m}}{\pi \bar{\alpha}} \gg 1$$

and, hence, (10) can be written as

$$T = \exp \left[- \frac{(1.66 \pi \bar{\alpha} k \bar{m})^{\frac{1}{2}}}{\delta} \right] , \quad (19)$$

which, upon substitution for $\bar{\alpha}$ and \bar{m} , becomes

$$T = \exp \left\{ - \left[\frac{1.66 \pi k \alpha_s}{2\delta^2} \left(\frac{\theta_s}{\theta} \right)^{\frac{1}{2}} \frac{p_o^2}{p_s} \frac{\Phi(\theta)w}{g} \left(\varphi(z)^2 - \varphi(z')^2 \right) \right]^{\frac{1}{2}} \right\} \quad (20)$$

To compute the cooling rates, we require dT/dz .

Letting

$$F = \frac{1.66 \pi k \alpha_s}{2\delta^2} \left(\frac{\theta_s}{\theta} \right)^{\frac{1}{2}} \frac{p_o^2}{p_s} \frac{\Phi(\theta)w}{g}, \quad (21)$$

we obtain for the vertical derivative of the transmittance

$$\frac{dT}{dz} = \frac{F \varphi(z)^2}{[\varphi(z)^2 - \varphi(z')^2]^{\frac{1}{2}}} \exp \left\{ - \left[F \left(\varphi(z)^2 - \varphi(z')^2 \right)^{\frac{1}{2}} \right] \right\}. \quad (22)$$

For the 15μ CO₂ band, centered at 667 cm^{-1} and extending over 170 cm^{-1} , Rodgers and Walshaw (1966) obtained the parameters k , δ , and α_s by fitting detailed quantum-mechanical calculations of line positions and intensities to the random model for band transmission. We use their values for the evaluation of transmission: $\alpha_s = 0.07 \text{ cm}^{-1}$; $k/\delta = 718.7 \text{ g}^{-1} \text{ cm}^2$; and $\pi\alpha_s/\delta = 0.448$. For the constant temperature correction, we assume $\theta = 200^\circ\text{K}$.

The downward flux of infrared radiation at the surface, $F_{\downarrow g}$, required for Equation (5), is given by

$$F_{\downarrow g} = - T(o, Z) B(Z) + B(o) + \int_o^Z T(o, z') \frac{dB}{dz}(z') dz'. \quad (23)$$

The blackbody flux $B(\theta)$ is the integral of the Planck function at temperature θ over the spectral interval $n_1 = 582 \text{ cm}^{-1}$ to $n_2 = 752 \text{ cm}^{-1}$. To a high approximation for this spectral region and Martian temperatures it can be computed from

$$B(\theta) = \frac{\pi c_1 \theta^4}{c_2^4} \left[\exp \left(- \frac{c_2 n}{\theta} \right) \right] \left[\frac{c_2^3 n^3}{\theta^3} + 3 \frac{c_2^2 n^2}{\theta^2} + 6 \frac{c_2 n}{\theta} + 6 \right] \Bigg|_{n=n_2}^{n=n_1} \quad (24)$$

where $c_1 = 1.191 \times 10^{-5} \text{ erg cm sec}^{-1} \text{ steradian}^{-1}$ and $c_2 = 1.4389 \text{ cm deg}^{-1}$.

1.4 Solar Heating

For the solar heating, we shall assume that only the near infrared bands of carbon dioxide contribute to heating. Although small amounts of water vapor are present in the Martian atmosphere, the contribution of this gas to the solar heating rate and to the final temperature distribution is negligible compared to carbon dioxide (see Ohring and Mariano, 1966). We shall follow the method of Houghton (1963), which is based upon the experimental absorption data of Howard, et al (1955), Burch, et al (1960), and Seeley and Houghton (1961).

For a given time of year and latitude, the average amount of solar energy absorbed from a pressure level p to the top of the atmosphere during a Martian day can be written as

$$E = \left(\sum_{\ell} I_{0\ell} \overline{\cos \psi} A_{\ell} \right) r \quad (25)$$

where $I_{0\ell}$ is the intensity of solar radiation per wavenumber n at the top of the atmosphere in the ℓ -th absorption band, $\overline{\cos \psi}$ is the average cosine of the solar zenith angle for the day, A_{ℓ} is the integrated absorption of the ℓ -th band for the atmospheric column extending from the top of the atmosphere to the pressure level p along a slant path parallel to the solar beam, r is the fraction of the day that the sun is shining, and the summation extends over the carbon dioxide absorption bands. The heating rate at a pressure level p can be determined from

$$\left(\frac{d\theta}{dt} \right)_s = \frac{g}{c_p} \overline{\cos \psi} \cdot r \sum_{\ell} I_{0\ell} \frac{dA_{\ell}}{dp}. \quad (26)$$

Houghton's (1963) expressions for the integrated absorption are:

$$\text{Weak bands } (\bar{pm} < x_{\ell}) \quad A_{\ell} = a_{\ell} (\bar{pm})^{\frac{1}{2}} \quad (27)$$

$$\text{Strong bands } (\bar{pm} > x_{\ell}) \quad A_{\ell} = b_{\ell} + c_{\ell} \log_{10}(\bar{pm}) \quad (28)$$

where p is in mb, m is in atmo-cm of CO_2 , and a_{ℓ} , b_{ℓ} , c_{ℓ} , and x_{ℓ} are the empirically determined constants for the ℓ -th band. For a path extending from the top of an atmosphere with a constant mixing ratio, w , to a level whose pressure is p_i

$$\bar{p} = \frac{\int p dm}{m} = \frac{p_i}{2} \quad (29)$$

and

$$m = \frac{10^3 w}{g \rho_c} \cdot \overline{\sec \psi} \cdot p_i \quad (30)$$

where ρ_c is the density of CO_2 at STP.

With these equations for mean pressure and path length, the integrated absorption in cm^{-1} down to the level p_i is

$$A_\ell(p_i) = \begin{cases} a_\ell \left(\frac{1}{2} \frac{10^3 w}{g \rho_c} \overline{\sec \psi} \right)^{\frac{1}{2}} p_i, & \bar{p}_i^m < x_\ell \\ b_\ell + 2c_\ell (.435) \ln_e(p_i) + c_\ell (.435) \ln_e \left(\frac{1}{2} \frac{10^3 w}{g \rho_c} \overline{\sec \psi} \right) & \bar{p}_i^m > x_\ell \end{cases} \quad (31)$$

Differentiating with respect to p , we have

$$\frac{dA_\ell}{dp_i} = \begin{cases} a_\ell \left(\frac{1}{2} \frac{10^3 w \overline{\sec \psi}}{g \rho_c} \right)^{\frac{1}{2}} & \bar{p}_i^m < x_\ell \\ \frac{2c_\ell (.435)}{p_i} & \bar{p}_i^m > x_\ell \end{cases} \quad (32)$$

The empirical constants for the near-infrared absorption bands, after Houghton (1963), are shown in Table 1 along with the values of I_o at Mars' mean distance from the sun.

For the solar radiation reaching the surface, S_g , we may write

$$S_g = (1 - A)(S_o r \overline{\cos \psi} - E_g) , \quad (33)$$

where S_o is the intensity of solar radiation at Mars' distance from the sun, A is the Martian planetary albedo, and E_g is the amount of solar energy absorbed in the atmosphere, which is given by

$$E_g = \left(\sum I_{o\ell} \overline{\cos \psi} A_{g\ell} \right) r , \quad (34)$$

where $A_{g\ell}$ is determined from (31).

Table 1

Constants for the near-infrared CO₂ bands.

Band (μ)	I_o erg cm ⁻² sec ⁻¹ (cm ⁻¹) ⁻¹	a	b	c	x
2.0	18.3	0.23			
1.6	25.0	0.02	weak only		
1.4	27.2	0.02			
4.3	5.6	8.4	- 11	37	15.4
2.7	11.8	1.87	- 136	65	910

To determine the average zenith angle, for a given day on Mars, we make use of the relationship

$$\cos \psi = \sin \varphi \sin \delta + \cos \varphi \cos \delta \cos h \quad (35)$$

where φ is latitude, δ is declination of sun and h is the hour angle. The average value of $\cos \psi$ for a given day is

$$\overline{\cos \psi} = \frac{1}{h_o} \int_0^{h_o} (\sin \varphi \sin \delta + \cos \varphi \cos \delta \cos h) dh \quad (36)$$

where h_o is the hour angle between noon and sunrise or sunset, which is given by

$$\cos h_o = -\tan \varphi \tan \delta. \quad (37)$$

Upon integration of (36), we obtain

$$\overline{\cos \psi} = \sin \varphi \sin \delta + \frac{\sin h_o \cos \varphi \cos \delta}{h_o}. \quad (38)$$

The fraction of the day that the sun shines is given by

$$r = \frac{h_o}{\pi}. \quad (39)$$

1.5 Numerical Methods

The temperature profile and surface temperature are computed using an iterative procedure. During each cycle the net rate of change of temperature $(d\theta/dt)_{net}$, is computed from Equations (1) through (5). The atmosphere is divided into n layers of equal pressure thicknesses, Δp . The temperature profile at the beginning of the iteration cycle (say, the τ -th cycle) consists of the temperatures at the interfaces of the n layers (see Figure 1), $\theta_1^\tau, \theta_2^\tau, \dots, \theta_{n+1}^\tau$ located at the pressures p_1 (surface pressure), p_2, \dots , and p_{n+1} respectively.

The following steps are then executed.

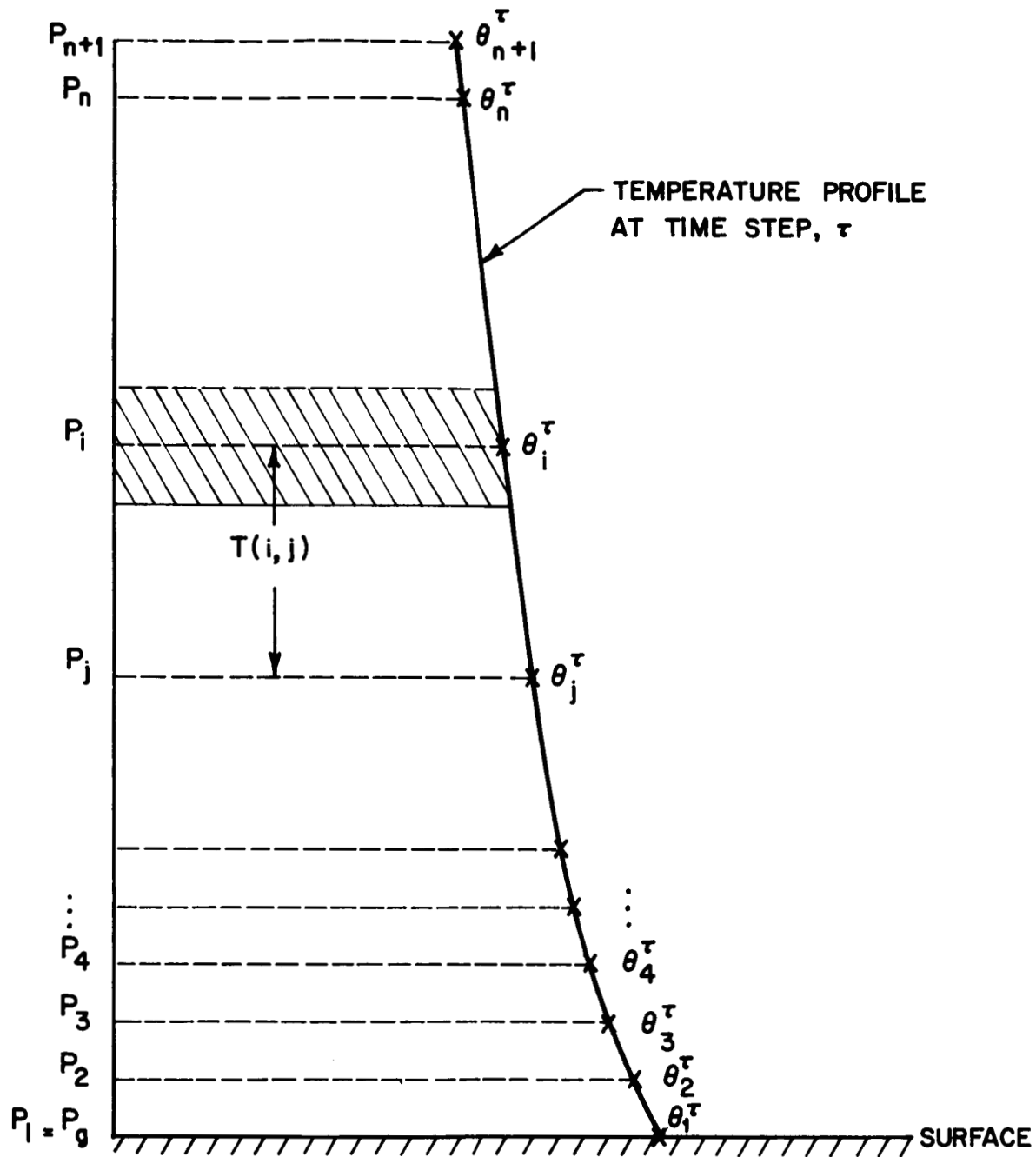


Figure 1. Schematic diagram of computational model at time step, τ .

Step (1): The infrared cooling rate is computed at each interface from

$$\begin{aligned}
 \left(\frac{d\theta}{dt} \right)_{i,IR}^{\tau} &= - \frac{g}{c_p} \frac{C(z_i)}{p_i} \\
 &= \frac{g}{c_p} \frac{1}{p_i} \left\langle - B(\theta_{n+1}^{\tau}) \left(\frac{dT}{dz} \right)_{i,n+1} \right. \\
 &\quad + \left\{ \sum_{j=1}^{i-2} \frac{1}{2} \left[\left(\frac{dT}{dz} \right)_{i,j} + \left(\frac{dT}{dz} \right)_{i,j+1} \right] \cdot \left[B(\theta_{j+1}^{\tau}) - B(\theta_j^{\tau}) \right] \right. \\
 &\quad + \left(\frac{dT}{dz} \right)_{i-\frac{1}{2}} \left[B(\theta_i^{\tau}) - B(\theta_{i-1}^{\tau}) \right] + \left(\frac{dT}{dz} \right)_{i+\frac{1}{2}} \left[B(\theta_{i+1}^{\tau}) - B(\theta_i^{\tau}) \right] \\
 &\quad \left. \left. + \sum_{j=i+1}^n \frac{1}{2} \left[\left(\frac{dT}{dz} \right)_{i,j} + \left(\frac{dT}{dz} \right)_{i,j+1} \right] \cdot \left[B(\theta_{j+1}^{\tau}) - B(\theta_j^{\tau}) \right] \right\} \right\rangle \quad (40)
 \end{aligned}$$

where $\left(\frac{dT}{dz} \right)_{i,j}$ is given by

$$\left(\frac{dT}{dz} \right)_{i,j} = \pm \frac{F^{\frac{1}{2}} \varphi_i^2}{[|\varphi_i^2 - \varphi_j^2|]^{\frac{1}{2}}} \exp \left\{ - \left[F(|\varphi_i^2 - \varphi_j^2|) \right]^{\frac{1}{2}} \right\} \quad \begin{array}{ll} i < j \\ i > j \end{array} \quad (41)$$

where F is defined by (21).

Step (2): The solar heating rate is computed at each interface from

$$\left(\frac{\partial \theta}{\partial t} \right)_{i,S} = \left(\sum_{\ell} I_{o,\ell} \overline{\cos \psi} \frac{dA_{\ell}}{dp_i} \right) r . \quad (42)$$

Step (3): The rate of change of temperature due to radiation is computed at each interface from

$$\left(\frac{\partial \theta}{\partial t} \right)_{i,RAD}^{\tau} = \left(\frac{\partial \theta}{\partial t} \right)_{i,S} + \left(\frac{\partial \theta}{\partial t} \right)_{i,IR}^{\tau} \quad (43)$$

Step (4): The loss of energy by the Martian surface due to convection is computed as follows. The convective temperature profile, $\{\theta_i^*\}$, with the surface temperature $\theta_g = \theta_1^*$, is computed for each successive level in the atmosphere from the equation

$$\frac{\theta_i^*}{\theta_{i-1}^*} = \left(\frac{p_i}{p_{i-1}} \right)^{\frac{\gamma-1}{\gamma}} \quad (i = 2, 3, \dots) \quad (44)$$

where $\gamma = c_p/c_v$, the ratio of the specific heat at constant pressure to the specific heat at constant volume, for the Martian atmosphere. The first computed convective temperature, θ_2^* , is compared with the new radiative temperature

$$(\theta_i)_{rad}^{\tau+1} = \theta_i^\tau + \left(\frac{\partial \theta}{\partial t} \right)_{i,rad}^\tau \Delta t, \quad (i = 2) \quad (45)$$

where Δt is the increment of time for the τ -th cycle. If $(\theta_2)_{rad}$ is superconvective, the net rate of change of temperature, $(\partial \theta / \partial t)_{net}$, is computed from the equation, (for $i = 2$)

$$\theta_i^* = \theta_i^\tau + \left(\frac{\partial \theta}{\partial t} \right)_{i,net}^\tau \Delta t. \quad (46)$$

The above procedure is continued until the level where the new radiative temperature is not superconvective (say, $i = t$) is attained. This level ($i = t$) defines the top of the convective layer that extends to the surface. The new surface temperature, $\theta_g^{\tau+1}$, is now computed from (5) where

$$\int_{p_t}^{p_g} \left(\frac{\partial \theta}{\partial t} \right)_{net}^\tau dp \cong \sum_{i=2}^{t-1} \left(\frac{\partial \theta}{\partial t} \right)_{i,net}^\tau \Delta p \quad (47)$$

$$\int_{p_t}^{p_g} \left(\frac{\partial \theta}{\partial t} \right)_{rad}^\tau dp \cong \sum_{i=2}^{t-1} \left(\frac{\partial \theta}{\partial t} \right)_{i,rad}^\tau \Delta p \quad (48)$$

$$(F_g)^\tau = \sum_{j=1}^n \frac{1}{2} \left[B(\theta_j^\tau) + B(\theta_{j+1}^\tau) \right] (T_{1j} - T_{1,j+1}) \quad (49)$$

(obtained from an integration by parts of (23)) and the solar radiation reaching the surface, S_g , is computed from (33). If the first new radiative temperature $(\theta_2)_{rad}^{\tau+1}$ is not superconvective, the model assumes that there is no convective layer that reaches the surface and (5) reduces to

$$0 = S_g + (F_g)^\tau - (\sigma \theta_g^4)^{\tau+1}. \quad (50)$$

The new radiative temperatures $(\theta_i)_{rad}^{\tau+1}$ for $i > t$ are also compared to their corresponding convective values, θ_i^* . If one or more temperatures (say, from $i=\ell$ to $i=\ell+k$) are super convective, the net rates of change of temperature, $(\partial \theta / \partial t)_i^{\text{net}}$ ($i = \ell, \ell+1, \dots, \ell+k$) are computed from (46). Also, in order to satisfy Equation (2), the new radiative temperatures above the level, $\ell+k$, (say, from $\ell+k+1$ to $\ell+k+m$) are lowered to their corresponding convective values, where $(\partial \theta / \partial t)_i^{\text{net}}$ ($i = \ell+k+1$ to $\ell+k+m$) is also computed from (46) and,

$$\sum_{i=\ell+1}^{\ell+k+m-1} \left[\left(\frac{\partial \theta}{\partial t} \right)_i^{\text{net}} - \left(\frac{\partial \theta}{\partial t} \right)_i^{\text{rad}} \right] \Delta p = 0. \quad (51)$$

For the remaining new radiative temperatures that are not superconvective,

$$\left(\frac{\partial \theta}{\partial t} \right)_i^{\text{net}} = \left(\frac{\partial \theta}{\partial t} \right)_i^{\text{rad}}, \quad (52)$$

and thus Equation (1) is satisfied.

Step (5): The new temperature profile, $\{\theta_i^{\tau+1}\}$ is computed from the equations

$$\theta_i^{\tau+1} = \theta_i + \left(\frac{\partial \theta}{\partial t} \right)_i^{\text{net}} \Delta t \quad (i \geq 2, 3, \dots, n) \quad (53)$$

and

$$\theta_1^{\tau+1} = \theta_g^{\tau+1} \quad (54)$$

and the τ -th interation cycle is completed. The iteration procedure is continued until the net rates of change of temperature, $(\partial \theta / \partial t)_{\text{net}}$ are less than a prescribed convergence criterion, ϵ .

1.6 Atmospheric Composition, Surface Pressure and Other Input Parameters

To perform the calculations with the thermal equilibrium model, information is required on the atmospheric composition and surface pressure on Mars. The results of recent spectroscopic observations (Spinrad et al, 1966; Owen, 1966; and Belton and Hunten, 1966) and the Mariner IV occultation experiment (Kliore et al, 1965) indicate that the surface pressure is about 5 to 10 mb and the atmosphere is predominantly carbon dioxide. For our computations, we assume an atmosphere composed of 60 percent (by mass) CO₂ with a surface pressure of 10 mb. The remainder of the atmosphere is probably argon or nitrogen — or a combination of the two — both of which are inactive as absorbers of radiation. We assume that the remaining gas is all nitrogen.

Trace amounts of water vapor — ~ 15 μ precipitable cm — have been detected in the Martian atmosphere (Kaplan et al, 1964). However, previous calculations (Ohring and Mariano, 1966) suggest that inclusion of this gas in our model would not substantially change the results. Therefore, it is not included in the computations.

Several other input constants are required in the computations. The intensity of solar radiation at the top of the Martian atmosphere is taken as

$$S_0 = \frac{s.c.}{R^2}$$

where s.c. = 2 cal cm⁻² min⁻¹ is the solar constant for Earth and R is the Mars-Sun distance in astronomical units. The variation of R with time of year is included in the calculations.

The planetary albedo of Mars is taken as 0.3 (de Vaucouleurs, 1964) and is assumed to be invariant with latitude and season. The convective lapse-rate is assumed to be the dry adiabatic lapse-rate. For the assumed atmospheric composition, the required thermodynamic constants are $(\gamma - 1)/\gamma = 0.269$ and $c_p = 0.858 \times 10^7$ erg gm⁻¹(°K)⁻¹. The iterations continued until the net rates of temperature change were less than the prescribed convergence criterion of $\epsilon = 0.05$ deg day⁻¹.

1.7 Results and Discussion

Before computing the average surface temperatures and atmospheric temperature profiles on Mars as a function of latitude and season, two preliminary sets of computations were performed. The first set was intended to compare results for an assumed model atmosphere (60% CO₂; p_o = 10 mb) with those for a 100 percent CO₂, p_o = 5 mb model atmosphere. The pure CO₂ atmosphere is also compatible with present observations and has been used in other calculations of Martian temperatures (see, for example, Leovy, 1966). The second set of computations was designed to determine the minimum number of layers in the computational model required to yield a reasonably accurate picture of the vertical temperature structure. Both sets of computations were performed for a time of maximum insolation - southern hemisphere summer solstice, latitude 80°S.

The results of the first set of computations are shown in Figure 2, where the computed temperatures are plotted as a function of p/p_o, the ratio of atmospheric pressure to surface pressure. The thermodynamic constants for the 5 mb, 100 percent CO₂ atmosphere are $(\gamma-1)/\gamma = 0.257$ and $c_p = 0.736 \times 10^7 \text{ erg gm}^{-1} (\text{°K})^{-1}$. The average surface temperature for the 10 mb case is slightly higher - 255°K versus 254°K - than for the 5 mb case. This is due to the slightly greater greenhouse effect (83 m STP of CO₂ at 10 mb pressure versus 69 m STP of CO₂ at 5 mb pressure) in the 10 mb atmospheric model. In addition, the greater adiabatic constant, $(\gamma-1)/\gamma$, for the 10 mb case also tends to increase the surface temperature, since the convective flux required to maintain an adiabatic temperature profile from the surface to the tropopause is less. The most significant feature of the computed temperature profiles, however, is the small temperature differences for the two different model atmospheres. The maximum temperature difference is 7°K and occurs at the upper levels. This result indicates that the temperatures computed with our assumed model atmosphere would also be representative of a 5 mb, 100 percent CO₂ model.

The results of the second set of computations are shown in Figure 3. In this set, a 10-layer computational model was compared to a 4-layer computational model. As can be seen, there is no appreciable difference in the computed temperature profiles. Therefore, the 4-layer model was used in computing the latitudinal distribution of temperature profiles for each of the four Martian seasons.

The computed temperature distributions are shown in Figures 4, 5, 6 and 7 in the form of latitudinal cross-sections - one for each season - extending from north pole to south pole. The vertical coordinate is the pressure plotted on a logarithmic scale; p = 1 mb corresponds to about 20 km altitude, p = 0.1 mb to about 40 km. Temperatures were computed at even 20-degree latitude intervals.

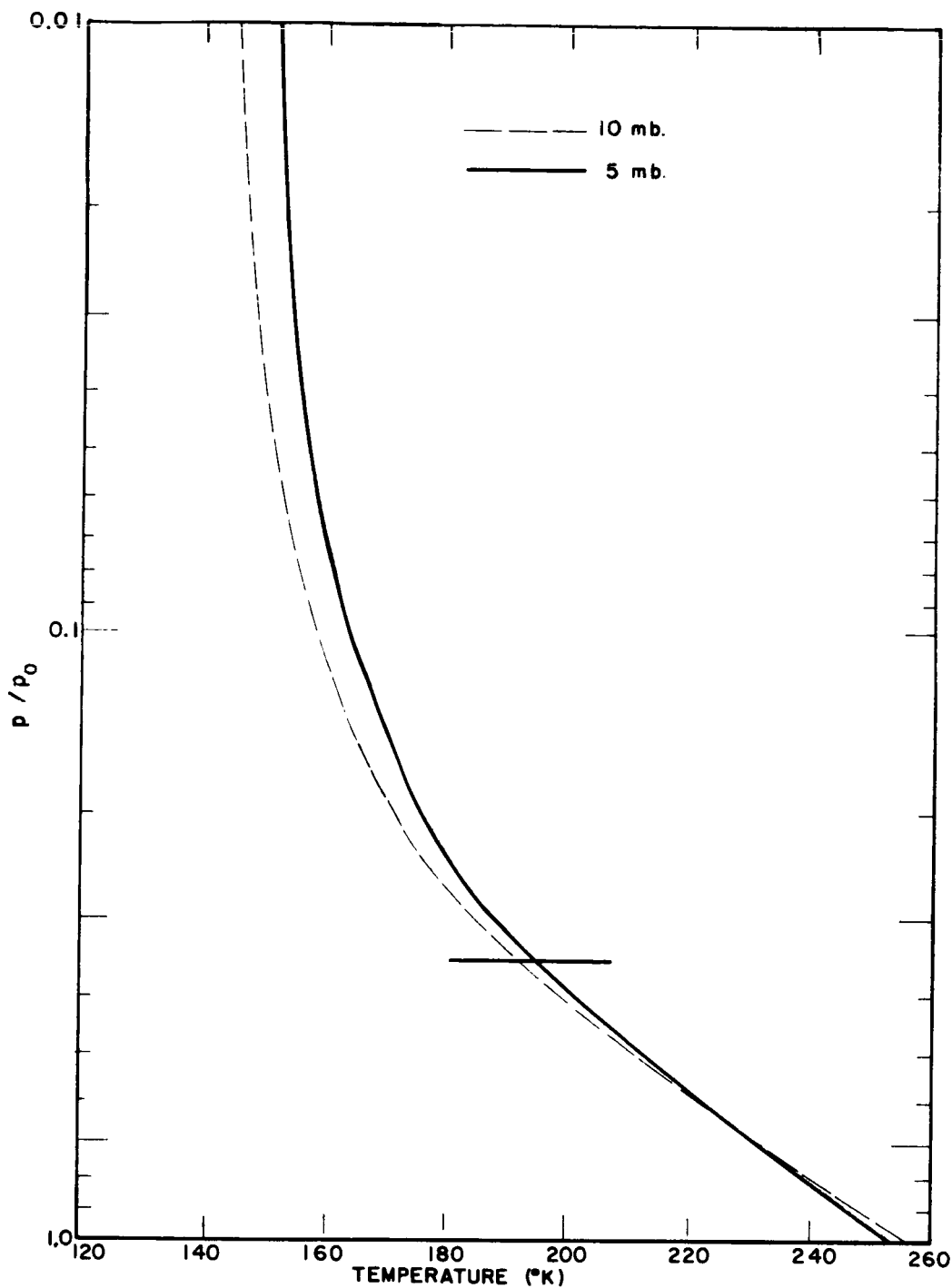


Figure 2. Comparison of Martian temperature profiles computed for 10 mb, 60% CO_2 atmosphere (dashed line) and 5 mb, 100% CO_2 atmosphere (solid line) for Southern Hemisphere summer solstice, latitude 80°S. Tropopause indicated by short horizontal line.

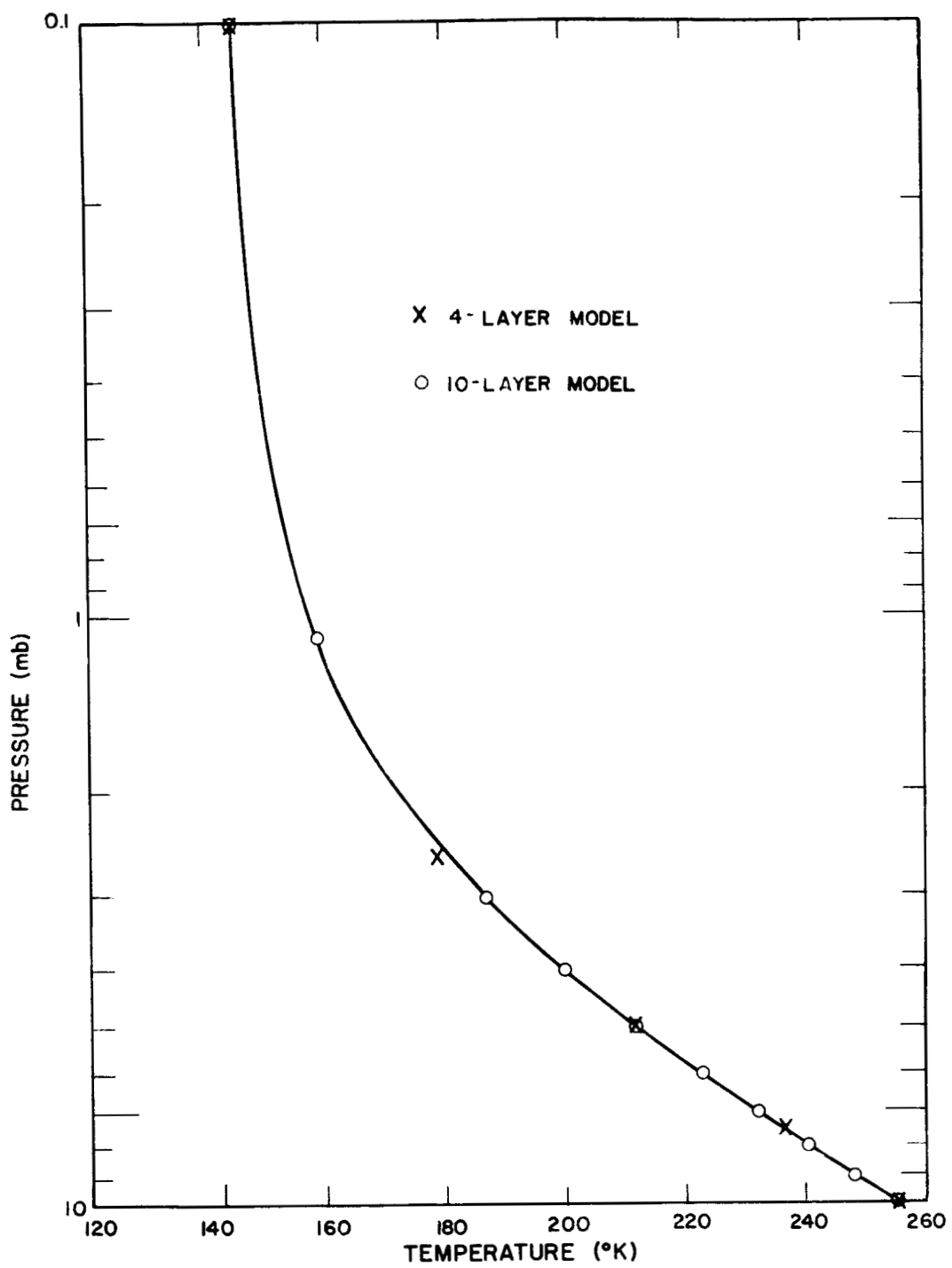


Figure 3. Comparison of Martian temperature profiles computed with 4-layer model (x) and 10-layer model (o) for Southern Hemisphere summer solstice, latitude 80° S.

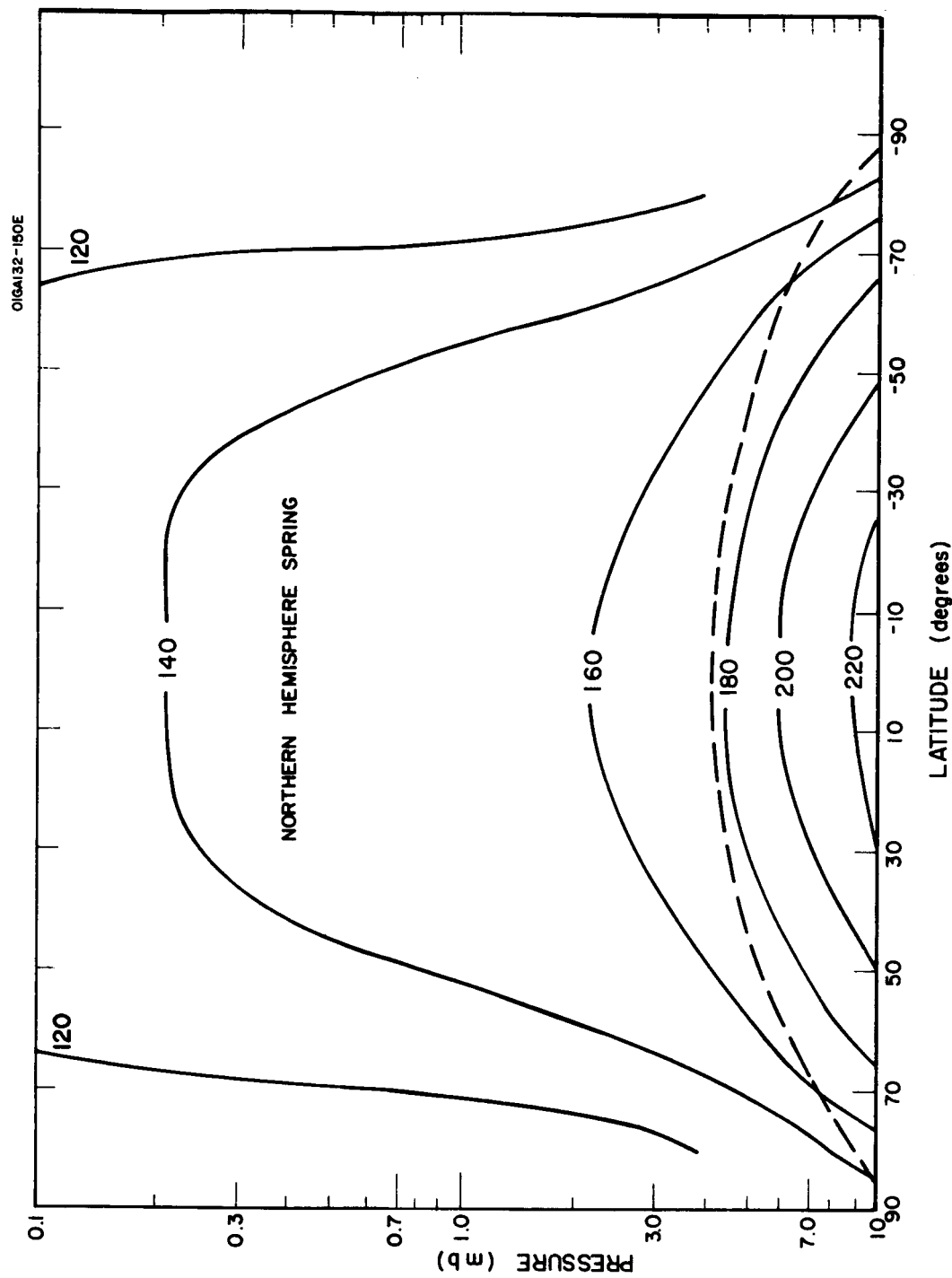


Figure 4. Computed latitudinal temperature cross-section for Northern Hemisphere spring equinox on Mars. Temperatures in $^{\circ}$ K; tropopause indicated by dashed line.

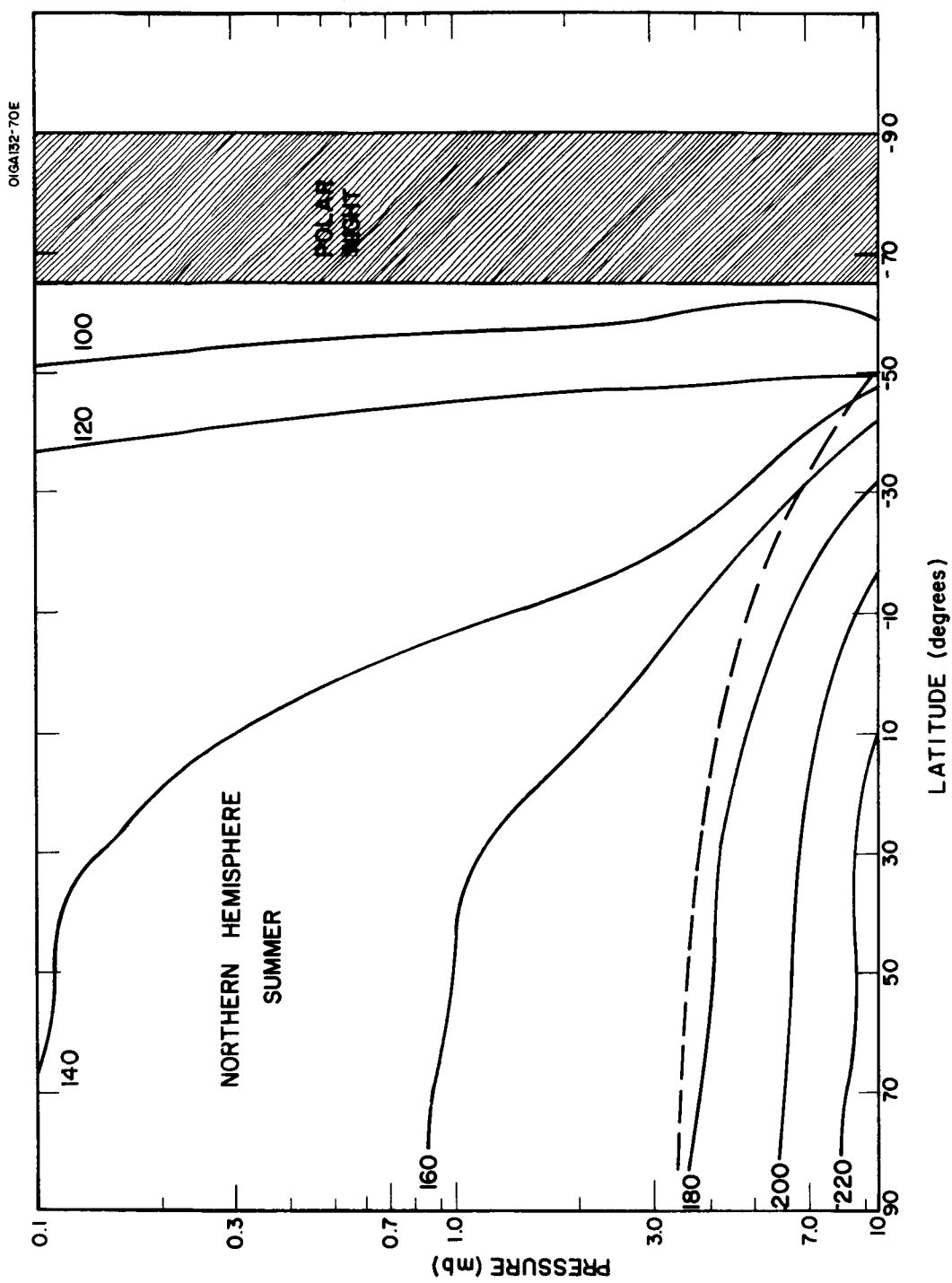


Figure 5. Computed latitudinal temperature cross-section for Northern Hemisphere summer solstice on Mars. Temperatures in $^{\circ}\text{K}$; tropopause indicated by dashed line.

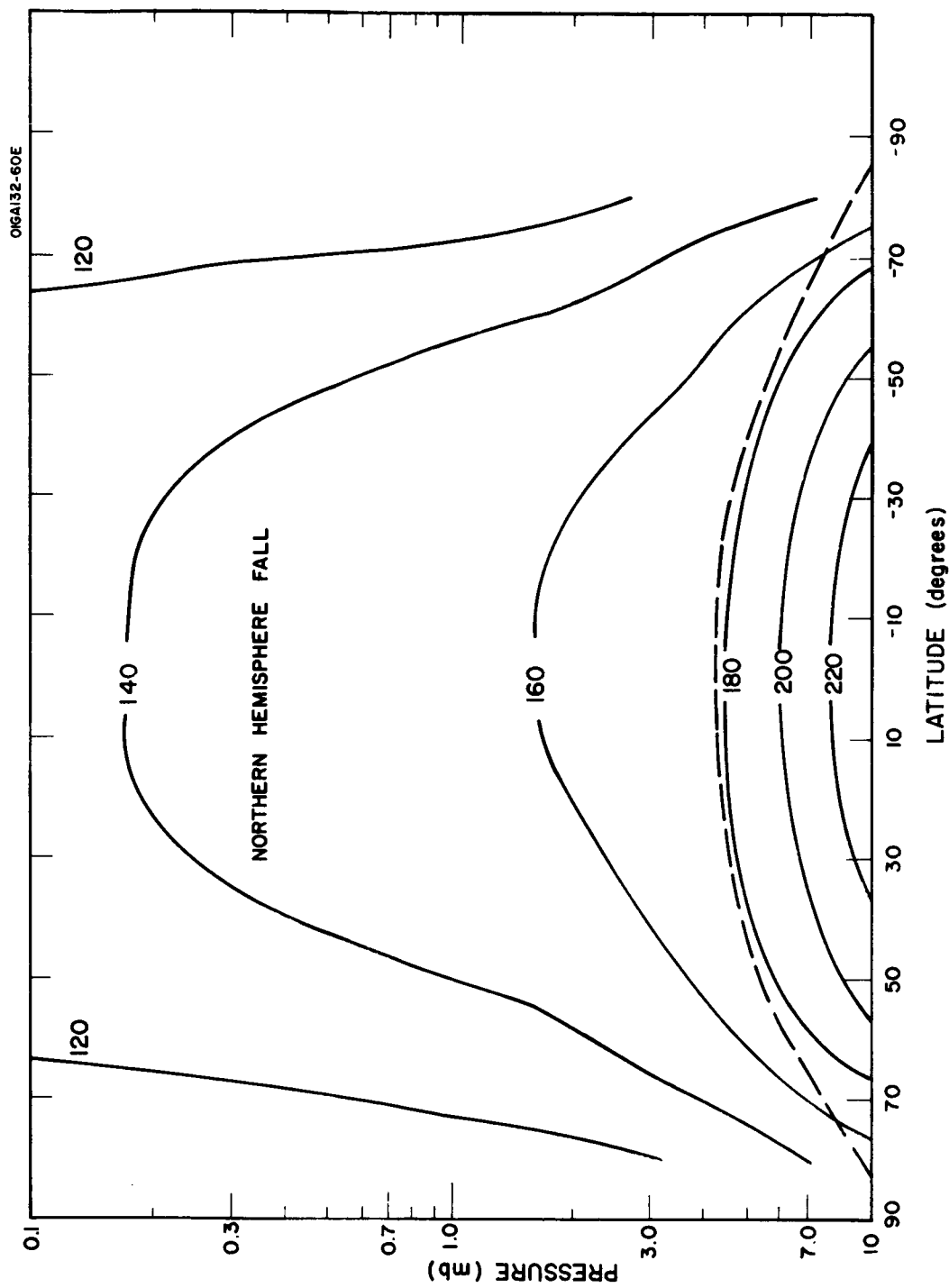


Figure 6. Computed latitudinal temperature cross-section for Northern Hemisphere fall equinox on Mars. Temperatures in $^{\circ}\text{K}$; tropopause indicated by dashed line.

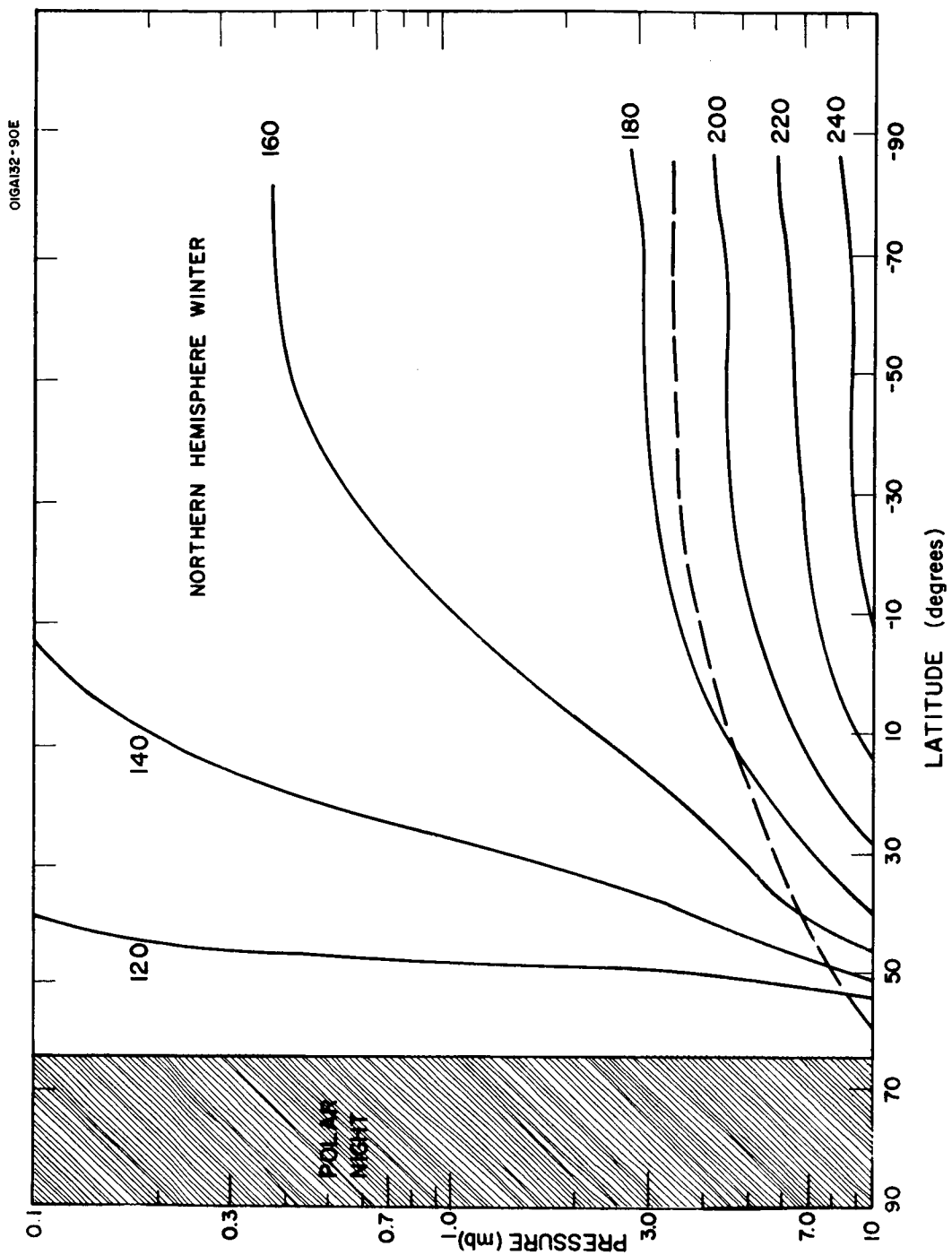


Figure 7. Computed latitudinal temperature cross-section for Northern Hemisphere winter solstice on Mars. Temperatures in $^{\circ}\text{K}$; tropopause indicated by dashed line.

Before describing the features of the computed temperature distributions, we should discuss the representativeness of these computed temperatures. The major heat transport processes not included in the model are latitudinal transport of heat by the atmospheric circulation and conductive exchange between the planetary surface and the subsurface. The atmospheric circulation would transport heat from the regions of maximum insolation (equinoctial equator or summer pole) to the regions of minimum insolation (equinoctial poles and winter pole). The effect of such transport would be a decrease of temperature at equatorial latitudes during the equinoxes and at polar latitudes during summer, and an increase of temperature at polar latitudes during the equinoxes and in winter. The effect of conductive exchange between the surface and subsurface would be similar. Downward heat conduction into the subsurface would lower the temperature at points with maximum insolation. Upward heat conduction to the surface would raise the temperature at points of minimum insolation. Of these two processes, the effect of latitudinal transport of heat energy by the circulation is probably much more important. Smagorinsky et al (1965) obtained excellent agreement between computed and observed temperatures for the Earth's atmosphere with a model that includes the effect of the circulation but neglects conductive heat exchange.

Another heat transfer mechanism - release of latent heat due to changes of phase of CO₂ - would become important at high latitudes if the Martian polar caps are composed of solid CO₂ (Leighton and Murray, 1966; Leovy, 1966). This mechanism would tend to increase the surface temperature during the period that the cap is forming and decrease the surface temperature during the period that the cap is melting. The effect of the possible condensation of CO₂ is not allowed for in the present model.

From the above discussion we may conclude that the computed temperatures are probably somewhat too high at equatorial latitudes during the equinoxes and at polar latitudes during the summer. They are too low at polar latitudes during the equinoxes and during winter. The computed temperatures should be most representative at middle latitudes during the equinoxes and at equatorial latitudes during the solstices.

The major features of the computed temperature cross-sections are:

1. The extremely small latitudinal temperature gradients in the summer hemisphere, with the maximum temperature occurring at the pole.
2. The decrease of tropopause altitude - dashed line - with latitude from a maximum at the equator during the equinoctial seasons and at the summer pole during the solstices.
3. The relatively isothermal vertical structure at high latitudes during the equinoxes and in winter.

The average planetary surface temperatures for the four seasons are listed in Table 2. The temperature differences between the two equinoxes and between the two solstices are due to differences in the planet's distance from the sun.

It is of interest to compare the computed temperatures with observational indications of Martian temperatures and with other theoretical estimates. Indications of surface temperature are available from microwave and infrared observations. Unfortunately, both the infrared and microwave observations are of the sunlit side of the planet and therefore are representative of daytime temperatures rather than the average daily temperatures that are computed in our model. However, the microwave observations refer to temperatures at levels a few centimeters below the surface. At such levels, the effect of diurnal temperature variations would be minimal, and the observed temperatures may be close to the daily average temperatures. Unfortunately, the microwave observations do not resolve the disk. Thus, to make a comparison we must average our computed surface temperatures to obtain a planetary average surface temperature. This temperature can then be compared with the microwave observations. Our computed planetary average surface temperature is 208°K . The microwave observations yield an average temperature of about 215°K to 220°K , when corrected for a surface emissivity of 0.89 and normalized to a mean Mars-sun distance (Dent et al, 1965; Hughes, 1966; Kellerman, 1966). The uncertainty in this temperature, due to observational errors, is about $\pm 5\%$. The agreement between the computed and observed planetary average temperature can be considered excellent.

Theoretical calculations of the latitudinal and seasonal distributions of the diurnal variation of Martian surface temperature have been performed by Leovy (1966) and Leighton and Murray (1966). Figures 8 and 9 show comparisons of our computed surface temperatures with the daily average surface temperatures of Leovy. Leovy models the atmospheric radiative exchange in a fashion similar to but simpler than ours. His treatment of convection is somewhat different from ours and he also includes the effect of conductive heat transfer between surface and subsurface. His computations are for a 5 mb surface pressure, 100 percent CO_2 atmosphere with an albedo that varies with latitude and whose average value is about 0.23. Because of a generally lower albedo, his surface temperature should be a few degrees lower than ours. However, the results are in excellent agreement except at polar regions during the equinoxes and winter. When Leovy's surface temperature falls below the condensation temperature of CO_2 ($\sim 145^{\circ}\text{K}$), he permits atmospheric CO_2 to condense. The release of latent heat of condensation maintains the polar temperatures during these seasons at 145°K . This effect is not included in our computations.

A comparison of our computed latitudinal distribution of annual surface temperature with that of Leighton and Murray (1966) is shown in Figure 10. Leighton and Murray parameterize the exchange of heat energy between the surface and atmosphere, but do include the effects of conductive

Table 2

Average planetary surface temperatures.

Season	Average Planetary Surface Temperature (°K)
Northern Hemisphere Spring Equinox	210
Northern Hemisphere Summer Solstice	194
Northern Hemisphere Fall Equinox	217
Northern Hemisphere Winter Solstice	212

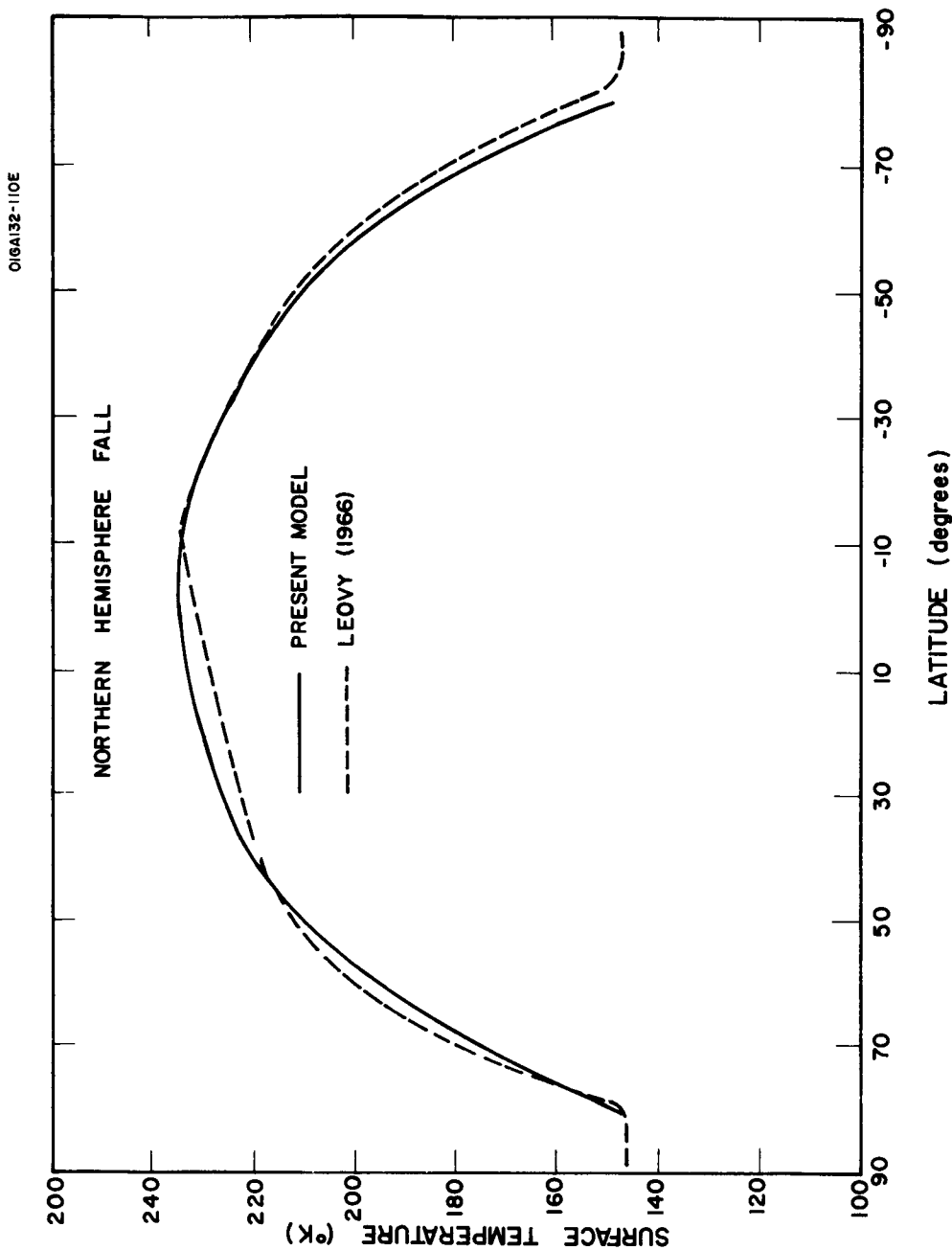


Figure 8. Comparison of computed latitudinal variation of Martian surface temperature for Northern Hemisphere fall equinox with that of Leovy (1966). Solid line - present model; dashed line - Leovy (1966).

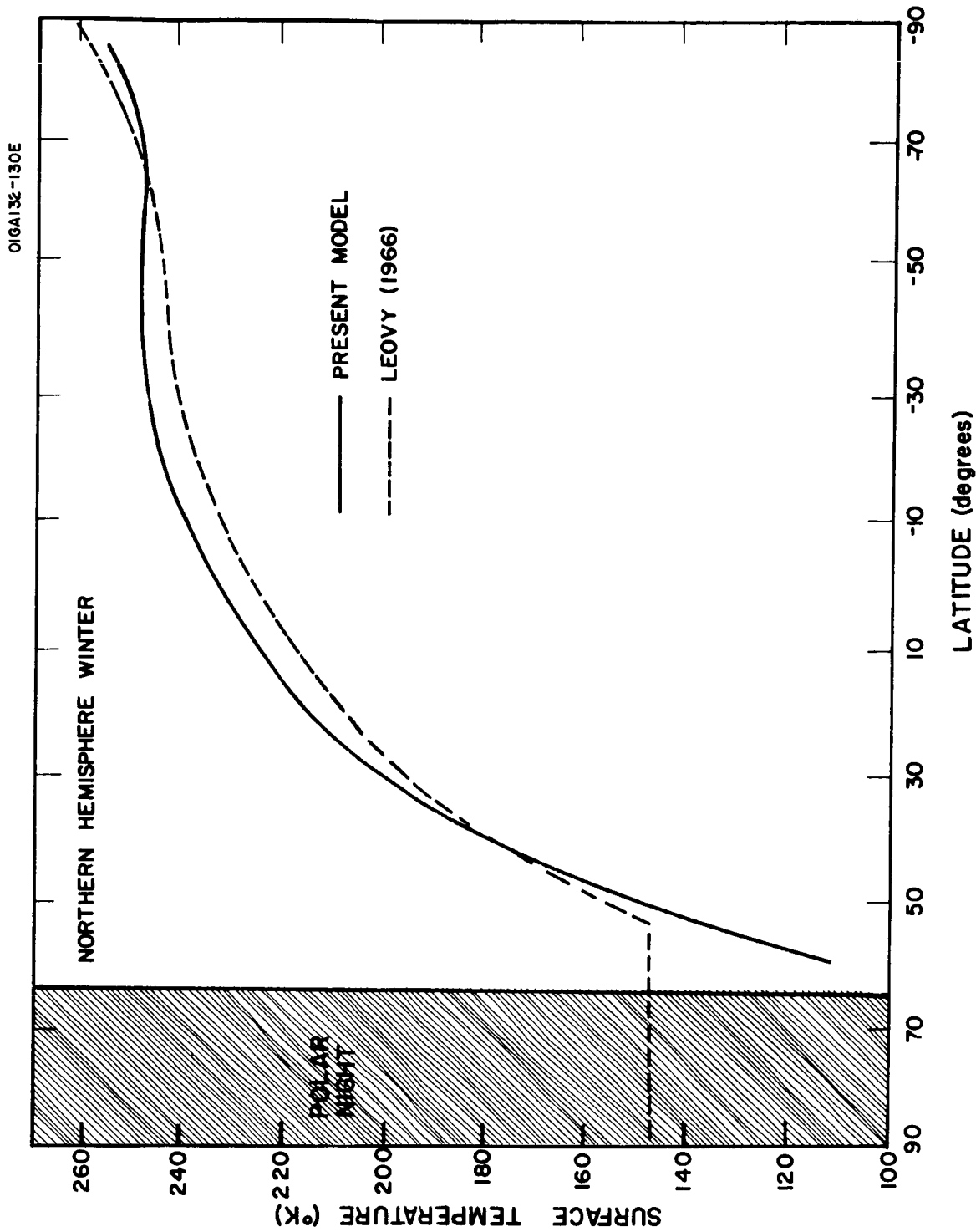


Figure 9. Comparison of computed latitudinal variation of Martian surface temperature for Northern Hemisphere winter solstice with that of Leovy (1966). Solid line - present model; dashed line - Leovy (1966).

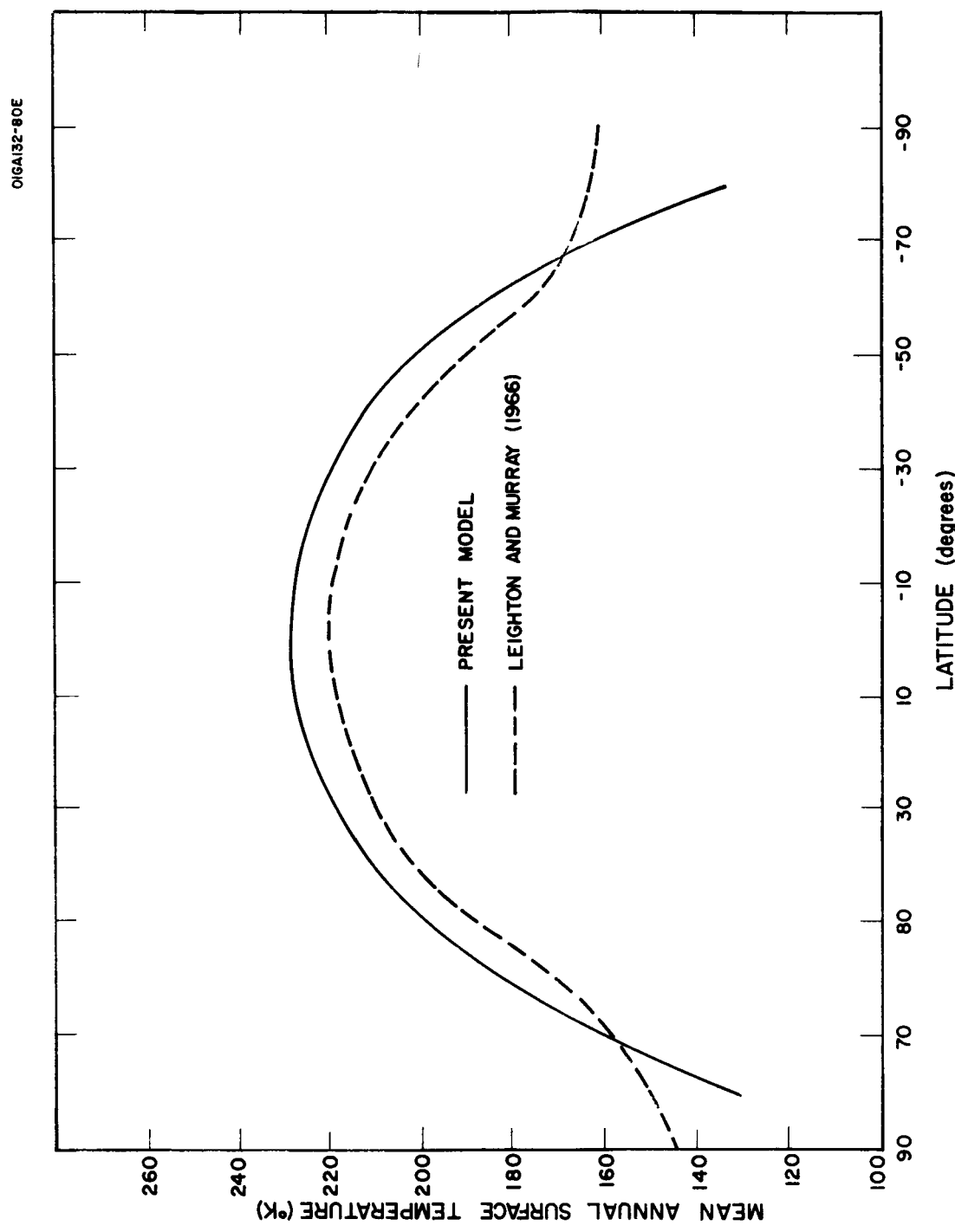


Figure 10. Comparison of computed latitudinal variation of mean annual Martian surface temperature with that of Leighton and Murray (1966). Solid line - present model; dashed line-Leighton and Murray (1966).

heat exchange between surface and subsurface and the effect of the release of latent heat due to condensation of CO₂. Their assumed albedo is 0.15. The comparison indicates that their temperatures are some 8 to 10°K lower than ours at low and middle latitudes. Since their assumed albedo is lower than ours, their computed temperatures should not be lower but higher than ours at these latitudes. The reason for the discrepancy may be their simplified modelling of heat exchange between surface and atmosphere. Their polar temperatures are higher than ours because they include the effect of condensation of atmospheric CO₂. Generally speaking, the results of all three theoretical models - ours, Leovy's, and Leighton and Murray's - are in excellent agreement on the latitudinal variations of surface temperature.

There is no observational information available on the latitudinal and seasonal variations of the Martian vertical temperature distribution with which to compare our results. There are also no theoretical estimates except those from Leovy's (1966) two layer atmosphere model. In Figures 11 and 12 we compare our latitudinal distributions of computed temperature at the atmospheric level, $p/p_0 = 0.31$, where p is pressure and p_0 is surface pressure, with those of Leovy for the same atmosphere level. In general, our computed temperatures are generally 20°K to 35°K lower than Leovy's. The reason for this difference is not immediately obvious. It may be that Leovy has overestimated the convective heat flux, which would lead to higher atmospheric temperatures and lower surface temperatures in his model. This would also explain why his surface temperatures agree quite well with ours despite his lower albedos.

A rough comparison can be made between our computed temperatures and the temperatures inferred from the Mariner IV occultation experiment.

Figure 13 shows a temperature profile computed for the latitude and time of year at which the Mariner IV occultation experiment during immersion was performed. Immersion occurred at 50°S latitude in late winter at a local time of 1 P.M. when the solar zenith angle was 67°. Our computations were performed for 50°S latitude and solar declination angle of +15° (corresponding to the day of the occultation measurement). The temperature near the surface derived from the immersion occultation experiment was 175°K ± 25°K (Kliore et al, 1965). This is presumably an average temperature of the lower Martian atmosphere. In addition, it was found that there was no obvious change of scale height with altitude in the first 30 km. Our calculations indicate a surface temperature of 173°K and a decrease of temperature with altitude to less than 120°K at $p = 0.1$ mb (~ 40 km). Our average temperature (pressure weighted) for the first 40 km would be about 150°K. Two factors would cause the computed temperatures to be less than the actual temperatures. The present computation represents the average diurnal temperature for the day and location of encounter. One would expect the average diurnal temperature to be less than the 1 P.M. temperature, which should be close to the maximum daily temperature. In addition, latitudinal heat transport is neglected

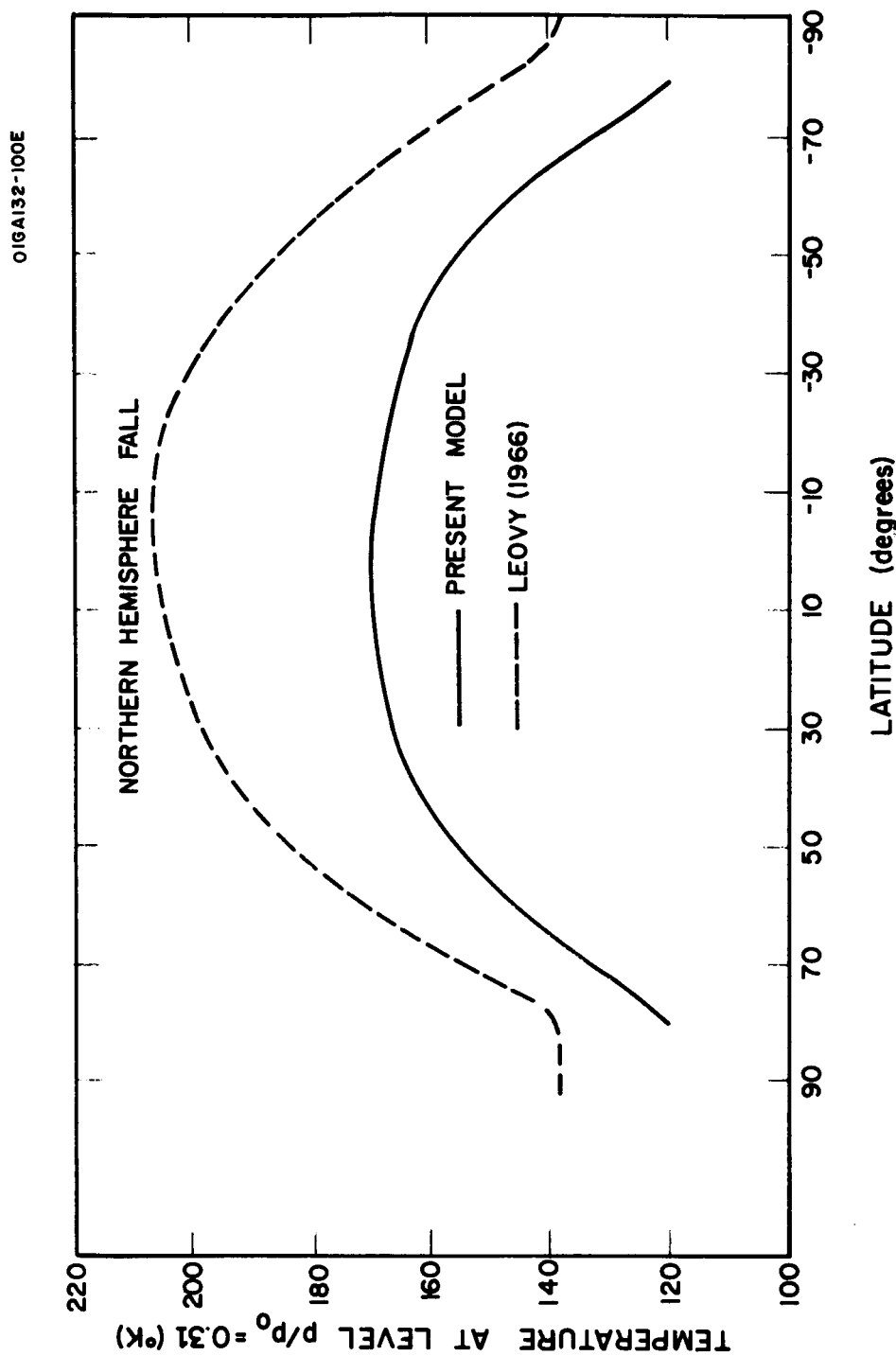


Figure 11. Comparison of computed latitudinal variation of Martian temperature at atmospheric level $p/p_0=0.31$ for Northern Hemisphere fall equinox with that of Leovy (1966). Solid line-present model; dashed line - Leovy (1966).

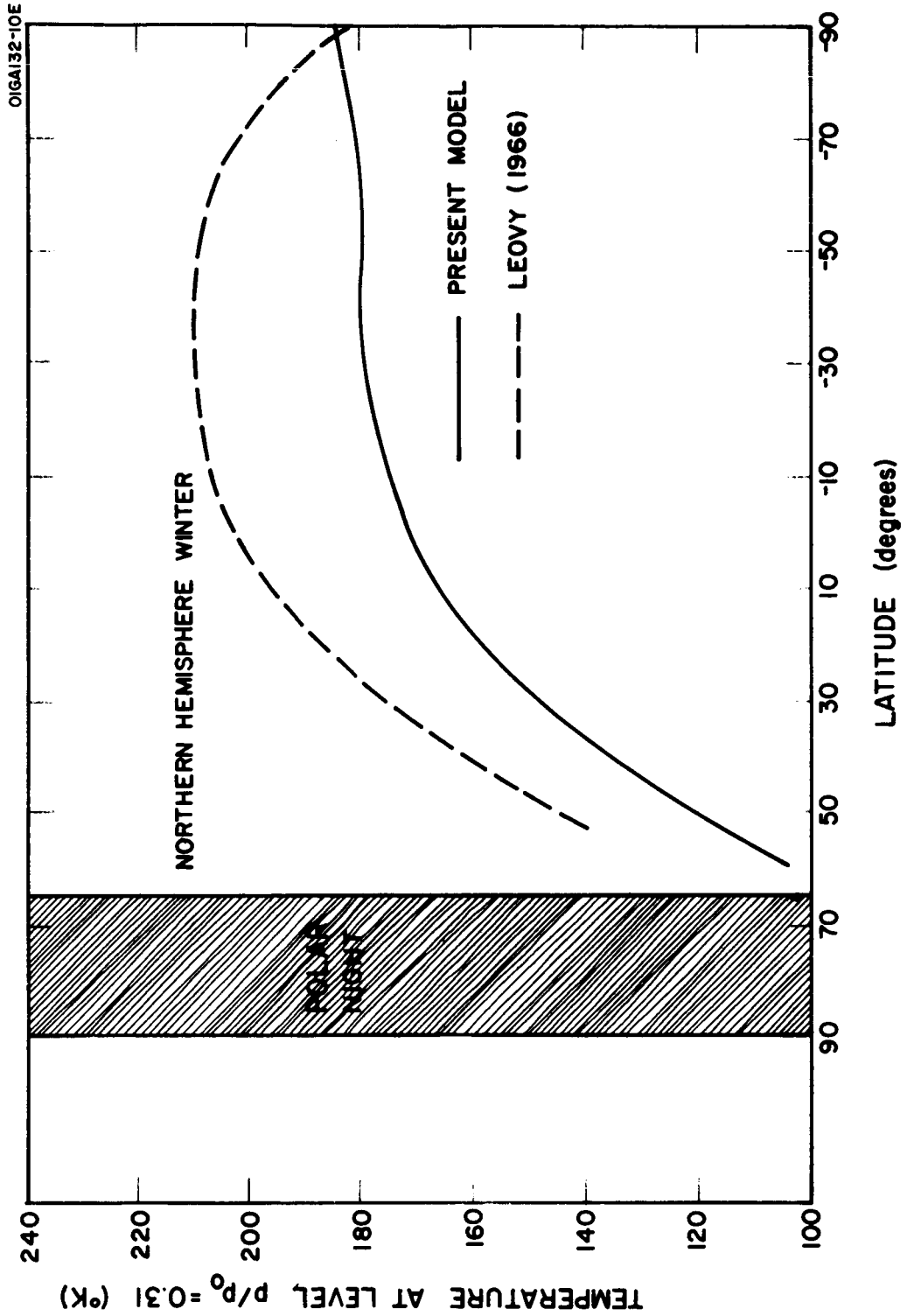


Figure 12. Comparison of computed latitudinal variation of Martian temperature at atmospheric level $p/p_0=0.31$ for Northern Hemisphere winter solstice with that of Leovy (1966). Solid line - present model; dashed line - Leovy (1966).

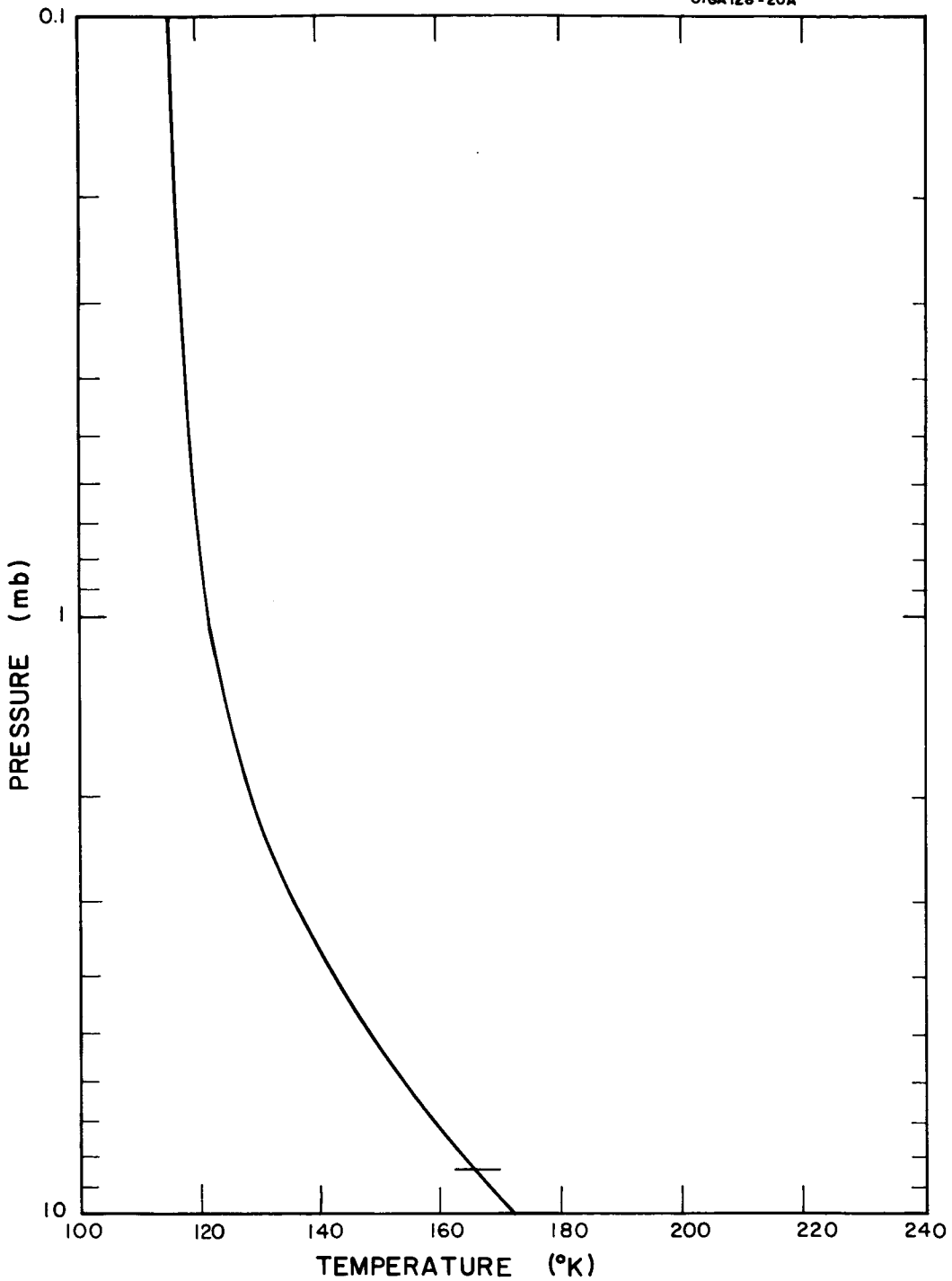


Figure 13. Computed temperature profile of the Martian atmosphere for the date of the Mariner IV immersion occultation experiment (50°S , solar declination $+15^{\circ}$, late Southern Hemisphere winter).

in the model. At this latitude during winter, one would expect latitudinal heat transport to increase the computed temperatures somewhat. An addition of 20°K to our computed values would be a reasonable correction for these effects and would place the computed temperature in excellent agreement with temperature derived from the immersion experiment. However, our computed temperatures do suggest that the scale height would vary by about 30 percent from the surface to about 40 km, which is not in agreement with the immersion observations.

Figure 14 shows a computed temperature profile for the latitude and solar declination on the day of emmersion, which occurred at 60°N at night during late summer. According to Kliore et al (1966) the temperature at emmersion was 220°K and according to Fjeldbo et al (1966) the apparent lapse rate was greater at emmersion than on immersion. Our calculations indicate a surface temperature of 222°K and a decrease of temperature with altitude to less than 135°K at 1.0 mb. Our average temperature for the first 40 km would be about 180°K . Since at the local time, season, and latitude of emmersion, both diurnal effects and latitudinal heat transport processes would tend to decrease our computed temperatures, it must be concluded that the computed temperatures for emmersion are not in good agreement with the observed temperature on emmersion. Our results for emmersion do indicate a greater lapse rate in the first 30 km, in agreement with the observations.

Whether the thermal equilibrium temperature profile is a good estimate of the actual daily average temperature profile for a particular time of year may be questioned on the grounds that a certain amount of time is necessary for an initial temperature profile to become a thermal equilibrium temperature profile. It will be recalled that, in computing the thermal equilibrium temperature, an initial temperature profile begins the iterative process of the computational model and, after a certain number of iterations, the final temperature profile is approached. Thus, the equilibrium temperature profile is the steady state solution to the convective and radiative equations governing the temperatures in the Martian atmosphere, which is approached asymptotically through the iterative cycles of the computational model. In the computational model all the atmospheric parameters (i.e. surface pressure, CO_2 mass mixing ratio, solar insolation, etc.) remain constant during the time required to reach equilibrium. In the actual case, the one atmospheric parameter that definitely changes with time is the average solar insolation. In our computations, it was implicitly assumed, however, that this change was negligibly small during the time necessary for a given initial temperature profile to approach asymptotically the steady state, thermal equilibrium temperature profile. The validity of this assumption was studied in the following manner.

Starting with a thermal equilibrium profile for a particular latitude and time of year, we computed temperature profiles at successive 10-day time steps for an annual cycle using the basic computational model to

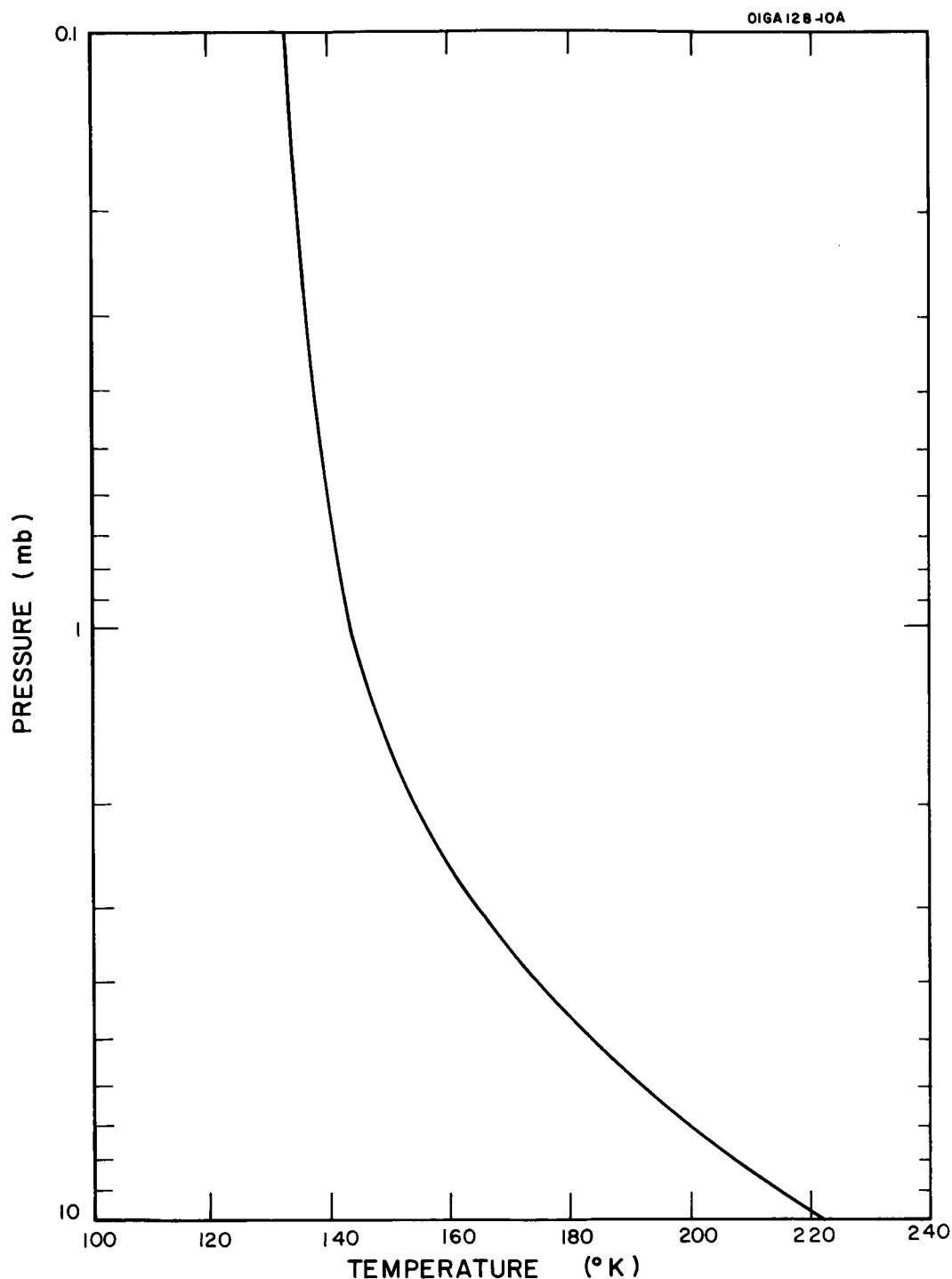


Figure 14. Computed temperature profile of the Martian atmosphere for the date of the Mariner IV emmersion occultation experiment (60° N, solar declination $+15^{\circ}$, late Northern Hemisphere summer).

determine the change in temperature during a single time step of 10 days. From one time step to the next the average solar insolation changes such that during the τ -th time step, the average solar insolation is given by

$$\bar{S}_o(\tau) = \frac{1}{2} [S_o(\tau) + S_o(\tau-1)]$$

where $S_o(\tau)$ and $S_o(\tau-1)$ are the average solar insolations at the end and beginning of the 10-day period of the τ -th time step. The temperatures computed in this manner can then be checked against the thermal equilibrium temperatures.

Computations were performed for Martian latitudes 0° and 80°N . The initial temperature profiles were the thermal equilibrium temperature profiles for the Northern Hemisphere spring equinox and for a date 45 days before the Northern Hemisphere spring equinox, respectively. Figures 15 and 16 are graphs of the daily average surface temperature as a function of time for 0° and 80°N respectively. Included in Figures 15 and 16 are the respective thermal equilibrium surface temperatures for the first day of the four Martian seasons. (Only 3 seasons appear in Figure 16, as the Northern Hemisphere winter solstice occurs during the polar night.)

As can be seen, the thermal equilibrium surface temperatures are in excellent agreement with the "time dependent" surface temperatures except at 80°N during the spring and autumnal equinoxes, when a maximum temperature difference of about 25°K occurs. Therefore, the computed equilibrium temperature profiles should give reasonable estimates of the seasonal variations of Martian temperatures.

1.8 Concluding Remarks

Martian pole-to-pole temperature cross-sections from the surface to about 40 km altitude for each season have been computed with a thermal equilibrium model. The computed average temperatures should be closest to the actual average temperatures at middle latitudes during the equinoxes and at low latitudes during the solstices. Because the model does not allow for latitudinal transport of heat energy by the atmospheric circulation and the possible condensation of carbon dioxide, the computed temperatures are too low at polar latitudes during the equinoxes and winter and probably too high at equatorial latitudes during the equinoxes and at polar latitudes during summer. The major features of the computed temperature cross-sections are:

- (1) The extremely small latitudinal temperature gradients in the summer hemisphere, with the maximum temperature occurring at the pole.

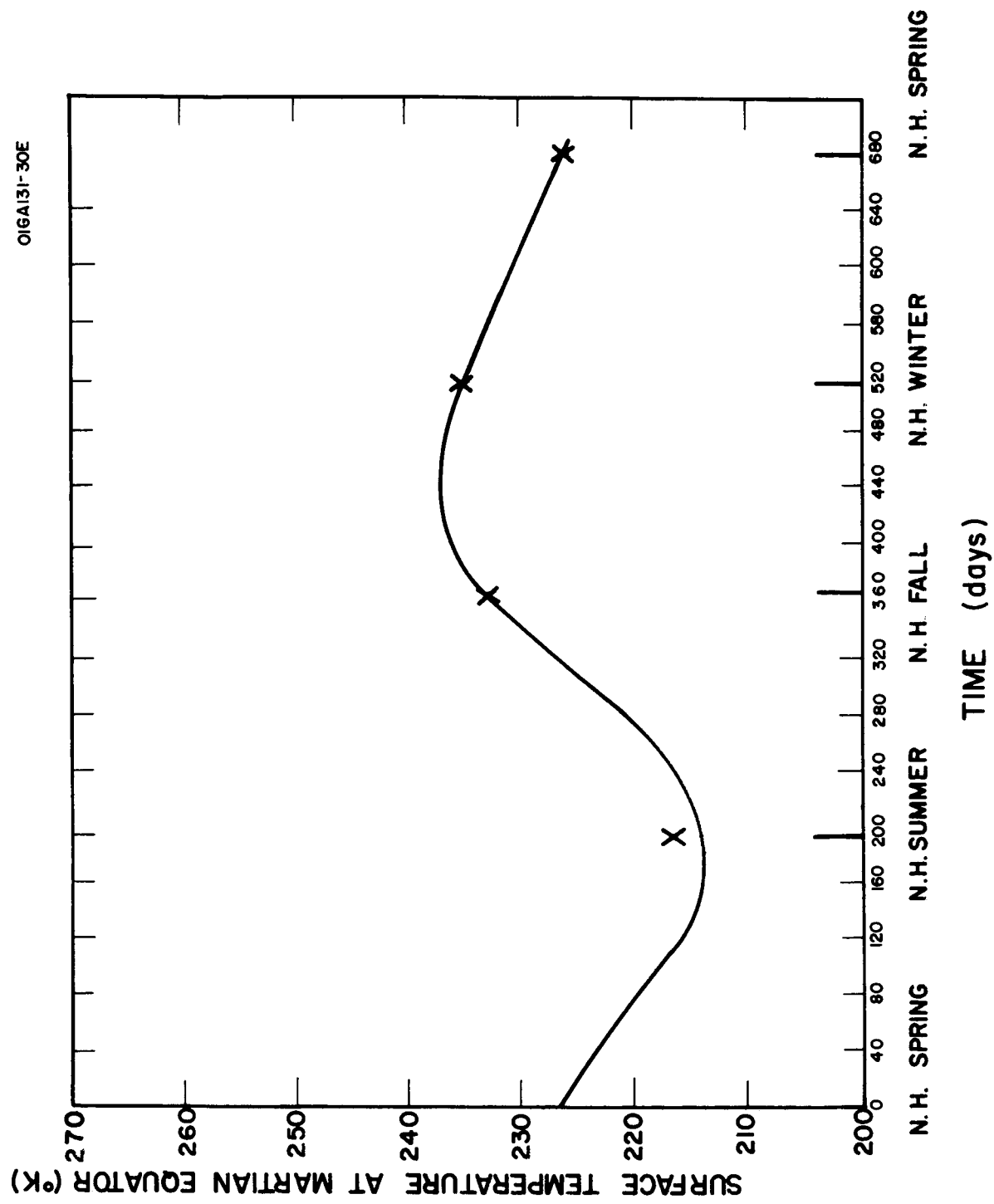


Figure 15. Martian surface temperature as a function of time at equator.
 Solid line: time dependent case starting with initial thermal equilibrium condition at Northern Hemisphere spring equinox.
 X: computed on basis of thermal equilibrium.

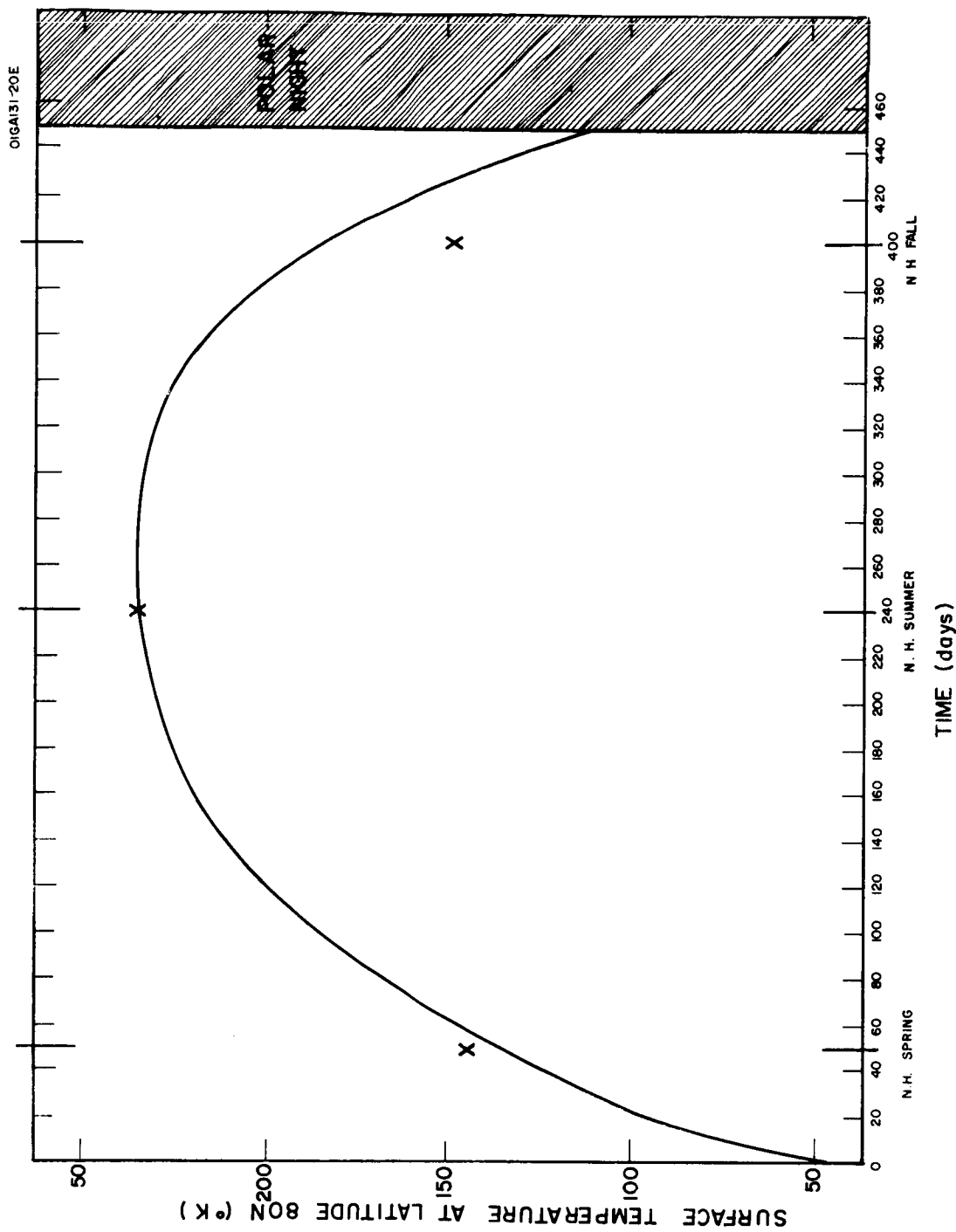


Figure 16. Martian surface temperature as a function of time at 80°N .
 Solid line: time dependent case starting with initial thermal equilibrium condition at 45 days prior to spring equinox.
 X: computed on the basis of thermal equilibrium.

(2) The decrease of tropopause altitude with latitude from a maximum at the equator during the equinoctial seasons and at the summer pole during the solstices.

(3) The relatively isothermal vertical structure at high latitudes during the equinoxes and winter.

Comparisons of the present results with other theoretical studies and with the microwave and Mariner IV observations of Martian temperatures yield generally good agreement. Further theoretical studies of temperatures of the surface and lower atmosphere of Mars should include the effects of latitudinal heat transport, release of latent heat of condensation, conductive heat exchange between surface and sub-surface, atmospheric water vapor radiative transfer, and analyses of the diurnal temperature wave.

2. THE GENERAL CIRCULATION OF THE MARTIAN ATMOSPHERE

Wen Tang

2.1 SEASONAL VARIATIONS OF THE MEAN ZONAL WIND VELOCITY AND TEMPERATURE OF THE MARTIAN ATMOSPHERE

2.1.1 Introduction. More than one and half decades ago, the general circulation of the Martian atmosphere was essentially inferred from telescopic observations of the movement of yellow clouds and radiometric observations of the surface temperature (Hess and Panofsky, 1951). In 1961, Mintz applied dynamic stability theory to the Martian atmosphere to determine the type of general circulation on the planet - symmetric or wave type.

Recently, Tang (1966) used the new data on atmospheric composition and surface pressure (Kliore, 1966) and a general circulation model for steady state and symmetrical regime to study the mean zonal and meridional winds in the northern hemisphere and the stability of the symmetrical regime in the Martian atmosphere during the equinoctial seasons. The purpose of the present work is to study the seasonal mean zonal winds and temperatures at the middle of the Martian atmosphere with the use of a simple dynamic model.

2.1.2 General Theory. Based upon the principle of conservation of energy, Adem (1962) developed a simple model of the general circulation for the Earth's atmosphere. His model yields mean monthly meridional profiles of zonal wind and temperature that agree well with observed mean profiles. We can apply this model to Mars.

We shall outline the concept involved in this model. For the details of the theory and the basic mathematical developments we refer the reader to Adem (1962). If the constituents of the atmosphere and the temperature are known, the energy emitted from an atmospheric layer can be calculated. From the balance of radiational energy, one can evaluate the excess of radiational energy at an atmospheric level and at the surface, if the atmospheric and surface temperatures, insolation, and albedo are known. Conversely, the atmospheric and surface temperatures can be computed if the excesses of both atmospheric and surface radiation energy are known. Two equations with four unknowns arise from writing down the radiation budget equations for the surface and atmosphere. Two more equations are needed to determine these quantities uniquely. One of these two is the energy equation, which essentially indicates that the rate of change of thermal energy due to meridional turbulent transport is equal to the rate of change of thermal energy due to radiation plus the rate of change of conduction of sensible heat and the molecular transformation. The fourth equation may be considered as an empirical equation which is used to evaluate some unknown with observational data. With these four equations the meridional profiles of the temperature for different seasons can be determined. By using the geostrophic wind equation, the meridional profile of mean zonal wind can be obtained from the computed meridional temperature profile.

The final governing equation for the latitudinal variation of atmospheric temperature is (Adem, 1962)

$$\frac{d^2}{d\phi^2} \bar{T}'_m + c_6^2 \bar{T}'_m = - \frac{c_1}{c_7 K} I_d - \frac{c_o}{c_7 K} + \frac{J - c_4 \bar{E}_3}{c_7 K} \quad (55)$$

where

\bar{T}'_m = the deviation of mean atmospheric temperature at latitude ϕ from the mean atmospheric temperature at a given latitude for a given season.

ϕ = Latitude

I_d = The insolation during one day

J = The rate of change of the conduction of sensible heat and the molecular transformation function.

\bar{E}_3 = The excess mean radiational energy at the surface of Mars.

c_6 = $(1 - A c_2) / c_7 K$

\bar{K} = Eddy viscosity

c_7 = $- c_3 (A_1) (1 + \beta A / 2) / r_o^2$

r_o = Radius of Mars

A_1 = $c_v / 2 (p_o^{*} - p_o)$

A = $2H_o / (4T_o + \beta H_o)$

p_o = Pressure

c_v = Specific heat at constant volume

g = Gravitational acceleration of Mars

H_o = Height of the top of the absorbing gases

T_o = The temperature at height H_o

β = The mean lapse rate

and

c_o, c_1, c_3 , and c_4 = coefficients of the following equation

$$(1-A) \bar{T}'_m = c_0 + c_1 I_d + c_3 \bar{E}_A + c_4 \bar{E}_s \quad (56)$$

The quantity \bar{E}_A is the excess of the mean radiational energy of the Martian atmosphere. The boundary conditions are that the temperature gradients both at the equator and poles are zero, that is,

$$\frac{d}{d\phi} \bar{T}'_m = 0 \quad \text{at } \phi = 0 \text{ and } \frac{\pi}{2} \quad (57)$$

The solution to the differential Equation (55) and boundary conditions in Equation (57) is

$$\begin{aligned} \bar{T}'_m(\phi) = & \frac{c_1}{c_6 c_7 K} \left\{ \int_0^\phi I_d(\psi) \sin(\psi - \phi) d\psi \right. \\ & + \frac{1}{2} \left[\int_0^\pi I_d(\psi) \cosh c(\psi - \frac{\pi}{2}) d\psi \right] \frac{(\cos c_6 \phi + \sin c_6 \phi)}{\sinh c_6 \pi/2} \\ & \left. - \frac{c_0 - J}{c_6 c_1} \right\} \end{aligned} \quad (58)$$

The quantity J is an unknown quantity. It can be evaluated by applying Equation (58) to a latitude for which we have a good estimate of the atmospheric temperature from observational or other theoretical results.

The wind field is determined from simple geostrophic wind relations. If the latitudinal temperature deviation is known, then the mean zonal and meridional wind velocity can be simply written as

$$f \bar{u} = - \frac{R}{r_o} \frac{\partial \bar{T}'_m}{\partial \phi} \quad (59)$$

and

$$\bar{v} = 0$$

respectively, where f = Coriolis parameter for Mars and R = gas constant for Martian atmosphere.

The solution of Equation (55) is valid in a region bounded by the equator and one of the poles, and is a function of the parameter J . In order to eliminate J and to obtain the meridional distribution of mean atmospheric temperatures, $\bar{T}(\phi)$, for one hemisphere, it is necessary to know a mean atmospheric temperature, $\bar{T}(\phi_1)$, at a given latitude, ϕ_1 . And, to obtain the meridional distribution of mean atmospheric temperatures for both hemispheres it is necessary to know mean atmospheric temperatures for two latitudes, $\bar{T}_N(\phi_1)$ and $\bar{T}_S(\phi_2)$, the former temperature somewhere in the Northern Hemisphere ($0 \leq \phi_1 \leq \pi/2$), and the latter temperature somewhere in the Southern Hemisphere ($-\pi/2 \leq \phi_2 \leq 0$). One of the inherent difficulties in the computational model, however, is that the mean atmospheric temperature and wind profiles are computed separately for each hemisphere, and in general the mean temperature will be discontinuous at the equator, unless the input mean temperatures, \bar{T}_N and \bar{T}_S , are specified at the equator. The cause of this discontinuity is the lack of observational data necessary for accurate estimates of \bar{T}_N and \bar{T}_S .

In the present computations the input mean atmospheric temperatures, \bar{T}_N and \bar{T}_S , were obtained from theoretical computations (House, 1966) based on radiative processes alone. House's mean atmospheric temperatures at $35^\circ N$ and $35^\circ S$ are considered representative of the actual Martian atmospheric temperatures at these latitudes, as the effect of meridional transport are considered to be a minimum at these latitudes. Therefore, in the present computations, rather than using the equatorial temperatures of the theoretical computations of House (1966) as the input temperatures for both hemispheres such that temperature discontinuities at the equator could have been avoided, the input temperatures, \bar{T}_N and \bar{T}_S , were the theoretical temperatures at $35^\circ N$ and $35^\circ S$ respectively. As expected, discontinuities in the mean atmospheric temperature at the equator occurred. A maximum temperature discontinuity of about $25^\circ K$ occurred in the temperature profile for the Northern Hemisphere winter solstice. The temperature discontinuities were eliminated by performing a second set of computations where the input temperatures for both hemispheres were specified at the equator and equal to the mid-point of the temperature discontinuity.

2.1.3 Results and Discussion. Meridional profiles of the mean zonal wind and mean atmospheric temperature during the summer and winter solstices and spring and fall equinoxes were constructed. The meteorological parameters used in these computations are as follows:

- P_o = Surface pressure = 5 mb
- β = Atmospheric lapse rate = $3.75^\circ K km^{-1}$
- α_1 = Percentage of solar radiation absorbed by the surface = 70 percent
- α_2 = Percentage of solar radiation absorbed by the atmosphere = 0 percent
- H_o = Level at which the absorbing gas is 1/10 of that at the surface = 21 km
- R = Gas constant = $1.87 \times 10^6 cm^2 sec^{-2} deg^{-1}$

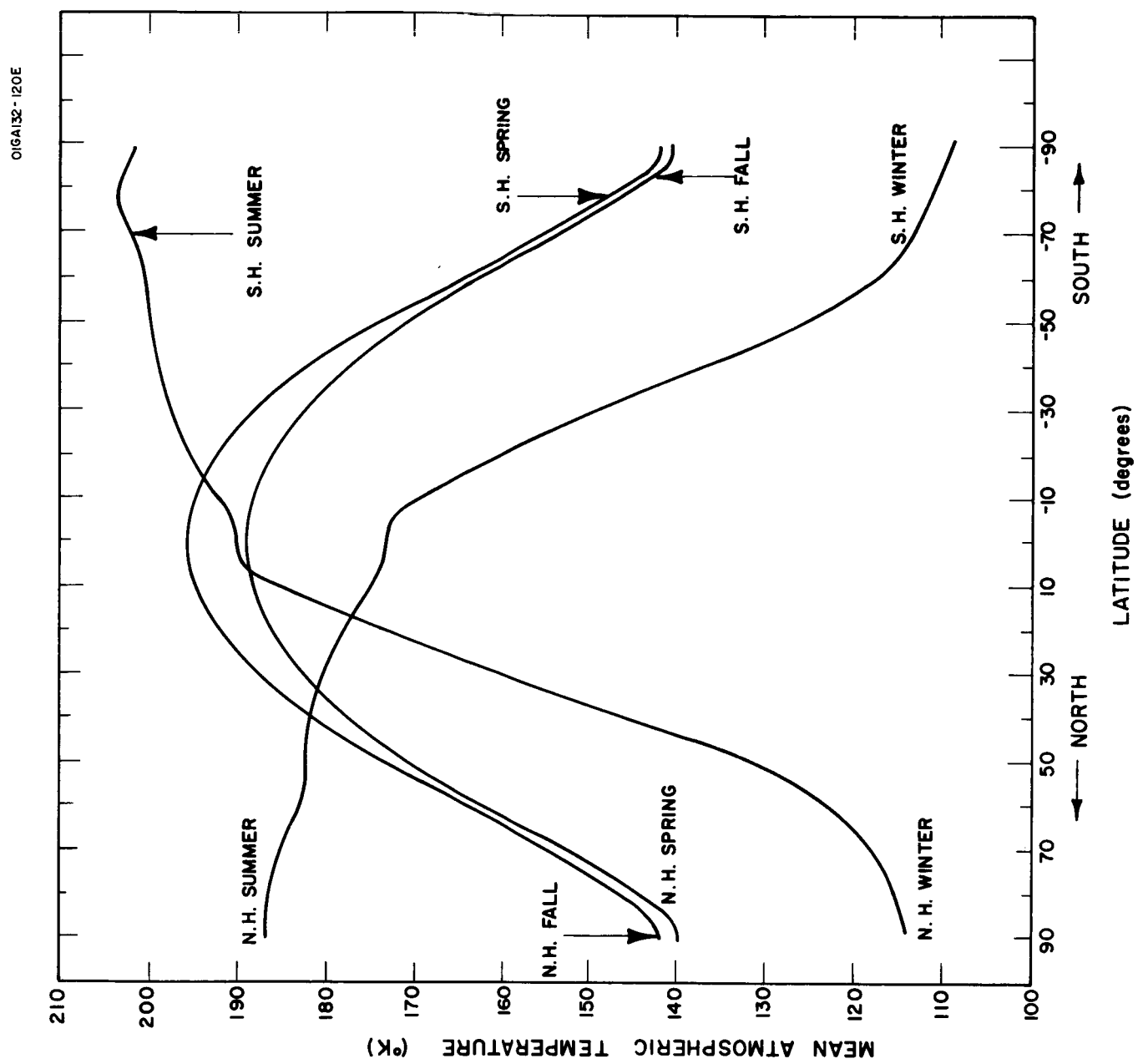


Figure 17. Latitudinal profile of mean atmospheric temperature for the four Martian seasons.

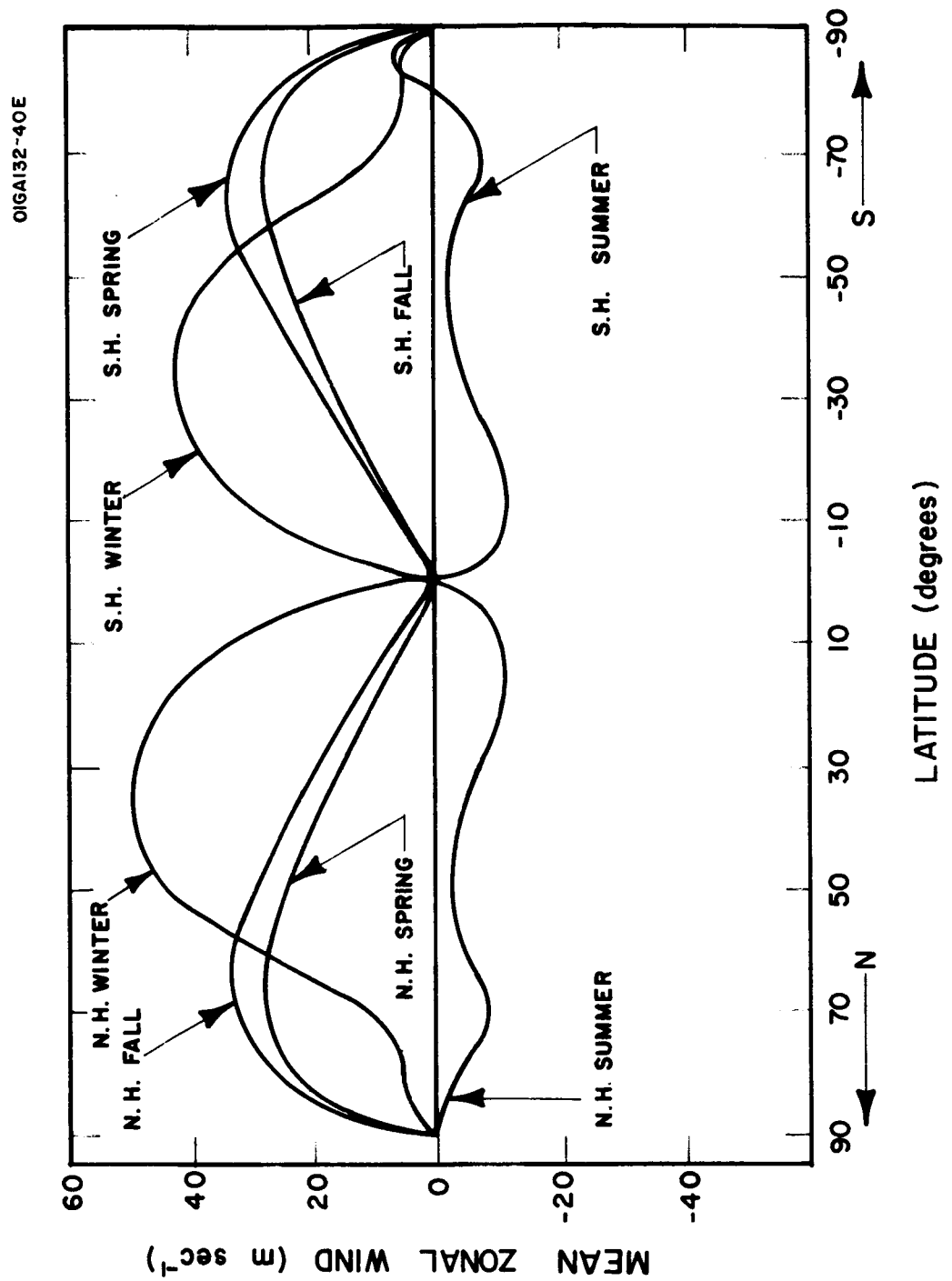


Figure 18. Latitudinal profile of mean zonal wind for the four Martian seasons.

g = Gravitational acceleration = 380 cm sec^{-2}

Ω = Angular velocity = $6.57 \times 10^{-5} \text{ sec}^{-1}$

K = Eddy exchange coefficient = $10^{10} \text{ cm}^2 \text{ sec}^{-1}$

r_o = Radius of Mars = 3400 km

c_v = Specific heat of constant volume = $0.158 \text{ cal gm}^{-1} \text{ deg}^{-1}$

The input temperatures, \bar{T}_N and \bar{T}_S , at 35°N and 35°S respectively, for the four seasons are as follows:

	Northern Hemisphere Winter	Northern Hemisphere Spring	Northern Hemisphere Summer	Northern Hemisphere Fall
$\bar{T}_N (\text{°K})$	160	180	190	188
$\bar{T}_S (\text{°K})$	205	180	145	184

The computed mean atmospheric temperature profiles for the four Martian seasons are shown in Figure 17. The extreme temperatures are found to occur in the Southern Hemisphere. The highest mean atmospheric temperature is about 205°K and occurs at 80°S during the Southern Hemisphere summer solstice. The lowest mean atmospheric temperature is about 108°K and occurs at the South Pole during the Southern Hemisphere winter solstice. It is interesting to note that the difference between the maximum and minimum mean atmospheric temperature, at the North Pole is smaller than the corresponding difference at the South Pole. This is a result of the planet's being closer to the sun during the Southern Hemisphere summer solstice. It is also interesting to note that the highest mean atmospheric temperature in the Northern Hemisphere occurs at the equator during the autumnal equinox. For both equinoctial seasons the mean atmospheric temperature profiles are symmetric about the equator. The temperature profiles of Figure 17 were compared to the mid-atmospheric temperatures of the thermal equilibrium model discussed in the previous section (see Figures 4 through 7). In the region bounded by the latitudes 50°N and 50°S the corresponding temperatures differ by at most 10°K . In the regions about the North and South Poles, the present temperatures are higher than the thermal equilibrium temperatures for all seasons except the summer solstice. This is due mainly to the meridional transport of heat from the warmer equatorial regions to the polar regions, which is included in the present model.

The temperatures computed from the Mariner IV occultation measurements by Kliore (1966) are about 220°K at 60°N latitude and about 175°K at 50°S latitude. These measurements were made during the late Northern Hemisphere summer (declination of sun = +15 degrees). The Mariner IV temperatures are much higher (about 40°K) than the corresponding mid-atmospheric temperatures as interpolated for

this time of year from Figure 17. If the temperatures of Figure 17 are reasonable estimates of the actual mid-atmospheric temperatures of Mars, one can conclude that the Mariner IV temperatures are representative of the atmospheric temperatures in the vicinity of the Martian surface.

The mean zonal wind profiles, based upon the geostrophic assumption, for the four Martian seasons are shown in Figure 18. The maximum mean zonal winds occur at latitudes 35°N and 35°S during the Northern Hemisphere winter solstice, and are about 50 and 40 msec^{-1} , respectively. During the Northern fall and spring equinoxes, the maximum mean zonal winds occur at about 65°N and 65°S latitudes and are about 30 msec^{-1} . During all seasons except summer the winds are westerly. In the summer seasons of both hemispheres, maximum easterlies of 10 msec^{-1} occur at 10°N and 10°S ; secondary maximums of 5 msec^{-1} occur at 70°N and 70°S . At middle latitudes the easterlies are relatively weak and about 2 msec^{-1} . The double peak phenomenon in the latitudinal profile was also formed in previous work (Tang, 1966), although the model used was different.

During winter the maximum westerlies occur further south and are stronger than in spring or fall. This is similar to the jet stream migration in the Earth's atmosphere. The wind profiles suggest that a wave regime may be present during the winter and during late spring and early fall. The mean wind at middle latitudes for the equinoctial seasons is about 30 msec^{-1} , which is slightly higher (5 msec^{-1}) than we obtained previously for a symmetrical regime (Tang, 1966). One expects a higher mean wind at middle latitudes in the wave regime than in the symmetrical regime (Charney, 1959). The computed wind velocity is larger than that of Earth as also found previously in Tang (1966).

In summary, this fairly simple model yields quantitative results on the latitudinal and seasonal variations of mid-atmospheric temperature and zonal wind for Mars. The reliability of the results is open to question because of some of the assumptions inherent in the model and some of the uncertainties in the input data for Mars. The first of these obstacles to reliability can be overcome with the use of an improved general circulation model — such as the numerical model discussed in the next section. The second obstacle to reliability can be overcome as new observational data and analytical studies become available.

2.2 A NUMERICAL MODEL OF THE MARTIAN ATMOSPHERIC GENERAL CIRCULATION

2.2.1 Introduction. As an extension to our previous study of the general circulation of the Martian atmosphere (Tang, 1966) and the recent work presented in the last section, a nonsteady, asymmetrical model is being developed. This model, a combination of the last two models, is a modification of Chen's circulation model which was originally developed for the Earth's atmosphere (Chen, 1965). It includes time variations, eddy transports, and some of the effects of the physical characteristics of the Martian surface (e.g., surface albedo, thermal conductivity, etc.) on the atmospheric circulation. Our main goal is to determine the seasonal variations of the basic zonally averaged motion of the Martian atmosphere and of the underlying surface temperature. The calculations of the surface temperature will be based upon the principle of conservation of energy among radiation, eddy conduction of the atmosphere and thermal conduction of the planetary surface. We shall also examine the influence of large-scale surface thermal conditions on the development of wave disturbances in the hemispheric flow patterns in the nonsteady case.

2.2.2 Basic Model. The fundamental equations are the quasi-geostrophic vorticity equation, the equation of state, the equation of continuity, and the first law of thermodynamics. By a zonally averaging process, we obtain two sets of the above equations. One set consists of the zonally-averaged equations for the mean flow; the other set consists of the finite amplitude perturbation equations for the disturbed flow. Both sets of equations are nonsteady and nonlinear. In the thermodynamic equation we consider not only the radiational processes but also the turbulent heat exchange processes in the atmosphere and heat conduction of the underlying planetary surface. The set of zonal averaged equations for the mean flow and the set of finite amplitude perturbation equations are:

$$\begin{aligned} \frac{\partial \bar{u}_1}{\partial t} - f_o \bar{v}_1 &= - \frac{\partial}{\partial y} (\bar{u}'_1 \bar{v}'_1) + a \frac{\partial^2 \bar{u}_1}{\partial y^2} - k_i (\bar{u}_1 - \bar{u}_3) \\ \frac{\partial \bar{u}_3}{\partial t} - f_o \bar{v}_3 &= - \frac{\partial}{\partial y} (\bar{u}'_3 \bar{v}'_3) + a \frac{\partial^2 \bar{u}_3}{\partial y^2} - k \left(\frac{3}{2} \bar{u}_3 - \frac{1}{2} \bar{u}_1 \right) + k_i (\bar{u}_1 - \bar{u}_3) \quad (60) \\ f_o \frac{\bar{\omega}_2}{p_2} &= \Lambda^2 \left\{ \frac{\partial}{\partial t} (\bar{\psi}_1 - \bar{\psi}_3) + \frac{\partial}{\partial y} [\bar{v}'_2 (\bar{\psi}'_1 - \bar{\psi}'_3)] - \frac{R}{f_o c_p} (\bar{Q}_r + \bar{Q}_t) \right\} . \end{aligned}$$

$$\begin{aligned}
\nabla^2 \frac{\partial \psi'_1}{\partial t} + \bar{u}_1 \frac{\partial \zeta'_1}{\partial x} + v'_1 \left(\frac{\partial \bar{\zeta}_1}{\partial y} + \beta \right) + u'_1 \frac{\partial \zeta'_1}{\partial x} + v_1 \frac{\partial \zeta'_1}{\partial y} - f_o \frac{\omega'_2}{p_2} &= a \nabla^2 \zeta'_1 - k_i (\zeta'_1 - \zeta'_3) \\
\nabla^2 \frac{\partial \psi'_3}{\partial t} + \bar{u}_3 \frac{\partial \zeta'_3}{\partial x} + v'_3 \left(\frac{\partial \bar{\zeta}_3}{\partial y} + \beta \right) + u'_3 \frac{\partial \zeta'_3}{\partial x} + v'_3 \frac{\partial \zeta'_3}{\partial y} + f_o \frac{\omega'_2}{p_2} &= \\
&= a \nabla^2 \zeta'_3 - k \left(\frac{3}{2} \zeta'_3 - \frac{1}{2} \zeta'_1 \right) + f_o \frac{\omega'_4}{p_2} + k_i (\zeta'_1 - \zeta'_3) , \tag{61}
\end{aligned}$$

$$\begin{aligned}
f_o \frac{\omega'_2}{p_2} &= \Lambda^2 \left[\frac{\partial}{\partial t} (\psi'_1 - \psi'_3) + \bar{u}_2 \frac{\partial}{\partial x} (\psi'_1 - \psi'_3) - (\bar{u}_1 - \bar{u}_3) v'_2 + u'_2 \frac{\partial}{\partial x} (\psi'_1 - \psi'_3) + \right. \\
&\quad \left. + v'_2 \frac{\partial}{\partial y} (\psi'_1 - \psi'_3) - \frac{R}{f_o c_p} (Q'_r + Q'_t) \right] .
\end{aligned}$$

where $u, v, \omega = \frac{dx}{dt}, \frac{dy}{dt}, \frac{dp}{dt}$,

ζ = the relative vorticity,

$\beta = \frac{df_o}{dy}$,

f_o = the mean Coriolis parameter,

$k_i = \frac{\mu g}{\alpha_2 p_2}^2$,

μ = dynamic coefficient of eddy viscosity in the vertical direction,

a = the coefficient of kinematic eddy viscosity in the lateral direction,

$\alpha_2 = \frac{\phi_1 - \phi_3}{p_2}$,

p_2 = pressure at middle of atmosphere,

∇^2 = Laplacian operator,

k = a proportional constant for the frictional stress near surface,

g = acceleration of gravity,

ϕ = geopotential,

t = time,

$$\Lambda^2 = \frac{f_o^2}{RT_2} \left(\frac{\theta_2}{\theta_1 - \theta_3} \right) - \text{a measure of static stability}$$

θ = potential temperature,

$\psi = \phi/f_o$ = geostrophic stream function,

R = gas constant for Martian atmosphere,

c_p = specific heat at constant pressure for Martian atmosphere,

Q_r, Q_t = rate of heating per unit mass due to radiation and turbulence, respectively,

($\overline{\quad}$) = zonal averaged quantity

(\quad)' = perturbed quantity,

and the subscripts 0, 1, 2, 3, and 4 represent the pressure levels at $p = 0$,

$\frac{1}{4} p_s, \frac{1}{2} p_s, \frac{3}{4} p_s$ and p_s , and p_s is the atmospheric pressure at surface of Mars.

The various heat exchange processes are modeled as follows. The radiative heating or cooling of the atmosphere per unit mass consists of three major parts: the absorption of solar radiation; the absorption of surface emitted long wave radiation; and the upward and downward emission of long wave radiation. The solar radiation is a function of time and latitude. Long wave radiation is a function of the surface temperature and the mean temperature of an entire atmospheric column, both of which vary with time, latitude, and longitude. The turbulent heat exchange process includes both horizontal and vertical exchanges. A simple austauach hypothesis is used in this model. The eddy transport of heat from the planetary surface is a function of atmospheric and surface temperature. Since both the radiative and turbulent heat exchange processes between surface and atmosphere depend upon the surface temperature, it is important to include the effects of a nonuniform Martian surface on the surface temperature. For example, the polar caps, bright areas, and dark areas are evidently composed of different materials with different thermal properties. Therefore, in the equation of thermal conduction of the Martian surface, which is used to obtain the surface temperature, the thermal conductivity and diffusivity (Carslaw and Jaeger, 1959) are expressed as functions of Martian longitude and latitude, using Sinton and Strong's (1960) values for dark and bright areas and Geiger's (1965) values for ice. We have written expressions for thermal conductivity and diffusivity as two different truncated Fourier series in horizontal coordinates for the planet Mars, according to the dark and bright area distribution, as

$$\begin{aligned}
\lambda^*(x,y) &= \lambda_{oo}^* + \lambda^{*\prime} = \lambda_{oo}^* + \\
&+ \sum_{m=1}^6 \left[(\lambda^{*\prime})_{m1} \cos m \frac{2\pi}{L} x + (\lambda^{*\prime})_{m2} \sin m \frac{2\pi}{L} x \right] \cos \frac{\pi}{2W} y + \\
&+ \sum_{m=1}^6 \left[(\lambda^{*\prime})_{m3} \cos m \frac{2\pi}{L} x + (\lambda^{*\prime})_{m4} \sin m \frac{2\pi}{L} x \right] \sin \frac{\pi}{W} y + \\
&+ \sum_{m=1}^6 \left[(\lambda^{*\prime})_{m5} \cos m \frac{2\pi}{L} x + (\lambda^{*\prime})_{m6} \sin m \frac{2\pi}{L} x \right] \cos \frac{3\pi}{2W} y,
\end{aligned} \tag{62}$$

$$\begin{aligned}
b^*(x,y) &= b_{oo}^* + b^{*\prime} = b_{oo}^* + \\
&+ \sum_{m=1}^6 \left[(b^{*\prime})_{m1} \cos m \frac{2\pi}{L} x + (b^{*\prime})_{m2} \sin m \frac{2\pi}{L} x \right] \cos \frac{\pi}{2W} y + \\
&+ \sum_{m=1}^6 \left[(b^{*\prime})_{m3} \cos m \frac{2\pi}{L} x + (b^{*\prime})_{m4} \sin m \frac{2\pi}{L} x \right] \sin \frac{\pi}{W} y + \\
&+ \sum_{m=1}^6 \left[(b^{*\prime})_{m5} \cos m \frac{2\pi}{L} x + (b^{*\prime})_{m6} \sin m \frac{2\pi}{L} x \right] \cos \frac{3\pi}{2W} y.
\end{aligned} \tag{63}$$

where L = the length of the latitude circle at 45° N or S,

$2W$ = the length of one-half of the meridian ($y = W$ at pole and $y = -W$ at equator).

The coefficients of the set of Fourier series for representing these thermal parameters are ready to be determined by solving two 36×36 matrices. Similarly, the Fourier series for Martian surface albedo are also ready to be determined. Solutions of these matrices will be obtained with the use of an IBM 7094.

The total heating rate per unit mass of atmosphere at different positions on Mars has been written in an analytical form. Values of the insolation and latitudinal derivative of the insolation as a function of time of year, at six hour intervals, smoothing out diurnal variations, are being obtained.

Since the surface temperature is important for the nonadiabatic heating of the atmosphere, we must solve the heat conduction equation and mean zonal motion equation simultaneously. As a first step in the solution of the problem, we are going to obtain the mean zonal surface temperature and mean zonal motion as a function of time for a period of a Martian year without considering eddy momentum transport.

To keep the model consistent, the solutions of all perturbation (finite amplitude) quantities are expressed in the form of double Fourier series. For example, the perturbed motion may be written as

$$\begin{aligned}\psi'_1(x, y, t) = & \sum_{m=1}^6 \left[(\psi'_1)_{m1} \cos m \frac{2\pi}{L} x + (\psi'_1)_{m2} \sin m \frac{2\pi}{L} x \right] \cos \frac{\pi}{2W} y + \\ & + \sum_{m=1}^6 \left[(\psi'_1)_{m3} \cos m \frac{2\pi}{L} x + (\psi'_1)_{m4} \sin m \frac{2\pi}{L} x \right] \sin \frac{\pi}{W} y + \quad (64) \\ & + \sum_{m=1}^6 \left[(\psi'_1)_{m5} \cos m \frac{2\pi}{L} x + (\psi'_1)_{m6} \sin m \frac{2\pi}{L} x \right] \cos \frac{3\pi}{2W} y,\end{aligned}$$

where subscripts 1 represents level 1, L is the length of the latitude circle at 45°N , and $(\psi'_1)_{m1}$, etc. are the Fourier coefficients which are the functions of the time t. The coefficients of these Fourier series are to be obtained by an electronic computer.

2.2.3 The Working Equations.

2.2.3.1 The Working Equations For the Mean Surface Temperature. The basic finite difference equation for the time differential of the Martian surface temperature can be simply written as

$$b^* \frac{\partial^2}{\partial z^2} T^* t + \Delta t = \frac{T^* t + \Delta t - T^* t}{\Delta t} \quad (65)$$

where b^* = the temperature-conduction coefficient of the Martian surface

Δt = the time interval used in the computation

T^* = the surface temperature

z = the vertical distance from surface

and the superscripts represent the time as indicated. The quantity T^{*t} is the initial input for each time step and is obtained from the prior step.

The boundary condition at the surface of Mars is the energy balance equation, which simply states that the total energy is a balance among the short and long wave radiations arriving at the surface, the long wave radiation emitted by the Martian surface, and the heat fluxes conducted to the atmosphere through an eddy transport process and to the soil through molecular conduction. The boundary conditions can be written as

$$\left[\lambda^* \frac{\partial T^*}{\partial z} + \frac{\lambda}{H_2} T^* + \sigma T^{*4} \right]^{t+\Delta t} = \left[\frac{\lambda}{H_2} T_2 + S_4 + \sigma T_2^4 - F(T_2) \right]^{t+\Delta t}$$

at $z = 0$,

and

(66)

$$T^{*t+\Delta t} = 0$$

at $z = -\infty$

where λ = the eddy heat transfer coefficient of the Martian atmosphere

λ^* = the molecular heat conduction coefficient of the Martian surface

σ = the Stefan-Boltzmann constant

H_2 = the thickness between level 2 and level 4 (level 4 corresponds to the surface level and level 2 is the constant pressure level at which the pressure is one-half of the surface pressure)

T_2 = the temperature at level 2 = $\frac{f_o}{R_o} (\psi_1 - \psi_3)$

(ψ_1, ψ_3) = stream functions at level 1 and 3 respectively (level 1 is the constant pressure level at which the pressure is one-fourth of the surface pressure and level 3 is the constant pressure level at which the pressure is three-fourths of the surface pressure)

T^* = the temperature at level 4

S_4 = the solar radiation reaching the surface of Mars.

$$F(T) = \left[c_1 \exp \left(-\frac{c_2}{\ell T} \right) \left(\frac{T}{c_2 \ell^3} + \frac{3T^2}{c_2^2 \ell^2} + \frac{6T^3}{c_2^3 \ell} + \frac{6T^4}{c_2^4} \right) \right]_{\ell_1}^{\ell_2} \\ + \left[c_1 \exp \left(-\frac{c_2}{\ell T} \right) \left(\frac{T}{c_2 \ell^3} + \frac{3T^2}{c_2^2 \ell^2} + \frac{6T^3}{c_2^3 \ell} + \frac{6T^4}{c_2^4} \right) \right]_{\ell_3}^{\ell_4} \quad (67)$$

where $\ell_1 = 0$, $\ell_2 = 13\mu$, $\ell_3 = 17\mu$, and $\ell_4 = \infty$; $c_1 = 3.7413 \times 10^{-5}$ erg cm² sec⁻¹ and $c_2 = 1.4388$ cm deg.

For practical purposes, the flux of long wave radiation from the atmosphere, E, may be assumed as

$$E = \epsilon_a \sigma T^4$$

where ϵ_a is the emissivity of the Martian atmosphere and is approximately equal to 0.16 on the average (House, 1966). If the following relation is valid (Adem, 1962)

$$E = \sigma T^4 - F(T) \quad (68)$$

then the corresponding F may be written

$$F = (1 - \epsilon_a) \sigma T^4 = 0.84 \sigma T^4 \quad (69)$$

In the actual computation, we shall use this approximation rather than (67).

The final solution for surface temperature, T^* , satisfying the difference equation and the boundary conditions as specified above, is

$$\bar{T}^{*t+\Delta t}|_{z=0} = \frac{\bar{L}}{\frac{\lambda_{oo}^*}{\sqrt{b_{oo}^* \Delta t}} + \left(\frac{\lambda}{H_2} + 4\bar{T}^{*3} \right)} \\ + \frac{\frac{\lambda_{oo}^*}{\sqrt{b_{oo}^* \Delta t}} \bar{T}^{*t}}{\frac{\lambda_{oo}^*}{\sqrt{b_{oo}^* \Delta t}} + \left(\frac{\lambda}{H_2} + 4\bar{T}^{*3} \right)} \quad (70)$$

where

$$\bar{L} = \left[\left(\frac{\lambda}{H_2} - \frac{F(\bar{T})}{\bar{T}_2} + 4\sigma \bar{T}_2^3 \right) \frac{f_o}{R} (\bar{\psi}_1 - \bar{\psi}_3) + \bar{s}_4 \right]^{t+\Delta t} \quad (71)$$

$(\lambda_{oo}^*, b_{oo}^*)$ = the mean values of the heat conduction and temperature-conduction coefficients of the surface respectively,

and the bars over T, L, ψ , and S represent the mean zonal values.

Since L is a function of ψ_1 and ψ_3 , we must solve for T^* simultaneously with the mean zonal motion by a finite time interval step-by-step process for about 1-1/2 Martian years. Based upon previous experience, a time interval of 6 hours would be appropriate for the grid size adopted in this model; an integration will need about 4000 time steps.

2.2.3.2 The Working Equations For Mean Zonal Wind Velocities. The basic zonal wind velocities for different meridional grid points at levels 1 and 3 can be obtained by solving the following six simultaneous equations. These equations will be used as working equations in the numerical computations. They are listed below.

$$\begin{aligned} \frac{\partial}{\partial t} \bar{u}_{1+1} + \frac{\partial}{\partial t} \bar{u}_{3+1} &= R_1 \bar{u}_{1+1} + R_2 \bar{u}_{1+0} + 0 + R_3 \bar{u}_{3+1} + R_2 \bar{u}_{3+0} \\ &\quad - \frac{\partial}{\partial y} (\overline{u'_1 v'} + \overline{u'_3 v'_3})_{+1} , \end{aligned} \quad (72)$$

$$\begin{aligned} \frac{\partial}{\partial t} \bar{u}_{1+0} + \frac{\partial}{\partial t} \bar{u}_{3+0} &= R_2 \bar{u}_{1+1} + R_1 \bar{u}_{1+0} + R_2 \bar{u}_{1-1} + R_2 \bar{u}_{3+1} + R_3 \bar{u}_{3+0} + R_2 \bar{u}_{3-1} \\ &\quad - \frac{\partial}{\partial y} (\overline{u'_1 v'} + \overline{u'_3 v'_3})_{+0} , \end{aligned} \quad (73)$$

$$\begin{aligned} \frac{\partial}{\partial t} \bar{u}_{1-1} + \frac{\partial}{\partial t} \bar{u}_{3-1} &= R_2 \bar{u}_{1+0} + R_1 \bar{u}_{1-1} + R_2 \bar{u}_{3+0} + R_3 \bar{u}_{3-1} \\ &\quad - \frac{\partial}{\partial y} (\overline{u'_1 v'} + \overline{u'_3 v'_3})_{-1} , \end{aligned} \quad (74)$$

$$\begin{aligned}
& - R_o \frac{\partial}{\partial t} \bar{u}_{1+1} + \frac{\partial}{\partial t} \bar{u}_{1+0} + R_o \frac{\partial}{\partial t} \bar{u}_{3+1} - \frac{\partial}{\partial t} \bar{u}_{3+0} = R_4 \bar{u}_{1+1} + R_5 \bar{u}_{1+0} + R_7 \bar{u}_{3+1} \\
& + R_8 \bar{u}_{3+0} - R_2 \bar{u}_{3-1} - \frac{w^2}{4} \frac{\partial^3}{\partial y^3} (\overline{u'_1 v'_1} - \overline{u'_3 v'_3})_{+1} \\
& - 2\Lambda^2 \frac{\partial^2}{\partial y^2} [\overline{v'_2(\psi'_1 - \psi'_3)}]_{+1} - R_{10} \left\{ \frac{\partial}{\partial y} [(1 - \bar{\Gamma}) \bar{s}_o] \right. \\
& \left. - \frac{\partial F(T^*)}{\partial y} \Big|_{z=0} - \lambda_{oo}^* \frac{\partial}{\partial y} \left(\frac{\partial T^*}{\partial z} \right)_{z=0} \right\}_{+1}, \tag{75}
\end{aligned}$$

$$\begin{aligned}
& \frac{\partial}{\partial t} \bar{u}_{1+1} - R_o \frac{\partial}{\partial t} \bar{u}_{1+0} + \frac{\partial}{\partial t} \bar{u}_{1-1} - \frac{\partial}{\partial t} \bar{u}_{3+1} + R_o \frac{\partial}{\partial t} \bar{u}_{3+0} - \frac{\partial}{\partial t} \bar{u}_{3-1} \\
& = R_5 \bar{u}_{1+1} + R_6 \bar{u}_{1+0} + R_5 \bar{u}_{1-1} + R_8 \bar{u}_{3+1} + R_9 \bar{u}_{3+0} + R_8 \bar{u}_{3-1} \\
& - \frac{w^2}{4} \frac{\partial^3}{\partial y^3} (\overline{u'_1 v'_1} - \overline{u'_3 v'_3})_{+0} - \frac{w^2}{4} 2\Lambda^2 \frac{\partial^2}{\partial y^2} [\overline{v'_2(\psi'_1 - \psi'_3)}]_{+0}
\end{aligned}$$

$$- R_{10} \left\{ \frac{\partial}{\partial y} [(1 - \bar{\Gamma}) \bar{s}_o] - \frac{\partial F(T^*)}{\partial y} \Big|_{z=0} - \lambda_{oo}^* \frac{\partial}{\partial y} \left(\frac{\partial \bar{T}^*}{\partial z} \right)_{z=0} \right\}_{+0}, \tag{76}$$

$$\begin{aligned}
& \frac{\partial}{\partial t} \bar{u}_{1+0} - R_o \frac{\partial}{\partial t} \bar{u}_{1-1} - \frac{\partial}{\partial t} \bar{u}_{3+0} + R_o \frac{\partial}{\partial t} \bar{u}_{3-1} = R_2 \bar{u}_{1+1} + R_5 \bar{u}_{1+0} + R_4 \bar{u}_{1-1} \\
& - R_2 \bar{u}_{3+1} + R_8 \bar{u}_{3+0} + R_7 \bar{u}_{3-1} - \frac{w^2}{4} \frac{\partial^3}{\partial y^3} (\overline{u'_1 v'_1} - \overline{u'_3 v'_3})_{-1} \\
& - \frac{w^2}{4} 2\Lambda^2 \frac{\partial^2}{\partial y^2} [\overline{v'_2(\psi'_1 - \psi'_3)}]_{-1} - R_{10} \left\{ \frac{\partial}{\partial y} [(1 - \bar{\Gamma}) \bar{s}_o] \right. \\
& \left. - \frac{\partial F(T^*)}{\partial y} \Big|_{z=0} - \lambda_{oo}^* \frac{\partial}{\partial y} \left(\frac{\partial \bar{T}^*}{\partial z} \right)_{z=0} \right\}_{-1}, \tag{77}
\end{aligned}$$

$$\text{where } R_0 = 2 \left(1 + \frac{1}{4} \Lambda^2 W^2 \right) ,$$

$$R_1 = \frac{k}{2} - 8 \frac{a}{W} ,$$

$$R_2 = \frac{4a}{W^2} ,$$

$$R_3 = -\frac{3}{2}k - 8 \frac{a}{W^2} ,$$

$$R_4 = 20 \frac{a}{W^2} + k + 4a\Lambda^2 - \frac{W^2}{4} \frac{\Lambda^2}{c_p} \frac{g}{2p_2} \frac{\partial}{\partial y} \left[\sigma \bar{T}_2^4 - F(\bar{T}_2) \right] \frac{1}{\partial \bar{T}_2} + 4k_i ,$$

$$R_5 = 16 \frac{a}{W^2} - \frac{k}{2} - 2a\Lambda^2 - 2k_i ,$$

$$R_6 = 24 \frac{a}{W^2} + k + 4a\Lambda^2 + \frac{W^2}{4} \frac{\Lambda^2}{c_p} \frac{g}{2p_2} \frac{\partial}{\partial y} \left[\sigma \bar{T}_2^4 - F(\bar{T}_2) \right] \frac{1}{\partial \bar{T}_2} + 4k_i ,$$

$$R_7 = -20 \frac{a}{W^2} - 3k - 4a\Lambda^2 - \frac{W^2}{4} \frac{\Lambda^2}{c_p} \frac{g}{2p_2} \frac{\partial}{\partial y} \left[\sigma \bar{T}_2^4 - F(\bar{T}_2) \right] \frac{1}{\partial \bar{T}_2} - 4k_i ,$$

$$R_8 = 16 \frac{a}{W^2} + \frac{3}{2}k + 2a\Lambda^2 + 2k_i ,$$

$$R_9 = -24 \frac{a}{W^2} - 3k - 4a\Lambda^2 - \frac{W^2}{4} \frac{\Lambda^2}{c_p} \frac{g}{2p_2} \frac{\partial}{\partial y} \left[\sigma \bar{T}_2^4 - F(\bar{T}_2) \right] \frac{1}{\partial \bar{T}_2} - 4k_i ,$$

$$R_{10} = \frac{W^2}{4} \frac{\Lambda^2}{c_p} \frac{Rg}{f_o p_2} ,$$

u_{1-2} , u_{1-1} , u_{1+0} , u_{1+1} , and u_{1+2} = quantity u at level 1 on the points $y = W$, $-\frac{1}{2}W$, 0 , $\frac{1}{2}W$, and w respectively

a = radius of Mars,

W = one half of the distance between pole and equator,

c_p = specific heat of Martian atmosphere at constant pressure,

f_o = Coriolis parameter,

p_2 = atmospheric pressure at level 2,

g = gravitational acceleration,

R = gas constant

k = a proportional constant for frictional stress in vertical direction,

k_i = internal friction,

$$\Lambda^2 = \frac{f_o^2}{RT_2} \times \frac{\theta_2}{\theta_1 - \theta_3},$$

$\theta_1, \theta_2, \theta_3$ = potential temperature at levels 1, 2, and 3, respectively.

2.2.3.3 The Working Equation For the Finite Amplitude Perturbed Motion.

Substituting the perturbation of heating per unit mass into Equation (62), eliminating ω_z , using the Fourier series and keeping all the nonlinear terms yields the following working equations of atmospheric disturbance.

$$M_1 \frac{\partial}{\partial t} (\psi'_1)_{mn} + \Lambda^2 \frac{\partial}{\partial t} (\psi'_3)_{mn} = - M_2 (\psi'_1)_{mn} + M_3 (\psi'_1)_{mn+1} - M_4 (\psi'_3)_{mn} + \\ + M_5 (\psi'_3)_{mn+1} + M_{11} (T'_{z=0})_{mn} + M_6 \lambda_{oo}^* \left(\frac{\partial T'^*}{\partial z} \Big|_{z=0} \right) + N_{mn}, \quad (78)$$

$$M_1 \frac{\partial}{\partial t} (\psi'_1)_{mn+1} + \Lambda^2 \frac{\partial}{\partial t} (\psi'_3)_{mn+1} = - M_3 (\psi'_1)_{mn} - M_2 (\psi'_1)_{mn+1} - M_5 (\psi'_3)_{mn} - \\ - M_4 (\psi'_3)_{mn+1} + M_{11} (T'_{z=0})_{mn+1} + M_6 \lambda_{oo}^* \left(\frac{\partial T'^*}{\partial z} \Big|_{z=0} \right)_{mn+1} + N_{mn+1}, \quad (79)$$

$$\Lambda^2 \frac{\partial}{\partial t} (\psi'_1)_{mn} + M_1 \frac{\partial}{\partial t} (\psi'_3)_{mn} = - M_7 (\psi'_1)_{mn} + M_8 (\psi'_1)_{mn+1} - M_9 (\psi'_3)_{mn} + \\ + M_{10} (\psi'_3)_{mn+1} - M_{11} (T'_{z=0})_{mn} - M_6 \lambda_{oo}^* \left(\frac{\partial T'^*}{\partial z} \Big|_{z=0} \right)_{mn} + \tilde{N}_{mn} \quad (80)$$

$$\begin{aligned}
& \Lambda^2 \frac{\partial}{\partial t} (\psi'_1)_{mn+1} + M_1 \frac{\partial}{\partial t} (\psi'_3)_{mn+1} = - M_8 (\psi'_1)_{mn} - M_7 (\psi'_1)_{mn+1} - \\
& - M_{10} (\psi'_3)_{mn} - M_9 (\psi'_3)_{mn+1} - M_{11} (T_{z=0}^{*'})_{mn+1} - M_6 \lambda_{oo}^* \left(\frac{\partial T^{*'}}{\partial z} \Big|_{z=0} \right)_{mn+1} + \tilde{N}_{mn+1} \\
& (m = 1, 2, \dots, 6, \quad n = 1, 3, 5)
\end{aligned} \tag{81}$$

where

$$\begin{aligned}
M_1 &= - \left[(m^2 + 2j^2) \frac{4\pi^2}{L^2} + \Lambda^2 \right], \\
M_2 &= (m^2 + 2j^2) \frac{4\pi^2}{L^2} (a M_1 - k_i) - 4 \left[4\sigma \bar{T}_2^3 T_2' - F (\bar{\bar{T}}_2 + \bar{T}_2 + T_2') + \right. \\
&\quad \left. + F (\bar{\bar{T}}_2 + \bar{T}_2) \right] \frac{g\Lambda^2}{2p_2 c_p} \frac{1}{T_2'} \\
M_3 &= m \frac{2\pi}{L} \left[- M_1 \bar{u}_{1+0} - \beta + \frac{4}{W^2} (\bar{u}_{1+1} - 2\bar{u}_{1+0} + \bar{u}_{1-1}) - \Lambda^2 (\bar{u}_{1+0} - \bar{u}_{3+0}) \right], \\
M_4 &= (m^2 + 2j^2) \frac{4\pi^2}{L^2} (a\Lambda^2 + k_i) + 4 \left[4\sigma \bar{T}_2^3 T_2' - F (\bar{\bar{T}}_2 + \bar{T}_2 + T_2') + \right. \\
&\quad \left. + F (\bar{\bar{T}}_2 + \bar{T}_2) \right] \frac{g\Lambda^2}{2p_2 c_p} \frac{1}{T_2'} \\
M_5 &= m \frac{2\pi\Lambda^2 u_{1+0}}{L}, \\
M_6 &= \frac{\Lambda^2 R g}{2p_2 f_0 c_p}, \\
M_7 &= M_4 + (m^2 + 2j^2) \frac{4\pi^2}{L^2} \cdot \left(\frac{k}{2} + k_i \right), \\
M_8 &= - m \frac{2\pi\Lambda^2 u_{3+0}}{L}, \\
M_9 &= M_2 - (m^2 + 2j^2) \frac{4\pi^2}{L^2} \cdot \left(\frac{3k}{2} + k_i \right)
\end{aligned}$$

$$M_{10} = m \frac{2\pi}{L} \left[- M_1 \bar{u}_{3+0} - \beta + \frac{4}{W^2} (\bar{u}_{3+1} - 2\bar{u}_{3+0} + \bar{u}_{3-1}) + \Lambda^2 (\bar{u}_{1+0} - \bar{u}_{3+0}) \right],$$

$$M_{11} = \frac{g\Lambda^2 R}{f_o p_2 c_p} \left[- F (\bar{T}_4' + \bar{T}_4 + T_4') + F (\bar{T} + \bar{T}_4) \right] \frac{1}{T_4'}$$

$j=1$ when $n=1$, $j=2$ when $n=3$, and $j=3$ when $n=5$. N_{mn} are the terms derived from the quadratic terms of the vorticity advection and the temperature advection at level 1 and \tilde{N}_{mn} are the terms derived from the quadratic terms of the vorticity advection and the temperature advection at level 3.

It is planned to integrate these equations numerically using the Runge-Kutta method. As a first approximation, we assume that the non-linear terms in Equations (72) to (77) can be neglected. Then these six equations for the mean zonal winds will be solved simultaneously with the solution for the mean surface temperature.

During the next year, the equations for the mean zonal velocities and the mean zonal temperatures will be programmed. Once the mean zonal velocities and temperatures are obtained, they can be used as input to the perturbation equations, solutions of which will provide information on the longitudinal variations of the circulation and temperature field. The perturbation equations for this problem will be also completed during the next year.

REFERENCES

- Adem, J., 1962: On the theory of the general circulation of the atmosphere. Tellus, 14, 102-105.
- Belton, M. J., and D. M. Hunten, 1966: The abundance and temperature of CO₂ in the Martian atmosphere. Ap. J., 145, 454-467.
- Burch, D. E., D. Gryvnak, and D. Williams, 1960: Infrared absorption by carbon dioxide, Report, Ohio State University.
- Carslaw, H. S., and J. C. Jaeger, 1959: Conduction of Heat in Solids. Oxford University Press, London, 510 pp.
- Charney, J., 1959: On the general circulation of the atmosphere. The Atmosphere and the Sea in Motion. The Rockefeller Institute Press, New York, 509 pp.
- Chen, Y-S, 1965: A numerical experiment on the atmospheric circulation based on the two-level quasi-geostrophic model. Scientia Sinica, 14, 246-266.
- Curtis, A., and R. Goody, 1956: Thermal radiation in the upper atmosphere. Proc. Roy. Soc. (A), 236, 193-206.
- Dent, W. A., M. J. Klein, and H. D. Aller, 1965: Measurements of Mars at λ 3.75 cm from February to June 1965. Ap. J., 142, 1685-1688.
- de Vaucouleurs, G., 1964: Geometric and photometric parameters of the terrestrial planets. Icarus, 3, 187-235.
- Fjeldbo, G., W. Fjeldbo, and V. Eshleman, 1966: Models for the atmosphere of Mars based upon the Mariner 4 occultation experiment. J. Geophys. Res., 71, 2307-2316.
- Geiger, R., 1965: The Climate near the Ground. Harvard University Press, Cambridge, Mass., 611 pp.
- Goody, R., 1957: The atmosphere of Mars. Weather, 12, 3.
- Hess, S. L., and H. L. Panofsky, 1951: Compendium of Meteorology. Amer. Meteor. Soc., Boston, Mass., 1334 pp.
- Houghton, J. T., 1963: The absorption of solar infrared radiation by the lower stratosphere. Quart. J. Roy. Met. Soc., 89, 319-331.
- House, F., 1966: The seasonal climatology of Mars. In Contributions to Planetary Meteorology. GCA Tech. Rpt. No. 66-8-N, Final Report under Contract NASW-1227.
- Howard, J.N., D. L. Burch, and D. Williams, 1955: Near infrared transmission through synthetic atmospheres. G.R.P. 40 (astia AD-87679).

REFERENCES (Cont.)

- Hughes, M. P., 1966: Planetary observations at a wavelength of 6 cm. Planetary and Space Sci., 14, 1017-1022.
- Kaplan, L., G. Munch, and H. Spinrad, 1964: An analysis of the spectrum of Mars. Ap. J., 139, 1-15.
- Kellerman, K. I., 1966: The thermal radio emission from Mercury, Venus, Mars, Saturn, and Uranus. Icarus, 5, 478-490.
- Kliore, A., D. Cain, G. Levy, V. Eshleman, G. Fjeldbo, and F. Drake, 1965: Occultation experiment: Results of the first direct measurements of Mars atmosphere and ionosphere. Science, 149, 1243-1248.
- Kliore, A., D. Cain, G. Levy, V. Eshleman, G. Fjeldbo, and F. Drake, 1966: Preliminary results of the Mariner IV occultation measurements of the atmosphere of Mars. In: Proceedings of the Caltech-JPL Lunar and Planetary Conference, Sept. 13-18, 1965, 257-266.
- Kliore, A., D. Cain, and G. Levy, 1966: Radio occultation measurements of the Martian atmosphere over two regions by the Mariner IV space probe. COSPAR, Internat. Space Science Symp., 7th, Vienna, May 10-19, 1966.
- Leighton, R.B., and B.C. Murray, 1966: Behavior of carbon dioxide and other volatiles on Mars. Science, 153, 136-144.
- Leovy, C.B., 1966: Radiative-convective equilibrium calculations for a two-layer Mars atmosphere. Rand Memo. RM-5017, 41 pp.
- Manabe, S., and R.F. Strickler, 1964: Thermal equilibrium of the atmosphere with convective adjustment. J. Atmos. Sci., 21, 361-385.
- Mintz, Y., 1961: The general circulation of planetary atmospheres. The Atmospheres of Mars and Venus. Pub. 944, NAS-NRO, Wash., D.C.
- Ohring, G., and J. Mariano, 1966: The vertical temperature distribution in the Martian atmosphere. J. Atmos. Sci., 23, 251-255.
- Owen, T., 1966: The composition and surface pressure of the Martian atmosphere: Results from the 1965 opposition. Ap. J., 146, 257-270.
- Prabhakara, C., and J. S. Hogan, Jr., 1965: Ozone and carbon dioxide heating in the Martian atmosphere. J. Atmos. Sci., 22, 97-109.
- Rodgers, C.D., and C.D. Walshaw, 1966: The computation of infrared cooling rates in planetary atmospheres. Quart. J. Roy. Met. Soc., 92, 67-92.
- Seeley, J. S., and J. T. Houghton, 1961: Spectroscopic observations of the vertical distribution of some minor constituents of the atmosphere. Infrared Phys., 1, 116-132.

REFERENCES (Cont.)

Sinton, W. M., and J. Strong, 1960: Radiometric observations of Mars.
Ap. J., 131, 459-469.

Smagorinsky, J., S. Manabe, and J. L. Halloway, Jr., 1965: Numerical results from a nine-level general circulation model of the atmosphere. Mon. Wea. Rev., 93, 727-768.

Spinrad, H., R. A. Schorn, R. Moore, L. P. Giver, 1966: High dispersion spectroscopic observations of Mars. I. The CO₂ content and surface pressure. Ap. J., 146, 331-338.

Tang, W., 1966: A study of the general circulation of the Martian atmosphere based upon the result of the occultation experiment from Mariner IV. Proc. of the 9th COSPAR meeting, Vienna, Austria, 1966. (In print).

PRECEDING PAGE BLANK NOT FILMED.

APPENDIX

PRECEDING PAGE BLANK NOT FILMED.

APPENDIX

ACCURACY OF LORENTZ LINE SHAPE

At high altitudes (low pressures) the shape of absorption lines changes from a Lorentz shape, which is assumed in our calculations of Martian temperatures, through a mixed shape to the Doppler shape. The height in the Martian atmosphere at which the transition to a Doppler shape takes place can be estimated following Rodgers and Walshaw (1966). A mixed line consists of a Doppler core and Lorentz wings. If the line is fully absorbed as far out as the Lorentz wings, the Doppler core makes no contribution to the transmission gradient. The point at which the Lorentz wings begin is given by

$$k_{\nu_L} = k_{\nu_D} \quad (A-1)$$

where k_{ν_L} is the Lorentz absorption coefficient and k_{ν_D} is the Doppler absorption coefficient. Substituting the complete expressions for these absorption coefficients, we obtain

$$\frac{k}{\pi} \frac{\alpha_L}{\nu^2 + \alpha_L^2} = \frac{k}{\alpha_D \sqrt{\pi}} \exp\left(-\frac{\nu^2}{\alpha_D^2}\right) \quad (A-2)$$

where k is the line intensity, ν is measured from the line center, and α_L and α_D are the Lorentz and Doppler half-widths. With $x = \nu/\alpha_D$ and $y = \alpha_L/\alpha_D$, (A-2) becomes

$$y = \sqrt{\pi} (x^2 + y^2) e^{-x^2}. \quad (A-3)$$

If the criterion of blackness is taken to be about 2 percent transmission, then a Lorentz line is "black" out to that frequency at which the transmission is 0.02, or

$$T = \exp(-k_{\nu} m) = \exp - \left[\frac{k \alpha_m}{\pi(\nu^2 + \alpha_L^2)} \right] = 0.02. \quad (A-4)$$

This corresponds to a value of x given by

$$x = y \left[\frac{km}{4\pi\alpha_L} - 1 \right]^{1/2}. \quad (A-5)$$

The amount of absorber, m , between a pressure level p and the top of the atmosphere, and the average Lorentz half-width, α_L , for such a path are given by

$$m = \frac{wp}{g} \quad \text{and} \quad \alpha_L = \frac{\alpha_{L_s} p}{2p_s} \quad (\text{A-6})$$

where α_{L_s} is the Lorentz half-width at STP. Substituting these values into (A-5), we obtain

$$x = y \left[\frac{kwp_s}{2g\pi\alpha_{L_s}} - 1 \right]^{1/2}. \quad (\text{A-7})$$

Letting $\eta = kwp_s / 2\pi\alpha_{L_s} g$, and combining (A-7) with (A-3), we obtain

$$y\eta \sqrt{\pi} \exp \left[-y^2(\eta-1) \right] = 1. \quad (\text{A-8})$$

This relationship determines the height above which Doppler broadening must be considered. According to Rodgers and Walshaw (1966), the value of η for the 15μ CO₂ band in the Earth's atmosphere is 1200. For a Martian CO₂ mass mixing ratio of 0.5 and gravitational acceleration of 373 cm sec^{-2} , the value of η in the Martian atmosphere is 2.9×10^3 as large, or 3.5×10^6 . From (A-8), we then obtain a value of y equal to 1.62×10^{-3} for Mars' atmosphere. Since

$$y = \frac{\alpha_L}{\alpha_D} = 1.62 \times 10^{-3},$$

and $\alpha_D = 7 \times 10^{-4}$ (Rodgers and Walshaw, 1966), then $\alpha_L = 1.13 \times 10^{-6}$. The pressure level in the Martian atmosphere corresponding to this value of α_L is given by

$$p = \frac{\alpha_L}{\alpha_{L_s}} p_s$$

and is equal to 1.6×10^{-2} mb. Thus, below (in height) pressure levels of 1.6×10^{-2} mb, the neglect of Doppler broadening is justified. For a Martian atmosphere scale height of 9 km and surface pressure of 10 mb, this corresponds to a height of 58 km.

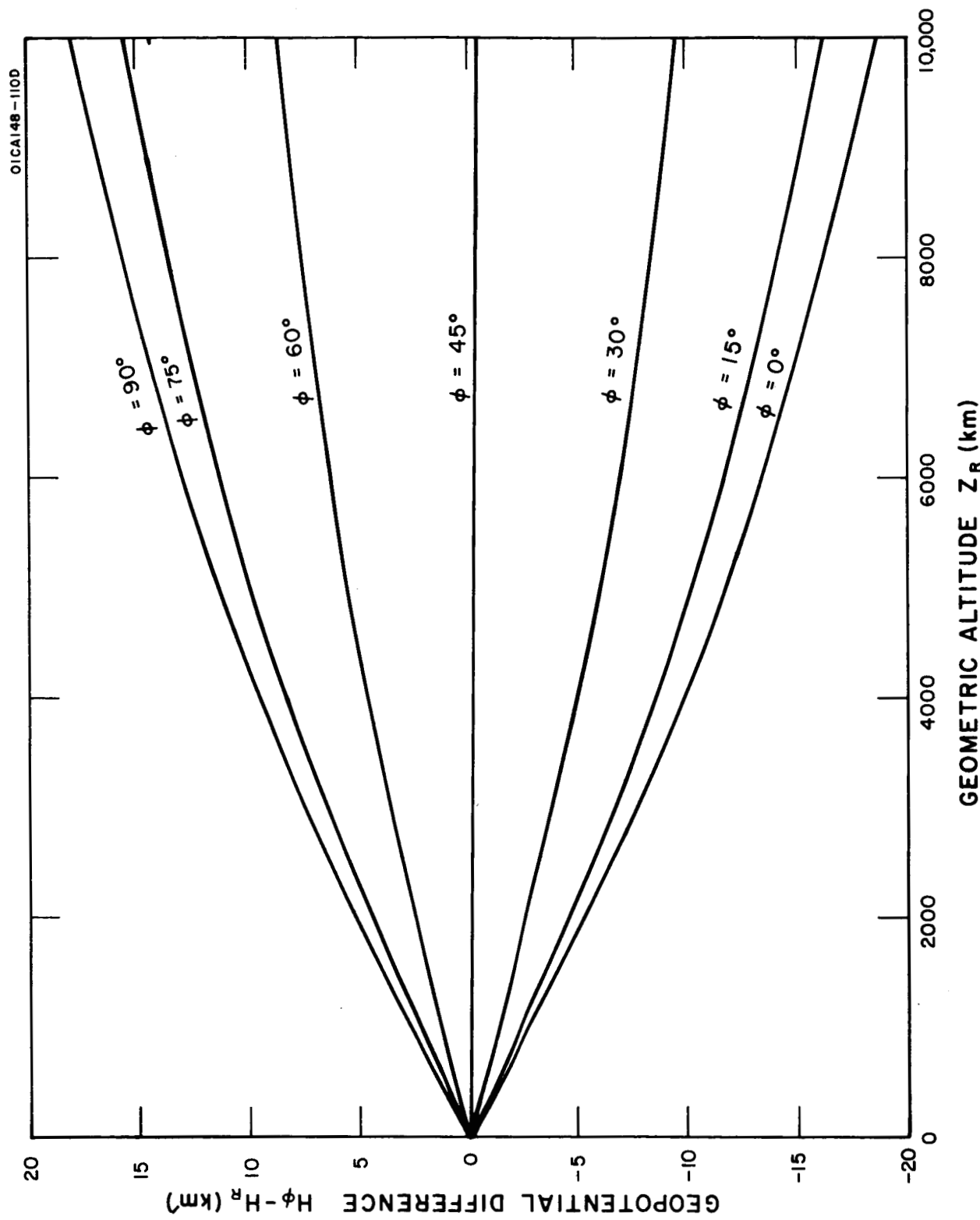


Figure 3.1B. Geopotential differences between geometric-altitude surfaces at a reference latitude, and the same geometric-altitude surfaces at each of seven other latitudes, all as a function of geometric altitude 0 to 10,000 km.

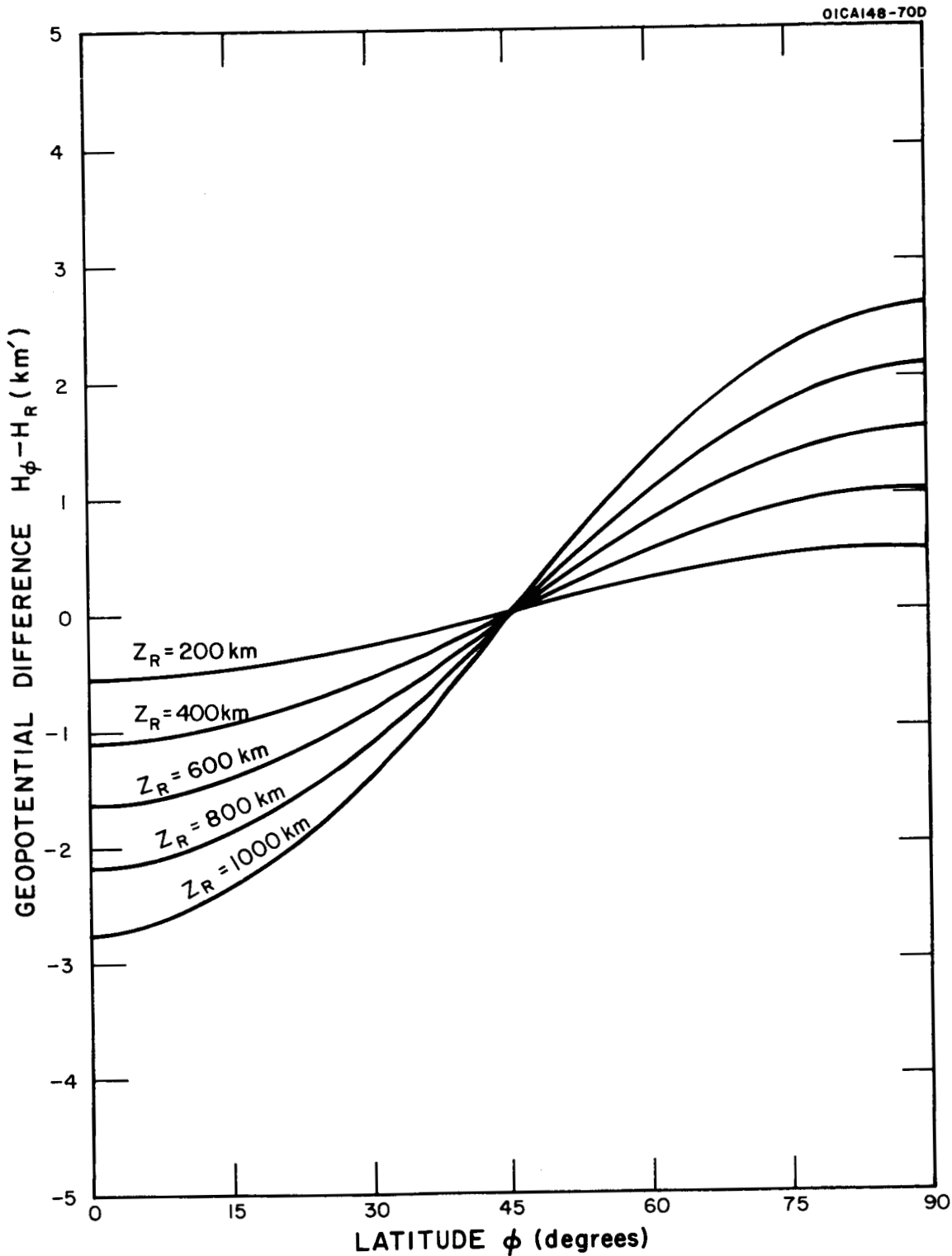


Figure 3.2A. Geopotential differences between each of five geometric-altitude surfaces (from 200 to 1,000 km) at a reference latitude, and the same geometric-altitude surfaces at other latitudes, all as a function of latitude, from 0 to 90 degrees.

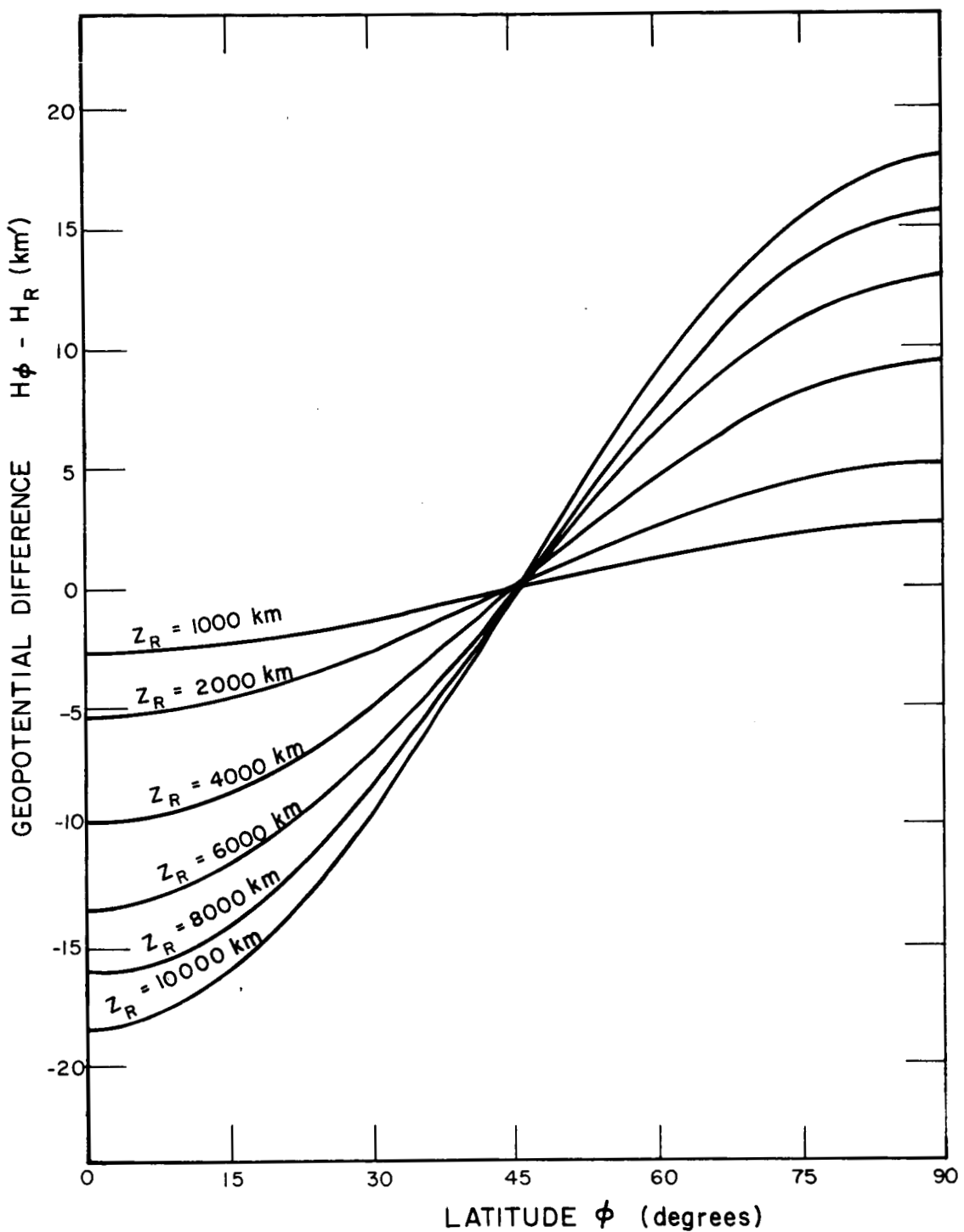


Figure 3.2B. Geopotential differences between each of six geometric altitude surfaces (from 1,000 to 10,000 km) at a reference latitude and the same geometric-altitude surfaces at other latitudes, all as a function of latitudes from 0 to 90 degrees.

SECTION VII

SPECIFIC DESCRIPTION OF TABLES 4A AND 4B

Tables 4A and 4B are formally arranged to present geopotential differences $H_\phi - H_R$ for various latitudes as a function of the second argument pair such that the differences $H_\phi - H_R$ are related to the integral values of H_R through the non-integral values of Z_R . The concept of the variation of values of $H_\phi - H_R$ as a function of H_R , implicit in the basic format of these tables provides the same difficulty of comprehension as that provided by the format of Tables 2A and 2B. Tables 4A and 4B are more understandable when considered as the variation in the values of $H_\phi - H_R$ as a function of latitude (columns 3 through 9) for each member of a large set of equal-geometric-altitude surfaces Z_R (column 2) equivalent at the reference latitude to a corresponding set of geopotential altitudes H_R (column 1) expressed in integral multiples of one m' or one km'.

Tables 4A and 4B are intended primarily to provide the geopotential adjustment required when atmospheric models expressed as a function of geopotential altitude at the reference latitude R are applied to other latitudes. Column 10 of Table 4A contains values of $H_S - H_R$ as a function of H_R corresponding to geometric altitudes between sea level and 700 km. As in Table 3 no values of $H_S - H_R$ are given for altitudes above 700 km.

Figures 4.1A, 4.1B, 4.2A, and 4.2B provide the graphical representations of the data of Tables 4A and 4B. In this instance, as in the previous cases, the figure notation follows that discussed for the figures associated with Tables 1A and 1B. No values of $H_S - H_R$ are given in these figures.

TABLE 4A

GEOPOTENTIAL DIFFERENCES BETWEEN A SERIES OF GEOMETRIC-ALTITUDE SURFACES AT A
REFERENCE LATITUDE AND THE SAME GEOMETRIC-ALTITUDE SURFACES AT OTHER LATITUDES,
INCLUDING THOSE IN THE US STANDARD ATMOSPHERE, ALL AS A FUNCTION OF THE
GEOPOTENTIAL EQUIVALENT OF THE EQUAL GEOMETRIC-ALTITUDE SURFACES, 0 TO
1,000 km²

GEOPOTENTIAL ALTITUDE	GEOMETRIC ALTITUDE	LATITUDE φ (DEG)							
		0	15	30	45	60	75	90	
H _R (m')	Z _R (m)	H _φ -H _R	H _S -H _R						
0.	0.0	-0.0	-0.0	-0.0	-0.0	0.0	0.0	0.0	-0
250.	2500.0	-0.7	-0.6	-0.3	-0.0	0.3	0.6	0.6	-0
500.	5000.0	-1.3	-1.2	-0.7	-0.0	0.6	1.1	1.3	-0
750.	7500.0	-2.0	-1.7	-1.0	-0.0	1.0	1.7	1.9	-0
1000.	10000.1	-2.7	-2.3	-1.4	-0.1	1.3	2.2	2.6	-0
1250.	12500.2	-3.4	-2.9	-1.7	-0.1	1.6	2.8	3.2	-0
1500.	15000.3	-4.0	-3.5	-2.1	-0.1	1.9	3.4	3.9	-0
1750.	17500.4	-4.7	-4.1	-2.4	-0.1	2.2	3.9	4.5	-0
2000.	20000.6	-5.4	-4.7	-2.7	-0.1	2.5	4.5	5.2	-0
2250.	22500.7	-6.0	-5.2	-3.1	-0.1	2.9	5.0	5.8	-0
2500.	25000.9	-6.7	-5.8	-3.4	-0.1	3.2	5.6	6.5	-0
2750.	27501.1	-7.4	-6.4	-3.8	-0.1	3.5	6.2	7.1	-0
3000.	30001.4	-8.0	-7.0	-4.1	-0.2	3.8	6.7	7.8	-0
3250.	32501.6	-8.7	-7.6	-4.4	-0.2	4.1	7.3	8.4	-0
3500.	35001.9	-9.4	-8.2	-4.8	-0.2	4.4	7.8	9.1	-0
3750.	37502.2	-10.1	-8.7	-5.1	-0.2	4.8	8.4	9.7	-0
4000.	40002.5	-10.7	-9.3	-5.5	-0.2	5.1	9.0	10.4	-0
4250.	42502.8	-11.4	-9.9	-5.8	-0.2	5.4	9.5	11.0	-0
4500.	45003.1	-12.1	-10.5	-6.2	-0.2	5.7	10.1	11.7	-0
4750.	47503.5	-12.7	-11.1	-6.5	-0.2	6.0	10.6	12.3	-0
5000.	50003.9	-13.4	-11.7	-6.8	-0.2	6.4	11.2	13.0	-0
5250.	52504.3	-14.1	-12.2	-7.2	-0.3	6.7	11.8	13.6	-0
5500.	55004.7	-14.8	-12.8	-7.5	-0.3	7.0	12.3	14.3	-0
5750.	57505.2	-15.4	-13.4	-7.9	-0.3	7.3	12.9	14.9	-0
6000.	60005.6	-16.1	-14.0	-8.2	-0.3	7.6	13.4	15.6	-0
6250.	62506.1	-16.8	-14.6	-8.6	-0.3	8.0	14.0	16.2	-0
6500.	65006.6	-17.4	-15.2	-8.9	-0.3	8.3	14.6	16.9	-0
6750.	67507.1	-18.1	-15.7	-9.2	-0.3	8.6	15.1	17.5	-0
7000.	70007.7	-18.8	-16.3	-9.6	-0.4	8.9	15.7	18.2	-0
7250.	72508.2	-19.5	-16.9	-9.9	-0.4	9.2	16.3	18.8	-0
7500.	75008.8	-20.1	-17.5	-10.3	-0.4	9.5	16.8	19.5	-0
7750.	77509.4	-20.8	-18.1	-10.6	-0.4	9.9	17.4	20.1	-0
8000.	800010.0	-21.5	-18.7	-11.0	-0.4	10.2	17.9	20.8	-0
8250.	825010.7	-22.2	-19.2	-11.3	-0.4	10.5	18.5	21.4	-0
8500.	850011.3	-22.8	-19.8	-11.6	-0.4	10.8	19.1	22.1	-0
8750.	875012.0	-23.5	-20.4	-12.0	-0.4	11.1	19.6	22.7	-0
9000.	900012.7	-24.2	-21.0	-12.3	-0.5	11.5	20.2	23.4	-0
9250.	925013.4	-24.8	-21.6	-12.7	-0.5	11.8	20.7	24.0	-0
9500.	950014.2	-25.5	-22.2	-13.0	-0.5	12.1	21.3	24.7	-0
9750.	975014.9	-26.2	-22.8	-13.4	-0.5	12.4	21.9	25.3	-0

TABLE 4A CONTINUED

GEOPOTENTIAL	GEOMETRIC ALTITUDE	0	15	30	45	60	LATITUDE ϕ (DEG)		
							$H_{\phi-H_R}$	$H_{\phi-H_R}$	$H_{\phi-H_R}$
									H_{S-H_R}
10000.	10015.7	-26.9	-23.3	-13.7	-5	12.7	22.4	26.0	-0
10250.	10266.5	-27.5	-23.9	-14.0	-5	13.0	23.0	26.6	-0
10500.	10517.3	-28.2	-24.5	-14.4	-5	13.4	23.6	27.3	-0
10750.	10768.2	-28.9	-25.1	-14.7	-5	13.7	24.1	27.9	-0
11000.	11019.0	-29.6	-25.7	-15.1	-6	14.0	24.7	28.6	-0
11500.	11520.8	-30.9	-26.8	-15.8	-6	14.6	25.8	29.9	-0
12000.	12022.6	-32.2	-28.0	-16.5	-6	15.3	26.9	31.2	-0
12500.	12524.6	-33.6	-29.2	-17.1	-6	15.9	28.0	32.5	-0
13000.	13026.6	-34.9	-30.4	-17.8	-7	16.6	29.2	33.8	-0
13500.	13528.7	-36.3	-31.5	-18.5	-7	17.2	30.3	35.1	-0
14000.	14030.9	-37.6	-32.7	-19.2	-7	17.8	31.4	36.4	-0
14500.	14533.1	-39.0	-33.9	-19.9	-7	18.5	32.5	37.7	-0
15000.	15035.4	-40.3	-35.0	-20.6	-8	19.1	33.7	39.0	-0
15500.	15537.8	-41.7	-36.2	-21.3	-8	19.8	34.8	40.3	-0
16000.	16040.3	-43.0	-37.4	-21.9	-8	20.4	35.9	41.6	-0
16500.	16542.9	-44.4	-38.6	-22.6	-8	21.0	37.1	42.9	-0
17000.	17045.5	-45.7	-39.7	-23.3	-9	21.7	38.2	44.2	-0
17500.	17548.3	-47.1	-40.9	-24.0	-9	22.3	39.3	45.5	-0
18000.	18051.1	-48.4	-42.1	-24.7	-9	23.0	40.4	46.8	-0
18500.	18553.9	-49.8	-43.2	-25.4	-9	23.6	41.6	48.2	-0
19000.	19056.9	-51.1	-44.4	-26.1	-10	24.2	42.7	49.5	-0
19500.	19560.0	-52.5	-45.6	-26.8	-10	24.9	43.8	50.8	-0
20000.	20063.1	-53.8	-46.8	-27.5	-10	25.5	44.9	52.1	-0
20500.	20566.3	-55.2	-47.9	-28.1	-10	26.2	46.1	53.4	-0
21000.	21069.6	-56.5	-49.1	-28.8	-11	26.8	47.2	54.7	-0
21500.	21572.9	-57.9	-50.3	-29.5	-11	27.4	48.3	56.0	-0
22000.	22076.4	-59.2	-51.5	-30.2	-11	28.1	49.5	57.3	-0
22500.	22579.9	-60.6	-52.6	-30.9	-11	28.7	50.6	58.6	-0
23000.	23083.5	-61.9	-53.8	-31.6	-12	29.4	51.7	59.9	-0
23500.	23587.1	-63.3	-55.0	-32.3	-12	30.0	52.8	61.2	-0
24000.	24090.9	-64.7	-56.2	-33.0	-12	30.6	54.0	62.5	-0
24500.	24594.7	-66.0	-57.3	-33.7	-12	31.3	55.1	63.8	-0
25000.	25098.7	-67.4	-58.5	-34.4	-13	31.9	56.2	65.2	-0
25500.	25602.7	-68.7	-59.7	-35.0	-13	32.6	57.4	66.5	-0
26000.	26106.7	-70.1	-60.9	-35.7	-13	33.2	58.5	67.8	-0
26500.	26610.9	-71.4	-62.0	-36.4	-13	33.8	59.6	69.1	-0
27000.	27115.1	-72.8	-63.2	-37.1	-14	34.5	60.8	70.4	-0
27500.	27619.4	-74.1	-64.4	-37.8	-14	35.1	61.9	71.7	-0
28000.	28123.8	-75.5	-65.6	-38.5	-14	35.8	63.0	73.0	-0
28500.	28628.3	-76.8	-66.8	-39.2	-14	36.4	64.2	74.3	-0
29000.	29132.9	-78.2	-67.9	-39.9	-15	37.1	65.3	75.6	-0
29500.	29637.5	-79.6	-69.1	-40.6	-15	37.7	66.4	77.0	-0

TABLE 4A CONTINUED

GEOPOTENTIAL	GEOMETRIC ALTITUDE	LATITUDE ϕ (DEG)							
		0	15	30	45	60	75	90	
H_R (m)	Z_R (m)	$H_\phi - H_R$	$H_\phi - H_R$	$H_\phi - H_R$	$H_\phi - H_R$	$H_\phi - H_R$	$H_\phi - H_R$	$H_\phi - H_R$	$H_S - H_R$
30000.	30142.2	-80.9	-70.3	-41.3	-1.5	38.3	67.6	78.3	-0.0
30500.	30647.0	-82.3	-71.5	-42.0	-1.5	39.0	68.7	79.6	-0.0
31000.	31151.9	-83.6	-72.7	-42.7	-1.6	39.6	69.8	80.9	-0.0
31500.	31656.8	-85.0	-73.8	-43.3	-1.6	40.3	70.9	82.2	-0.0
32000.	32161.9	-86.3	-75.0	-44.0	-1.6	40.9	72.1	83.5	-0.0
33000.	33172.2	-89.1	-77.4	-45.4	-1.7	42.2	74.4	86.1	-0.0
34000.	34182.8	-91.8	-79.7	-46.8	-1.7	43.5	76.6	88.8	-0.0
35000.	35193.7	-94.5	-82.1	-48.2	-1.8	44.8	78.9	91.4	-0.0
36000.	36205.0	-97.2	-84.5	-49.6	-1.8	46.1	81.2	94.0	-0.0
37000.	37216.6	-99.9	-86.8	-51.0	-1.9	47.4	83.4	96.7	-0.0
38000.	38228.5	-102.6	-89.2	-52.4	-1.9	48.6	85.7	99.3	-0.0
39000.	39240.7	-105.4	-91.5	-53.7	-2.0	49.9	88.0	101.9	-0.0
40000.	40253.2	-108.1	-93.9	-55.1	-2.0	51.2	90.2	104.6	-0.0
41000.	41266.1	-110.8	-96.3	-56.5	-2.1	52.5	92.5	107.2	-0.0
42000.	42279.3	-113.5	-98.6	-57.9	-2.1	53.8	94.8	109.8	-0.0
43000.	43292.8	-116.3	-101.0	-59.3	-2.2	55.1	97.1	112.5	-0.0
44000.	44306.6	-119.0	-103.4	-60.7	-2.2	56.4	99.4	115.1	-0.0
45000.	45320.8	-121.7	-105.8	-62.1	-2.3	57.7	101.6	117.7	-0.0
46000.	46335.3	-124.5	-108.1	-63.5	-2.3	59.0	103.9	120.4	-0.0
47000.	47350.0	-127.2	-110.5	-64.9	-2.4	60.3	106.2	123.0	-0.1
48000.	48365.2	-129.9	-112.9	-66.3	-2.4	61.6	108.5	125.7	-0.1
49000.	49380.6	-132.7	-115.2	-67.7	-2.5	62.9	110.8	128.3	-0.1
50000.	50396.3	-135.4	-117.6	-69.1	-2.5	64.2	113.0	131.0	-0.1
51000.	51412.4	-138.1	-120.0	-70.5	-2.6	65.5	115.3	133.6	-0.1
52000.	52428.8	-140.9	-122.4	-71.9	-2.6	66.8	117.6	136.3	-0.1
53000.	53445.6	-143.6	-124.8	-73.2	-2.7	68.1	119.9	138.9	-0.1
54000.	54462.6	-146.3	-127.1	-74.6	-2.7	69.4	122.2	141.5	-0.1
55000.	55480.0	-149.1	-129.5	-76.0	-2.8	70.7	124.5	144.2	-0.1
56000.	56497.7	-151.8	-131.9	-77.4	-2.8	72.0	126.8	146.8	-0.1
57000.	57515.7	-154.6	-134.3	-78.8	-2.9	73.2	129.0	149.5	-0.1
58000.	58534.0	-157.3	-136.7	-80.2	-2.9	74.5	131.3	152.2	-0.1
59000.	59552.7	-160.0	-139.0	-81.6	-3.0	75.8	133.6	154.8	-0.1
60000.	60571.7	-162.8	-141.4	-83.0	-3.0	77.2	135.9	157.5	-0.1
61000.	61591.0	-165.5	-143.8	-84.4	-3.1	78.5	138.2	160.1	-0.1
62000.	62610.6	-168.3	-146.2	-85.8	-3.1	79.8	140.5	162.8	-0.1
63000.	63630.6	-171.0	-148.6	-87.2	-3.2	81.1	142.8	165.4	-0.1
64000.	64650.9	-173.8	-151.0	-88.6	-3.2	82.4	145.1	168.1	-0.1
65000.	65671.5	-176.5	-153.4	-90.0	-3.3	83.7	147.4	170.8	-0.1
66000.	66692.4	-179.3	-155.8	-91.5	-3.3	85.0	149.7	173.4	-0.1
67000.	67713.6	-182.0	-158.2	-92.9	-3.4	86.3	152.0	176.1	-0.1
68000.	68735.2	-184.8	-160.5	-94.3	-3.4	87.6	154.3	178.7	-0.1
69000.	69757.1	-187.5	-162.9	-95.7	-3.5	88.9	156.6	181.4	-0.1

TABLE 4A CONTINUED

GEOPOTENTIAL ALTITUDE	GEOMETRIC ALTITUDE	LATITUDE ϕ (DEG)							
		0	15	30	45	60	75	90	
H_R (m)	Z_R (m)	$H_\phi - H_R$	$H_\phi - H_R$	$H_\phi - H_R$	$H_\phi - H_R$	$H_\phi - H_R$	$H_\phi - H_R$	$H_S - H_R$	
70000.	70779.4	-190.3	-165.3	-97.1	-3.5	90.2	158.9	184.1	-0.1
71000.	71801.9	-193.1	-167.7	-98.5	-3.6	91.5	161.2	186.7	-0.1
72000.	72824.8	-195.8	-170.1	-99.9	-3.7	92.8	163.5	189.4	-0.1
73000.	73848.0	-198.6	-172.5	-101.3	-3.7	94.1	165.8	192.1	-0.1
74000.	74871.5	-201.3	-174.9	-102.7	-3.8	95.4	168.1	194.7	-0.1
75000.	75895.4	-204.1	-177.3	-104.1	-3.8	96.7	170.4	197.4	-0.1
76000.	76919.6	-206.9	-179.7	-105.5	-3.9	98.0	172.7	200.1	-0.2
77000.	77944.1	-209.6	-182.1	-106.9	-3.9	99.3	175.0	202.8	-0.2
78000.	78968.9	-212.4	-184.5	-108.3	-4.0	100.7	177.3	205.4	-0.2
79000.	79994.1	-215.2	-186.9	-109.7	-4.0	102.0	179.6	208.1	-0.2
80000.	81019.6	-217.9	-189.3	-111.2	-4.1	103.3	181.9	210.8	-0.2
81000.	82045.4	-220.7	-191.7	-112.6	-4.1	104.6	184.2	213.5	-0.2
82000.	83071.5	-223.5	-194.1	-114.0	-4.2	105.9	186.6	216.1	-0.2
83000.	84098.0	-226.2	-196.5	-115.4	-4.2	107.2	188.9	218.8	-0.2
84000.	85124.8	-229.0	-198.9	-116.8	-4.3	108.5	191.2	221.5	-0.2
85000.	86151.9	-231.8	-201.4	-118.2	-4.3	109.8	193.5	224.2	-0.2
86000.	87179.4	-234.5	-203.8	-119.6	-4.4	111.2	195.8	226.9	-0.2
87000.	88207.2	-237.3	-206.2	-121.1	-4.4	112.5	198.1	229.5	-0.2
88000.	89235.3	-240.1	-208.6	-122.5	-4.5	113.8	200.4	232.2	-0.2
89000.	90263.7	-242.9	-211.0	-123.9	-4.5	115.1	202.8	234.9	-0.2
90000.	91292.5	-245.6	-213.4	-125.3	-4.6	116.4	205.1	237.6	-0.2
92000.	93351.0	-251.2	-218.2	-128.1	-4.7	119.1	209.7	243.0	-0.2
94000.	95410.8	-256.8	-223.1	-131.0	-4.8	121.7	214.4	248.4	-0.2
96000.	97472.0	-262.3	-227.9	-133.8	-4.9	124.3	219.0	253.7	-0.3
98000.	99534.4	-267.9	-232.8	-136.7	-5.0	127.0	223.7	259.1	-0.3
100000.	101598.2	-273.5	-237.6	-139.5	-5.1	129.6	228.3	264.5	-0.3
102000.	103663.3	-279.1	-242.4	-142.4	-5.2	132.3	233.0	269.9	-0.3
104000.	105729.7	-284.7	-247.3	-145.2	-5.3	134.9	237.6	275.3	-0.3
106000.	107797.5	-290.2	-252.2	-148.1	-5.4	137.5	242.3	280.7	-0.3
108000.	109866.6	-295.8	-257.0	-150.9	-5.5	140.2	247.0	286.1	-0.3
110000.	111937.0	-301.4	-261.9	-153.8	-5.6	142.8	251.6	291.6	-0.4
112000.	114008.7	-307.0	-266.7	-156.6	-5.7	145.5	256.3	297.0	-0.4
114000.	116081.7	-312.6	-271.6	-159.5	-5.8	148.2	261.0	302.4	-0.4
116000.	118156.1	-318.2	-276.5	-162.3	-5.9	150.8	265.7	307.8	-0.4
118000.	120231.8	-323.9	-281.4	-165.2	-6.0	153.5	270.4	313.2	-0.4
120000.	122308.8	-329.5	-286.2	-168.1	-6.1	156.1	275.1	318.7	-0.4
125000.	127507.3	-343.5	-298.5	-175.2	-6.4	162.8	286.8	332.3	-0.5
130000.	132714.0	-357.6	-310.7	-182.4	-6.7	169.5	298.6	345.9	-0.5
135000.	137929.2	-371.8	-323.0	-189.6	-6.9	176.2	310.4	359.6	-0.6
140000.	143152.7	-385.9	-335.3	-196.8	-7.2	182.9	322.2	373.3	-0.6
145000.	148384.7	-400.1	-347.6	-204.1	-7.5	189.6	334.0	387.0	-0.7
150000.	153625.0	-414.3	-359.9	-211.3	-7.7	196.3	345.9	400.7	-0.8
155000.	158873.9	-428.5	-372.3	-218.6	-8.0	203.1	357.8	414.5	-0.8
160000.	164131.1	-442.7	-384.7	-225.8	-8.3	209.8	369.6	428.3	-0.9
165000.	169396.9	-457.0	-397.1	-233.1	-8.5	216.6	381.6	442.1	-1.0

TABLE 4A CONTINUED

GEOPOTENTIAL	GEOMETRIC ALTITUDE	LATITUDE ϕ (DEG)							
		0	15	30	45	60	75	90	
	H_R (km')	Z_R (m)	$H_\phi - H_R$						
170.	174671.2	-471.4	-409.5	-240.4	-8.8	223.4	393.5	455.9	-1.1
175.	179954.0	-485.7	-421.9	-247.7	-9.1	230.2	405.5	469.8	-1.1
180.	185245.4	-500.0	-434.4	-255.1	-9.3	237.0	417.5	483.7	-1.2
185.	190545.4	-514.4	-446.9	-262.4	-9.6	243.8	429.5	497.6	-1.3
190.	195853.9	-528.8	-459.4	-269.7	-9.9	250.6	441.5	511.5	-1.4
195.	201171.1	-543.3	-472.0	-277.1	-10.1	257.5	453.6	525.5	-1.5
200.	206496.9	-557.8	-484.6	-284.5	-10.4	264.3	465.6	539.5	-1.6
205.	211831.3	-572.2	-497.1	-291.9	-10.7	271.2	477.8	553.5	-1.7
210.	217174.5	-586.8	-509.8	-299.3	-10.9	278.1	489.9	567.6	-1.8
215.	222526.3	-601.3	-522.4	-306.7	-11.2	285.0	502.0	581.6	-2.0
220.	227886.8	-615.9	-535.1	-314.2	-11.5	291.9	514.2	595.7	-2.1
225.	233256.1	-630.5	-547.8	-321.6	-11.8	298.8	526.4	609.8	-2.2
230.	238634.2	-645.1	-560.5	-329.1	-12.0	305.7	538.6	624.0	-2.3
235.	244021.0	-659.8	-573.2	-336.5	-12.3	312.7	550.8	638.2	-2.5
240.	249416.7	-674.5	-586.0	-344.0	-12.6	319.6	563.1	652.4	-2.6
245.	254821.2	-689.2	-598.7	-351.5	-12.8	326.6	575.4	666.6	-2.8
250.	260234.5	-703.9	-611.5	-359.0	-13.1	333.6	587.7	680.9	-2.9
255.	265656.7	-718.7	-624.4	-366.6	-13.4	340.6	600.0	695.2	-3.1
260.	271087.8	-733.5	-637.2	-374.1	-13.7	347.6	612.4	709.5	-3.3
265.	276527.8	-748.3	-650.1	-381.7	-13.9	354.7	624.8	723.8	-3.4
270.	281976.7	-763.2	-663.0	-389.3	-14.2	361.7	637.1	738.2	-3.6
275.	287434.7	-778.0	-675.9	-396.9	-14.5	368.7	649.6	752.6	-3.8
280.	292901.5	-792.9	-688.9	-404.5	-14.8	375.8	662.0	767.0	-4.0
285.	298377.4	-807.9	-701.9	-412.1	-15.1	382.9	674.5	781.4	-4.2
290.	303862.4	-822.8	-714.8	-419.7	-15.3	390.0	687.0	795.9	-4.4
295.	309356.3	-837.8	-727.9	-427.4	-15.6	397.0	699.4	810.4	-4.6
300.	314859.4	-852.8	-740.9	-435.0	-15.9	404.2	712.0	824.9	-4.8
310.	325892.7	-882.9	-767.1	-450.4	-16.5	418.4	737.1	854.0	-5.3
320.	336962.7	-913.1	-793.3	-465.7	-17.0	432.8	762.4	883.2	-5.8
330.	348069.4	-943.4	-819.6	-481.2	-17.6	447.1	787.7	912.6	-6.3
340.	359212.9	-973.8	-846.1	-496.7	-18.2	461.5	813.1	942.0	-6.9
350.	370393.6	-1004.4	-872.6	-512.3	-18.8	476.0	838.5	971.5	-7.5
360.	381611.6	-1035.0	-899.2	-527.9	-19.3	490.5	864.1	1001.2	-8.1
370.	392867.1	-1065.8	-925.9	-543.6	-19.9	505.1	889.8	1030.9	-8.8
380.	404160.2	-1096.6	-952.7	-559.4	-20.5	519.7	915.5	1060.7	-9.5
390.	415491.1	-1127.6	-979.6	-575.2	-21.0	534.4	941.4	1090.7	-10.3
400.	426860.2	-1158.6	-1006.6	-591.0	-21.6	549.1	967.3	1120.7	-11.1
410.	438267.4	-1189.8	-1033.7	-606.9	-22.2	563.9	993.4	1150.9	-11.9
420.	449713.1	-1221.1	-1060.9	-622.9	-22.8	578.7	1019.5	1181.1	-12.8
430.	461197.4	-1252.5	-1088.2	-638.9	-23.4	593.6	1045.7	1211.5	-13.7
440.	472720.5	-1284.0	-1115.5	-654.9	-23.9	608.5	1072.0	1242.0	-14.7
450.	484282.7	-1315.6	-1143.0	-671.1	-24.5	623.5	1098.4	1272.6	-15.7
460.	495884.0	-1347.3	-1170.5	-687.3	-25.1	638.5	1124.9	1303.2	-16.8
470.	507524.8	-1379.1	-1198.2	-703.4	-25.7	653.7	1151.5	1334.0	-17.9
480.	519205.2	-1411.1	-1225.9	-719.7	-26.3	668.8	1178.1	1364.9	-19.1
490.	530925.4	-1443.1	-1253.7	-736.1	-26.9	684.0	1204.9	1395.9	-20.4

TABLE 4A CONCLUDED

GEOPOTENTIAL ALTITUDE	H_R (km ²)	Z_R (m)	LATITUDE ϕ (DEG)							
			0	15	30	45	60	75	90	$H_S - H_R$
500.	542685.6	-1475.3	-1281.7	-752.5	-27.5	699.2	1231.7	1427.0	-21.7	
510.	554486.1	-1507.5	-1309.7	-768.9	-28.1	714.5	1258.6	1458.2	-23.0	
520.	566327.0	-1539.9	-1337.8	-785.5	-28.7	729.8	1285.6	1489.5	-24.5	
530.	578208.5	-1572.4	-1366.0	-802.0	-29.3	745.2	1312.7	1520.9	-26.0	
540.	590130.9	-1604.9	-1394.4	-818.7	-29.9	760.6	1339.9	1552.4	-27.5	
550.	602094.4	-1637.6	-1422.7	-835.3	-30.5	776.2	1367.3	1584.1	-29.2	
560.	614099.1	-1670.4	-1451.2	-852.0	-31.2	791.7	1394.6	1615.8	-30.9	
570.	626145.3	-1703.3	-1479.8	-868.8	-31.8	807.3	1422.1	1647.6	-32.6	
580.	638233.3	-1736.3	-1508.5	-885.6	-32.3	823.0	1449.7	1679.6	-34.5	
590.	650363.1	-1769.4	-1537.2	-902.5	-33.0	838.6	1477.3	1711.6	-36.4	
600.	662535.1	-1802.7	-1566.1	-919.5	-33.6	854.4	1505.1	1743.7	-38.4	
610.	674749.4	-1836.0	-1595.1	-936.5	-34.2	870.1	1532.9	1775.9	-40.5	
620.	687006.4	-1869.4	-1624.1	-953.5	-34.8	886.0	1560.8	1808.3	-42.7	
630.	699306.1	-1903.0	-1653.3	-970.7	-35.5	901.9	1588.8	1840.8	-44.9	
640.	711648.8	-1936.6	-1682.5	-987.9	-36.1	917.9	1616.9	1873.3		
650.	724034.8	-1970.4	-1711.9	-1005.1	-36.8	933.9	1645.1	1906.0		
660.	736464.4	-2004.3	-1741.3	-1022.3	-37.3	950.0	1673.4	1938.8		
670.	748937.6	-2038.2	-1770.8	-1039.7	-38.0	966.0	1701.8	1971.6		
680.	761454.8	-2072.3	-1800.4	-1057.1	-38.7	982.2	1730.2	2004.6		
690.	774016.2	-2106.5	-1830.1	-1074.5	-39.2	998.5	1758.8	2037.7		
700.	786621.9	-2140.8	-1859.9	-1092.0	-39.9	1014.7	1787.5	2070.9		
710.	799272.3	-2175.2	-1889.8	-1109.6	-40.6	1031.0	1816.2	2104.2		
720.	811967.5	-2209.8	-1919.8	-1127.2	-41.2	1047.3	1845.0	2137.5		
730.	824708.0	-2244.4	-1949.9	-1144.8	-41.8	1063.8	1873.9	2171.1		
740.	837493.8	-2279.1	-1980.1	-1162.5	-42.5	1080.2	1902.9	2204.7		
750.	850325.1	-2314.0	-2010.4	-1180.3	-43.1	1096.7	1932.0	2238.4		
760.	863202.4	-2348.9	-2040.7	-1198.2	-43.8	1113.3	1961.2	2272.2		
770.	876125.8	-2383.9	-2071.1	-1216.0	-44.4	1130.0	1990.5	2306.1		
780.	889095.4	-2419.1	-2101.7	-1234.0	-45.1	1146.6	2019.8	2340.1		
790.	902111.7	-2454.4	-2132.4	-1252.0	-45.8	1163.3	2049.3	2374.3		
800.	915174.8	-2489.8	-2163.2	-1270.0	-46.4	1180.0	2078.8	2408.4		
820.	941442.7	-2560.9	-2224.9	-1306.3	-47.7	1213.8	2138.2	2477.3		
840.	967901.0	-2632.3	-2287.0	-1342.7	-49.0	1247.7	2198.0	2546.5		
860.	994551.8	-2704.3	-2349.5	-1379.5	-50.4	1281.8	2258.0	2616.1		
880.	1021397.3	-2776.7	-2412.4	-1416.4	-51.8	1316.1	2318.4	2686.1		
900.	1048439.5	-2849.5	-2475.7	-1453.6	-53.2	1350.6	2379.2	2756.5		
920.	1075680.8	-2922.7	-2539.3	-1490.8	-54.5	1385.4	2440.4	2827.4		
940.	1103123.1	-2996.5	-2603.3	-1528.5	-55.9	1420.2	2501.9	2898.7		
960.	1130768.9	-3070.5	-2667.7	-1566.3	-57.3	1455.4	2563.8	2970.4		
980.	1158620.3	-3145.1	-2732.5	-1604.3	-58.7	1490.7	2626.0	3042.5		
1000.	1186679.8	-3220.0	-2797.5	-1642.5	-60.0	1526.2	2688.6	3115.0		

TABLE 4B

GEOPOTENTIAL DIFFERENCES BETWEEN A SERIES OF GEOMETRIC-ALTITUDE SURFACES AT A
REFERENCE LATITUDE AND THE SAME GEOMETRIC-ALTITUDE SURFACES AT OTHER LATITUDES,
ALL AS A FUNCTION OF THE GEOPOTENTIAL EQUIVALENT
OF THE EQUAL GEOMETRIC-ALTITUDE SURFACES, 0 to 3,900 km'

GEOPOTENTIAL ALTITUDE	GEOMETRIC ALTITUDE	LATITUDE ϕ (DEG)						
		0	15	30	45	60	75	90
H_R (km')	Z_R (km)	$H_\phi - H_R$	$H_\phi - H_R$	$H_\phi - H_R$	$H_\phi - H_R$	$H_\phi - H_R$	$H_\phi - H_R$	$H_\phi - H_R$
1000.	1186.68	-3.22	-2.80	-1.64	-0.06	1.53	2.69	3.12
1020.	1214.95	-3.30	-2.86	-1.68	-0.06	1.56	2.75	3.19
1040.	1243.43	-3.37	-2.93	-1.72	-0.06	1.60	2.81	3.26
1060.	1272.13	-3.45	-3.00	-1.76	-0.06	1.63	2.88	3.34
1080.	1301.04	-3.52	-3.06	-1.80	-0.07	1.67	2.94	3.41
1100.	1330.18	-3.60	-3.13	-1.84	-0.07	1.71	3.01	3.48
1120.	1359.54	-3.68	-3.20	-1.88	-0.07	1.74	3.07	3.56
1140.	1389.12	-3.76	-3.26	-1.92	-0.07	1.78	3.14	3.63
1160.	1418.93	-3.84	-3.33	-1.96	-0.07	1.82	3.20	3.71
1180.	1448.97	-3.91	-3.40	-2.00	-0.07	1.86	3.27	3.79
1200.	1479.24	-3.99	-3.47	-2.04	-0.07	1.89	3.33	3.86
1220.	1509.75	-4.07	-3.54	-2.08	-0.08	1.93	3.40	3.94
1240.	1540.50	-4.15	-3.61	-2.12	-0.08	1.97	3.47	4.02
1260.	1571.49	-4.23	-3.68	-2.16	-0.08	2.01	3.54	4.10
1280.	1602.73	-4.31	-3.75	-2.20	-0.08	2.05	3.60	4.17
1300.	1634.21	-4.40	-3.82	-2.24	-0.08	2.08	3.67	4.25
1320.	1665.94	-4.48	-3.89	-2.28	-0.08	2.12	3.74	4.33
1340.	1697.92	-4.56	-3.96	-2.33	-0.09	2.16	3.81	4.41
1360.	1730.16	-4.64	-4.03	-2.37	-0.09	2.20	3.88	4.49
1380.	1762.66	-4.73	-4.11	-2.41	-0.09	2.24	3.95	4.57
1400.	1795.42	-4.81	-4.18	-2.45	-0.09	2.28	4.02	4.65
1420.	1828.45	-4.89	-4.25	-2.50	-0.09	2.32	4.09	4.73
1440.	1861.74	-4.98	-4.33	-2.54	-0.09	2.36	4.16	4.82
1460.	1895.31	-5.06	-4.40	-2.58	-0.09	2.40	4.23	4.90
1480.	1929.15	-5.15	-4.47	-2.63	-0.10	2.44	4.30	4.98
1500.	1963.27	-5.23	-4.55	-2.67	-0.10	2.48	4.37	5.06
1520.	1997.67	-5.32	-4.62	-2.71	-0.10	2.52	4.44	5.15
1540.	2032.36	-5.41	-4.70	-2.76	-0.10	2.56	4.52	5.23
1560.	2067.34	-5.49	-4.77	-2.80	-0.10	2.60	4.59	5.32
1580.	2102.61	-5.58	-4.85	-2.85	-0.10	2.65	4.66	5.40
1600.	2138.18	-5.67	-4.93	-2.89	-0.11	2.69	4.73	5.49
1620.	2174.05	-5.76	-5.00	-2.94	-0.11	2.73	4.81	5.57
1640.	2210.22	-5.85	-5.08	-2.98	-0.11	2.77	4.88	5.66
1660.	2246.70	-5.94	-5.16	-3.03	-0.11	2.81	4.96	5.74
1680.	2283.49	-6.03	-5.23	-3.07	-0.11	2.86	5.03	5.83
1700.	2320.60	-6.12	-5.31	-3.12	-0.11	2.90	5.11	5.92
1720.	2358.03	-6.21	-5.39	-3.17	-0.12	2.94	5.18	6.00
1740.	2395.78	-6.30	-5.47	-3.21	-0.12	2.99	5.26	6.09
1760.	2433.86	-6.39	-5.55	-3.26	-0.12	3.03	5.34	6.18
1780.	2472.28	-6.48	-5.63	-3.31	-0.12	3.07	5.41	6.27

TABLE 4B CONTINUED

GEOPOTENTIAL	GEOMETRIC ALTITUDE	0	LATITUDE ϕ (DEG)					
			15	30	45	60	75	90
H_R (km')	Z_R (km)	$H_\phi - H_R$	$H_\phi - H_R$	$H_\phi - H_R$	$H_\phi - H_R$	$H_\phi - H_R$	$H_\phi - H_R$	$H_\phi - H_R$
1800.	2511.03	-6.57	-5.71	-3.35	-0.12	3.12	5.49	6.36
1820.	2550.12	-6.66	-5.79	-3.40	-0.12	3.16	5.57	6.45
1840.	2589.56	-6.76	-5.87	-3.45	-0.13	3.20	5.64	6.54
1860.	2629.35	-6.85	-5.95	-3.49	-0.13	3.25	5.72	6.63
1880.	2669.50	-6.94	-6.03	-3.54	-0.13	3.29	5.80	6.72
1900.	2710.00	-7.04	-6.12	-3.59	-0.13	3.34	5.88	6.81
1920.	2750.88	-7.13	-6.20	-3.64	-0.13	3.38	5.96	6.90
1940.	2792.12	-7.23	-6.28	-3.69	-0.13	3.43	6.04	7.00
1960.	2833.73	-7.32	-6.36	-3.74	-0.14	3.47	6.12	7.09
1980.	2875.73	-7.42	-6.45	-3.79	-0.14	3.52	6.20	7.18
2000.	2918.11	-7.52	-6.53	-3.83	-0.14	3.56	6.28	7.28
2020.	2960.89	-7.61	-6.62	-3.88	-0.14	3.61	6.36	7.37
2040.	3004.06	-7.71	-6.70	-3.93	-0.14	3.66	6.44	7.46
2060.	3047.63	-7.81	-6.79	-3.98	-0.15	3.70	6.52	7.56
2080.	3091.61	-7.91	-6.87	-4.03	-0.15	3.75	6.61	7.65
2100.	3136.00	-8.01	-6.96	-4.08	-0.15	3.80	6.69	7.75
2120.	3180.81	-8.11	-7.04	-4.13	-0.15	3.84	6.77	7.84
2140.	3226.05	-8.20	-7.13	-4.19	-0.15	3.89	6.85	7.94
2160.	3271.71	-8.30	-7.22	-4.24	-0.15	3.94	6.94	8.04
2180.	3317.82	-8.40	-7.30	-4.29	-0.16	3.99	7.02	8.14
2200.	3364.37	-8.51	-7.39	-4.34	-0.16	4.03	7.11	8.23
2220.	3411.37	-8.61	-7.48	-4.39	-0.16	4.08	7.19	8.33
2240.	3458.82	-8.71	-7.57	-4.44	-0.16	4.13	7.28	8.43
2260.	3506.74	-8.81	-7.66	-4.49	-0.16	4.18	7.36	8.53
2280.	3555.13	-8.91	-7.74	-4.55	-0.17	4.23	7.45	8.63
2300.	3603.99	-9.02	-7.83	-4.60	-0.17	4.28	7.53	8.73
2320.	3653.34	-9.12	-7.92	-4.65	-0.17	4.32	7.62	8.83
2340.	3703.19	-9.22	-8.01	-4.71	-0.17	4.37	7.71	8.93
2360.	3753.53	-9.33	-8.10	-4.76	-0.17	4.42	7.79	9.03
2380.	3804.37	-9.43	-8.20	-4.81	-0.18	4.47	7.88	9.13
2400.	3855.73	-9.54	-8.29	-4.87	-0.18	4.52	7.97	9.23
2420.	3907.62	-9.64	-8.38	-4.92	-0.18	4.57	8.06	9.33
2440.	3960.03	-9.75	-8.47	-4.97	-0.18	4.62	8.14	9.44
2460.	4012.98	-9.86	-8.56	-5.03	-0.18	4.67	8.23	9.54
2480.	4066.48	-9.96	-8.66	-5.08	-0.19	4.72	8.32	9.64
2500.	4120.53	-10.07	-8.75	-5.14	-0.19	4.78	8.41	9.75
2520.	4175.14	-10.18	-8.84	-5.19	-0.19	4.83	8.50	9.85
2540.	4230.33	-10.28	-8.94	-5.25	-0.19	4.88	8.59	9.96
2560.	4286.10	-10.39	-9.03	-5.30	-0.19	4.93	8.68	10.06
2580.	4342.46	-10.50	-9.13	-5.36	-0.20	4.98	8.78	10.17

TABLE 4B CONTINUED

GEOPOTENTIAL	GEOMETRIC ALTITUDE	0	LATITUDE ϕ (DEG)					
			15	30	45	60	75	90
H_R (km')	Z_R (km)	$H_\phi - H_R$	$H_\phi - H_R$	$H_\phi - H_R$	$H_\phi - H_R$	$H_\phi - H_R$	$H_\phi - H_R$	$H_\phi - H_R$
2600.	4399.42	-10.61	-9.22	-5.41	-20	5.03	8.87	10.27
2620.	4456.99	-10.72	-9.32	-5.47	-20	5.09	8.96	10.38
2640.	4515.18	-10.83	-9.41	-5.53	-20	5.14	9.05	10.49
2660.	4574.00	-10.94	-9.51	-5.58	-20	5.19	9.14	10.59
2680.	4633.46	-11.05	-9.60	-5.64	-21	5.24	9.24	10.70
2700.	4693.57	-11.17	-9.70	-5.70	-21	5.30	9.33	10.81
2720.	4754.33	-11.28	-9.80	-5.75	-21	5.35	9.42	10.92
2740.	4815.78	-11.39	-9.90	-5.81	-21	5.40	9.52	11.03
2760.	4877.90	-11.50	-9.99	-5.87	-21	5.46	9.61	11.14
2780.	4940.72	-11.62	-10.09	-5.93	-22	5.51	9.71	11.25
2800.	5004.25	-11.73	-10.19	-5.98	-22	5.56	9.80	11.36
2820.	5068.49	-11.84	-10.29	-6.04	-22	5.62	9.90	11.47
2840.	5133.47	-11.96	-10.39	-6.10	-22	5.67	9.99	11.58
2860.	5199.19	-12.07	-10.49	-6.16	-23	5.73	10.09	11.69
2880.	5265.67	-12.19	-10.59	-6.22	-23	5.78	10.19	11.80
2900.	5332.91	-12.30	-10.69	-6.28	-23	5.84	10.28	11.91
2920.	5400.94	-12.42	-10.79	-6.34	-23	5.89	10.38	12.03
2940.	5469.76	-12.54	-10.89	-6.40	-23	5.95	10.48	12.14
2960.	5539.39	-12.65	-11.00	-6.46	-24	6.00	10.58	12.25
2980.	5609.85	-12.77	-11.10	-6.52	-24	6.06	10.67	12.37
3000.	5681.15	-12.89	-11.20	-6.58	-24	6.11	10.77	12.48
3020.	5753.30	-13.0	-11.3	-6.6	-24	6.2	10.9	12.6
3040.	5826.33	-13.1	-11.4	-6.7	-24	6.2	11.0	12.7
3060.	5900.24	-13.2	-11.5	-6.8	-25	6.3	11.1	12.8
3080.	5975.05	-13.4	-11.6	-6.8	-25	6.3	11.2	12.9
3100.	6050.78	-13.5	-11.7	-6.9	-25	6.4	11.3	13.1
3120.	6127.45	-13.6	-11.8	-6.9	-25	6.5	11.4	13.2
3140.	6205.07	-13.7	-11.9	-7.0	-26	6.5	11.5	13.3
3160.	6283.66	-13.8	-12.0	-7.1	-26	6.6	11.6	13.4
3180.	6363.24	-14.0	-12.1	-7.1	-26	6.6	11.7	13.5
3200.	6443.83	-14.1	-12.2	-7.2	-26	6.7	11.8	13.6
3220.	6525.44	-14.2	-12.4	-7.3	-27	6.7	11.9	13.8
3240.	6608.11	-14.3	-12.5	-7.3	-27	6.8	12.0	13.9
3260.	6691.84	-14.5	-12.6	-7.4	-27	6.9	12.1	14.0
3280.	6676.66	-14.6	-12.7	-7.4	-27	6.9	12.2	14.1
3300.	6862.59	-14.7	-12.8	-7.5	-27	7.0	12.3	14.2
3320.	6949.65	-14.8	-12.9	-7.6	-28	7.0	12.4	14.4
3340.	7037.87	-14.9	-13.0	-7.6	-28	7.1	12.5	14.5
3360.	7127.26	-15.1	-13.1	-7.7	-28	7.2	12.6	14.6
3380.	7217.86	-15.2	-13.2	-7.8	-28	7.2	12.7	14.7

TABLE 4B CONCLUDED

GEOPOTENTIAL ALTITUDE	GEOMETRIC ALTITUDE	0	LATITUDE ϕ (DEG)						75	90
			15	30	45	60	$H_{\phi}-H_R$	$H_{\phi}-H_R$		
H_R (km')	Z_R (km)		$H_{\phi}-H_R$	$H_{\phi}-H_R$	$H_{\phi}-H_R$	$H_{\phi}-H_R$	$H_{\phi}-H_R$	$H_{\phi}-H_R$	$H_{\phi}-H_R$	$H_{\phi}-H_R$
3400.	7309.7	-15.	-13.	-7.8	-0.3	7.3	13.	15.		
3420.	7402.7	-15.	-13.	-7.9	-0.3	7.3	13.	15.		
3440.	7497.1	-16.	-14.	-8.0	-0.3	7.4	13.	15.		
3460.	7592.7	-16.	-14.	-8.0	-0.3	7.5	13.	15.		
3480.	7689.7	-16.	-14.	-8.1	-0.3	7.5	13.	15.		
3500.	7788.1	-16.	-14.	-8.2	-0.3	7.6	13.	15.		
3520.	7887.8	-16.	-14.	-8.2	-0.3	7.6	13.	16.		
3540.	7988.9	-16.	-14.	-8.3	-0.3	7.7	14.	16.		
3560.	8091.5	-16.	-14.	-8.4	-0.3	7.8	14.	16.		
3580.	8195.6	-16.	-14.	-8.4	-0.3	7.8	14.	16.		
3600.	8301.2	-17.	-14.	-8.5	-0.3	7.9	14.	16.		
3620.	8408.3	-17.	-15.	-8.6	-0.3	8.0	14.	16.		
3640.	8517.0	-17.	-15.	-8.6	-0.3	8.0	14.	16.		
3660.	8627.3	-17.	-15.	-8.7	-0.3	8.1	14.	16.		
3680.	8739.2	-17.	-15.	-8.8	-0.3	8.1	14.	17.		
3700.	8852.9	-17.	-15.	-8.8	-0.3	8.2	14.	17.		
3720.	8968.2	-17.	-15.	-8.9	-0.3	8.3	15.	17.		
3740.	9085.4	-18.	-15.	-9.0	-0.3	8.3	15.	17.		
3760.	9204.3	-18.	-15.	-9.0	-0.3	8.4	15.	17.		
3780.	9325.1	-18.	-15.	-9.1	-0.3	8.5	15.	17.		
3800.	9447.8	-18.	-16.	-9.2	-0.3	8.5	15.	17.		
3820.	9572.4	-18.	-16.	-9.2	-0.3	8.6	15.	18.		
3840.	9698.9	-18.	-16.	-9.3	-0.3	8.7	15.	18.		
3860.	9827.6	-18.	-16.	-9.4	-0.3	8.7	15.	18.		
3880.	9958.2	-19.	-16.	-9.4	-0.3	8.8	15.	18.		
3900.	10091.1	-19.	-16.	-9.5	-0.3	8.8	16.	18.		

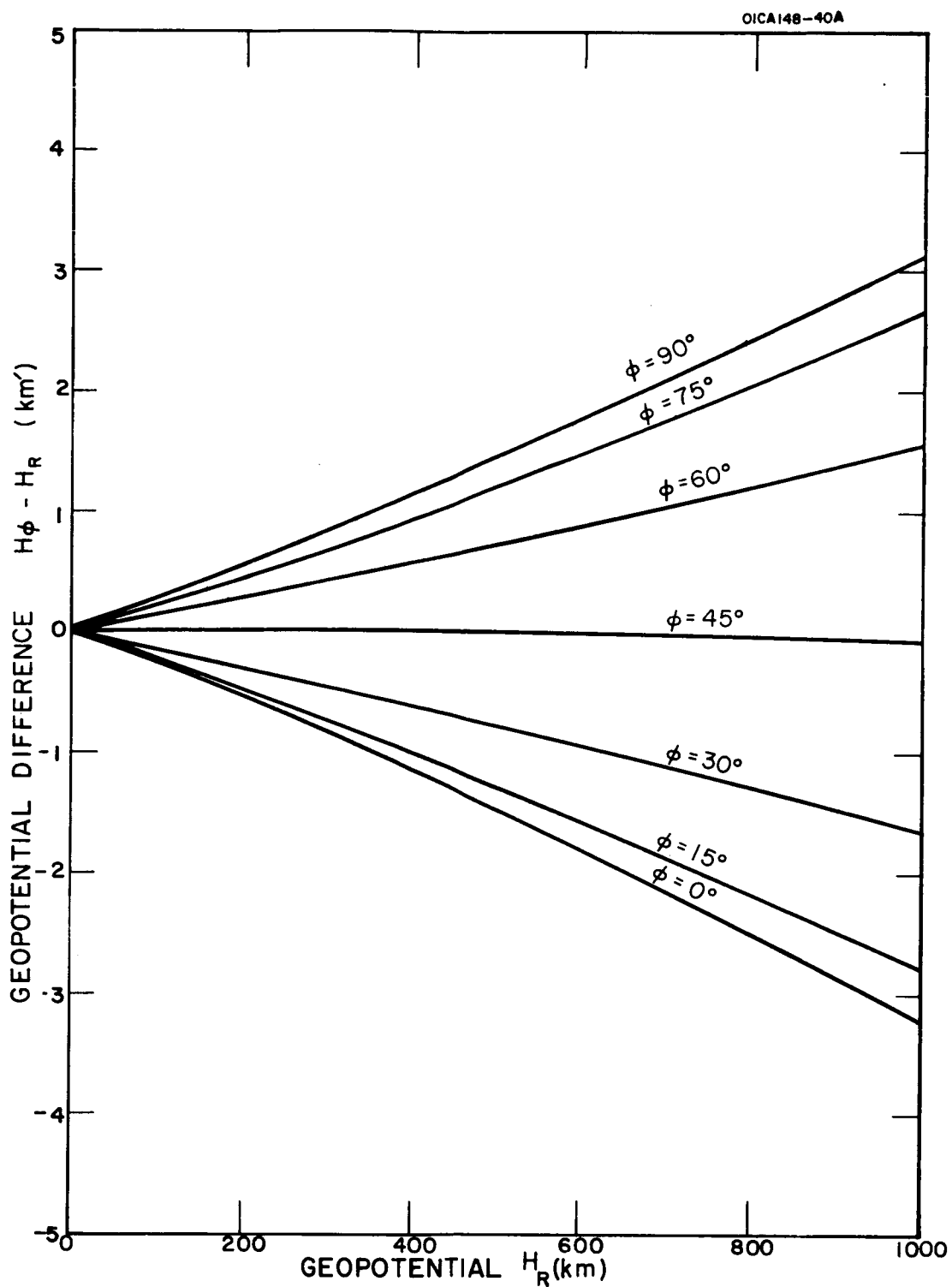


Figure 4.1A. Geopotential differences between geometric-altitude surfaces at a reference latitude, and the same geometric altitude surfaces at seven other latitudes, all as a function of the geopotential equivalent of the equal geometric-height surfaces, 0 to 1,000 km'.

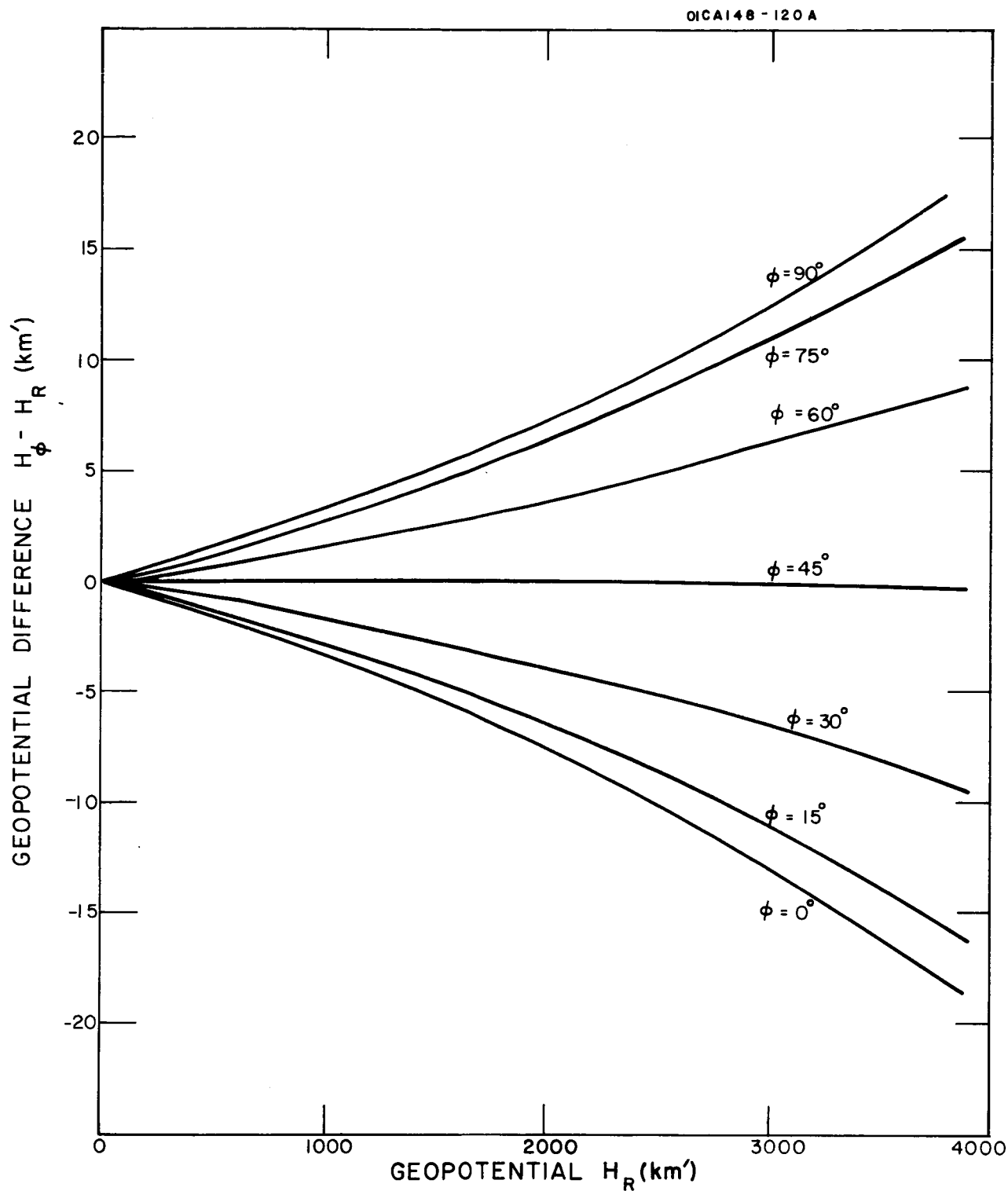


Figure 4.1B. Geopotential differences between geometric-altitude surfaces at a reference latitude, and the same geometric-altitude surfaces at seven other latitudes all as a function of the geopotential equivalent of the equal geometric-height surfaces, 0 to 10,000 km'.

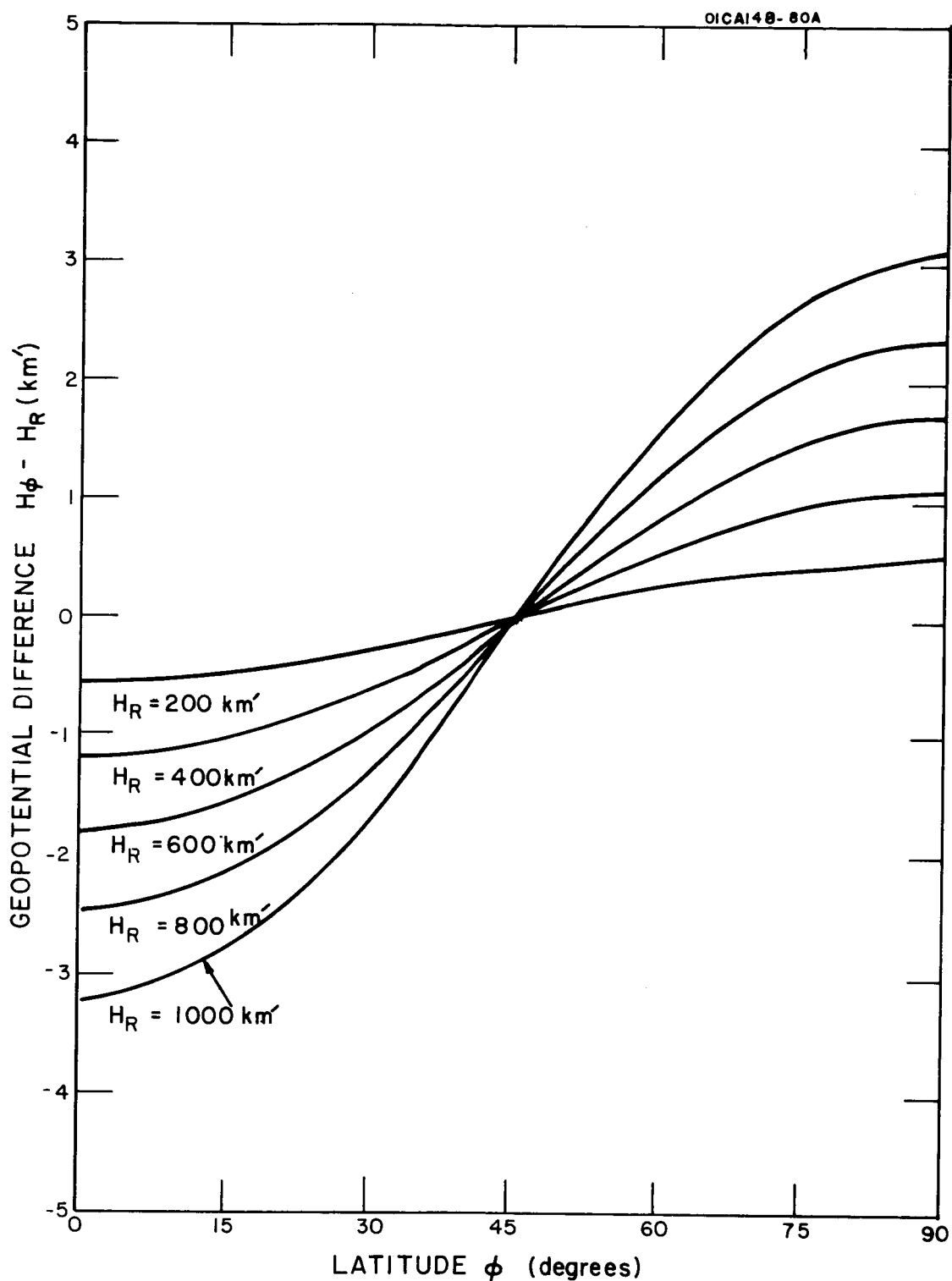


Figure 4.2A. Geopotential differences between each of give geometric-altitude surfaces, expressed in the equivalent geopotential (200 to 1000 km') at a reference latitude, and the same five surfaces at other latitudes, all as a function of latitude from 0 to 90 degrees.

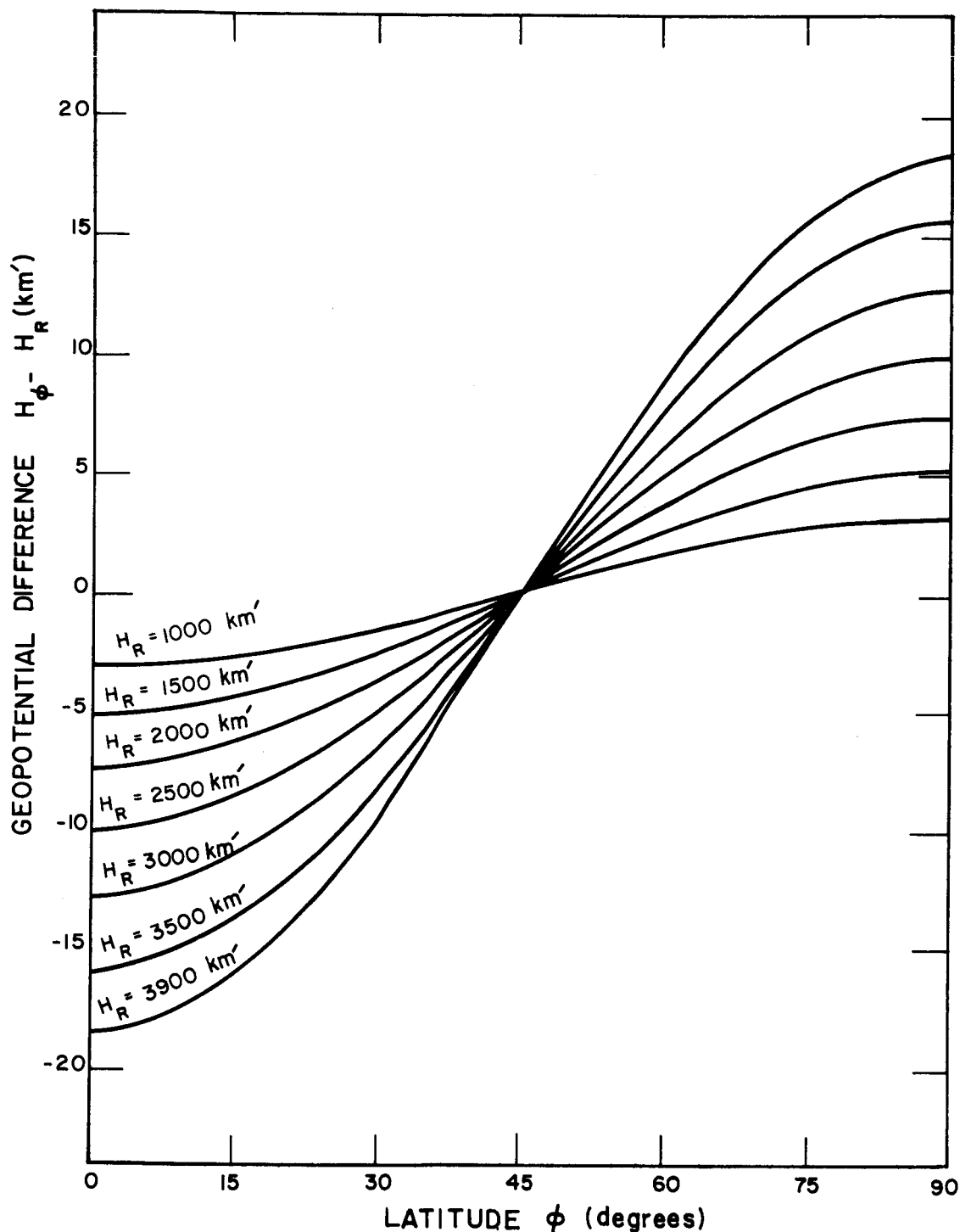


Figure 4.2B. Geopotential differences between each of seven geometric-altitude surfaces expressed in the equivalent geopotential (200 to 1,000 km') at a reference latitude, and the same seven surfaces at other latitudes, all as a function of latitude from 0 to 90 degrees.

SECTION VIII

UNCERTAINTY CONSIDERATIONS

The method employed in relating geopotential H and geometric altitude Z in the United States Standard Atmosphere is very sophisticated and is assumed to involve a very small error between H and Z . The closeness of fit between the empirically derived values, H_S and Z_S , and the corresponding Standard Atmosphere values, H and Z , respectively, implies a similarly small error between H_S and Z_S . The method employed in computing the relationships between H_R and Z_R , between H_R and Z_ϕ , between Z_R and H_ϕ , or between Z_R and H_ϕ , as presented in this document, is a considerably simpler but somewhat less accurate one than that employed in the Standard. Consequently, the differences $(Z_S - Z_R)$ and $(H_S - H_R)$ may be considered to be approximately δZ_R and δH_R , the uncertainties in Z_R and H_R respectively, resulting from the less precise computational function employed in obtaining these values. From the tabulations of $H_S - H_R$, the value of δH_R is seen to be less than one geopotential meter for altitudes of 175 km and below, and is seen to increase to 33.2 geopotential meters at 700 km altitude. From $Z_S - Z_R$, the value of δZ_R is seen to be about 40 meters for values of H_R equivalent to $Z_R = 700$ km.

While values of δH_R and δZ_R are thus known, the values of δH_ϕ and δZ_ϕ , the uncertainties in H_ϕ and Z_ϕ respectively are not known, and could not be determined without a recalculation of the values of H_ϕ and Z_ϕ using the techniques employed in the calculation of the Standard Atmosphere. It is reasonable to assume, however, that the values of δH_ϕ and δZ_ϕ are similar in magnitude but not necessarily in sign to the values of δH_R and δZ_R respectively. Accordingly one may assume that, for latitudes 0° , 15° , 30° , 60° , 75° , and 90° , the uncertainties in the differences $(Z_\phi - Z_R)$ are of the order of $2\delta Z_R$, while the uncertainties in the differences $(H_\phi - H_R)$ are of the order of $2\delta H_R$.

With such assumptions, the uncertainties in the differences $(H_\phi - H_R)$ for latitudes 30° and 60° are seen to range from about 1 percent at 200 km to about 6.8 percent at 700 km. Determined in this manner the percentage uncertainties in the differences $(H_\phi - H_R)$ and $(Z_\phi - Z_R)$ for the latitudes more remote from the reference latitude are smaller than for latitudes 30° and 60° since the differences are greater. It is quite possible, however, that the estimated values of δH_ϕ and δZ_ϕ for the latitudes more remote from the reference latitude might also be greater for these latitudes.

Latitude 45° is so close to the reference latitude R that the uncertainty in H_ϕ for this altitude must be very nearly identical with the value of δH_R and the uncertainty in the difference $(H_\phi - H_R)$ for $\phi = 45^\circ$ must be very small.

Significant Figures

For altitudes below 1000 km (Tables 1A, 2A, 3A, and 4A) the results of the calculations are given to the nearest tenth of a meter (geometric or geopotential). It is apparent from the discussion of uncertainty in the tabulated values of $H_\phi - H_R$ or $Z_\phi - Z_R$ that the apparent precision implied by the tabulations to one tenth of a meter is unwarranted for altitudes above 80 km. Tabulations to the nearest meter are similarly unwarranted above about 200 km, while tabulations to the nearest 10 meters are unwarranted above 500 km. The listing of values of H_R and Z_R to one tenth of a meter was justifiably retained to altitudes of 700 km, however, in order to obtain correct values of the uncertainties, $(H_S - H_R)$ and $(Z_S - Z_R)$, which do warrant the 0.1 meter tabulations. Between 700 and 1000 km the same format in H_R and Z_R was retained for the sake of uniformity alone.

The value of $H_S - H_R$, that is δH_R , if it were available for altitudes of about 1000 km, would probably be close to 100 meters and could be expected to increase to the order of kilometers at higher altitudes. Consequently, for altitudes above 1000 km, the format of the tables has been changed so that all values are presented in kilometers rather than in meters. Furthermore, the number of significant figures in the differences $H_\phi - H_R$ and $Z_\phi - Z_R$ is decreased to four or three for geometric altitudes between 1000 and 3600 km and is further reduced to two for greater altitudes. From 1000 to 3600 km the non-integral member of the argument pair is tabulated to the nearest hundredth of a kilometer, while at greater altitudes it is tabulated to the nearest tenth of a kilometer.

REFERENCES

1. ICAO (International Civil Aviation Organization), 1954
The ICAO Standard Atmosphere - Calculations by NASA
NACA Tech Note 3182, Langley Aeronautical Lab. Langley Field, Va.
2. Minzner, R.A. and Ripley, W.S., Dec. 1956
The ARDC Model Atmosphere, 1956
Air Force Surveys in Geophysics No. 86, AFCRC IN-56-204.
3. Minzner, R.A., Ripley, W.S. and Condron, T.P., 1958
United States Extension to the ICAO Standard Atmosphere
United States Government Printing Office, Washington, D.C.
4. Minzner, R.A., Champion, K.S.W. and Pond, H.L., 1959
The ARDC Model Atmosphere, 1959
Air Force Surveys in Geophysics, No. 115, AFCRC-TR-59-267.
5. United States Standard Atmosphere, 1962.
National Aeronautics and Space Administration, United States
Air Force and United States Weather Bureau, Government Printing
Office, Washington, D.C.
6. Cole, A.E. and Kantor, A.J., Dec 1963
Air Force Interim Supplemental Atmospheres to 90 Kilometers.
Air Force Surv. Geophys., 153, AFCRL-63-936.
7. Harrison, L.P., 1951
Relation Between Geopotential and Geometric Height.
Unpublished Paper Adapted for Smithsonian Meteorological Tables,
Sixth Ed., Edited by R.S. List, pp 217-218, Washington, D.C.
8. List, R.S., Editor, 1951
Smithsonian Meteorological Tables, Sixth Ed.
Publication 4014, Smithson. Misc. Collec. V114, Washington, D.C.
9. Jacchia, L.G., Dec. 1964
Static Diffusion Models of the Upper Atmosphere with Empirical
Temperature Profiles.
Smithsonian Inst. Astrophysical Observatory, Special Report 170.
10. Minzner, R.A., 1966
Standard Atmosphere Suppliments, 1966
GCA Tech Rpt., 66- -A, Final Rpt. Cont. Af19(628)-6085 in Prep.

REFERENCES (continued)

11. Minzner, R.A., 1966
Studies of Atmospheric Structure and variability of the Earth's Atmosphere, GCA Tech. Rpt. 66-14-N, Final Report, Contract NASW-1225.
12. Committee on Extension of the Standard Atmosphere (COESA), 1966
United States Standard Atmosphere Supplements, 1966.
Government Printing Office, Washington, D.C. (To be published).

APPENDIX A

VALUES OF r_ϕ AND g_ϕ EMPLOYED IN THE CALCULATION
OF GEOPOTENTIAL AT VARIOUS LATITUDES

ϕ	r_ϕ	g_ϕ
$45^\circ 32' 33''$	6,356,766	9.80665
0°	6,334,984	9.78036
15°	6,337,838	9.78381
30°	6,345,653	9.79324
45°	6,356,360	9.80616
60°	6,367,103	9.81911
75°	6,374,972	9.82860
90°	6,377,862	9.83208

PRECEDING PAGE BLANK NOT FILMED.

APPENDIX B
PROGRAM FOR TABLE 2

C PROGRAM IV

```
DIMENSION R0(8),G0(8),ZZ(8),DZ(8),DA(7),DD(8),DF(7)
A=.4858124E-02
B=-.1338918E-06
C=.1903029E-10
D=.8288881E-16
E=-.1822113E-22
G=9.80665
R=6356766.
DO 1 I=1,7
  READ 100,R0(I),G0(I)
1  R0(I)=R0(I)*1.E+03
  K=I
  Z=44000.
5  H=Z*(1./(1.+Z/R))
  DO 2 J=1,7
    ZZ(J)=R0(J)*H/(G0(J)/G*R0(J)-H)
    DZ(J)=ZZ(J)-Z
    IF (DZ(J)) 41,42,42
41  DD(J)=DZ(J) -.05
    DA(J)=DZ(J)/1000.+.05
    DF(J)=DZ(J)/1000.+.5
    DZ(J)=(DZ(J)/1000.+.005)
    GO TO 2
42  DD(J)=DZ(J) +.05
    DA(J)=DZ(J)/1000.+.05
    DF(J)=DZ(J)/1000.+.5
    DZ(J)=(DZ(J)/1000.+.005)
2  CONTINUE
ZA=Z/1000.
HA=H/1000.+.05
HG=H/1000.+.005
26 IF (ZA-1000.) 53,53,28
53  DZ(8)=+(A+B*Z+C*Z**2+D*Z**3+E*Z**4)
    DZ(8)=DZ(8)/((1.-H/R)*(1.-H/R-DZ(8)/R))
    DD(8)=DZ(8)+.05
    IF (Z-170000.) 25,27,27
25  PUNCH 107, Z,H,DD(1),DD(2),DD(3),DD(4),DD(5),DD(6),DD(7),DD(8)
    GO TO 16
27  IF (ZA-710.) 29,47,47
29  PUNCH 107,ZA,H,DD(1),DD(2),DD(3),DD(4),DD(5),DD(6),DD(7),DD(8)
    GO TO 16
```

```

C PROGRAM IV CONCLUDED
47 PUNCH 107,ZA,H,DD(1),DD(2),DD(3),DD(4),DD(5),DD(6),DD(7)
   IF (ZA-10000.) 16,28,28
28 K=K+1
   IF (ZA-35000.) 14,20,20
14 PUNCH 101, ZA,HG,DZ(1),DZ(2),DZ(3),DZ(4),DZ(5),DZ(6),DZ(7)
20 PUNCH 104,ZA,HA,DF(1),DF(2),DF(3),DA(4),DF(5),DF(6),DF(7)
16 IF (K-10) 22,13,13
13 PUNCH 103
   K=0
22 IF (ZA-100000.) 12,21,21
12 IF (Z-110000.) 33,44,44
33 Z=Z+250.
   GO TO 5
44 IF (Z-320000.) 66,77,77
66 Z=Z+500.
   GO TO 5
77 IF (Z-900000.) 88,99,99
88 Z=Z+1000.
   GO TO 5
99 IF (Z-1200000.) 91,92,92
91 Z=Z+2000.
   GO TO 5
92 IF (Z-3000000.) 35,36,36
35 Z=Z+5000.
   GO TO 5
36 IF (Z-8000000.) 37,38,38
37 Z=Z+10000.
   GO TO 5
38 IF (Z-50000000.) 10,11,11
10 Z=Z+20000.
   GO TO 5
11 Z=Z+50000.
   GO TO 5
100 FORMAT(F9.0,F8.0)
101 FORMAT (F7.0,F9.2,F7.2,6F8.2)
103 FORMAT (1H )
104 FORMAT (F7.0,F8.1,F6.0,2F8.0,F9.1,F7.0,2F8.0)
107 FORMAT (F10.0,F9.1,3F8.1,F6.1,3F8.1,F6.1)
21 END

```

APPENDIX C
PROGRAM FOR TABLE 4

C PROGRAM II

```

DIMENSION RU(8),GO(8),HH(8),DZ(8),DA(8),DD(8),DH(8),DF(7)
A=.2579651E-02
B=-.2161710E-07
C=.1807561E-10
D=.9153012E-16
E=.2006785E-22
G=9.80665
R=6356766.
DO 1 I=1,7
READ 100,R0(I),GO(I)
1 R0(I)=R0(I)*1.E+03
K=C
H=44000.
5 Z=H/(1.-H/R)
DO 2 J=1,7
HH(J)=GO(J)/G*RU(J)*Z/(RU(J)+Z)
DH(J)=HH(J)-H
IF (DH(J)) 41,42,42
41 DD(J)=(DH(J)-.05)
DA(J)=(DH(J)/1000.-.05)
DF(J)=DH(J)/1000.-.5
DH(J)=(DH(J)/1000.-.005)
GO TO 2
42 DD(J)=(DH(J)+.05)
DA(J)=(DH(J)/1000.+.05)
DF(J)=DH(J)/1000.+.5
DH(J)=(DH(J)/1000.+.005)
2 CONTINUE
HH=H/1000.
ZA=Z/1000.+.05
ZG=Z/1000.+.005
26 IF (HH-1000.) 53,53,28
53 DZ(8)=-(A+B*Z+C*Z**2+D*Z**3+E*Z**4)
DD(8)=DZ(8)-.05
IF (H-170000.) 25,27,27
25 PUNCH 107, H,Z,DD(1),DD(2),DD(3),DD(4),DD(5),DD(6),DD(7),DD(8)
GO TO 16
27 IF (HH-640.) 29,47,47
29 PUNCH 107,HH,Z,DD(1),DD(2),DD(3),DD(4),DD(5),DD(6),DD(7),DD(8)
GO TO 16
47 PUNCH 107,HH,Z,DD(1),DD(2),DD(3),DD(4),DD(5),DD(6),DD(7)
IF (HH-1000.) 16,28,28

```

```

C PROGRAM II CONCLUDED
28 K=K+1
    IF (HH-3020.) 14,20,20
14 PUNCH 101, HH,ZG,DH(1),DH(2),DH(3),DH(4),DH(5),DH(6),DH(7)
    GO TO 16
20 PUNCH 104, HH,ZA,DF(1),DF(2),DA(3),DA(4),DA(5),DF(6),DF(7)
16 IF (K=10) 22,13,13
13 PUNCH 103
    K=0
22 IF (HH-3900.) 12,21,21
12 IF (H-11000.) 33,44,44
33 H=H+250.
    GO TO 5
44 IF (H-32000.) 66,77,77
66 H=H+500.
    GO TO 5
77 IF (H-90000.) 88,99,99
88 H=H+1000.
    GO TO 5
99 IF (H-120000.) 91,92,92
91 H=H+2000.
    GO TO 5
92 IF (H-300000.) 35,36,36
35 H=H+5000.
    GO TO 5
36 IF (H-800000.) 37,38,38
37 H=H+10000.
    GO TO 5
38 H=H+20000.
    GO TO 5
103 FORMAT (1H )
104 FORMAT (F7.0,F8.1,F6.0,F8.0,F9.1,2F8.1,F7.0,F8.0)
101 FORMAT (F7.0,F9.2,F7.2,6F8.2)
107 FORMAT (F9.0,F10.1,3F8.1,F6.1,3F8.1,F6.1)
100 FORMAT(F9.0,F8.0)
21 END

```